Fetal and infant brain development in individuals with and without a familial risk of autism spectrum disorder

Pote, Inês

Awarding institution:
King's College London

Fetal and infant brain development in individuals with and without a familial risk of autism spectrum disorder

Inês Pote

A thesis submitted for the degree of
Doctor of Philosophy

Institute of Psychiatry, Psychology & Neuroscience
King's College London

2017

Acknowledgements

I would first like to thank my supervisors, Dr. Grainne McAlonan, Prof. Mary Rutherford, and Prof. Declan Murphy for their constant support and guidance throughout this journey. I am indebted to them for their continuous feedback but also for their overwhelming patience.

Thank you also to the fantastic BIBS team, including both current and past members (Dr. Grainne McAlonan, Rali Dimitrova, Judit Ciarrusta, Emily Perry, Johanna Kangas, Ayesha Javed, Dr. Hannah Dickson, Maria Gudbrandsen, Vladi Stoencheva, Emma Quinlan, Li Faye Lim, Dee Howley, and Vera D'Almeida) – working alongside you has been an absolute pleasure. I am also extremely grateful to all the researchers at the Centre for the Developing Brain and at Imperial College London, who somehow always found the time to help. I am especially thankful to Alice Davidson, Dr. Vanessa Kyriakopoulou, Dr. Christina Malamateniou, Dr. Lucilio Cordero Grande, Dr. Antonis Makropoulos, Dr. Paul Aljabar, and Dr. Maria Kuklisova-Murgasova. Many thanks also to everyone who was involved in scanning, particularly the research nurses, radiologists, and radiographers – you all made Monday mornings something I actually looked forward to!

I would also like to thank Dr. Eileen Daly and Dr. Jamie Horder for their advice and expertise, as well as Dr. Vaheshta Sethna for her constant source of encouragement. To my colleagues at the IoPPN – thank you for everything – this whole experience would have been very different without you. I am particularly grateful to Laura Ajram and Alice Durieux for their incessant moral support, often disguised in the form of sushi, cake, wine, and beer.

Many thanks also to my flatmates for providing a stable and comforting environment at home, as well as my friends, especially Tess, Bea, Ellie, Bélène, Amelie, Louis, Tomás, Pedro, Teresa, Carmo, Sara, and Pie. Although scattered around the world, your constant pick-me-ups have been what has encouraged me to carry on, and I cannot thank you enough for that. Special thanks also to Tobi, with R&R schedules always conveniently booked for the times in which I needed him most.

Finally, and most importantly, I would like to thank my family (Mami, Papi, Mari, and Ant) for reassuring me. You kept me sane, and our 5-way conference calls kept me happy. Thank you.

Statement of contribution

The work presented in this thesis would not have been possible without the help and contribution of several people. They have all been duly recognised in the relevant sections of the methodology, but their names appear in full only here:

AB: Anna Blasi
AD: Alice Davidson
AF: Annabel Forsdyke
AM: Antonis Makropoulos
AN: Alexandra Nolan
AS: Asel Shamenkova
CC: Celeste Cheung
CDR: Chelo Del Rosario
CK: Christopher Kelly
DC: David Cox
DH: Dee Howley
EH: Emer Hughes
GP: Greg Pasco
JA: Joanna Allsop
JBC: José Bueno Conde
JC: Judit Ciarrusta
JK: Johanna Kangas
JM: James Morphett
JS: Jasmine Siew
JW: Julia Wurie
KP: Kelly Pegoretti
LB: Laura Bozicevic
LC: Lucilio Cordero Grande
MB: Madeleine Barnett
MF: Matt Fox
MG: Maria Gudbrandsen
MK: Michelle Krishnan
MR: Mary Rutherford
MS: Maryann Sharma
NT: Nora Tusor
OC: Olivia Carney
PW: Paul Wellman
RD: Rali Dimitrova
SA: Sophie Arulkumaran
SW: Siying Wang
TC: Tony Charman
VS: Vaheshta Sethna
VLS: Vladi Stoencheva

Although not acknowledged elsewhere, the BIBS (Brain Imaging in Babies) team deserves special mention. The team was involved with overall study design, participant recruitment, and data collection. Current and past members include: Dr. Grainne McAlonan, Rali Dimitrova, Judit Ciarrusta, Emily Perry, Johanna Kangas, Ayesha Javed, Dr. Hannah Dickson, Maria Gudbrandsen, Vladi Stoencheva, Emma Quinlan, Li Faye Lim, Dee Howley, and Vera D'Almeida.

List of related publications and presentations

Publications

Pote I, Sethna V, Wang S, Blasi A, Charman T, Daly E, Johnson MH, Kuklisova-Murgasova M, Lloyd-Fox S, Mercure E, Williams S, Murphy DG, McAlonan G. (2016). Mother-infant interactions and regional brain volumes in infancy: an MRI study. *Brain Structure and Function*, 1–10.

Pote I, Wang S, Sethna V, Blasi A, Daly E, Kuklisova-Murgasova M, Lloyd-Fox S, Mercure E, Busuulwa P, Charman T, Williams SCR, Johnson MH, Murphy DGM, McAlonan GM, and the BASIS Team. Brain anatomy and outcomes in very young infants at high familial risk of autism (*under review with Psychological Medicine)*.

Oral presentations

Pote I, Dimitrova R, Ciarrusta J, Perry E, Quinlan E, Kangas J, Allsop JM, Fox M, Hughes E, Murphy DGM, Rutherford MA, McAlonan GM. The developmental trajectory of glutamate in the human brain: from neonatal life to early infancy. In: Society for the Study of Behavioural Phenotypes (SSBP) International Research Symposium, 9th to 11th of September 2016 (Sienna, Italy).

Pote I, Sethna V, Wang S, Gudbrandsen M, Daly E, Perry E, Adams KPH, Kuklisova-Murgasova M, Busuulwa P, Watson C, Kangas J, Stoencheva V, Williams SCR, Murphy DGM, McAlonan GM, Craig M. The influence of maternal antenatal depression on infant brain volume. In: World Congress of the World Association for Infant Mental Health (WAIMH), 29th of May to 2nd of June 2016 (Prague, Czech Republic).

Sethna V, **Pote I**, Wang S, Gudbrandsen M, Blasi A, McCusker C, Daly E, Perry E, Adams KPH, Kuklisova-Murgasova M, Busuulwa P, Lloyd-Fox S, Murray L, Johnson M, Williams SCR, Murphy DGM, Craig M, McAlonan GM. Mother-infant interactions and regional brain volumes in infancy: an MRI study. In: World Congress of the World Association for Infant Mental Health (WAIMH), 29th May to 2nd of June 2016 (Prague, Czech Republic).

Pote I, Wang S, Sethna V, Blasi A, Daly E, Kuklisova-Murgasova M, Lloyd-Fox S, Mercure E, Charman T, Williams SCR, Johnson MH, Murphy DGM, McAlonan GM. Cerebellum enlargement in 4-6 month-old infants at high familial risk of autism spectrum disorder. In: European Congress of Radiology (ECR), 2nd to 6th of March 2016 (Vienna, Austria).

Sethna V, **Pote I**, Wang S, Blasi A, Charman T, Daly E, Johnson MH, Kuklisova-Murgasova M, Lloyd-Fox S, Mercure E, Williams S, Murphy DG, McAlonan GM. Is there a relationship between mother-infant interactions and regional brain volumes? An MRI study of 4-month-old infants. In: Annual Meeting of the UK and Ireland Marcé Society (UKIMS), 17th of September 2015 (London, UK).

Poster presentations

Pote I, Wang S, Sethna V, Blasi A, Daly E, Kuklisova-Murgasova M, Lloyd-Fox S, Mercure E, Charman T, Williams SCR, Johnson MH, Murphy DGM, McAlonan GM. Cerebellum enlargement in 4-6 month-old infants at high familial risk of autism spectrum disorders. In: International Meeting for Autism Research (IMFAR), 13th to 16th of May 2015 (Salt Lake City, USA); Poster 124.114.

Abstract

There is currently very little known about early brain development; even less about how normal development may be disrupted in individuals genetically predisposed to neurodevelopmental conditions, including autism spectrum disorder (ASD). Hence, by using magnetic resonance imaging (MRI) to examine the structure and chemistry of the fetal, neonatal, and infant human brain, my intention was to provide further insight into early neurodevelopment. The additional focus on individuals with a familial risk of ASD, also aimed to detect any potential deviations from typical brain development that may be associated with an ASD risk status.

The first experimental study of this thesis used MRI at 1.5T to reveal that the early environment – specifically, mother-infant interactions – is associated with variations in brain biology, within a sample of assumed-to-be typically developing individuals. Therefore, the next study, which compared brain volume in infants with and without a familial risk of ASD also incorporated measures of mother-infant interactions. In this second study, subcortical and cerebellar enlargements were identified in 4-6 month-old infants at risk of ASD, and larger volumes were associated with more autistic symptoms at 36 months. Within the high-risk group, a higher measure of maternal sensitivity was correlated with lower subcortical brain volumes.

Next, to examine even earlier development and to estimate when differences between risk groups might first appear, fetuses and neonates with and without a familial risk of ASD were scanned using advanced MRI protocols at 3T. At both these timepoints, the cortex and cerebellum were identified as the fastest growing brain regions. In addition, fetuses at risk of ASD had smaller cortical volumes when compared to low-risk controls. Postnatally, within the first month of life, neonates at risk of ASD also had smaller intracranial and total brain volumes, as well as a smaller lentiform nucleus. Placed together with the infant findings, these studies suggest that an ASD genetic risk constrains brain growth in the perinatal period, but is

associated with volumetric expansion of both subcortical and cerebellar regions in infancy. The subcortical region also appeared to be particularly affected by the abnormal growth trajectory of high-risk participants, as differences in this region were observed amongst high-risk individuals at *both* neonatal and infant timepoints.

The subcortex was therefore selected as a region-of-interest in the final study, which mapped metabolic maturation from fetal to early postnatal life using magnetic resonance spectroscopy. In both low and high-risk groups, choline and myo-inositol decreased significantly with age, whilst N-acetylaspartate and creatine increased. In contrast, glutamate (measured as glutamate and glutamine; Glx) decreased from fetal to neonatal life, with a marked 'dip' around the time of birth before increasing in early infancy. The sample size at the 4-6 month timepoint also permitted an explicit comparison of low and high-risk infants, and because previous studies of older cohorts have linked glutamate abnormalities to ASD, Glx levels were compared between groups. The results showed, for the first time, that high-risk infants have significantly elevated levels of Glx at 4-6 months of age, when compared to low-risk controls.

In conclusion, both the volume and biochemistry of the human brain undergoes rapid change in the late prenatal and early postnatal periods. Moreover, individuals with a familial risk of ASD already show differences in brain maturation from fetal life, including neurochemical pathways modulating the balance of neuronal excitation and inhibition. This is well before the onset of autistic symptoms, and therefore, has important implications for ASD in terms of risk (and resilience) pathways.

Table of contents

List of figures

Chapter 1

Chapter 2

Chapter 4

Chapter 5

Chapter 6

Chapter 7

Chapter 8

List of tables

Chapter 2

Chapter 4

Chapter 5

Chapter 6

Chapter 7

List of abbreviations

^{1}HMRS	Proton (^{1}H) Magnetic Resonance Spectroscopy
ADHD	Attention Deficit Hyperactivity Disorder
ADI-R	Autism Diagnostic Interview – Revised
ADOS-2	Autism Diagnostic Observation Schedule – Second Edition
ANCOVA	Analysis of co-variance
Ankrd11	Ankyrin repeat domain containing protein 11
ASD	Autism Spectrum Disorder
BAP	Broader Autism Phenotype
BASIS	British Autism Study of Infant Siblings
BBFE	Balanced fast field echo sequence
BMI	Body Mass Index
B_0	External Magnetic Field
Cho	Choline
CNV	Copy Number Variant
Cr	Creatine
CSF	Cerebrospinal Fluid
CSS	Calibrated Severity Score
CW	Corrected age in weeks
DAWBA	Development and Well-Being Assessment
dHCP	Developing Human Connectome Project
Draw-EM	Developing Brain Region Annotation with Expectation-Maximisation
DSM-5	Diagnostic and Statistical Manual of Mental Disorders – Fifth Edition
E/I	Excitatory/Inhibitory
EDD	Expected Date of Delivery
ELC	Early Learning Composite
EM	Expectation-Maximisation Algorithm
FID	Free Induction Decay

FOV	Field of View
GABA	*y*-aminobutyric acid
Glx	Glutamate and glutamine
GMM	Gaussian Mixture Model
GRS	Global Rating Scales
GW	Gestational age in weeks
HPA	Hypothalamic-pituitary-adrenal
ICC	Intraclass Correlation
ICD	International Classification of Diseases
Ins	Myo-inositol
IRTK	Image Registration Toolkit
MRI	Magnetic Resonance Imaging
MSEL	Mullen Scales of Early Learning
NAA	N-acetylaspartate
Ppm	Parts per million
PRESS	Point Resolved Spectroscopy
RD	Reference Date
REC	Research Ethics Committee
RF	Radiofrequency
SAR	Specific Absorption Rate
SCQ	Social Communication Questionnaire
SD	Standard Deviation
SENSE	SENSitivity Encoding
SNAPIR	Snapshot Inversion-Recovery Sequence
SNR	Signal to Noise Ratio
SPM	Statistical Parametric Mapping software
SPSS	Statistical Package for the Social Sciences
SS	Standard Score
SVR	Snapshot MRI with Volume Reconstruction

T1	Longitudinal (or spin-lattice) relaxation time
T1 IR-TSE	T1-weighted inversion recovery turbo spin echo sequence
T2	Transverse (or spin-spin) relaxation time
T2ssFSE	T2-weighted dynamic single shot fast spin echo sequence
T2ssTSE	T2-weighted single shot turbo spin echo sequence
T2 TSE	T2-weighted multishot turbo spin echo sequence
T2w	T2-weighted sequence
TE	Echo Time
TR	Repetition Time
US	Ultrasound

Chapter 1: Introduction

1.1. Motivation and rationale

New imaging modalities have hugely advanced our understanding of the brain. However, our knowledge of how the early prenatal and postnatal periods shape brain development is limited. By examining the structure and chemistry of the fetal, neonatal, and infant human brain, the studies included in this thesis have therefore attempted to improve our understanding of very early brain development. In addition, these studies have considered how factors that disrupt typical developmental trajectories may lead to aberrant neurodevelopmental processes, and subsequently impact upon behavioural outcomes. Specifically, this exploratory section of the research has been accomplished by studying very young individuals with and without a genetic (or familial) risk of autism spectrum disorder (ASD).

As the name implies, ASD is a complex neurodevelopmental disorder that encompasses a broad spectrum of conditions. Although traditionally conceptualised as a categorical condition, this view has recently been challenged, and the disorder is now considered to exist as a continuum. Whilst a large proportion of affected individuals are highly dependent upon others, many on the spectrum lead much more autonomous lives. Moreover, it has become increasingly recognised that the presence of ASD-like traits (for example, deficits in social functioning, communication difficulties, and rigid personalities) – often referred to as the broader autism phenotype (BAP) (Bolton et al., 1998; Piven et al., 1997) – may also be evident in first-degree relatives of individuals with the disorder, and especially in siblings (Georgiades et al., 2013; Pisula and Ziegart-Sadowska, 2015). In addition, as many as 70% of individuals with ASD suffer from co-occurring difficulties, including intellectual disability, attention deficits, motor abnormalities, sleep disruptions, and mood disorders such as anxiety and/or depression. This has led some to propose that many of these co-occurring conditions may share common risk pathways (Rommelse et al., 2010).

Individuals with a familial risk of ASD, by virtue of having an older sibling with a diagnosis of the condition, are thus an important group to study, even in the absence of outcome data. Not only is this because infant siblings may (or may not) go on to receive an ASD diagnosis, but because they can provide important insights into what biological pathways are targeted by risk factors. Hence, the studies included in this thesis have sought to detect subtle deviations from typical brain development that may be associated with an ASD risk status, while recognising that the majority of participants studied will not go on to receive a diagnosis of the core disorder (but may display other related difficulties). In addition, potential environmental influences that may modulate the effect of risk of ASD on brain biology were also explored.

The introductory chapter of this thesis begins by describing what is currently known about normal brain development, as well as how it may be altered by some of the risk factors associated with ASD. The next section describes some of the key behavioural milestones that a child is expected to reach from 0-2 years, along with the most common departures from these targets in individuals who go on to receive an ASD diagnosis. Subsequently, since the studies included in this thesis have used magnetic resonance imaging (MRI) to examine the neuroanatomy and neurochemistry of very young individuals, the chapter then goes on to provide a fundamental background on the principles of MRI, and on the practicalities of imaging at fetal, neonatal, and infant timepoints. An overview of ASD is then provided, followed by an account of the main findings from brain structural and spectroscopic studies of the disorder. The chapter concludes with the main aims and hypotheses of the current thesis.

A note on choice of language:

The term *normal* and *typical* will be used interchangeably in this thesis. However, both terms are really quite ambiguous, particularly when used in the context of early brain development. The truth is that there is no real boundary or cut-off score for what is defined as typical or normal. For instance, there is now evidence indicating that ASD-like traits, aside from being present in first-degree relatives of individuals with ASD, are also distributed in a continuum

within the general population (Constantino and Todd, 2003; Hoekstra et al., 2007). This is true for many other behavioural and psychological traits. Indeed, as our understanding of individual differences progresses, we are beginning to appreciate that behaviour should in itself also be viewed as a spectrum, with individuals who receive a diagnosis of a disorder considered to lie on the more atypical end of the spectrum (Plomin et al., 2016).

1.2. Normal brain development

Human brain development involves a series of complex processes that begin shortly after conception and continue throughout adolescence; arguably, throughout one's lifetime. Both genetic and environmental factors mediate brain development to such an extent, that a disruption in either system could dramatically compromise neurodevelopmental outcome (for review see Roth and Sweatt, 2011; Sale et al., 2014). This introductory section will focus on the main events leading up to the formation of the mature human brain, with development described in four stages: the pre-embryonic period (encompassing the first 2 gestational weeks), the embryonic period (from the 3rd to the 8th gestational week), the fetal period (extending through to the end of gestation), and the postnatal period (referring to the developmental processes taking place after birth).

1.2.1. Pre-embryonic development

Conception refers to the process by which the male spermatozoon combines with the female oocyte inside the fallopian tube, to fertilise an oocyte and form the zygote – a single-cell embryo containing 46 chromosomes, half of which come from the spermatozoon and half from the oocyte. As soon as it is formed, the zygote undergoes cleavage, dividing repeatedly whilst moving down the fallopian tube to form the morula. With the presence of progesterone, the fallopian tube relaxes, allowing the morula to move inside the uterus. Here, the morula develops into the blastocyst – a fluid-filled cavity with a collection of cells located at one end. Blastocyst implantation follows shortly after, when the outer cells of the blastocyst bind to the epithelial cells of the endometrium (the inner layer of the uterus), enabling it to become embedded within the uterine wall (Figure 1.1). Then, the embryoblast cells of the blastocyst go on to form the embryo, whilst the outer trophoblast cells form the placenta.

Genetic mutations and epigenetic modifications (that is, heritable changes in gene expression that occur independent of alterations to the DNA sequence) can play a critical role in the pre-embryonic period (Zhu, 2009), and potentially affect psychopathology in later life. For instance, epigenetic modifications of the paternal spermatozoon, including changes in DNA

methylation, have been shown to contribute to an elevated risk of ASD in the offspring (Feinberg et al., 2015), and may be associated with advanced paternal age (Flanagan et al., 2006; Reichenberg et al., 2006). Indeed, infants born to parents but especially fathers of an advanced age, are at a higher risk of neurodevelopmental conditions such as ASD (Croen et al., 2007; Hultman et al., 2011; Reichenberg et al., 2006). This elevated risk could also be due to the increased number of spontaneous (*de novo*) mutations associated with older spermatozoon (Buwe et al., 2005; Crow, 2000; Kong et al., 2012). Hence, it seems that both genetic and epigenetic modifications associated with aging, may contribute to an increased risk of having offspring with ASD.

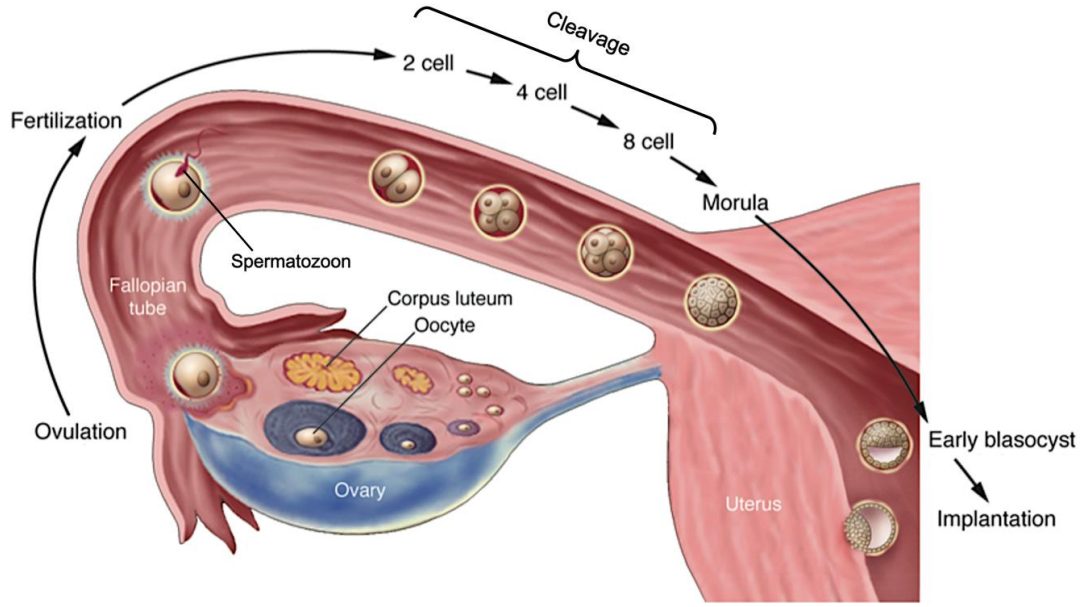

Figure 1.1: The pre-embryonic period.
The pre-embryonic period consists of a series of chronological processes, beginning with conception (or fertilisation, as referred to above) and terminating with the implantation of the blastocyst. This image was adapted from Dey (2010).

1.2.2. Embryonic development

In humans, the embryonic period extends from the end of the 2nd gestational week (at approximately 12 days post-conception), through to the 8th gestational week. The main processes involved at this time include gastrulation and neurulation, which together 'set the scene' for brain development, by establishing the basic structure and organisation of the

nervous system. This period is so fundamental to development that a failure in any of its processes could result in serious neural defects, or worse, compromise the viability of the embryo (Copp and Greene, 2013).

1.2.2.1. Gastrulation: the formation of the neural plate

Human brain development starts in the 3rd gestational week with the differentiation of the neural progenitor cells; a process commonly referred to as gastrulation (Figure 1.2). This process begins with the epiblast and hypoblast, which together comprise the oval-shaped two-layered structure that is the embryo. At this point, the embryo is positioned between the two major placental sacs: the amniotic sac, located above the embryo (and which will eventually surround it), and the yolk sac, positioned below it (Stiles, 2008). The onset of gastrulation is defined by the appearance of a slit-like opening in the upper layer of the embryo, referred to as the primitive streak. The primitive streak provides the epiblast cells with access to lower regions of the embryo, and as the cells migrate towards the streak, they pass through the primitive node and receive molecular signals that induce gene expression (Stiles, 2008). As they pass through the primitive streak, the epiblast cells are displaced to produce the ectoderm, composed of both epidermal ectodermal and neuroectodermal stem cells. Likewise, hypoblast cells produce the endoderm, which will eventually give rise to structures of the gut and respiratory system. Between these two newly formed layers, the mesoderm develops, eventually producing structures such as the muscle, bone, and vasculature. Moreover, whilst the epidermal ectodermal cells of the ectoderm go on to produce structures such as the skin and sweat glands, the neuroectodermal cells are what give rise to the brain and central nervous system. Neuroectodermal cells are also referred to as neural progenitor cells and the region of the embryo containing them is the neural plate; hence, gastrulation can be defined as the formation of the neural plate.

The differentiation of neural progenitor cells requires complex genetic signalling. In addition to the first set of signals sent out, the primitive node generates a second set, which informs the neural progenitor cells of their specific regional identity. Neural progenitors formed from the

first epidermal cells, for instance, will produce the basic building blocks of the forebrain. Conversely, neural progenitors formed from some of the later migrating cells will help to produce some of the more caudal structures such as the spinal cord. Thus by the end of gastrulation, not only do we have a neural plate with the necessary progenitor cells for future development, but we also have a clearly defined spatial organisation of the embryonic nervous system, with front-back (anterior-posterior), right-left, and top-bottom (dorsal-ventral) axes (Stiles, 2008).

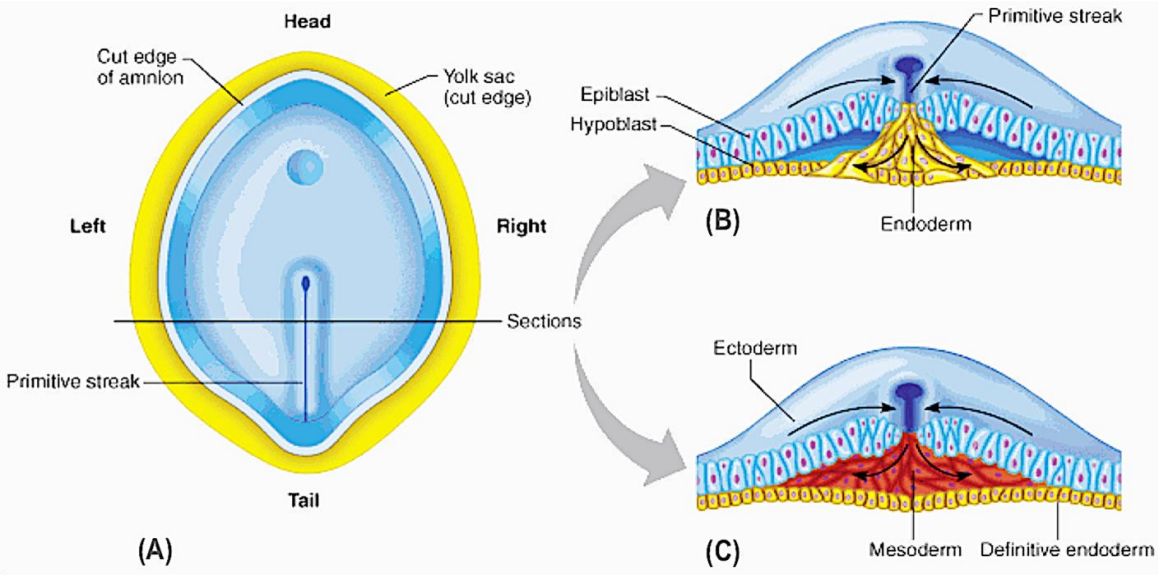

Figure 1.2: The process of gastrulation.

(A) The superior view of the two-layered embryo, formed by **(B)** the epiblast and hypoblast, is shown. During gastrulation, epiblast cells move towards lower regions of the embryo to form the ectoderm, whilst the hypoblast cells go on to produce the endoderm. In between the two layers, **(C)** the mesoderm develops. This image was adapted from Marieb and Hoehn (2007).

1.2.2.2. Neurulation: the formation of the neural tube

Neurulation comprises of a set of processes that give rise to the first identifiable neural structure, the neural tube, from which the central nervous system develops. Neurulation begins as soon as gastrulation is complete, with the appearance of two ridges alongside each end of the neural plate (Copp et al., 2003). Over the course of several days, the ridges rise, converge inward, and fuse to form a hollow tube (Figure 1.3). The fusion of the tube begins

from the centre and ends with the closing of the anterior neuropore (at the most rostral end of the tube), followed by the posterior neuropore (at the most caudal end). When the process is complete, the neural progenitors form a single layer of cells that line the centre of the neural tube. The hollow cavity within it develops to become the brain's ventricular system (Copp et al., 2003; O'Rahilly and Müller, 2008).

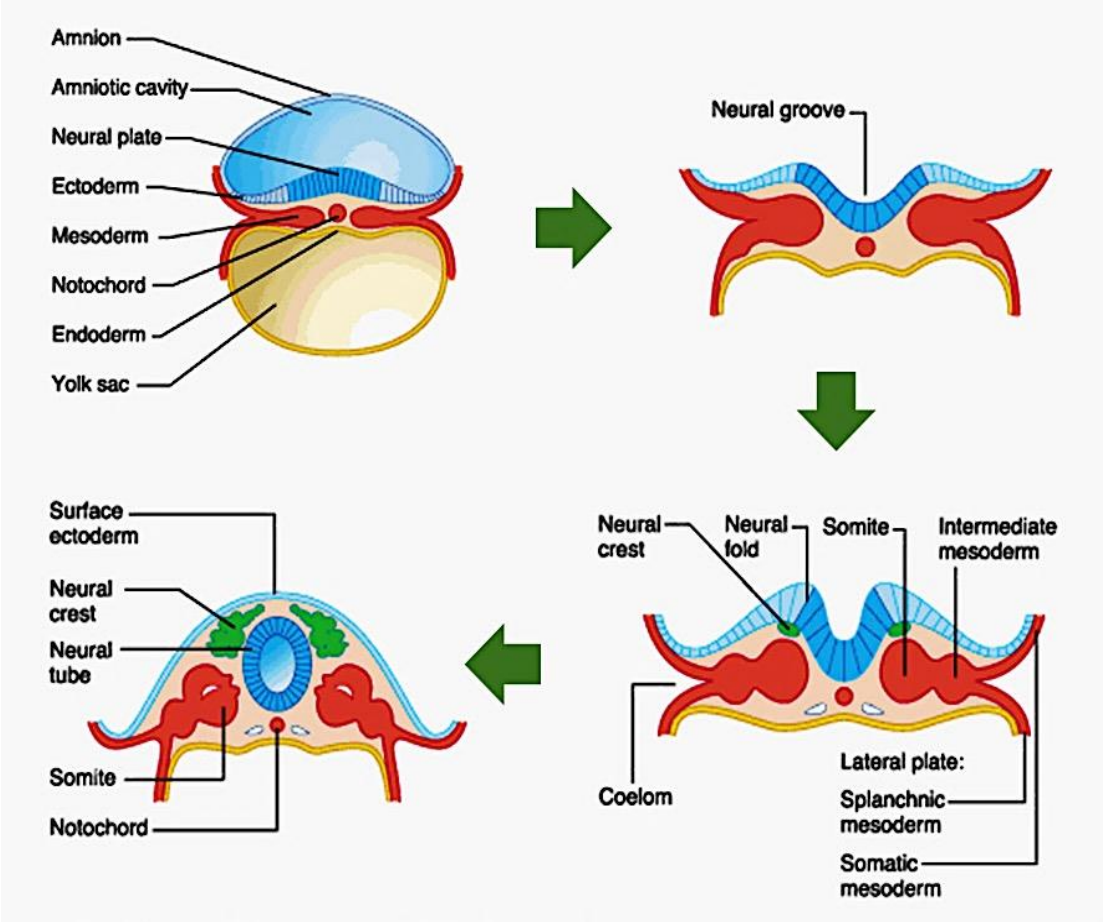

Figure 1.3: The process of neurulation.
Neurulation begins with the appearance of two ridges either side of the neural plate. Over the course of several days, these ridges rise and converge inwards to produce the neural tube, which will later develop into the central nervous system. This image was adapted from Marieb and Hoehn (2007).

Neural tube defects affect 1 in every 1000 pregnancies and can result in severe congenital malformations (Copp and Greene, 2013). Prenatal exposure to anti-epileptic drugs such as sodium valproate, which cross the placenta and enter the circulation of the developing

embryo, can cause a 20-fold increase in neural tube defects (Alsdorf and Wyszynski, 2005). Moreover, exposure to sodium valproate during pregnancy can also contribute to an increased risk of neurologic abnormalities and neurodevelopmental disorders, including ASD (Christensen et al., 2013; Williams et al., 2001). The mechanism(s) underlying the disruptive effects of sodium valproate on neurodevelopment are not fully understood. Potential explanations include the induction of oxidative stress and the inhibition of histone deacetylase, which can result in epigenetic alterations (for review see Ornoy, 2009). Fortunately, supplementation of folic acid during pregnancy appears to prevent some neural tube defects (Smithells et al., 1980, 2011), and has also been associated with a reduced risk of ASD (Schmidt et al., 2012; Suren et al., 2013). Mechanisms for how folate may impact upon ASD risk are not yet known. However, plausible suggestions implicate suppression of oxidative stress (Solon et al., 2008), as well as epigenetic alterations involving increases in methylation (Pufulete et al., 2005).

1.2.2.3. The end of the embryonic period

After neurulation, during the final period of embryonic development, the shape of the neural tube changes dramatically. At first, the anterior end of the tube undergoes expansion and folding to form the three primary brain vesicles: the prosencephalon, mesencephalon, and rhombocephalon – also known as the embryonic precursors of the forebrain, midbrain, and hindbrain, respectively (O'Rahilly and Müller, 2008). From here onwards the mesencephalon does not divide further, but the remaining two primary vesicles do. The prosencephalon divides into the telencephalon and diencephalon, whilst the rhombocephalon separates into the metencephalon and myelencephalon. Hence, by the end of the embryonic period, five secondary brain vesicles will have emerged and aligned themselves along the rostral-caudal axis of the embryo, establishing the primary organisation of the brain (O'Rahilly and Müller, 2008; Stiles and Jernigan, 2010). Eventually, the telencephalon will become what we know of as the cerebrum, encompassing the cerebral hemispheres and cortex. The embryonic region of the diencephalon will form the hypothalamus and thalamus, whilst the mesencephalon will develop into the midbrain. In turn, the metencephalon will go on to form the pons and

cerebellum, whereas the myelencephalon will become the medulla oblongata, leading on to the spinal cord (Figure 1.4).

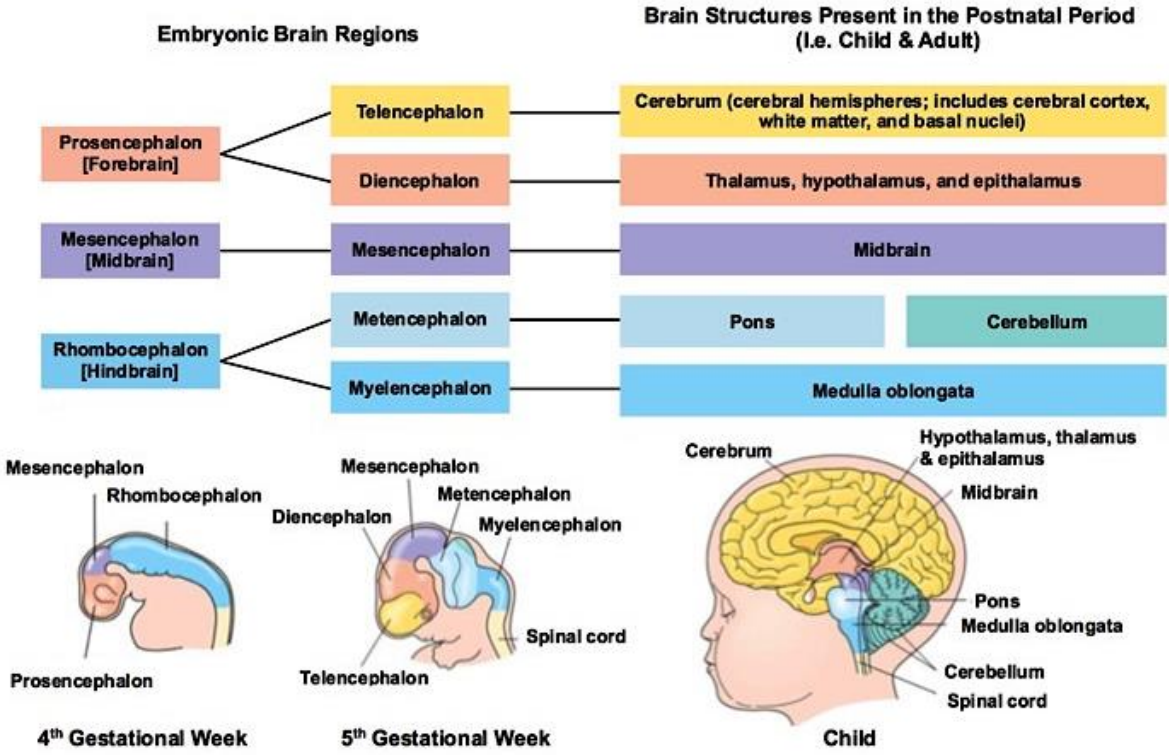

Figure 1.4: Embryonic brain regions and their equivalent postnatal brain structures. As shown in the schematic above, the embryonic brain region of the prosencephalon splits into the telencephalon and diencephalon, which will eventually become the cerebrum, hypothalamus, and thalamus. The mesencephalon develops, but does not divide, and goes on to form the midbrain. Finally, the metencephalon matures into the pons and cerebellum, whereas the myelencephalon gives rise to the medulla oblongata, leading on to the spinal cord. This image was adapted from Marieb and Hoehn (2007).

1.2.3. Prenatal development

Prenatal (or fetal) development is initiated after the end of the embryonic period. It extends up until the end of gestation, culminating at birth, and ideally around forty weeks gestation. Although longer gestational periods are more favourable to neural development (Davis et al., 2011), it is extremely common for births to occur within a range of this age.

The main processes of fetal development involve the proliferation, migration, and differentiation of neurons (Stiles and Jernigan, 2010). Together, they contribute to dramatic changes in brain morphology, from the emergence of cortical and subcortical structures, through to the establishment of major neural pathways.

1.2.3.1. Neuron proliferation

Neuron proliferation refers to the production of neurons, of which the human brain has billions. The number of neural progenitor cells available at the end of gastrulation, however, is far too small to accommodate the expected neuron population size. Therefore, one of the first steps in proliferation involves the production of more neural progenitor cells. Fortunately, progenitors are mitotic cells that undergo symmetrical cell division, resulting in the generation of two identical neural progenitors from just one (Paridaen and Huttner, 2014). With time, this mode of division begins to shift into an asymmetrical process, whereby each neural progenitor cell produces both one neuron and one neural progenitor (Paridaen and Huttner, 2014; Wodarz and Huttner, 2003). In humans, at the peak of proliferation, neurons are produced at a rate of 250,000 per minute, such that the proliferative process is largely complete by mid-gestation (Rakic, 1995).

Neurons are almost exclusively produced in the proliferative region of the ventricular zone, located at the centre of the neural tube, in what will later become the region of the lateral ventricles. In the brains of individuals with neurodevelopmental disorders, there is often a concentration of abnormalities within this region (Cardoso et al., 2009; Olsén et al., 1997). For example, infants exposed to the rubella infection during pregnancy, which in itself is a risk factor for ASD (Carvill and Marston, 2002; Chess, 1977), are more likely to develop abnormalities of the proliferative region, including periventricular leukomalacia, periventricular cysts, and dilated perivascular spaces (Rorke and Spiro, 1967; Sugita et al., 1991). In addition, some of these abnormalities have been identified in individuals with idiopathic ASD, and are associated with some of the core ASD symptoms (Blackmon et al., 2016), suggesting that neuron proliferation may carry with it inherent vulnerabilities.

1.2.3.2. Neuron migration

Unlike neural progenitors, neurons are post-mitotic cells. Once formed, they are incapable of further dividing and instead, they migrate away from the proliferative zones towards the developing cortex (Figure 1.5) (for review see Nadarajah and Parnavelas, 2002). The first neurons to leave the proliferative zone only need to travel for very short distances and thus migrate via somal translocation (Nadarajah et al., 2001). In somal translocation (Figure 1.5A), neurons extend their basal processes enabling the nucleus to move through them, such that by the end of translocation the nucleus has moved out of the ventricular zone and into the cortex.

Later on in development, as the brain becomes larger and the cortex begins to thicken, neurons are required to travel away from the ventricular zone for longer distances. Hence, radial migration (Figure 1.5B) becomes the primary mode of travel (Nadarajah and Parnavelas, 2002). Radial glial guides are a specific type of glial cell, which provide support to the neurons and act as the main protagonists in this migratory process (Rakic, 1971, 1972). The glial guides are comparable to neurons during somal translocation, in the sense that they too extend their basal processes. However, unlike in somal translocation, the nucleus of the glia remains within the ventricular zone. The basal processes are what guide the migrating neurons, allowing them to move up along the glia and out towards the cortex. Importantly, one radial glial is enough to support many migratory neurons (Rakic, 1972).

In the late 1990's, the proliferative region of the ganglionic eminences, mainly responsible for producing interneurons, was identified (Anderson et al., 1997). Alongside this discovery, it was found that interneurons migrating away from the ganglionic eminences travel via a different mode of migration, known as tangential migration (Anderson et al., 2001; Corbin et al., 2001; Marín and Rubenstein, 2001). In tangential migration (Figure 1.5C), neurons are guided by signalling pathways along their route (Huang, 2009; Valiente and Marín, 2010). This enables them to traverse for long distances, through multiple tangential tracts, to the cerebral cortex.

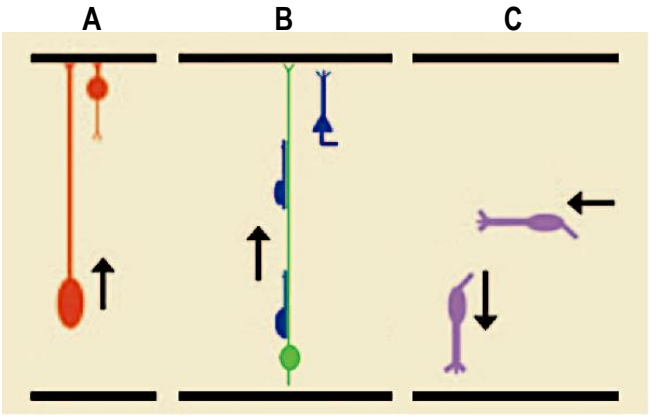

Figure 1.5: Modes of neuronal migration.
During early development, neurons migrate via **(A)** somal translocation. Later on, as neurons travel for longer distances, the primary mode of neuronal migration changes to **(B)** radial migration, with radial glia (in green) supporting neurons (in blue). Interneurons travel via **(C)** tangential migration. This image was adapted from Nadarajah et al., (2003).

Once neurons reach their final destination, they begin to organise themselves into the six-layered structure of the cortex (Figure 1.6). Formation of the cerebral cortex occurs in an orderly 'inside-out' manner (Angevine and Sidman, 1961), with each layer comprising a distinct type of neuron. An exception to this orderly formation occurs at the very start, with the earliest set of migrating neurons leaving the ventricular zone to form the preplate (Marin-Padilla, 1978). The next set of migrating neurons splits the preplate into the marginal zone and the subplate; within these two regions, the cortical plate emerges (Marin-Padilla, 1978). As soon as the cortical plate is present, the first neurons to arrive there will go on to form the deepest layer of the cortex (that is, layer VI), and all subsequent sets of migrating neurons will successively form more superficial layers (from layer V to I).

Certain embryonic layers including the marginal zone and the subplate, are transient structures, which disappear by the end of the fetal period (Bystron et al., 2008; Kostovic, 2002). These structures, however, are crucial for normal brain development. The appropriate development of the subplate, for instance, is essential for both cortical development and synaptogenesis (Ghosh and Shatz, 1993; Kostovic and Rakic, 1990). Specifically, it is the

concurrent process of cortical plate maturation and subplate dissolution, which signals the beginning of cortical connectivity.

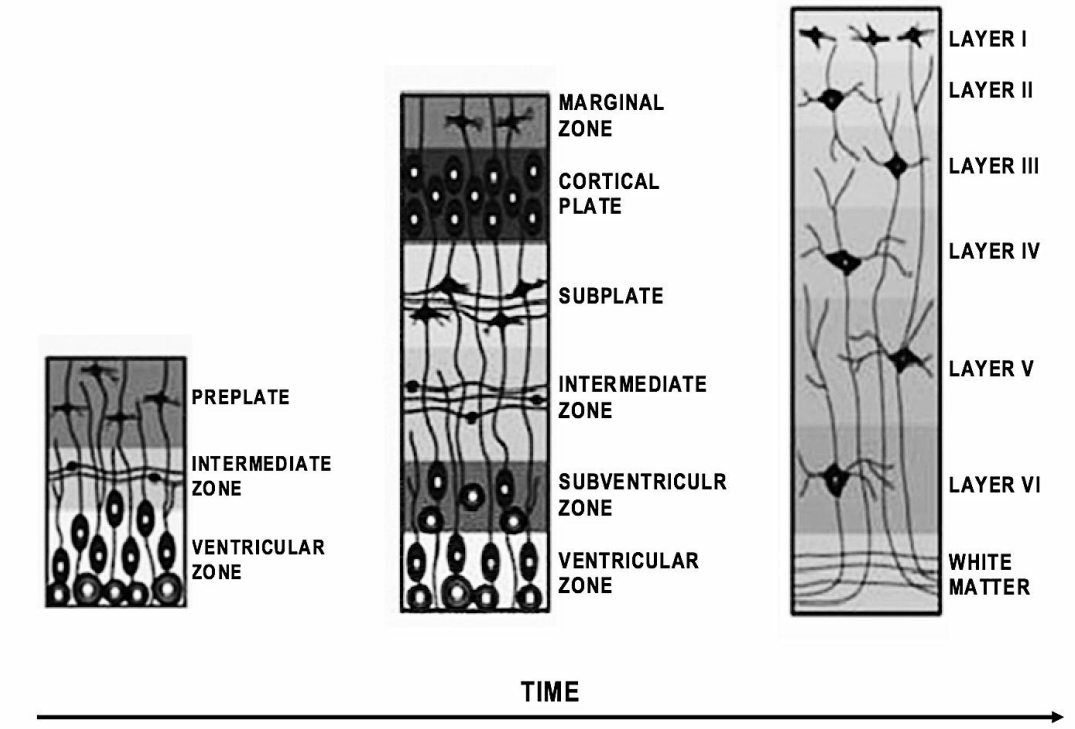

Figure 1.6: The development of the six-layered cortex.
As shown in the first panel on the left, the earliest set of migrating neurons leaving the ventricular zone form the preplate. With the next set of migrating neurons, the preplate splits into the marginal zone and subplate. In between these newly formed layers, the cortical plate develops, as illustrated in the middle panel above. The panel on the right displays the six-layered cortex, formed once the brain is fully mature. Image adapted from Stiles (2008).

Altogether, the orderly process of neuronal migration is crucial for the normal development of the cortex. Reelin, produced by Cajal-Retzius cells in the marginal zone, is essential to migration as it plays an important role in the signalling pathway that helps to position neurons in their appropriate cortical layers (Huang, 2009; Pearlman et al., 1998; Rice and Curran, 2001). As such, mutations in the Reelin gene have resulted in mutant mice with a highly disrupted cerebral cortex (Caviness and Sidman, 1973; Goffinet, 1984). In addition, post-mortem reports have shown lowered levels of Reelin and Reelin mRNA in the brain tissue of individuals with ASD (Fatemi et al., 2005). The failure of neurons to migrate towards the cortex and/or the over proliferation of neurons in the ventricular zone can result in patches of heterotopic grey matter within white matter regions, and these have been identified in a range

of neurodevelopmental disorders (for review see Gleeson and Walsh, 2000). For example, in a recent post-mortem study examining the brains of 13 ASD participants and 14 age-matched controls (aged 4-60 years), subcortical, periventricular, hippocampal, and cerebellar heterotopias were detected in the brains of 4 ASD cases, compared to none of the controls (Wegiel et al., 2010). Together with evidence of abnormalities in the cortical minicolumn (that is, the vertical column encompassing all cortical layers of the brain) (Casanova et al., 2002, 2006), findings suggest that neuron migration may be disrupted in ASD.

1.2.3.3. Neuron differentiation

Once they have arrived safely at their cortical destinations, neurons then need to become integrated into brain networks. This process, largely overseen by neuron differentiation, results in the derivation of the distinct neuron types necessary for the different layers of the cortex. Early in development, neural progenitor cells are multipotent and thus capable of producing any type of neuron. However, with time, progenitors begin to exhibit what is known as "fate restriction" – an epigenetic phenomena which limits the types of neurons that can be produced (Desai and McConnell, 2000; Frantz and McConnell, 1996; McConnell and Kaznowski, 1991), and which ultimately results in the end of differentiation.

Neuron differentiation also oversees the maturation of axonal and dendritic processes, which enable neurons to communicate and establish connections (or synapses) with one another. The establishment of connections, also known as synaptogenesis, is what facilitates information processing in the brain. Importantly, distinct neural pathways are responsible for transmitting different types of information. The thalamocortical and corticothalamic pathways, for instance, transmit sensorimotor information and are considered by some to be two of the most important pathways in the human brain. Guided by subplate neurons, these pathways begin to form towards the end of the second trimester and appear complete by the 26th week of gestation (Kostović and Jovanov-Milošević, 2006). In neuroimaging studies of ASD, however, functional and anatomical abnormalities have been identified in both these pathways

(Belmonte et al., 2004; Cheon et al., 2011; Nair et al., 2013, 2015), suggesting that atypical connectivity may be an underlying feature of this neurodevelopmental disorder.

1.2.3.4. Cortical development

The human brain begins as a smooth "lissencephalic" structure. However, as it expands, the cerebral cortex begins to fold so as to ensure that the brain is able to fit within the spatially limited cranium. Cortical folding, or gyrification, occurs in an orderly sequence and like most other processes described it follows a rostral-to-caudal developmental course (Rakic, 2006; Sur and Rubenstein, 2005). Gradually, this causes the brain to develop into a highly convoluted "gyrencephalic" structure, formed by an intricate pattern of gyri (ridges) and sulci (grooves).

Although there is some variability in the exact timing of when individual gyri and sulci emerge, data stemming from both post-mortem and *in vivo* MRI are in agreement. The first fold to form is the interhemispheric fissure, which refers to the deep groove dividing the two cerebral hemispheres. Development of the interhemispheric fissure begins in the rostral region as early as the 8th gestational week (Chi et al., 1977), but it is only fully formed by the 22nd week (Garel et al., 2001). Other primary sulci begin to form at the 14th week of gestation (GW 14), following a sequential pattern which includes the sylvian (GW 14-16), central (GW 20-24), and intraparietal (GW 25-26) sulci. By the 26th gestational week most primary sulci will have developed and from then on, the secondary sulci (GW 30-35) can begin to emerge (Chi et al., 1977; Garel et al., 2001). The tertiary sulci follow soon after, but their formation extends well into the postnatal period, illustrating the protracted nature of gyrification.

The development of the cerebral cortex is an extremely complex process, with faults in its appropriate completion implicated in the emergence of many neurodevelopmental disorders (Rubenstein, 2011). In a sulcal mapping study of ASD, for instance, affected children were observed to have anatomical abnormalities in the cortical surface (Levitt et al., 2003a). Researchers reported an anterior and superior shifting of several, sulci with the greatest

deviations from the norm localised to the frontal and temporal regions of the brain. Thus these findings indicate that there may be aberrant maturation of these specific brain regions in ASD – regions crucial for some of the functions commonly impaired in affected individuals.

1.2.4. Postnatal development

As already mentioned, brain development is far from complete after birth, continuing for an extended period of time during the postnatal period. Neurogenesis, for instance, has been shown to persist throughout adulthood (Eriksson et al., 1998) and should therefore be considered as a postnatal process too. Most essential in postnatal development, however, is the proliferation, migration, and differentiation of glial cells. Having said that, it is important to note that these processes actually begin prenatally. As glial progenitors themselves, radial glia are particularly vital for early cell formation as well as neuronal migration and positioning, existing in large numbers during the postnatal period. Moreover, although often overlooked, glial cells play a variety of critical roles in the nervous system. Aside from their function in neurodevelopment, they also provide support to the mature nervous system by regulating neuronal survival, modulating synaptic function, maintaining homeostasis, and intervening in the face of injury (for review see Jessen, 2004).

1.2.4.1. Glial proliferation, migration, and differentiation

Glial progenitor cells proliferate in the ventricular and subventricular zones as well as in the region of the ganglionic eminences, with different types of glia produced in different zones (Kessaris et al., 2006). Once formed, they migrate outward into the white matter and cortex as well as into the striatum and hippocampus, where they begin to differentiate. Glial progenitors can differentiate into a myriad of different classes of glia. The two main types of glia to differentiate at this time include astrocytes (which provide support to the neurons, modulate neuronal activity at the synapse, and respond to injury) and oligodendrocytes (which mainly produce myelin); together, they are commonly referred to as macroglia. Microglia (not to be confused with macroglia) are yet another type of glial cell, which amongst other things support immune function, modulate synaptic pruning, and help to regulate neuronal activity. Unlike

macroglia, microglia are formed from circulating monocytes, themselves derived from haematopoietic stem cells in the bone marrow. These monocytes travel past the blood-brain barrier into the brain, where they begin to differentiate into microglia during postnatal life (Chan et al., 2007). Unlike neural progenitors, glial progenitors are capable of continuing to proliferate whilst they migrate (Cayre et al., 2009). They therefore remain widespread throughout the brain for an indefinite period of time, so that they can differentiate into the required glial cell whenever needed (for instance, in response to injury).

1.2.4.2. Myelination

Oligodendrocyte progenitors differentiate by extending their processes and increasing their myelin expression, so that eventually they can begin to ensheath the axons of neighbouring neurons (Back et al., 2002; Nave and Werner, 2014). This procedure, commonly referred to as myelination, dramatically improves the efficiency of information transmission in the brain by working to accelerate axonal conduction (Jakovcevski and Zecevic, 2005). Myelin can also protect axons from damage and is thus of crucial importance to the developing brain. In addition, oligodendrocytes can synthesise a variety of trophic factors that contribute to both axonal integrity and neuronal survival. The interaction between oligodendrocytes and neurons has also been shown to influence the size and diameter of axons, and hence, support the functional maturation of developing pathways (McTigue and Tripathi, 2008).

In the typically developing brain, myelination is initiated around the second trimester of pregnancy (Brody et al., 1987; Kinney et al., 1994). Between the 21st and 25th gestational week, for instance, myelination is established in the medial longitudinal fasciculus and the inferior cerebellar peduncles (Jakovcevski and Zecevic, 2005). By the 28th week of gestation, myelin can be observed in the inferior colliculi, posterior brainstem, and ventrolateral nuclei of the thalamus. Later on, by 36 weeks gestation, myelination is evident in the corona radiata, posterior limb of the internal capsule, and corticospinal tracts (Counsell et al., 2002). Other brain regions such as the cerebral hemispheres are only myelinated after birth, which may explain why myelination is largely considered as a postnatal process.

In a recent neuroimaging study aimed at quantifying the regional progression of myelin during postnatal life (Deoni et al., 2011), the first evidence of myelination was identified in the region of the cerebellum and pons. This then progressed from the splenium of the corpus callosum and the optic radiations (by 3-4 months of postnatal life) into the occipital and parietal lobes (by 4-6 months), eventually advancing towards the frontal and temporal lobes (by 6-8 months). Evidence from post-mortem tissue suggests that the peak production of myelin terminates at approximately 8 months of age, with adult-like myelination evident by 2 years (Brody et al., 1987). It is important to note, however, that these are merely approximations and that different studies have reported subtle variations in these timings.

Furthermore, it is now known that an adequate diet, rich in protein and micronutrients, is crucial for appropriate myelination. A lack of vitamin B_{12}, for instance, may cause disruptions to myelination, resulting in white matter abnormalities and errors in neural connectivity (Black, 2008). In line with this, a recent post-mortem study showed that children with ASD (aged 4-9 years) had a 3-fold reduction in cortical B_{12} levels, when compared to age-matched controls, and researchers proposed that this deficit in B_{12} could contribute to impaired myelination in the disorder (Zhang et al., 2016).

1.2.5. Regressive events in the prenatal and postnatal periods

Brain development involves a dramatic overproduction of cells and synapses, followed by the partial removal of these via two major regressive events: cell death (or apoptosis) and synaptic pruning. These non-pathological processes are all necessary for normal brain maturation, but they each have a specified timing. For example, while neuronal apoptosis mainly occurs in the prenatal period, both glial cell death and synaptic pruning are typically considered as postnatal processes.

1.2.5.1. Apoptosis: programmed cell death

Apoptosis is responsible for the extensive loss of neurons that occurs towards the end of gestation (Rakic and Zecevic, 2000), resulting in maximal death rates of approximately 70% in

some cortical brain regions (Rabinowicz et al., 1996). The process of apoptosis involves a series of physiological events, which result in the breakdown of the nuclear chromatin of a cell, followed by its disintegration. The death of glial cell populations is also regulated by apoptosis, but as previously mentioned, this occurs a little later in the developmental time course, coinciding with the later process of glial proliferation.

The apoptotic cascade is regulated by a series of genes, which in turn can be influenced by various intrinsic and extrinsic factors. Some factors (such as oxidative stress) contribute to a more rapid cell death, whilst others (for example neurotrophic factors) protect the cell against apoptosis. According to the neurotrophic hypothesis, during development, neurons that have already established effective connections are able to obtain more neurotrophic factor and thus, are more likely to survive (Oppenheim, 1989). Prenatal apoptosis is therefore necessary for maintaining the most effective connections and hence, for strengthening the most functionally active neural pathways. However, apoptosis also plays a critical role in the elimination of cell populations that are no longer necessary (as is the case of neural progenitor cells), or that are no longer involved in the development of brain pathways. Finally, neuronal death can also be used to correct errors that may have occurred during earlier processes of cell proliferation and migration (Buss and Oppenheim, 2004). Apoptosis is therefore essential for the appropriate development of the brain, contributing to the strengthening of neural connections.

1.2.5.2. Synaptic pruning

Synaptogenesis (described in section 1.2.3.3 on page 39) results in an overproduction of connections, such that by the end of the first postnatal year, neuronal connectivity has reached a plateau nearly twice as high as that evidenced in the adult brain (Innocenti and Price, 2005). During childhood and adolescence, this exuberant connectivity slowly declines with the systematic elimination (or pruning) of up to 50% of synapses. The timing of synaptic pruning is largely dependent on that of synaptogenesis, and the two processes occur at different times in distinct brain regions (Huttenlocher, 1979; Huttenlocher and Dabholkar,

1997). For example, even though synaptogenesis in the primary visual cortex reaches its peak at around 6 months of age, neural connectivity in the visual cortex is the last to mature due to a more prolonged period of synaptic pruning in this region (Figure 1.7).

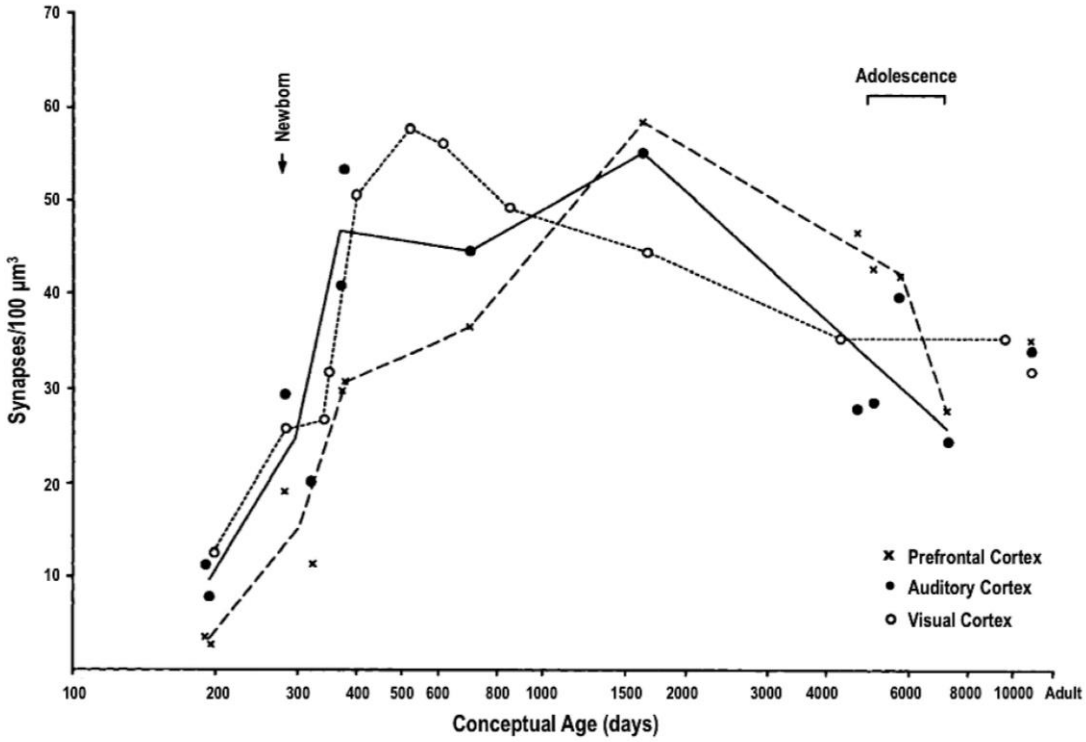

Figure 1.7: Synaptic pruning.
Synaptogenesis results in an overproduction of connections, with mean synaptic density peaking around the first year of life. However, during childhood and adolescence, this exuberant connectivity declines as synaptic pruning eliminates up to 50% of synapses. As shown in the graph above, adapted from Huttenlocher and Dabholkar (1997), different cortical regions undergo synaptogenesis and synaptic pruning at distinct times.

Alongside changes in the structure and organisation of the developing cortex, synaptic pruning results in the inherent fine-tuning and maturation of neuronal circuits (Tau and Peterson, 2010). Ultimately, these processes improve the efficiency of neurotransmission, critical for cognitive function. It is therefore not surprising that atypical patterns of connectivity, which can stem from delayed and/or inappropriate pruning, have recently been associated with a series of cognitive and neurodevelopmental disorders, like ASD (Geschwind and Levitt, 2007; Tau and Peterson, 2010). Evidence from genetic, animal, and neuroimaging work has

supported this and in turn, sparked interest in the notion that ASD may be a developmental disconnection syndrome, with high-order association areas of the brain partially disconnected during development (Geschwind and Levitt, 2007).

1.2.6. Plasticity and the role of experience in brain development

It should be clear by now that brain development follows a co-ordinated sequence of events; but contrary to what was originally thought, this process is vulnerable to change via the influence of extrinsic environmental factors (for review see Sale et al., 2014). For a continued maturation, for instance, the human brain is reliant on environmental inputs from its surroundings. The term "experience-expectant" development refers to exactly this – the notion that experience can shape brain development (Greenough et al., 1987). However, this is only possible because the developing brain is a plastic organ, receptive and malleable to incoming experiences which are then manifested biologically in a variety of forms, from cell proliferation, migration and integration, to axonal remodelling and synaptogenesis. Importantly, the possibility for neuroplasticity is heightened during sensitive periods of prenatal and postnatal life, but with time the brain becomes considerably less plastic (Ismail et al., 2016).

Early infant experiences, therefore, have the exceptional ability to either weaken or strengthen any given synapse. In doing so, they can help determine whether or not a connection is to become part of the permanent neural network, and hence, whether it maintains its functionality (as discussed in section 1.2.5.1 on page 43). Typical and appropriate experiences will help to shape major pathways, allowing for adequate patterns of cortical organisation to emerge. However, for this to occur, inputs via all major sensory systems (visual, auditory, somatic sensory, gustatory, olfactory, and vestibular) are required. If an input is lacking, certain brain regions may develop in an abnormal manner (Greenough et al., 1987).

1.2.6.1. Parent-infant interactions

Young infants mainly experience the early environment through interaction with their primary caregiver. Hence, parent-infant interactions are critical for child development, as they provide

an important source of sensory experience (Belsky and De Haan, 2011; Cabrera et al., 2011; Lugo-Gil and Tamis-LeMonda, 2008). Infants exposed to sensitive and responsive early care, for instance, will tend to manifest optimal brain, behavioural, and cognitive outcomes (Cabrera et al., 2011; Fleming et al., 1999; Lugo-Gil and Tamis-LeMonda, 2008). In contrast, infants exposed to insensitive rearing are at an increased risk of developing psychopathology in later life (Murray et al., 2010). Although the biological mechanisms mediating these associations are not yet fully understood, elevated levels of stress hormones have been identified in both children and adults who experienced early life adversity, such as parental loss and/or poor maternal care (Luecken, 1998; Lupien et al., 2011; Nicolson, 2004). It has also been proposed that elevations in stress hormones are likely to activate the hypothalamic-pituitary-adrenal (HPA) system (Atkinson et al., 2013), commonly referred to as the stress system. Consequently, this can result in inhibition of neurogenesis, acceleration of apoptosis, altered synaptic pruning (Teicher et al., 2006; Tupler and De Bellis, 2006), and perhaps also aberrant connectivity (Sarkar et al., 2014), leading to a disruption in normal brain development. Having said that, it is imperative that we do not disregard the importance of the normal temporary increases in stress hormones. These temporary increases play a protective role in the developing brain, and are considered essential for survival. It is only when stress hormones reach excessively high levels, or individuals are exposed to them for prolonged periods of time, that they can inflict harmful and chronic effects on the brain and other developing organs (Shonkoff et al., 2012).

All things considered, one can be sure that the innate plasticity of the developing brain confers great survival value, particularly when considering that positive environmental experiences can work advantageously to influence brain maturation and cognitive development. However, neuroplasticity becomes increasingly more important when we begin to think of what might happen when an infant is exposed to adverse environmental influences. Couple that with a genetic susceptibility, and we have an infant that is vulnerable to a deviation from the normal developmental track.

1.2.7. Metabolic development in the prenatal and postnatal periods

All the major maturational processes described thus far are thought to be accompanied by metabolic changes in the brain (Robertson and Cox, 2002). Preliminary evidence for this comes from studies using proton magnetic resonance spectroscopy (^{1}HMRS). This *in vivo* technique provides a non-invasive method for characterising the cellular biochemistry underlying processes such as proliferation, differentiation, migration, and myelination, but also cellular energetics, membrane turnover, and neuronal function. In addition, changes in brain metabolite concentrations often precede structural brain abnormalities (Fayed et al., 2006). ^{1}HMRS may thus be a useful tool for identifying early atypical brain features before they can be visualised on structural MRI. However, since brain metabolites are both age- and region-dependent (Huppi et al., 1995; Pouwels et al., 1999), understanding how the concentrations of different metabolites change during typical development is a crucial first step, prior to exploring the metabolic profile of atypical development. For instance, it is evident even upon brief inspection that there are vast differences between typical brain spectra acquired at birth and in adulthood (Figure 1.8).

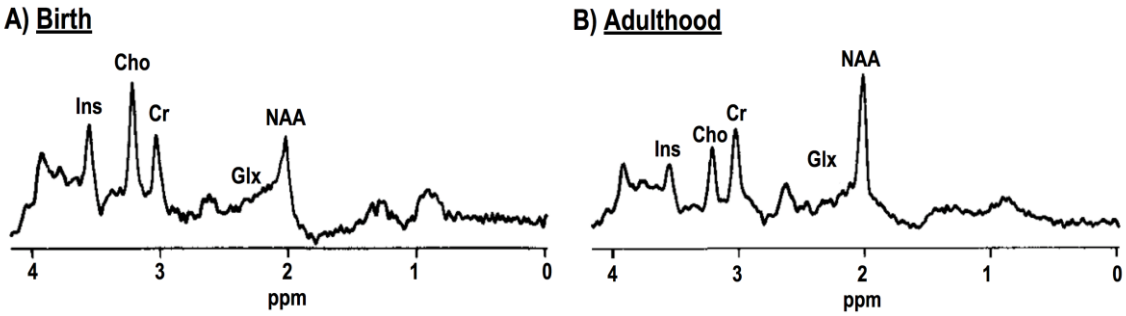

Figure 1.8: Differences in typical brain spectra acquired at birth and in adulthood. These spectra, sampled from the parieto-occipital cortex, clearly show the difference in the metabolic peaks present at **(A)** birth and in **(B)** adulthood. It is evident, for instance, that whilst N-acetylaspartate increases throughout development, choline decreases. Image adapted from Kreis et al., (1993). Abbreviations: Ins = Myo-inositol; Cho = Choline; Cr = Creatine; Glx = glutamate/glutamine; NAA = N-acetylaspartate; ppm = parts per million.

Although ^{1}HMRS has been widely used in both paediatric and adult settings for some time, studies of fetal ^{1}HMRS have only begun to emerge in the last fifteen years. The current consensus is that metabolic development begins in the fetal period and continues until around the third year of postnatal life. At this point, concentrations stabilise to reach adult levels (Figure 1.9), indirectly signalling successful maturation of the human brain (for review see Bertholdo et al., 2013; Dezortova and Hajek, 2008; Story et al., 2011).

In typical development, N-acetylaspartate (NAA) can be detected *in vivo* as early as 18 weeks gestation (Evangelou et al., 2016). From there on the NAA signal increases with age throughout pregnancy and postnatal life, until it becomes the most dominant spectroscopic peak at about 2 years of age (Blüml et al., 2013; Degnan et al., 2014; Evangelou et al., 2016; Girard et al., 2006a, 2006b; Heerschap et al., 2003; Kok et al., 2001, 2002; Ross and Bluml, 2001). In contrast, both myo-inositol and choline dominate the brain spectrum at short echo times from 22-28 weeks gestation (Girard et al., 2006a), but decrease with age during the prenatal and postnatal periods (Blüml et al., 2013; Cady et al., 1996; Degnan et al., 2014; Girard et al., 2006a, 2006b; Kimura et al., 1995; van der Knaap et al., 1990; Kok et al., 2002; Kreis et al., 1993; Pouwels et al., 1999; Story et al., 2013).

Until recently, creatine was thought to remain relatively stable throughout development, such that it became common practice to use creatine as a reference for calculating other metabolite ratios (Bertholdo et al., 2013; Brown et al., 2013; Kousi et al., 2013; Ross and Bluml, 2001). However, studies have now begun to report regional increases in creatine levels over the first 2 years of life, as well as immediately before birth (Blüml et al., 2013; Degnan et al., 2014; Evangelou et al., 2016; Girard et al., 2006a; Huppi et al., 1995; Kreis et al., 1993, 2002). Differences amongst clinical and control populations have also started to emerge (Suzuki et al., 2010). Consequently, this has led to the use of creatine as a reference metabolite being questioned (Rae, 2014; Turner and Gant, 2014).

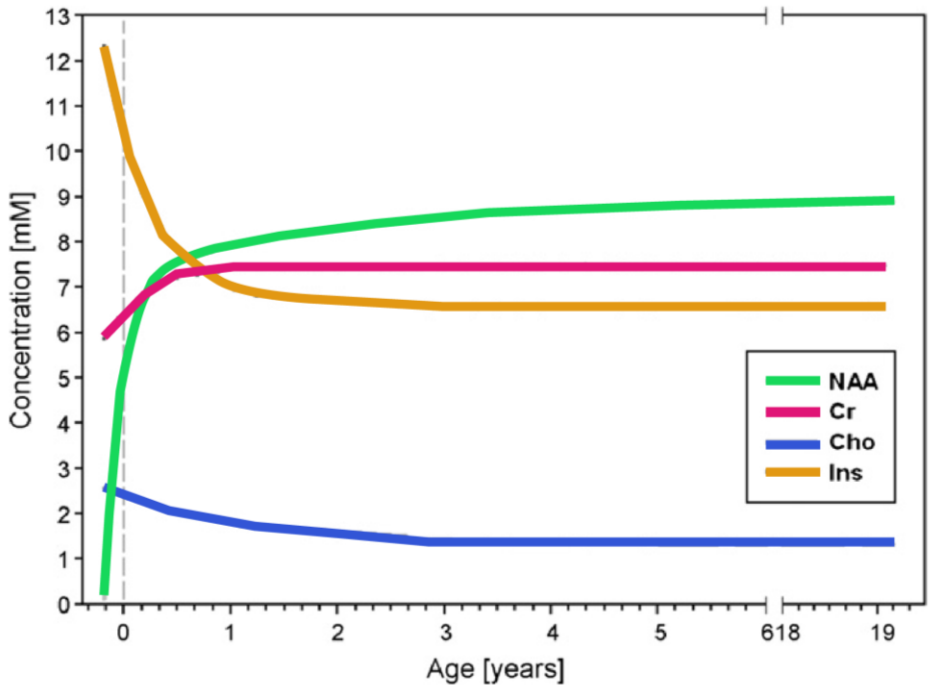

Figure 1.9: A representation of how metabolite concentrations vary with age. Although the most dynamic changes in brain biochemistry take place immediately before and after birth, metabolite concentrations only begin to stabilise at around three years of age. For example, while NAA increases in postnatal life, both myo-inositol and choline are found to decrease. In addition, recent evidence suggests that creatine increases over the first 2 postnatal years. This image was adapted from Dezortova and Hajek (2008). Abbreviations: NAA = N-acetylaspartate; Cr = Creatine; Cho = Choline; Ins = Myo-inositol.

Also unclear are the maturational changes that take place in glutamate and glutamine, commonly referred to as Glx. According to a prenatal report, Glx is clearly visible *in vivo* by 24 weeks gestation (Girard et al., 2006a), but no major changes in this metabolite have been observed with increasing gestational age (Girard et al., 2006a, 2006b). In postnatal studies, the majority of evidence suggests that brain maturation is accompanied by increases in Glx or glutamate (Blüml et al., 2013; Degnan et al., 2014; Kornhuber et al., 1993; Kreis et al., 2002). However, there is at least one report suggesting that Glx does not vary with postnatal age (Kreis et al., 1993). Thus, our understanding of how this metabolite changes with age remains inconsistent, especially with regards to its prenatal development. Nonetheless, glutamate is crucial for a variety of neurodevelopmental processes and so, understanding what happens to its concentration during these critical periods is of utmost importance.

1.2.7.1. N-acetylaspartate (NAA)

NAA is an essential amino acid found exclusively in the central and peripheral nervous system. The NAA peak is detected at 2.0 ppm on a ^{1}HMRS spectrum and is comprised of both NAA and N-acetylaspartylglutamate. In the typical brain, NAA is synthesised by L-aspartate N-acetyltransferase in neural mitochondria. It then diffuses along axons and is transferred to oligodendrocytes, where the deacetylation of NAA by aspartoacylase can take place (Ariyannur et al., 2008; Moffett et al., 2007; Patel and Clark, 1979). Although its exact function remains unclear, NAA is important for both the development and maintenance of the central nervous system. It is thought to be involved in processes such as migration, synaptogenesis, myelination, energy regulation, cellular signalling, mitochondrial function, protein synthesis, and the maintenance of neuronal integrity (Baslow, 2000; Coyle, 1997; Moffett et al., 2007).

Up until recently, NAA was thought to be predominantly present in neurons and therefore it was mainly considered as a neuronal marker (Demougeot et al., 2001; Moffett and Namboodiri, 2006; Simmons et al., 1991). However, a recent study reported that aside from being present in neuronal cell bodies, NAA is also present in high concentrations within oligodendrocytes (Nordengen et al., 2015). This suggests that NAA may be a marker for both neurons and oligodendrocytes. The increase in NAA evident from prenatal to late postnatal life is thus likely to reflect neural maturation, as well as oligodendrocyte proliferation and differentiation (Bhakoo and Pearce, 2000).

In the typically developed brain, NAA is present in high concentrations only in 'normal' neurons, axons, and oligodendrocytes, such that irregular levels are a good indicator of an abnormality. For instance, neonates suffering from hypoxic-ischemic encephalopathy (a type of brain injury caused by a reduction in the supply of oxygen to the brain), often show low levels of NAA (Barkovich et al., 1999). On the contrary, in Canavan's disease, aspartoacylase deficiency leads to an abnormal accumulation of NAA in the brain, which results in myelin degeneration and a series of symptoms including loss of motor skills, abnormal muscle tone, and seizures (Janson et al., 2006).

1.2.7.2. Creatine (Cr)

In ^{1}HMRS, the Cr peak is detected at 3.0 ppm and reflects both Cr and phosphocreatine. Synthesised in the liver and transported to the brain, these molecules are involved in the cellular energy exchange between adenosine triphosphate and adenosine diphosphate. Hence, Cr plays an essential role in the energy metabolism and equilibrium of cells, and is present in both neurons and glia (Bertholdo et al., 2013; Rae, 2014; Ross and Bluml, 2001; Urenjak et al., 1992). For instance, at birth, high levels of Cr can be found in the basal ganglia and thalamus; most likely because the metabolite is required for energy production during myelination of both these regions (Brighina et al., 2009; Huppi et al., 1995).

1.2.7.3. Choline (Cho)

Cho is a complex peak comprised of several Cho-containing compounds, including free Cho, phosphorylcholine, and glycerophosphorylcholine (Govindaraju et al., 2000; Rae, 2014). The Cho peak is evident at 3.2 ppm in a ^{1}HMRS spectrum, but it is representative of only a small percentage of the Cho present in brain tissue. This is because the majority of the metabolite is incorporated in substances such as myelin, undetectable using ^{1}HMRS. Cho-containing compounds are intermediates in the process of phospholipid metabolism. They are therefore considered essential components of cell membranes, used as markers for cell membrane formation, turnover, density, and integrity (Nelson, 2003; Sibtain et al., 2007; Soares and Law, 2009). In addition, Cho-containing compounds have been implicated in the process of myelination, which explains why Cho is predominantly found in the white matter (Bertholdo et al., 2013; Blüml et al., 1999; Pouwels and Frahm, 1998). It also explains why this metabolite is most prominent in the fetal spectrum and why, in typical brain development, progressive myelination results in the concentration of Cho decreasing with age (Girard et al., 2006b; Kok et al., 2002; Story et al., 2011). Once it has decreased, the Cho peak reaches a definite plateau, but only after 2 years of age when myelination is assumed to be largely complete (Kreis et al., 1993).

1.2.7.4. Myo-inositol (Ins)

Ins is a naturally occurring pentose sugar and an essential constituent of all living cells, both mature and immature. The metabolite is found in high concentrations throughout the central nervous system and can be reliably visualised using ^{1}HMRS at short echo times, with resonance at 3.6 ppm. Although primarily synthesised in glial cells and considered as an important glial marker (Brand et al., 1993; Kousi et al., 2013; Ross and Bluml, 2001), high concentrations of Ins have also been identified in neuronal populations (Novak et al., 1999). As a glial marker, increased levels of Ins are indicative of enhanced glial proliferation and/or augmented glial cell size, which can be suggestive of an inflammatory response (van der Graaf, 2010; Soares and Law, 2009). In addition, Ins plays an important part in the regulation of cell growth, neuronal plasticity, and the maintenance of osmolyte homeostasis (Fisher et al., 2002; Ross and Bluml, 2001). It is also a main product of myelin degradation, which explains why altered levels of Ins are commonly reported in patients with degenerative and demyelinating conditions (Lin et al., 2005; Wattjes et al., 2008).

1.2.7.5. Glutamate and glutamine (Glx)

In ^{1}HMRS, glutamate and glutamine resonate as a composite peak between 2.1 and 2.5 ppm. Given their similar chemical structures, it is not always possible to differentiate between the two metabolites. As a result, they are often measured together and referred to as Glx. Glutamate is the most abundant source of excitatory transmission in the nervous system and together with glutamine, it forms the important glutamate-glutamine neurotransmitter cycle. In this cycle, glutamate (mainly stored in neurons) is released into the synaptic cleft during neurotransmission. It is then transported out of the cleft by surrounding glia in order to be converted into glutamine. In turn, glutamine (mainly stored in glia) is released and taken up by neurons, where it is hydrolysed back to glutamate (Bak et al., 2006). Given that high levels of extracellular glutamate are considered to be excitotoxic, not only is this cycle critical for normal brain function, it also provides protection against excitotoxicity. Aside from its involvement in the redox cycle (van der Graaf, 2010; Soares and Law, 2009), glutamate also plays a critical role in a variety of neurodevelopmental processes, including the proliferation

and differentiation of oligodendrocytes, synaptogenesis, neural migration, plasticity, and cortical development (Gallo and Ghiani, 2000; Huttenlocher et al., 1982; Yuan et al., 1998).

1.2.7.6. γ-aminobutyric acid (GABA)

The measurement of GABA using ^{1}HMRS is technically challenging. Nonetheless, through pulse-editing sequences such as MEGA-PRESS, the metabolite can be identified at 1.9 ppm in a ^{1}HMRS spectrum (Mullins et al., 2014). GABA will not, however, be examined in this thesis, but it is an important metabolite to consider when studying early neurodevelopment.

GABA is synthesised from glutamate via the rate limiting enzyme glutamate decarboxylase (Bak et al., 2006). It is also the major inhibitory transmitter of the adult nervous system and hence, partly responsible for mediating the excitatory activity of glutamate. In adulthood, the inhibitory role of GABA is thought to be involved in both the maintenance and regulation of cognition, sleep, motor control, and anxiety (Rae, 2014). However, GABA is not always inhibitory; in early infancy it is excitatory. In brief, there is a developmental switch in the molecular machinery controlling the intracellular concentration of chloride which changes the functional role of GABA from excitatory to inhibitory (Ben-Ari, 2002). This switch is critical for normal brain development as it plays an important role in synaptic tuning and neuronal wiring, helping to establish appropriate neural connectivity. Thus, it is not surprising that irregularities in this developmental switch have been recently implicated in the manifestation of early atypical behaviours, as well as in neurodevelopmental disorders such as ASD (Ben-Ari, 2015; Cellot and Cherubini, 2014; LeBlanc and Fagiolini, 2011).

1.3. Key behavioural milestones

As highlighted in the previous section, the brain undergoes tremendous development from the early prenatal to the late postnatal period. Similarly, the first few years of life are marked by an astonishing increase in the amount and variety of skills that a child acquires. These skills tend to develop across specific age ranges, and are known as 'milestones'. Many individuals who go on to develop ASD or other neurodevelopmental disorders have delays in reaching specific behavioural milestones. Since ASD is a behaviourally defined condition, it is critical that we understand what the first observable indicators of future ASD may be. This introductory section will, therefore, focus on some of the key behavioural milestones that a child is expected to reach from 0-2 years, accompanied by a description of the most common departures from these targets reported in individuals who go on to receive an ASD diagnosis.

1.3.1. Birth

As soon as they are born, infants begin to interact socially, exhibiting a number of skills that facilitate engagement with others (Klin et al., 2003). For example, within the first few hours of life, newborn infants give preferential attention to people, preferring human faces over shapes and human voices over silence (Sheridan, 2008). They also prefer faces with eyes open (Batki et al., 2000), and favour their own mother's face and voice to that of a stranger's (Bushnell, 2001; Johnson et al., 1991). In addition, neonates are able to distinguish between a directed gaze and an averted gaze, orienting towards and fixating on a directed gaze more frequently and for longer periods of time (Farroni et al., 2002). Aside from their ability to engage in eye contact, newborn infants display spontaneous and imitative facial gestures, which helps them establish an interaction with their parents and/or carers within just a few days of birth (Sheridan, 2008). At this time, infants can respond to the emotional cues of others, an ability exemplified by 'contagious' crying (Geangu et al., 2010), and they are also able to produce vegetative sounds such as burping, sneezing, and coughing (Fenson et al., 1994).

1.3.2. Infancy: 1 to 6 months

One of the ways in which typically developing infants begin to respond to social cues in their environment is by smiling. Usually, social smiling is manifested over the first 2 months of life (Emde and Harmon, 1972), and is accompanied by gaze following, which involves orienting attention in response to another person's shift in gaze (Farroni et al., 2004). At this age, infants also begin to produce non-crying noises, such as cooing and gurgling sounds, and by as early as 2 months, some infants may begin to make vowel sounds, like "ah-ah" or "ooh-ooh" (Oller, 1978). Skill co-ordination becomes noticeable at around 3 months, when vocalizations become integrated with smiles, and eye contact becomes integrated with hand gestures. A little later on, by 6 months of age, infants are able to turn their bodies to the source of a sound, including that of a familiar voice across the room (Sheridan, 2008).

During this period of early infancy, typically developing infants begin to display a range of gross motor skills. At 1 month of age, infants tend to make jerky and uncontrolled movements with their arms and legs. Their hands are mostly kept closed with their thumbs turned in, but occasionally, infants will open their hands in order to grasp an adult's finger (Sheridan, 2008). By 3 months of age, the hands are more loosely open, and the body movements are generally less jerky and more continuous. When lying on their front in the prone position, infants are able to lift their head and upper chest, and they are also able to keep their head erect and steady for several seconds at a time. When pulled to sit, at around 4 months of age, infants can typically keep their head in line with their body, and by 6 months, head lag is very uncommon in typically developing infants (Bly, 1994). Infants also begin to roll over from front to back and back to front (Bly, 1994), and as their arm and hand muscles develop, they begin to use their hands in order to reach for and grasp objects.

During this period of postnatal life, most of the infants who develop ASD are progressing in much the same way as their typically developing peers. Studies comparing high-risk and low-risk infants, for instance, found no significant differences in the behaviours of each group at 6 months of age; infants who were later diagnosed with ASD showing typical engagement in

social interactions with others, manifested by normal rates of directed gaze, social smiling, and vocalization (Ozonoff et al., 2010; Rozga et al., 2011; Zwaigenbaum et al., 2005). There are however exceptions, and in a study conducted by Zwaigenbaum et al. (2005), some of the infants who later developed ASD were described as being more 'passive' than typically developing infants, with a marked decrease in their levels of attention and responsiveness to others. In a more recent study, similar findings were reported, and 6-month-old infants later diagnosed with ASD could be differentiated from age-matched controls by a diminished ability to attend spontaneously to social scenes and human faces (Chawarska et al., 2013). This, however, is not a consistently reported finding, as others have not identified a significant association between an ASD diagnosis and a 6-month-old's ability to orient or visually attend to a face (Elsabbagh et al., 2013a; Ozonoff et al., 2010). In addition, infant siblings who go on to develop ASD have been observed to produce significantly fewer vocalizations, including fewer cooing, laughing, and imitative sounds, as compared to their typically developing peers (Paul et al., 2011). Others have also reported that these infant siblings have limited motor control (Bryson et al., 2007), including a more frequent inability to keep their head in line with their body by 6 months of age (Flanagan et al., 2012). Although delays in reaching gross motor milestones are considered as an important warning sign for a range of neurodevelopmental disorders, including ASD, why these motor delays occur and whether they cause subsequent problems, is not fully understood.

To summarize, there are already some subtleties in the behaviours of 6-month-old infants who go on to develop ASD, as compared to those who do not. However, it is only after 6 months of age, that the difference between these groups of infants becomes increasingly noticeable. Over the next few months, while typically developing individuals gradually become more social and creative, those who are later diagnosed with ASD may acquire socio-communicative skills at a rate slower than the typical rate, or in some instances, demonstrate a general loss of these skills (Ozonoff et al., 2010).

1.3.3. Infancy: 6 to 12 months

By 9 months of age, typically developing infants have become very visually attentive to their environment, including to the people, objects, and activities around them (Sheridan, 2008). They are also able to respond to their name (Fenson et al., 1993) and can recognise the meaning of a few familiar words, such as “no” and “bye-bye” (Bergelson and Swingley, 2012). At this age, infants enjoy participating in vocal play; they begin to vocalize more deliberately with others and to babble loudly and repetitively using strings of syllables, like “adaba” and “agaga” (Sheridan, 2008). They also enjoy clapping their hands, and show interest in taking part in social games, like peek-a-boo (Hodapp et al., 1984).

As they reach 12 months of age, typically developing infants can produce most vowels and many consonants, and are babbling more often and loudly than before (Sheridan, 2008). They are now also able to recognise familiar people from a distance, as well as capable of locating sounds that originate from various directions. By the time of their first birthday, infants can follow the gaze of others (Corkum and Moore, 1998; Gredebäck et al., 2008; Senju et al., 2008) as well as alternate the direction of their own gaze between a person and an object, for instance, in order to initiate episodes of joint attention (Carpenter et al., 1998). Similarly, to elicit attention and initiate social interaction, infants begin to improve their skill co-ordination and to use a greater variety of gestures. For instance, it is very common for 12-month-old infants to point with their index figure at objects of interest, while looking back for a reaction from an adult, hoping to engage in shared attention (Bates and Dick, 2002).

Alongside the acquisition of fine motor skills, including the ability to grasp objects with their thumb and index finger, the development of gross motor skills continues. For example, at around 7-9 months of age, the majority of typically developing infants are crawling, and by the age of 12 months, they are able to walk with one or both hands held, and perhaps even entirely unassisted. In contrast, infants later diagnosed with ASD may not have the same strengths and co-ordination as their typically developing peers, and so can have a delayed onset of walking (Iverson and Wozniak, 2007).

Other studies have identified additional patterns of delay, with many of the infants who later receive an ASD diagnosis presenting with very specific atypical behaviours by the age of 12 months (Ozonoff et al., 2010; Zwaigenbaum et al., 2005). Deficits in social and visual attention, for instance, become apparent around the end of the first year of life, with infants having atypical eye contact (Klin et al., 2003; Ozonoff et al., 2010), including a decline in gaze and visual tracking (Ozonoff et al., 2010), as well as a delay in the ability to disengage visual attention (Elsabbagh et al., 2013b; Zwaigenbaum et al., 2005). Others have reported a poor co-ordination of point and gaze (Landa et al., 2007), fewer attempts to show and point (Rozga et al., 2011), as well as a general lack of response and interest in interacting with others, including a reduced frequency of looking at faces (Gillberg et al., 1990; Hoshino et al., 1987).

Overall, children with ASD tend to engage less in activities requiring joint attention, as compared to their typically developing peers (Charman, 2003; Chawarska et al., 2003). The ability to engage in joint attention is considered to play a critical role in the development of socio-communicative skills (Mundy et al., 1986; Tomasello et al., 2005), and therefore, it is possible that abnormalities in joint attention may lead to other difficulties in social cognition and language. As an example, 12-month-old infants who later receive an ASD diagnosis already have abnormalities in socio-communicative behaviours, including fewer directed vocalizations, gestures, social smiles (Landa et al., 2007; Ozonoff et al., 2010; Zwaigenbaum et al., 2005), and deficits in initiation and response to social interaction, such as a failure to respond to when their name is called (Feldman et al., 2012; Zwaigenbaum et al., 2005). A decreased expression of positive affect is also evident by the age of 1, and tends to be accompanied by extreme temperaments, ranging from alarming passivity to marked irritability (Gillberg et al., 1990; Hoshino et al., 1987). Finally, 12-month-old infants who later develop ASD are usually intensely interested in non-social stimuli, fixating on objects and playing with them in a stereotyped sensory-oriented manner (Zwaigenbaum et al., 2005). There is thus growing evidence to suggest that many of the infants who will eventually be diagnosed with ASD, have already started to appear ‘withdrawn’ by the age of 1.

1.3.4. Toddlerhood: 12 to 24 months

This pattern of social atypicality withdrawal amongst high-risk infants who develop ASD becomes increasingly more evident with age, particularly as typically developing infants begin to show a growing interest in social activities. From the age of 15 months, most toddlers will engage in functional play, by pushing a toy car and pretending to drink from an empty cup (Sheridan, 2008). A little later at 18 months of age, infants will enjoy simple picture books in the company of their parents, and by 24 months, they will spontaneously engage in role-play, make-believe, and pretend play. A toddler of similar age who goes on to develop ASD, is much less likely to engage in this type of imaginative play, and instead, may prefer to play in a more self-stimulatory way. It is not uncommon at this age, for example, for high-risk infants who develop ASD to continue fixating on toys, consequently displaying fewer functional and more non-functional repetitive behaviours (Christensen et al., 2010; Zwaigenbaum et al., 2005).

Throughout toddlerhood, infants become more mobile and begin to enjoy climbing onto furniture, walking upstairs, and running around unassisted (Sheridan, 2008). The range of behaviours that a toddler is able to exhibit increases markedly in the second year of life, as toddlers learn at least one novel behaviour a day, mostly through observation and imitation (Barr and Hayne, 2003). It is also through imitation that toddlers begin to acquire a more comprehensive vocabulary (Masur, 1995; Masur et al., 2002). First words typically emerge spontaneously and in the correct context around the first year of life. By 18 months of age, toddlers will usually produce between 6-20 recognisable words, although some may already be producing 50 words, and by 2 years, they will begin to put two or more words together to form simple sentences (Fenson et al., 1994). The auditory comprehension of a typically developing child develops even more quickly than the spoken language, as toddlers are able to understand many more words than the ones that they produce (Fenson et al., 1994). In contrast, toddlers who are later diagnosed with ASD tend to show a decreased comprehension of single words and an atypical production of language. In fact, a delay in the

production of the first words is one of the earliest 'red flags' for ASD (Short and Schopler, 1988), and one which has also been recently replicated in high-risk samples (Mitchell et al., 2006; Zwaigenbaum et al., 2005).

In conclusion, infants who later develop ASD tend to show specific deficits and delays in key behavioural milestones, from 12 months of age, with some subtle differences already evident at 6 months. Despite common areas of impairment, such as socio-communicative skills, individuals who go on to develop ASD still show an enormous variability in the expression and severity of their behaviours. Perhaps for this reason, no study has yet found a reliable predictor of ASD within the first year of life.

1.4. Magnetic Resonance Imaging (MRI)

MRI is a particularly safe, non-invasive, and non-ionising imaging technique, which has been increasingly used to examine the fetal, neonatal, and infant brain. In recent years, MRI has made it possible to study the anatomy and chemistry of the brain *in vivo*. As a result, huge advances have been made in our understanding of typical and atypical neurodevelopment.

1.4.1. The physics of MRI

1.4.1.1. Nuclear magnetic resonance

Nuclear magnetic resonance describes the quantum mechanical behaviour of nuclei within a magnetic field and provides the fundamental construct for MRI (Rabi et al., 1939). In order to obtain information about the anatomy and function of the body *in vivo*, MRI exploits the magnetic properties inherent to hydrogen nuclei – the most abundant nuclei in the human body. Hydrogen nuclei are comprised of a single proton (^1H) with a corresponding positive charge, and since protons are in constant precession (spinning around their own axes); their presence contributes to the induction of a magnetic moment. In the absence of a magnetic field, hydrogen nuclei are randomly oriented in space. However, as soon as an external magnetic field (B_0) is applied, the spins of the nuclei align their axis of rotation longitudinally to the applied field (Figure 1.10).

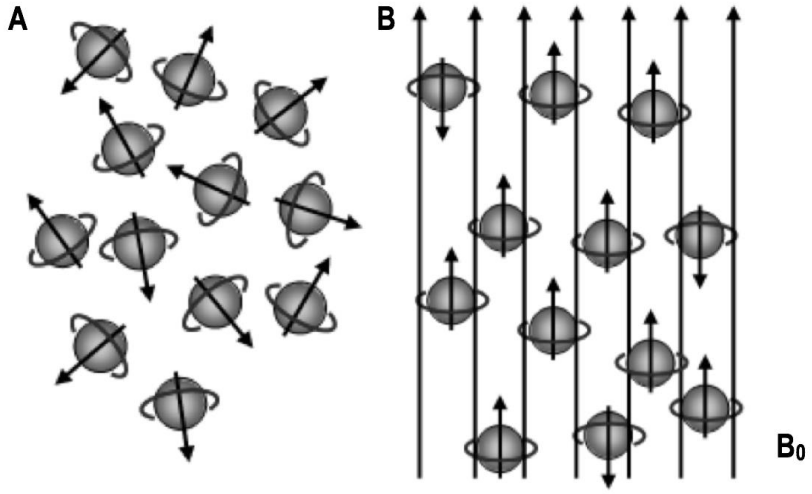

Figure 1.10: The application of an external magnetic field (B_0) to hydrogen nuclei. **(A)** In the absence of an external magnetic field (B_0=0), the hydrogen nuclei are in random orientation. **(B)** In the presence of an external magnetic field (B_0), the nuclei align themselves parallel or anti-parallel to the field.

Hydrogen nuclei can exist in one of two energy states: in the low-energy state, the nuclei align parallel to the field (spin up), whereas in the high-energy state the nuclei possess enough energy to oppose the magnetic field and hence, to align anti-parallel to it (spin down). With time, the nuclei continuously oscillate between the two energy states, favouring the state that requires less energy. Consequently, the number of nuclei aligned parallel to the magnetic field usually outnumbers that which are aligned anti-parallel to it. This gives rise to a net magnetisation, parallel to the external magnetic field, which is referred to as the longitudinal magnetisation. In normal circumstances and irrespective of energy state, the aligned nuclei continue to precess about their axes. The frequency of their precession is proportional to the applied magnetic field strength and is defined by the Larmor equation:

$$\omega_0 = \gamma \beta_0$$

Where ω_0 = precessional or Larmor frequency (MHz), γ = gyromagnetic ratio (MHz/T), and β_0 = magnetic field strength (T)

Nuclei often precess out of phase from one another, except when they are made to precess in phase. Nuclei that precess in phase give rise to a net magnetisation that is perpendicular to the magnetic field, termed transverse magnetisation. The vector sum of all the magnetic moments in a sample of nuclei refers to the net magnetisation vector, which is comprised of both longitudinal and transverse magnetisations.

1.4.1.2. Excitation, relaxation, and the MR signal detection

The application of a radiofrequency (RF) pulse, equal to the Larmor frequency, produces an overall excitation, which causes the nuclei to absorb energy and move onto a high-energy state. With an increased number of nuclei in the high-energy state, the longitudinal magnetisation is reduced. Consequently, the net magnetisation vector moves out of alignment with the magnetic field and in alignment with the precessing nuclei that are now in phase, and hence, inducing transverse magnetisation. The angle to which the net magnetisation vector realigns to is called the flip angle, and its magnitude depends on the amplitude and duration of

the applied RF pulse, normally 90°. The constant changing of the net magnetisation vector in the transverse plane causes an induced current in the coil, which can be measured, and is commonly referred to as the MR signal.

After the RF pulse has been applied, the nuclei eventually relax back into their low-energy states, realigning with the external magnetic field. In doing so they release the absorbed energy back into the surrounding tissue, or lattice, and re-establish thermal equilibrium in a process referred to as T1 longitudinal relaxation (or spin-lattice relaxation). In addition, as the nuclei relax back to their original energy states, the magnetic fields of the nuclei interact and exchange energy with one another. Ultimately, this leads to a loss of phase and a loss of signal, in a process known as T2 transverse relaxation (or spin-spin relaxation). In the presence of an applied 90° RF pulse, T1 is defined as the time taken for longitudinal relaxation to return to approximately 63% of its value, prior to the application of the RF pulse. In contrast, T2 is the time taken for transverse magnetisation to fall to approximately 37% of its original value after RF pulse application, corresponding to the 63% of transverse magnetisation that will be lost.

Multiple RF pulses are applied during a single MR examination. These are often referred to as pulse sequences and described in terms of their magnitude and frequency. The time taken between each RF pulse application is defined as the repetition time (TR), and it is largely responsible for the amount of T1 relaxation that can occur amidst two pulses. In addition, the echo time (TE) refers to the time taken between RF pulse application and MR signal detection, and controls the amount of T2 decay that occurs before the signal is read.

1.4.1.3. Image formation in structural MRI

Image formation does not occur directly from the MR signal received. Instead, the signal is first encoded in an intermediate form, known as the k-space. A Fourier transformation is then applied in order to reconstruct the k-space data into an appropriate MR image. The final image consists of a matrix of pixels, corresponding to the data previously encoded in the k-

space, with each pixel allocated to a specific spatial location and a particular shade on the grey-scale.

In medical imaging, the tissue contrast (that is, the difference in brightness between grey-scale shades) is one of the most important characteristics of an image, as it is what helps to visualise and delineate anatomical structures. The contrast of an MR image is highly dependent on both intrinsic and extrinsic properties. Intrinsic properties, for instance, are inherent to the tissue being imaged and depend on factors such as T1 recovery, T2 decay, and proton density. Tissues with high proton density (that is, with a large number of protons per unit volume of tissue) have a large component of transverse magnetisation and thus a high signal. In contrast, tissues with low proton density have a small component of transverse magnetisation and a low signal. Moreover, transverse magnetisation may decay faster in some tissues relative to others. If a signal takes a long time to decay, a low signal is detected in the region being imaged, and therefore, it appears dark in intensity.

Altering some of the extrinsic imaging parameters, such as TE, TR, and flip angle, can also produce images with different contrasts. To achieve a T1-weighted image, for example, the TR must be short enough so that tissues do not have sufficient time to fully recover before the next RF pulse is applied. In contrast, given that TE controls the amount of T2 decay that is allowed to occur before a signal is received, to produce a T2-weighted image, the TE must be long. MRI sequences can be designed to give images different weightings of T1 and T2, which will ultimately produce images of opposing contrasts. In a T2-weighted image, for instance, lipids have low signal intensity and appear dark, whereas water has high signal intensity and is bright. This explains why cerebrospinal fluid (CSF), which is largely composed of water, appears bright in a T2-weighted image, but very dark in a T1-weighted image (Figure 1.11). Moreover, in prenatal and postnatal periods when there is still limited myelination, T2-weighted images provide better tissue contrast and signal to noise ratio (SNR), when compared to T1-weighted images. Thus, the studies included in this thesis have only analysed T2-weighted images, largely focussing on the volume of different brain regions.

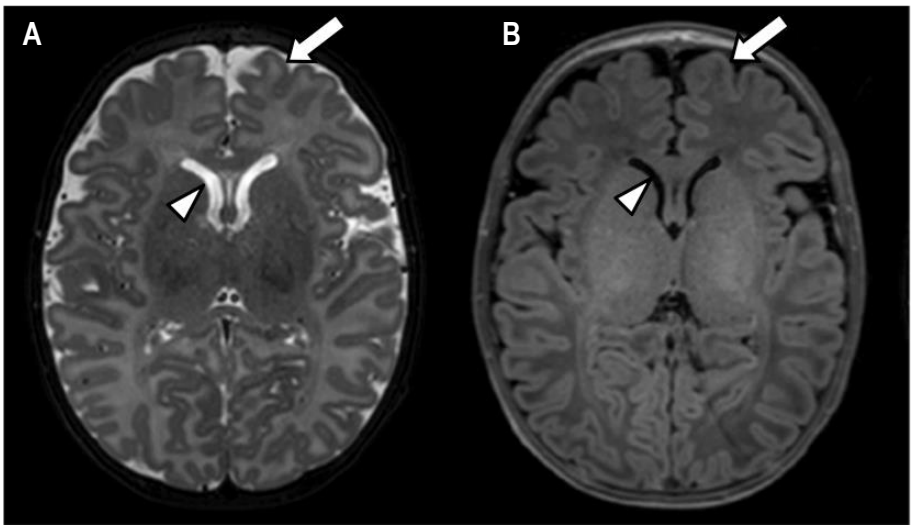

Figure 1.11: Tissue contrast in a T1-weighted and T2-weighted image.
The brain of a healthy term neonate scanned at an age of 40^{+1} corrected weeks is displayed above. In **(A)** the T2-weighted image, lipids have a low signal intensity and emerge as dark (arrow), but water has high intensity and appears bright in colour (arrowhead). Conversely, in **(B)** the T1-weighted image, lipids have high signal intensity and appear bright (arrow), whereas water has low signal intensity and appears dark (arrowhead). Note for instance, the difference in intensities between the lateral ventricles (arrowhead) and cortex (arrow).

1.4.1.4. Spectrum formation in ^{1}HMRS

^{1}HMRS is based on the same physical constructs as MRI. Instead of generating a structural image, however, it produces a chemical spectrum that provides information on the biochemistry of the tissue under study. More specifically, the ^{1}HMRS technique relies on the fact that hydrogen nuclei will resonate at different frequencies, depending on the tissue in which they are incorporated in and on the type of molecules surrounding them. This phenomenon is known as the chemical shift and it produces a change in the resonant frequency that is reliant on the molecular group attached to the hydrogen nuclei. The difference in the resulting frequency can then be used to identify which metabolites are present within the tissue being investigated.

The MR signal in ^{1}HMRS is recorded as a function of voltage over time; for a single RF pulse, this is denoted as the free induction decay (FID). Much like with the formation of anatomical images, a Fourier transformation is applied to the FID in order to reproduce the data in the

form of a chemical spectrum. In a ^{1}HMRS spectrum (Figure 1.12), peaks are positioned at different radiofrequencies. Each peak represents a different metabolite that can be identified by its specific frequency, expressed in parts per million (ppm) on the *x*-axis. The *y*-axis depicts the signal intensity of each metabolite, which is represented in arbitrary units. The signal intensity and the width of the peak are influenced by the spin-lattice and spin-spin relaxation times, whilst the area below the peak provides the metabolite concentration of the voxel under study. In principle, the area below the peak is proportional to the number of protons contributing to the MR signal. However, absolute concentrations cannot be accurately obtained without controlling for a series of confounding factors, including the pulse sequence and acquisition method. Hence, metabolite concentrations are often presented as relative ratios, expressed over what is considered to be a stable metabolite – Cr for example. Although commonly used, this technique is limited by the uncertainty of a given metabolite's stability (Jansen et al., 2006). It is also particularly problematic in the developing and atypical brain. Still, some argue that relative quantifications are actually more robust than absolute quantifications, and the truth is that the majority of studies continue to report relative ratios.

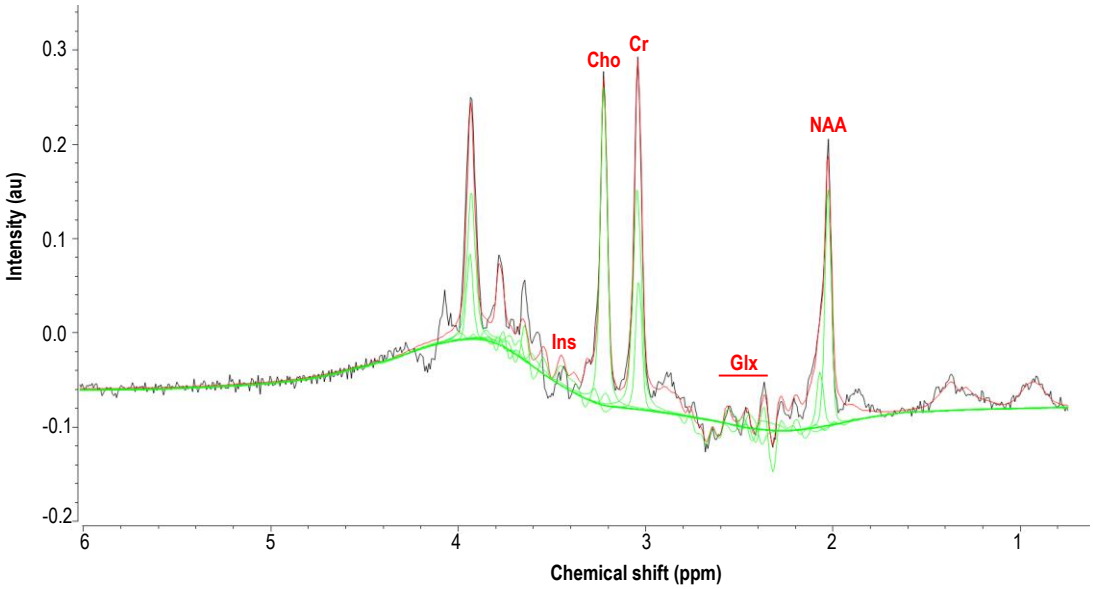

Figure 1.12: An example of a ^{1}HMRS spectrum acquired from a healthy neonate. The ^{1}HMRS spectrum is described by two axes – the vertical *y*-axis represents the signal intensity of metabolites, whilst the horizontal *x*-axis describes the frequency chemical shift in parts per million (ppm). The metabolite peaks for myo-inositol (Ins; 3.6 ppm), choline (Cho; 3.2 ppm), creatine (Cr; 3.0 ppm), glutamate/glutamine (Glx; 2.1-2.5 ppm), and N-acetylaspartate (NAA; 2.0 ppm) are indicated in red.

Metabolic profiles vary according to the brain region under study. However, they are also dependent on both pathology and age, which makes ^{1}HMRS an invaluable tool for assessing the function of the typical and atypical brain. In recent years, this particular imaging modality has been commonly used to assess the neonatal and infant brain, and increasingly so to examine the fetal brain. Thus, the studies included in this thesis have also used ^{1}HMRS to quantify the neurometabolic profile of the late prenatal and early postnatal periods. In order to detect metabolites with short spin-spin relaxation times, such as Glx and Ins, a short TE (55 ms) acquisition was used. Furthermore and although also visible at short TEs, NAA, Cho, and Cr were assessed using a longer TE (144 ms), as their long relaxation times allow for a more accurate quantification with this approach.

1.4.2. Imaging the fetal brain

At present, ultrasound (US) remains standard practice for the *in vivo* evaluation of fetal development in antenatal medicine. This is largely due to its many practical benefits; for example, its high safety profile, low cost, easy portability, and real-time use. However, US produces poor contrast resolution, which limits accurate anatomical delineations (Gholipour et al., 2011; Glenn, 2006; Rutherford, 2009). In addition, it lacks detailed visualisation of specific brain structures such as the cerebellum and cortex, particularly in the presence of an unfavourable fetal position. Compared to US, MRI has a larger field of view (FOV), which enables visualisation of the whole uterus and fetal body throughout gestation. It is also not limited by fetal position or maternal habitus, and has far better spatial and contrast resolution as well as higher SNR. Hence, MRI has recently been recognised as an invaluable complementary tool to US, often used to confirm diagnostic findings, evaluate suspected anomalies, monitor the progression of high-risk pregnancies, and provide a more comprehensive assessment of the fetal brain (Sévely and Manelfe, 2002).

Ever since its first application to fetal imaging in 1983 (Smith et al., 1984), when MRI was limited by long acquisition times and greatly affected by both fetal motion and maternal respiration (D'Ercole et al., 1993; Sévely and Manelfe, 2002), huge advances have been

made in fetal MRI (Figure 1.13). For example, the development of the single-shot rapid acquisition sequence in which each slice is acquired in less than one second, has revolutionised the field of fetal MRI, by allowing for good quality images to be produced in the presence of inevitable motion. Furthermore, advances in post-processing techniques, such as the offline registration and reconstruction of T2-weighted single-shot images, has enabled the production of 3D volumetric images with high SNR, high resolution, and relatively free of motion artefacts (Jiang et al., 2007).

Taken together, these techniques have greatly enhanced the visualisation and quantification of fetal brain development across a range of gestational ages. They have also improved the type of imaging analysis that can be accomplished with fetal data (Jiang et al., 2007; Rutherford, 2009; Sévely and Manelfe, 2002). As a result, the use of MRI for the *in vivo* study of the developing brain has enabled clinicians and researchers to examine both typical and atypical brain development (Gholipour et al., 2011).

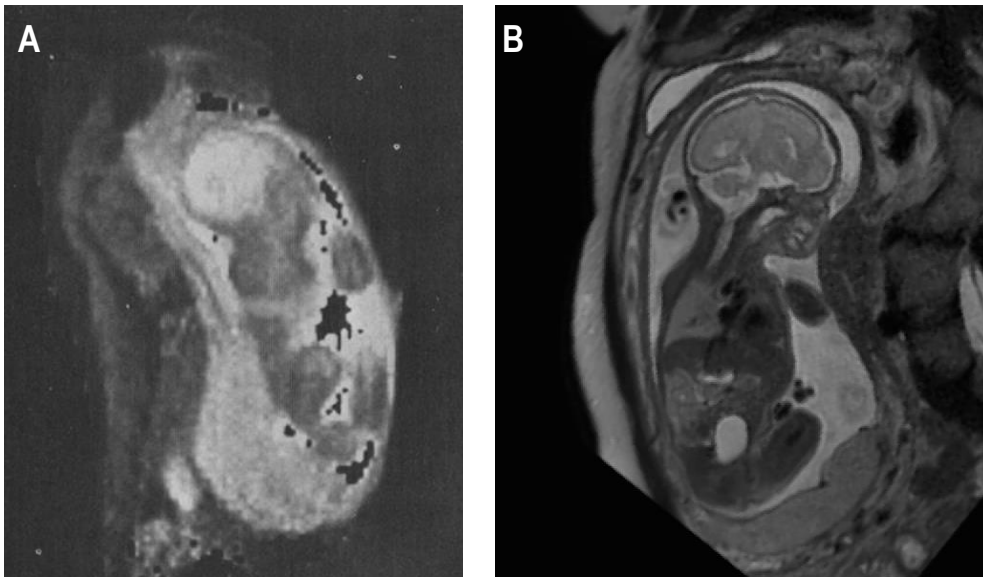

Figure 1.13: Advances in fetal MRI within the past 30 years.
(A) A T1-weighted image of a 32 week-old fetus acquired from a 0.04-0.08T MR scanner in 1983 (image obtained from Smith et al., 1984), and **(B)** a T2-weighted image of a 26^{+5} week-old fetus acquired on a 1.5T MR scanner in 2016.

1.4.2.1. Safety concerns and practicalities

MRI is considered to be a safe technique for use in pregnancy, despite some animal studies having reported an increased risk of developmental abnormalities and offspring mortality, subsequent to the use of MRI (Mevissen et al., 1994; Yip et al., 1994). However, these studies exposed animals to prolonged periods of MRI lasting up to 6 hours (Yip et al., 1994), and therefore, cannot be directly compared to human studies in which scanning times are considerably lower. For example, in a human study investigating the effects of MRI on 74 normal fetuses scanned at 0.5T, there were no reports of any adverse impacts upon fetal growth (Myers and Johnson, 2007). Other studies have also found no significant variations in fetal heart rates during scanning, and there is no current evidence stemming from human work to suggest that there are any adverse effects of fetal MRI on the health of either the pregnant woman or the fetus (Michel et al., 2002; Poutamo et al., 1998; Vadeyar et al., 2000). Hence, regulatory guidelines state that it is safe to use fetal MRI at 3T or less during the second and third trimester, but recommend that the use of MRI be carefully considered during the first trimester of pregnancy when the fetus is particularly vulnerable (Patenaude et al., 2014). However, in a recent study involving over 1.4 million pregnancies, it was reported that exposure to MRI during the first trimester of pregnancy was not significantly associated with any adverse effects on the fetus or the developing child (Ray et al., 2016). In light of this evidence it is therefore expected that future recommendations be made more lenient.

Other safety concerns associated with fetal MRI can easily be overcome, so long as precautionary measures are taken. One of the risks associated with fetal imaging, for example, relates to temperature. The slightest of increases in maternal body temperature could result in adverse effects on the developing fetus, including growth restriction and developmental defects (Chambers et al., 1998; Edwards et al., 2003; Kline et al., 1985). These adverse effects are thought to be a consequence of alterations in neurodevelopmental processes such as cell proliferation, migration, differentiation, and apoptosis. The effects are also largely dependent on the extent and duration of the temperature rise, as well as on the gestational age at which the insult occurs (Edwards et al., 2003). For instance, it appears that

the fetal brain is most sensitive to heat during the embryonic and mid-gestation periods. At this time, the fetus has no homeostatic mechanism to control its own body temperature, and instead, it is reliant on both maternal temperature and placental blood flow. Fetal temperature is assumed to be 0.5°C greater than that of the maternal temperature (Schroder and Power, 1997). Hence, it is important to ensure that the maternal temperature does not rise by more than 0.5°C while in the MRI scanner, and that the fetal temperature is kept under 38°C. As a result, it is a rule in some hospitals that whenever a fetal scan takes place, if the maternal temperature is ≥ 37.5°C, the scan is postponed. Alternatively, if there is no need to reschedule, the temperature in the scanning room is kept cool, and the expectant mother's temperature is monitored once again after the scan.

Another safety concern refers to the level of acoustic noise that is produced by the rapid changing of the currents within the gradient coils, and which gives rise to the characteristic knocking noise of the MR scanner (Rutherford et al., 2008; Sévely and Manelfe, 2002). Furthermore, although it is known that there is at least a 30 dB sound attenuation as noise passes through the maternal abdomen and amniotic fluid to the fetus, there is limited information regarding the level of noise heard by the fetus. To date, there has been no evidence of hearing impairments in children who have undergone MRI examination during fetal life (Kok et al., 2004; Reeves et al., 2010). Nonetheless, aside from protecting the mother's hearing with earplugs and headphones, it is also advised that imaging sequences be kept to a minimum of 100 dB. As a further precautionary measure, it is suggested that the more noisy sequences – for example, those used for diffusion tensor imaging – are acquired for only short periods of time.

Aside from this, claustrophobia and discomfort are common complaints during scanning. The small diameter of the bore also does not always allow for the imaging of patients with a high body mass index (BMI; ≥ 35 Kg m^{-2}). Women that are extremely claustrophobic (incapable of entering a lift, for example) are advised to not take part in fetal MRI, unless in cases of clinical need. In those circumstances, prism glasses can also be used in order to redirect the

women's line of sight and to make them feel more at ease. With regards to discomfort, pregnancy pillows are placed around the women's body to try and ensure the most comfortable position possible. Finally, because MRI is contraindicated in participants that have ferrous metal inside their body, anyone entering the MRI scanning room must complete a thorough metal check, which then needs to be approved by the designated radiographer.

1.4.3. Imaging the neonatal and infant brain

MRI has been far more extensively used to visualise and assess the neonatal and infant human brain, than it has been to assess the fetal brain. As with fetal imaging, it is commonly used to detect lesions, carry out diagnostic assessments, and predict outcomes. However, advances in imaging techniques have extended its role beyond visual assessments to allow for more robust analyses of volumetric data, metabolic profiles, connectivity, and function (Arichi, 2012; Ball et al., 2010; Counsell and Rutherford, 2002; Makropoulos et al., 2015; Malamateniou et al., 2013; Ramenghi et al., 2009; Varela et al., 2012; Xue et al., 2007). Importantly, the purpose of this thesis extends beyond the assessment of brain development during prenatal life, such that neurodevelopment will also be studied during neonatal and infant timepoints.

Similar safety precautions to those just highlighted for fetal imaging – regarding temperature, acoustic noise, and metallic implants – also need to be considered when scanning a neonate or infant. Hence, before entering the scanning room, it is necessary that a thorough metal check be complete to ensure that the individual is free of any ferrous metal. Special attention should be paid to neonates and infants that are being scanned for clinical reasons, as medical devices such as intravenous access lines and electroencephalograms are not always MR compatible. Aside from this, exposure to acoustic noise is also minimised by insulating the scanner bore with sound attenuating foam. The infant's ears are also protected with mouldable silicone-based dental putty and MiniMuff noise attenuators. In addition, an experienced clinician supervises the MR examination to monitor the infant's physiological parameters, including heart rate, oxygen saturation, and body temperature.

1.5. Autism Spectrum Disorder (ASD)

ASD is a heterogeneous neurodevelopmental condition, characterised by difficulties in reciprocal social communication and social interaction, as well as restricted and repetitive patterns of behaviour (American Psychiatric Association, 2013). The disorder affects approximately 1% of the general population (Baird et al., 2006; Baron-Cohen et al., 2009) and is more commonly diagnosed in males, with the most recent prevalence recorded at a ratio of 2-5:1 (Lai et al., 2015). In recent years there has been a tremendous increase in the number of ASD diagnoses, from an incidence of 0.04% in the 1990's to the current 1%. This rise may be explained, at least partly, by a broadening of the diagnostic criteria, improved service availability, and increased public awareness (Charman, 2002; Fombonne, 2005; Wing and Potter, 2002). Nonetheless, whether the current figure also reflects a true increase in the incidence of the disorder remains to be determined.

Currently, ASD is diagnosed exclusively based on its behavioural phenotype. Moreover, whilst initial symptoms have been identified as early as 12 months (Ozonoff et al., 2010; Volkmar and Chawarska, 2008; Zwaigenbaum et al., 2013), clinical diagnoses are not typically given before 2-3 years of age. Even then, diagnosis involves a lengthy clinical assessment with no biomarkers available to facilitate the process. In addition to the core deficits described, as many as 70% of individuals with ASD also suffer from co-occurring conditions. These include intellectual disability, ADHD, motor abnormalities, epilepsy, sleep disruptions, and affective difficulties such as anxiety and/or depression (Joshi et al., 2013; Matson and Nebel-Schwalm, 2007; Simonoff et al., 2008). Therefore, it is crucial that these conditions be carefully screened for and routinely evaluated as well as treated if possible.

Although some adults with ASD are able to live independently, the majority (58-78%) are described as having poor to very poor outcomes in terms of independent living, educational achievement, employment, and the establishment of meaningful relationships (Billstedt et al., 2011; Howlin et al., 2014). From a public health perspective, ASD's early onset, lifelong persistence, and associated co-morbidities, can cause considerable health and financial

burden to the individuals and their families (Howlin et al., 2004; Knapp et al., 2009; Woolfenden et al., 2012). Recent studies have also identified a 2.56-fold increase in the odds of premature mortality amongst individuals with ASD, relative to those in the general population (Hirvikoski et al., 2015; Schendel et al., 2016). This increase in likelihood of premature mortality does not appear limited to a specific cause of death, as it was found elevated for almost all of the ICD categories analysed (Hirvikoski et al., 2015). Despite this, evidence suggests that low-functioning individuals (that is, those with a co-existing intellectual disability) are more likely to die from neurological conditions such as epilepsy, whilst premature death in those that are high-functioning (with average or above average intellectual ability) will most likely be due to suicide (Hirvikoski et al., 2015).

1.5.1. Treatment and management

At present, there are no pharmacological treatments for the core symptoms of ASD (Ecker et al., 2013a), and even if they were to become available, it is uncertain whether they would be suited for young children. Therefore, the majority of work regarding the treatment and management of childhood ASD has mainly focused on developing behavioural therapies. Symptoms are thought to be particularly malleable in early infancy (Lord et al., 2005), most probably due to the heightened neuroplasticity at this time. In addition, this may partly explain the considerable progress made in recent years to develop interventions targeted at very young children (aged < 3 years). Some of these interventions have been designed by adapting existing treatments for older individuals, whilst others have attempted to incorporate aspects of the early infant environment, including parent-infant interactions (Dawson et al., 2010; Green et al., 2015; Oono et al., 2013; Rogers and Vismara, 2008; Volkmar and Pauls, 2003). Perhaps more importantly though, there is now evidence to suggest that early behavioural interventions are effective in decreasing core symptoms and improving outcomes (Zwaigenbaum et al., 2015).

As has been proposed with pharmacotherapy, it is unlikely that the treatment and management of ASD is possible with a “one-size-fit-all” approach (Ecker et al., 2013a).

Instead, as the field progresses towards targeted pharmacotherapies, it is likely that the development of stratified behavioural interventions will also emerge, particularly once we have understood which individuals respond best to which therapies. For early behavioural interventions to be successful, however, prompt referrals to appropriate services are required. Hence, the early identification of ASD has become a priority.

1.5.2. Aetiology

The exact aetiology of ASD remains unknown. Nonetheless, there is now considerable evidence to suggest that it is one of the most genetically determined psychiatric conditions (Sandin et al., 2014). While the estimated concordance rates in monozygotic twins is 60-99%, the rates in dizygotic twins range from 14-36% (Colvert et al., 2015; Hallmayer et al., 2011; Lichtenstein et al., 2010; Rosenberg et al., 2009). These figures highlight the importance of genetic influences on the pathogenesis of ASD; however, the incomplete concordance in monozygotic twins also indicates the significant role that is played by environmental factors (Hallmayer et al., 2011). Consequently, the current consensus is that ASD is caused by a complex interplay between both genetic and environmental risk factors (Hallmayer et al., 2011; Mandy and Lai, 2016; Rutter, 2005). In addition, ASD is largely viewed as a multifactorial condition with a highly heterogeneous phenotype. Some even suggest that there are probably many different kinds of "autisms", each with distinct developmental pathways (Abrahams and Geschwind, 2008).

1.5.2.1. Genetic risk factors

Most ASD cases are idiopathic, and recent advances in the field of genetics have identified over a thousand susceptibility genes (Abrahams and Geschwind, 2008). Nevertheless, clues to the molecular pathways implicated in the disorder come from the association of ASD with specific genetic syndromes and copy number variants (CNVs). For instance, syndromic forms of ASD such as fragile X syndrome (Hagerman et al., 2005), tuberous sclerosis (Shafali, 2015), Rett syndrome (Moretti and Zoghbi, 2006), and Phelan-McDermid syndrome (Durand et al., 2007) account for about 5% of all ASD cases (Miles, 2011). For the most part, the

functions of the genes involved in these conditions implicate synaptic dysfunction as a unifying cause in the pathogenesis of ASD (for review see Zoghbi and Bear, 2012). However, a substantial proportion of the ASD risk has been found to reside in high impact CNVs, involving microscopic deletions or duplications of DNA fragments. These variants have been associated with genes that code for proteins involved in various roles, including cell adhesion, neurotransmitter synthesis, and synaptic function, as well as neuronal differentiation and migration (Iossifov et al., 2012; Levy et al., 2011; O'Roak et al., 2012; Sanders et al., 2012). CNVs are responsible for 10-20% of all ASD cases (Miles, 2011). However, no single locus has been found to account for more than 1% (Abrahams and Geschwind, 2010), despite the fact that some loci have been more commonly implicated than others – perhaps especially those on chromosomal regions 7q11, 15q11-13, 16p11, and 22q11.2 (Jonas et al., 2014; Kumar et al., 2008; Sanders et al., 2011; Szafranski et al., 2010; Weiss et al., 2008). In addition, although some CNVs are dominantly inherited, the majority arise from *de novo* mutations, meaning that not all genetic causes of ASD are of familial origin – i.e. some arise for the first time in a new family member, as a result of a mutation in a germ cell or in the fertilised egg itself. Thus, a significant proportion of genetic risk arises *de novo.*

1.5.2.2. Environmental risk factors

As previously mentioned, genetic heritability is not thought to be the only cause of ASD, particularly since environmental risk factors have recently been found to play an important part in the emergence of the disorder (for review see Mandy and Lai, 2016). In fact, there is now evidence to suggest that some of the environmental factors implicated in ASD can impact neurodevelopmental outcome prior to birth, during the fetal period (Bale et al., 2010; Szatmari, 2011). For instance, there is an association between ASD and fetal exposure to gestational diabetes (Gardener et al., 2009), vitamin D deficiency (Cannell, 2008), and the presence of a viral or bacterial infection such as congenital rubella (Atladóttir et al., 2010; Chess, 1977). Maternal use of medication during pregnancy – specifically anticonvulsants such as sodium valproate (Williams et al., 2001), but also thalidomide (Strömland et al., 1994) and paracetamol (Liew et al., 2015) – has also been found to correlate with a higher incidence of

ASD, especially if ingested within the first trimester. Furthermore, there is now a growing body of evidence to suggest that women who are depressed or stressed during pregnancy, including those who take antidepressant medication, may also be at an increased risk (Boukhris et al., 2015; Croen et al., 2011; Kinney et al., 2008; Rai et al., 2013).

In addition to the impact of the prenatal environment, postnatal complications can also play a contributory role in the development of ASD. Associated factors include a breech presentation, caesarean delivery, induced labour, preterm birth, as well as a low Apgar score and low birth weight (Gardener et al., 2011; Glasson et al., 2004; Guinchat et al., 2012; Hultman et al., 2002; Johnson et al., 2010; Kuzniewicz et al., 2014; Landrigan, 2010). Specific congenital abnormalities such as ventriculomegaly and cerebellar anomalies, have also been linked to poor neurodevelopmental outcomes, often present in individuals with ASD, ADHD, and learning difficulties (Courchesne et al., 1994; Gilmore et al., 2001; Limperopoulos et al., 2007; Palmen et al., 2005). Furthermore, advanced paternal and/or maternal reproductive age has also been considered a risk factor (Croen et al., 2007; Hultman et al., 2011; Reichenberg et al., 2006), possibly due to the higher rate of *de novo* mutations and epigenetic alterations associated with older gametes (Crow, 2000; Reichenberg et al., 2006).

1.5.2.3. Gene-environment interactions

Many of the environmental factors thus far identified are unlikely to be sufficient in isolation to cause ASD. However, the emerging field of epigenetics has identified a number of gene-environment interactions, in which exposure to a given environmental insult can result in the manifestation of the disorder, if the exposed individual is already genetically susceptible (Bale et al., 2010; Rutter et al., 2006). Gene-environment interactions are mediated by epigenetic modifications of the genome, which result in altered gene expression, and may involve DNA methylation, histone modification, and non-coding RNAs (Borrelli et al., 2008; Franklin and Mansuy, 2010; Sweatt, 2009). Epigenetics may also help to explain the extensive heterogeneity of ASD, as well as the presence of the BAP in first-degree relatives of affected individuals.

1.5.3. Neuroanatomy

Despite an increase in studies using a range of investigational techniques, including genetic, animal, post-mortem, and neuroimaging work, the neurobiology of ASD remains unclear. The majority of studies investigating brain anatomical differences in individuals with ASD, compared to unaffected controls, have generated a series of inconsistent results. Partly accounting for these inconsistencies are demographic differences in cohorts, particularly with regards to age, gender, handedness, and ethnicity (Courchesne et al., 2011). In addition, there is significant diagnostic heterogeneity in the individuals who have been studied. Some groups have only included participants with high-functioning ASD, whereas others have studied more severe forms of the disorder, including individuals that suffer from associated co-morbidities such as intellectual disability and ADHD. Since it is likely that ASD subgroups have distinct neurobiological underpinnings, studies that include different behavioural phenotypes will probably confound results (Johnson and Myers, 2007). Moreover, neuroimaging studies can vary in terms of the scanning equipment used, imaging protocol run, and the analyses conducted. These factors are therefore all likely to explain, at least in part, the inconsistencies in the findings reported so far.

An additional significant complication is the age of subjects who are investigated. Age may be especially important in a disorder of brain maturation, as the dynamic changes that take place with time will be even more pronounced for individuals suffering from neurodevelopmental conditions (Courchesne et al., 2007). For instance, findings from observational studies including individuals from broad age-ranges (of 8-55 years, for example) cannot be restrained to a specific developmental timepoint. Moreover, most studies investigating structural brain differences in ASD, relative to age-matched typically developing controls, have been cross-sectional in design – restricting our understanding of the disorder's neurodevelopmental trajectory. In addition, the majority of these studies have been carried out in adults, adolescents, and children who already have ASD and so it is unknown if the brain differences that are detected underpin, or result from, having ASD. Consequently, very little is currently

known about early brain development in ASD, and there is limited knowledge on the brain biology of infants who go on to develop the disorder.

1.5.3.1. Studies of children, adolescents, and adults with ASD

Cross-sectional studies comparing brain volumes in children, adolescents, and adults with and without ASD, generally reveal a pattern of inconsistent findings. For example, whilst some have reported smaller-than-normal brain volumes in ASD (Lotspeich et al., 2004), others have observed larger volumes (Piven et al., 1995, 1996), and some have detected no significant differences in individuals with ASD compared to age-matched controls (Herbert et al., 2003; Kates et al., 2004). Partly driven by these discrepancies, recent reports have employed longitudinal designs in order to better understand the neurodevelopmental trajectory of ASD in later life. So far, these studies have revealed that after early adolescence, brain development in ASD is dominated by an accelerated age-related decline in total brain volume (Lange et al., 2015). Aside from an accelerated reduction of total grey matter in individuals with ASD (Hardan et al., 2009; Lange et al., 2015), the overall decline in total brain volume also appears to be accompanied by an unusually slow pattern of white matter growth, particularly evident in the temporal, parietal, and occipital lobes (Hua et al., 2013; Lange et al., 2015). Recent longitudinal studies in children, adolescents, and adults with ASD, therefore, provide initial evidence for an arrest in total brain volume growth, followed by a potentially accelerated decline from adolescence onwards.

Aside from this generalised difference in total brain growth, there is also evidence to implicate regional brain abnormalities in ASD. For example, neuroimaging studies of ASD have observed smaller volumes of the cerebellum (Courchesne et al., 1988; Levitt et al., 1999; McAlonan et al., 2002; Rojas et al., 2006), with differences in cerebellar morphometry identified as one of the key markers for classifying adults with ASD (Ecker et al., 2010). Post-mortem evidence corroborates these findings, particularly since cerebellar hypoplasia and a reduced size, packing density, and number of Purkinje cells, have been commonly reported in studies of adults and adolescents with ASD (Courchesne, 1997; Fatemi et al., 2012; Skefos et

al., 2014). Purkinje cell loss, for example, has been identified in 95% of the ASD post-mortem studies carried out between 1980 and 1997 (Courchesne, 1997). Since then, this finding has been replicated in other ASD samples, and appears prominent in both the cerebellar hemispheres and the vermis of affected individuals (Allen, 2005; Bailey et al., 1998; Palmen et al., 2004; Skefos et al., 2014). Indeed, the vermis is one of the most affected regions of the cerebellum, with numerous studies reporting hypoplasia of vermal lobules VI-VII (Allen, 2005; Courchesne et al., 1988, 1994, 2001, 2011; Kaufmann et al., 2003; Stanfield et al., 2008). Vermal hypoplasia has also been found to correlate with some ASD symptoms, namely stereotyped behaviours and repetitive movements (Kaufmann et al., 2003; Pierce and Courchesne, 2001), indicating that there may be a relationship in adulthood between vermal size and autistic symptoms.

Besides the cerebellum, other brain regions have been reported as significantly different between ASD and control groups. For example, the subcortical region has been frequently implicated in studies of ASD, with caudate overgrowth commonly reported in children, adolescents, and adults affected by the disorder (Haznedar et al., 2006; Herbert et al., 2003; Hollander et al., 2005; Langen et al., 2007; Rojas et al., 2006; Sears et al., 1999). Other subcortical regions such as the globus pallidus and putamen, have also been reported to be enlarged in older individuals with ASD (Herbert et al., 2003; Hollander et al., 2005; Langen et al., 2007; Sato et al., 2014; Turner et al., 2016). However, these studies are limited by their cross-sectional designs and the inclusion of participants from broad age-ranges. Thus, just as differences in total brain volume between ASD and control groups have started to be analysed longitudinally, so have differences in regional brain volumes.

In a recent longitudinal study focussed on the striatum (encompassing caudate and putamen), different growth trajectories were identified in children and adolescents with ASD, compared to typically developing controls (Langen et al., 2014). Specifically, ASD individuals demonstrated a significantly increased growth rate of the caudate nucleus, which was disproportional to overall brain growth and significantly associated with more rigid behaviours in autistic

individuals (Langen et al., 2014). Adding to this, others have also noted that the volume of the putamen and anterior cingulate cortex increases at an abnormally rapid rate in children and young adolescents with ASD, compared to controls (Hua et al., 2013). Taken together, these findings stand in stark contrast to the accelerated decline identified in total brain volume at similar ages, and suggest that different brain regions show distinct age-related volumetric trajectories in ASD.

In summary, although there has been progress in our understanding of brain anatomy in older individuals with ASD, more work is needed to further understand how the different regions implicated in the disorder, develop and change in later life. Moreover, it remains to be determined whether these atypical developmental trajectories are primary to ASD pathogenesis, or secondary to having the disorder (for example, in association with disease-related factors or as a consequence of treatment). Studying younger individuals at and around the time of clinical diagnosis may therefore inform us more about the potential biological underpinnings of the disorder.

1.5.3.2. Studies of toddlers and pre-school aged children with ASD

Prior studies of head circumference at birth suggest that the head (and therefore perhaps brain) size of infants who go on to develop ASD, is of either average (Dawson et al., 2007; Hazlett et al., 2005; Surén et al., 2013) or reduced size (Courchesne et al., 2003; Redcay and Courchesne, 2005), when compared to that of typically developing controls. However, some studies have reported that individuals with ASD subsequently show a sudden increase in head circumference (Courchesne et al., 2003; Dawson et al., 2007; Hazlett et al., 2005). For instance, in infants who were later diagnosed with ASD, head circumference increased between 1 to 2 months, and then again between 6 to 14 months, such that individuals with ASD already had larger head sizes by 6 months of age, when compared to controls (Courchesne et al., 2003). Importantly though, this pattern of accelerated head growth in the first postnatal year has not been observed by all (Surén et al., 2013; Zwaigenbaum et al., 2014). Early head overgrowth may therefore not necessarily reflect a pathological mechanism

that is common to all individuals with ASD. Rather, it may reflect a specific neurobiological subtype of the disorder (Zwaigenbaum et al., 2014).

Having said that, cross-sectional neuroimaging studies that directly measure brain volume as opposed to head circumference, have consistently shown that toddlers with ASD (aged 2-4 years) have larger total brain volumes than typically developing controls of similar ages (Carper and Courchesne, 2005; Courchesne, 2002; Courchesne et al., 2001; Hazlett et al., 2005; Sparks et al., 2002). Furthermore, recent evidence suggests that deviations in brain growth may begin before the age of 2. Longitudinal studies in toddlers, for example, have shown that affected individuals already have significantly larger brain volumes by 2.5 years of age, compared to those without ASD (Schumann et al., 2010). In addition, toddlers with ASD have enlarged cerebral cortices by 2 years of age (Hazlett et al., 2011) and thus, it is likely that there is accelerated brain growth in ASD prior to this age.

During the first few years of life there therefore appears to be an accelerated brain growth in young affected individuals, rather than an arrest or decline in brain growth, as evident in older individuals with ASD. However, as with findings from ASD studies in later life, affected toddlers also have specific regional abnormalities. That is, early overgrowth in ASD does not appear to be proportional throughout the brain, with neuroimaging evidence suggesting that enlargement may be localised to specific regions. For instance, multiple studies have observed significant overgrowth in the frontal, temporal, and cingulate cortices, but not in other brain regions, such as the occipital lobe (Carper and Courchesne, 2005; Carper et al., 2002; Schumann et al., 2010). The amygdala (located deep within the temporal lobes) has also been implicated in neuroimaging studies of young individuals with ASD. For example, in studies of toddlers (aged 1-5 years) who later received an ASD diagnosis, the volume of the amygdala was reported to be significantly enlarged and disproportional to total brain volume, when compared to that of toddlers who did not receive a diagnosis (Schumann et al., 2009). More recently, a longitudinal study reported similar results. Relative to typically developing children, the amygdala of children with ASD was significantly enlarged at both 3 and 4 years

of age. The growth of the amygdala between these two timepoints was also significantly greater in some, but not all children with ASD (Nordahl et al., 2012). Moreover, the size of the amygdala in toddlers with ASD has been found to positively correlate with overall symptom severity (Sparks et al., 2002), as well as social and communication impairments (Munson et al., 2006; Schumann et al., 2010) and joint attention scores (Mosconi et al., 2009). Thus, not only is there evidence that the amygdala is enlarged in young individuals with ASD, but also that it is associated with core autistic symptoms, and that increased growth rates may be present in only a subset of affected individuals.

1.5.3.3. Conclusions from structural studies of ASD

In conclusion, considerable progress has been made in recent years, with perhaps the most notable discovery being that (at least some) individuals with ASD appear to undergo a pattern of abnormal early brain development (Courchesne et al., 2007; Lange et al., 2015). Although this was originally proposed based on findings from cross-sectional investigations, it has now been confirmed by longitudinal studies. Taken together, prior work suggests that at birth, the head size of infants who go on to develop ASD is of either normal or small size, when compared to typically developing controls. However, there then appears to be a period of early brain overgrowth in toddlerhood and early childhood. This is followed by an arrested growth during adolescence and adulthood, which in some cases may lead to smaller-than-normal brain volumes in later life (Figure 1.14).

Based on the findings from a recent longitudinal study, the intersection between overgrowth and arrested growth in ASD has been proposed to occur between 10-15 years of age, when the growth curves of affected and unaffected individuals appear to converge (Lange et al., 2015). Nonetheless, it is not yet known when brain overgrowth in ASD begins, and in order to investigate this, future studies would benefit from inclusion of even younger populations. In line with this, more research is needed to investigate whether deviation from the normal trajectory is already evident in prenatal life, or whether disrupted growth is largely a postnatal event. Part of this thesis will therefore attempt to examine this.

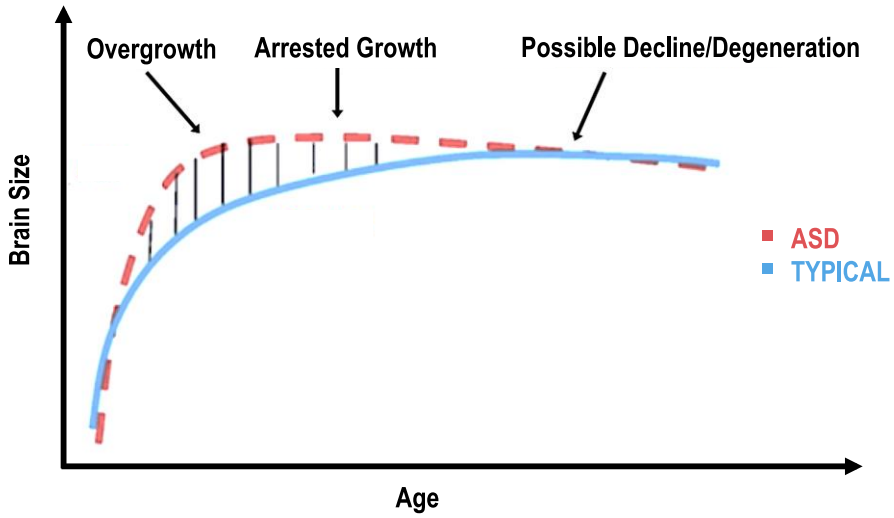

Figure 1.14: The aberrant neurodevelopmental trajectory of ASD.
Some individuals with ASD undergo an accelerated period of postnatal brain growth, which is followed by a period of arrested growth during adolescence, and a possible degeneration in later adulthood. In this figure, adapted from Courchesne et al., (2007), the blue line represents individuals with ASD, whilst the red represents those with typical development.

This thesis will also attempt to examine which brain regions (if any) are implicated from early on. As mentioned earlier, there is evidence that the neurodevelopmental trajectory of ASD is not proportional, with particular regions showing a significantly greater deviation in volume from the established norm. For instance, there is extensive evidence implicating the frontal, temporal, and cingulate cortices, as well as the cerebellum, amygdala, and subcortical regions, including components of the basal ganglia such as the caudate and putamen. These are also brain regions that mediate motor and high-order skills. Therefore, if their development is disrupted, this could result in a variety of social, emotional, cognitive, and motor dysfunctions – all of which are recognised areas of ASD deficit – and constitute an important direction for future research.

In addition, the underlying cause(s) of the putative and aberrant neurodevelopmental trajectory in ASD have yet to be established. A potential way forward is to study the *in vivo* neurochemistry of individuals with or at risk of the disorder.

1.5.4. Neurochemistry

Further insight into the underlying development of ASD has come from studies using ^{1}HMRS. However, here too there are inconsistencies in the literature (for review see Ford and Crewther, 2016), which can be explained by many of the same factors that affect structural studies, including differences in sample characteristics and imaging protocols.

1.5.4.1. NAA

To date, the majority of ^{1}HMRS studies carried out in children with ASD, support the notion that there are low levels of NAA across the brain (Aoki et al., 2012; DeVito et al., 2007; Ipser et al., 2012). For example, lower NAA has been identified in both grey and white matter brain regions (Corrigan et al., 2013; DeVito et al., 2007; Friedman et al., 2006; Levitt et al., 2003b), as well as in the cerebellum and the anterior cingulate cortex of autistic children (Chugani et al., 1999; DeVito et al., 2007; Fujii et al., 2010; Otsuka et al., 1999). In contrast, the NAA literature on adults with ASD is less clear, with autistic individuals exhibiting both lower (Suzuki et al., 2010; Tebartz Van Elst et al., 2014) and higher NAA levels (Brown et al., 2013; Murphy et al., 2002), as well as no significant differences (Bernardi et al., 2011; Hashimoto et al., 1997; Kleinhans et al., 2009; Page et al., 2006) when compared to age-matched controls.

Amongst its many roles (noted earlier in section 1.2.7.1 on page 51), NAA is considered to be a marker of neuronal integrity (Clark, 1998; Kleinhans et al., 2007). Lower levels of NAA are thus likely to indicate loss, dysfunction, or immaturity of neurons (Aoki et al., 2012; DeVito et al., 2007; Horder et al., 2013), as well as decline in axon count (Levitt et al., 2003b). These findings, therefore, do not support the hypothesis of increased neural and synaptic density as the basis for an early brain overgrowth in children with ASD. However, since the majority of ^{1}HMRS studies conducted in children have been carried out within, or shortly after 2-4 years of age, it could be that the low levels of NAA correspond to the period of arrested brain growth that follows early overgrowth. In addition, since NAA is cycled between neurons and oligodendrocytes, low levels of NAA in the young autistic brain may also signal errors in myelination and not in neurons *per se* (Moffett et al., 2007).

The abnormal levels of NAA identified in these studies might also contribute to the manifestation of some of the core symptoms of ASD. Lower NAA in the hippocampal-amygdala complex, for instance, has been linked with repetitive behaviours in adults with ASD (Kleinhans et al., 2009). Moreover, others have found NAA levels to correlate with deficits in communication (Fujii et al., 2010; Horder et al., 2013; Kleinhans et al., 2009), social responsiveness and functioning (Fujii et al., 2010; Kleinhans et al., 2009), and directed eye gaze (Levitt et al., 2003b).

1.5.4.2. Cr

Low levels of Cr have been identified in the cortex of ASD children (Corrigan et al., 2013; DeVito et al., 2007; Friedman et al., 2003; Hardan et al., 2008; Levitt et al., 2003b). In contrast, adult studies of ASD have reported elevated levels of Cr in the auditory and medial prefrontal cortex, as well as in the hippocampal-amygdala complex (Brown et al., 2013; Murphy et al., 2002; Page et al., 2006; Suzuki et al., 2010). Cr is present in both neurons and glia, and plays a critical role in the energy metabolism and equilibrium of cells (Bertholdo et al., 2013; Rae, 2014; Ross and Bluml, 2001; Urenjak et al., 1992). Hence, these findings suggest that there may be abnormalities in the energy metabolism and homeostasis of cells amongst individuals with ASD (Turner and Gant, 2014).

Cr levels have also been found to correlate with some of the core ASD symptoms, including impairments in social and repetitive domains (Kleinhans et al., 2009; Turner and Gant, 2014). In addition, they have been linked with associated symptoms, such as atypical motor learning and intellectual disability (Turner and Gant, 2014). Thus, it is possible that Cr may be involved in both the underlying pathophysiology of ASD, as well as in the development of co-morbid symptoms.

1.5.4.3. Cho

In ASD studies assessing Cho levels in children, evidence is inconsistent at present. For example, children with ASD have been reported to exhibit both lower (Corrigan et al., 2013;

DeVito et al., 2007; Fayed and Modrego, 2005; Friedman et al., 2003, 2006; Hardan et al., 2008; Levitt et al., 2003b) and higher Cho levels (Gabis et al., 2008; Levitt et al., 2003b; Vasconcelos et al., 2008), when compared to age-matched controls. By adulthood, however, results consistently report elevated levels of Cho in ASD individuals relative to controls (Bertholdo et al., 2013; Gabis et al., 2008; Murphy et al., 2002; Suzuki et al., 2010).

As mentioned earlier (please see section 1.2.7.3 on page 51), Cho is predominantly found in the white matter and has been largely implicated in the process of myelination. Thus, the abnormal levels of Cho observed in studies of ASD imply that there may be a dysfunction in myelination, which could underlie some of the developmental delays associated with the disorder (Baruth et al., 2013; Corrigan et al., 2013; Vasconcelos et al., 2008). Also, given that cholinergic pathways play a vital role in the development of cognition, an aberrant maturation of the cholinergic system may explain some of the behavioural abnormalities apparent in ASD; specifically, the deficits in attention orientation and sensory processing (Lam et al., 2006).

1.5.4.4. Ins

Thus far, the majority of ASD studies point towards low levels of Ins in both children and adults affected by the disorder, relative to typically developing controls (Bernardi et al., 2011; Friedman et al., 2003, 2006). However, there have been two studies reporting elevated levels of Ins in the hippocampal-amygdala complex, cerebellum, anterior cingulate cortex, and striatum of children with ASD (Gabis et al., 2008; Vasconcelos et al., 2008). In addition, aside from being considered as a glial marker, Ins also plays an important role in the regulation of cell growth and cell signalling (Fisher et al., 2002; Ross and Bluml, 2001). Evidence implicating low levels of Ins in ASD, therefore suggests that abnormalities in glial proliferation and cell signalling, may be present in affected individuals.

1.5.4.5. Glx

There has been a recent surge in the number of ASD studies either examining Glx or glutamate. This is mainly due to increasing evidence that the balance between excitatory

glutamate (E) and inhibitory GABA (I) – the E/I balance – is altered in individuals with ASD (for review see Rubenstein and Merzenich, 2003). However, spectroscopic findings remain inconsistent at present. For example, children with ASD have been reported to exhibit lower (Corrigan et al., 2013; DeVito et al., 2007; Kubas et al., 2012), higher (Bejjani et al., 2012; Doyle-Thomas et al., 2014), and no significant differences in Glx levels (Friedman et al., 2003, 2006; Hardan et al., 2008), when compared to typically developing controls. In addition, studies focussing on adult populations are similarly inconclusive (Aoki et al., 2012; Bernardi et al., 2011; Brown et al., 2013; Horder et al., 2013; Page et al., 2006; Tebartz Van Elst et al., 2014). Nonetheless, there is evidence that abnormalities in Glx may underlie some of the symptoms associated with ASD. For example, Glx levels have been found to correlate with deficits in motor and sensory regulation, as well as social interaction (Doyle-Thomas et al., 2014; Hardan et al., 2008; Tebartz Van Elst et al., 2014).

1.5.4.6. Conclusions from spectroscopic studies of ASD

Although many of the spectroscopic studies here reported have focussed on paediatric populations, no study has examined the neurochemistry of ASD in early infancy, prior to 3 years of age. In addition, not all studies in children are independent of medication; some have included participants on stimulants, antidepressants, anticonvulsants, and/or antipsychotics, further confounding the interpretation of results. Nonetheless, and despite discrepancies in the literature, the overall evidence points towards low levels of NAA, Cr, and Ins in young children with ASD relative to typically developing controls. Evidence from ASD studies assessing Cho and Glx is less clear. More research is therefore needed to fully understand if, and how, these brain metabolites differ in affected individuals, as well as in those at risk of developing the disorder.

1.5.5. Studying infants at risk of ASD

Studies from children, adolescents, and adults point toward differential maturation processes in both the neuroanatomy and neurochemistry of individuals with ASD, and highlight that the first years of life are key. In addition, and as alluded to throughout this introductory chapter,

both prenatal and early postnatal periods are crucial for normal brain development. More specifically, these critical periods play an important role in the appropriate establishment of the neural circuitry, which makes possible the development of the very skills that are impaired in ASD. It is thus highly probable that a neurodevelopmental disorder like ASD will be vulnerable to abnormal processes occurring during these early periods of development. Indeed, although the pathology of ASD remains unknown, its signature is most likely to be evident during fetal and/or early postnatal life, when clinical symptoms first begin to emerge.

To date, very few imaging studies have focused on these critical first years. However, there is now an increased recognition that ASD needs to be studied from a very early age and tracked throughout development. In order to study brain development in ASD prior to symptom manifestation, research has turned to 'infants at risk' who already have an older sibling with a diagnosis of the disorder. Given the disorder's genetic liability, infant siblings of diagnosed children have a considerably higher chance than the general population of developing ASD, or the BAP, with up to 20% developing ASD and perhaps a further 15-20% developing the BAP (Constantino et al., 2010; Georgiades et al., 2013; Ozonoff et al., 2011). In addition, many individuals at risk of ASD have early deficits in joint attention and delays in communication, neither of which are specific to ASD (Bedford et al., 2012). Therefore, prospective studies of infants at risk of ASD may help to identify neural markers that predate the emergence of symptoms, and provide novel insights into the neurodevelopmental processes underpinning risk and resilience for ASD and other behavioural difficulties common to many developmental problems.

The first MRI study using an infants at risk design to compare brain volume in 6 month-old siblings of infants with ASD, relative to those with typically developing siblings, reported no significant differences in intracranial, cerebellar, or lateral ventricular volumes, and no difference in head circumference (Hazlett et al., 2012). However, since then, other volumetric MRI studies have found evidence to suggest that enlarged corpus callosum (Wolff et al., 2012, 2015) and 'extra' CSF volume in the subarachnoid space (Shen et al., 2013), is present in

high-risk siblings by as early as 6 months of age. Increased area and thickness of the corpus callosum, as well as volume of subarachnoid CSF, also correlated with subsequent ASD symptom severity at 24 months – and these measures were proposed by the researchers as potentially predictive biomarkers of the disorder (Shen et al., 2013; Wolff et al., 2015). In addition, high-risk infants who later developed ASD had significantly larger total cerebral volumes at both 12-15 and 18-24 months, when compared with infants who did not develop ASD (Shen et al., 2013).

Alternative imaging modalities, such as diffusion tensor imaging and functional MRI, have proven useful in establishing other brain differences in infants at risk of ASD. For instance, there have been preliminary reports of differences in the development of white matter microstructure (Jin et al., 2015; Wolff et al., 2012). In line with this, connectivity abnormalities have enabled the differentiation of 6 month-old infants at high-risk of ASD, from those at low-risk, with a 76% accuracy (Jin et al., 2015). Moreover, prior to 6 months of age, irregularities in both brain function and behaviour can already be observed in infants at risk of ASD. For example, there are reports of high-risk infants aged 4-6 months showing a lack of early specialisation for human voice processing (Blasi et al., 2015; Lloyd-Fox et al., 2013) and a reduced sensitivity to social visual stimuli (Lloyd-Fox et al., 2013). Consistent with this, differences in the interaction of high-risk infants with their early caregivers, is evident by 6 months of age, with high-risk infants reported to be less lively than their low-risk peers (Doussard-Roosevelt et al., 2003; Wan et al., 2012, 2013).

Altogether, these studies have made critical first steps in advancing our understanding of atypical brain development within the context of infants at risk of ASD. However, as far as I am aware, there have not yet been any studies using ^{1}HMRS to examine neurochemical differences in these infants, nor have there been any structural studies investigating total and regional brain volumes in infants younger than 6 months. It is therefore not yet known whether there are any differences in brain structure and chemistry, present in individuals at risk of ASD prior to 6 months of age.

1.6. Aims and hypotheses

The over-arching aim of this thesis, therefore, was to investigate very early brain development, and to identify potential deviations from typical maturation that may be associated with a genetic risk of ASD. To do this, MRI measures of brain volume and chemistry were acquired in late prenatal and early postnatal life, from a sample of individuals at low and high-risk of ASD. Participants were considered to be at low-risk if they did not have a first-degree family relative with ASD, and at high-risk if they had a biological sibling with a diagnosis of the condition.

In the first study of this thesis (chapter 3), I worked with others to examine the association between observational measures of normative mother-infant interactions and regional brain volumes, in a typical sample of infants aged 3-6 months. The tested hypothesis was that there would be a significant association between brain and behaviour, and that this would be stronger in males.

In the next study (chapter 4), the objectives were to (i) compare total and regional brain volumes in 4-6 month-old infants with and without a familial risk of ASD; (ii) examine whether any early differences in brain volume were associated with ASD symptom severity and/or clinical diagnostic status at 36 months; and (iii) explore whether early mother-infant interactions moderated the extent of differences in brain volume and/or subsequent severity of symptoms. Given that larger volumes of extracerebral CSF in 6 month-old infants at risk of ASD have been reported in comparison to infants at low-risk (Shen et al., 2013), a group difference in CSF volume was predicted. In addition, it was hypothesised that mother-infant interactions would moderate the association between risk group and infant brain volume. No *a priori* hypothesis regarding the direction of these differences was made.

To build on the results of this previous study, subsequent studies examined brain development in individuals of even younger ages. The first of these studies focused on the

fetal period (chapter 5). It aimed to characterise volumetric brain growth across risk groups between 28-38 gestational weeks, and to compare volumes between groups. The next study (chapter 6) examined the neonatal period. Here, the goal was to characterise volumetric brain development across risk groups in the first month of life, as well as to compare brain volumes between groups. Both studies tested the hypothesis that there would be early brain differences in individuals at high-risk of ASD, relative to those at low-risk.

Finally, given that neurochemical abnormalities often precede and/or accompany structural brain differences (Fayed et al., 2006), the last study of this thesis (chapter 7) used spectroscopic data to examine key brain metabolites. By selecting the basal ganglia as the region-of-interest, this study aimed to characterise metabolic maturation from fetal to early infant life, and to compare brain metabolite ratios in 4-6 month-old infants with and without a familial risk of ASD. This was the first study to examine brain metabolites in infants genetically predisposed to ASD and therefore, no definite *a priori* hypotheses were made. However, given the current evidence suggesting that there is E/I imbalance in ASD (Nelson and Valakh, 2015; Rubenstein and Merzenich, 2003), it was proposed that if group differences did exist, these would be manifested by differences in Glx.

At this point, it is important to emphasise the exploratory nature of this research, as well as to highlight that the immediate results of this thesis will not inform outcome prediction, given that most of the studies set out below are not designed to examine categorical outcomes. Nonetheless, long-term follow-up studies will be conducted to specifically examine dimensions of cognition and behaviour that may be associated with ASD risk factors, as it is now known that children at risk of ASD who do not go on to receive an ASD diagnosis may still show signs of other difficulties that may require further support.

Chapter 2: Methodology

This thesis includes data collected as part of two distinct research projects: project 1 – an infant MRI study carried out at 1.5T, and project 2 – a serial MRI study conducted at 3T, incorporating fetal, neonatal, and infant data. Both projects were prospective in design, aimed at gaining a better understanding of very early typical and atypical brain development.

The first two experimental chapters of this thesis (chapters 3-4) are based on data acquired from project 1, while the final three chapters (chapters 5-7) report on findings from project 2.

2.1. Defining age: a brief note on terminology

For consistency, and to allow for easy comparisons between timepoints, the age of the participants included in this thesis has been reported in weeks. Moreover, given that some of the data incorporated in this thesis was collected at the fetal timepoint, participant age was defined based on the expected date of delivery (EDD). Initially, the EDD is determined based on the start of the last menstrual period, with an estimated 280 days (or 40 weeks) between these two dates. However, it is common for the EDD to be changed slightly subsequent to the first US scan, as this allows for a more direct measurement of fetal development. In this thesis, age was therefore defined based on the EDD obtained at US. The terms 'gestational' and 'corrected' age were used, as appropriate.

2.1.1. Gestational age

The term gestational age was used to describe the age of the fetus or the baby at birth; it was calculated according to this formula:

$$\text{Age (in weeks)} = (280 - (\text{EDD} - \text{RD})) / 7$$

Where EDD = expected date of delivery, RD = reference date, and (EDD – RD) is calculated in days.

In these circumstances, the reference date could either refer to the date of the fetal scan (used to calculate the gestational age at scan), or the date of delivery (used to calculate the gestational age at birth). Fetal scans were conducted from 28 weeks on (that is, 28 weeks ≤ Gestational Age < Birth) and only babies born at or over 34 gestational weeks were included.

2.1.2. Corrected age

Corrected (or adjusted) age was used to describe the postnatal age of a neonate or infant. Since the measure was also based on the EDD, it ensured that the baby's prematurity was accounted for, even if minor; for example, when referring to a baby born at 38 weeks gestation. This was important as it allowed for a fair developmental comparison between infants born at different gestational ages.

Corrected age was calculated according to the formula shown in the previous page; but in this case, the reference date referred to the date of examination, be it a scan or a behavioural assessment. For the purpose of the studies included in this thesis, the neonatal timepoint spanned the first month of life, with babies scanned from birth up to a corrected age of 47 weeks (that is, Birth ≤ Corrected Age ≤ 47 weeks). The infant timepoint included individuals that were a little older, aged between 50-75 corrected weeks (or 4-6 months of age).

Note: In this thesis, the majority of experimental chapters have reported age in weeks. However, since the first study is presented in the form of a published paper (chapter 3), infant age is referred to in terms of months, as this is what was originally submitted to the journal. In addition, there are other times in which age has been reported in months; however, this was mainly for ease of comprehension when discussing behavioural assessments carried out at 36 months.

2.2. Project 1: prospective infant imaging study at 1.5T

2.2.1. Ethical approval

This project received ethics approval from the UK National Research Ethics Service (REC 08/H0718/76, 06/MRE02/73, and 12/LO/2017). Written informed consent was obtained from parents on behalf of themselves and their child.

2.2.2. Recruitment strategy

Infants were eligible if they were aged between 50-75 corrected weeks (or between approximately 4-6 months of age). Recruitment was therefore conducted at any stage between pregnancy and the first few months of postnatal life. Infants in the high-risk group were recruited via the British Autism Study of Infant Siblings (BASIS), while those in the typical or low-risk group were recruited from the local community.

2.2.3. Study population

2.2.3.1. Typical community sample

Participants in this sample were assumed to be typically developing and representative of the general population. However, information on familial ASD risk was not collected. For logistical reasons, the age of participants in this sample ranged between 3-6 months.

2.2.3.2. Low-risk group

Participants were considered to be at low-risk if they had no family history of a first-degree biological relative with a diagnosis of ASD.

2.2.3.3. High-risk group

Participants were characterised as high-risk if they had one full sibling with a clinical diagnosis of ASD, confirmed by two expert clinicians with reference to the DAWBA (Development and Well-being Assessment; Goodman et al., 2000) and the SCQ (Social Communication Questionnaire; Rutter et al., 2003).

2.2.3.4. Exclusion criteria

Initial exclusion criteria prior to enrolment in the study included: (i) preterm infants (born < 36 weeks gestation), with (ii) contraindications for MRI (for example, metallic implants or pacemakers), (iii) clinically identified structural brain abnormalities, (iv) major antenatal or obstetric complications potentially altering infant development (such as perinatal asphyxia or seizures), (v) born to mothers with any current or past major psychiatric illness, and (vi) with a poor working knowledge of the English language (precluding informed consent for the study).

2.2.4. Experimental design

As part of this research project, all participants were assessed at 3/4-6 months of age. Those in the high-risk group were also followed-up at 36 months (Figure 2.1). During their first visit, participants underwent a structural MRI scan (which was part of a larger functional imaging study) and were video-recorded during a mother-infant interaction assessment. Basic demographic data on both the infant and the parents was also collected at this time. Then, at 36 months of age, participants in the high-risk group were behaviourally assessed using the Mullen Scales of Early Learning (MSEL; Mullen, 1995) and the Autism Diagnostic Observation Schedule (ADOS-2; Lord et al., 2012). The infants' parents were also interviewed using the Autism Diagnostic Interview (ADI-R; Lord et al., 1994).

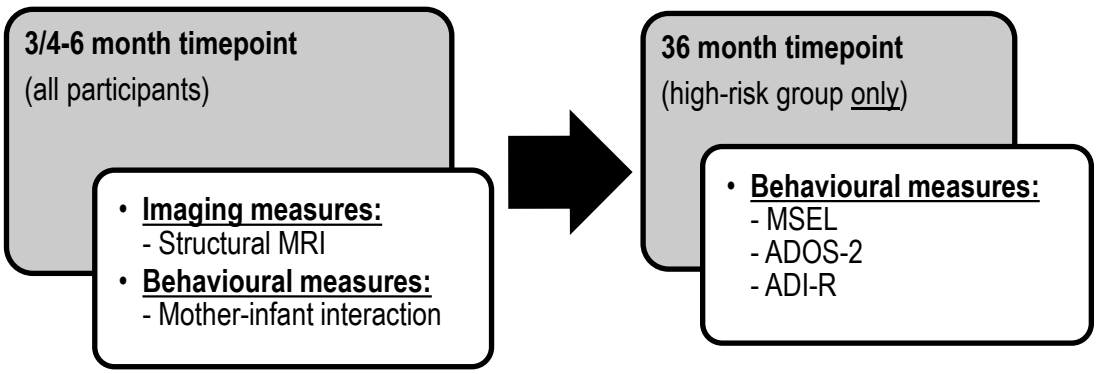

Figure 2.1: Schematic diagram illustrating the experimental design of project 1.
At 3/4-6 months, participants were assessed using both imaging and behavioural measures. Then, only participants in the high-risk group were followed-up for an outcome assessment at 36 months. Abbreviations: MSEL = Mullen Scales of Early Learning; ADOS-2 = Autism Diagnostic Observation Schedule - 2nd Edition; ADI-R = Autism Diagnostic Interview – Revised

2.2.5. Imaging procedures

Infants were scanned during natural sleep at the Centre for Neuroimaging in the Institute of Psychiatry, Psychology and Neuroscience at King's College London. Image acquisition took place on a 1.5T General Electric TwinSpeed MRI scanner (GE Medical Systems, Milwaukee, WI, USA), equipped with an 8-channel head radiofrequency coil.

2.2.5.1. Participant preparation

Prior to the MRI appointment, each family was given an information sheet detailing the purpose of the project and what to expect on the day of the scan. Given that all infants were scanned in natural sleep, without the use of sedation, appointment times were scheduled around the infant's usual naptime. On the scanning day, families were invited to come to the research facility an hour before the scheduled appointment. This allowed sufficient time for the infant to become familiar with the experimental setting, and to be fed, if necessary. The infant was then changed into metal-free clothes and weighed on a medical balance. Written informed consent was obtained from the parent on behalf of the infant, and a detailed metal check was conducted to ensure that the infant was safe to scan. Subsequently, the parent and infant were transferred into a dark, quiet room, to allow for the infant to fall asleep on a portable MR table.

Once asleep, the infant was swaddled in a cotton sheet and comfortably positioned in a Med-Vac Infant Immobilisation Bag (CFI Medical Solutions, Fenton, MI, USA), which provided neck support and restricted head movement during scanning. In order to minimise acoustic noise, the scanner bore was insulated with sound attenuating foam (Ultra Barrier, American Micro Industries, Chambersburg, PA, USA) and the infant's ears were protected with mouldable silicone-based dental putty (President Putty, Mahwah, NJ, USA). To further minimise any residual noise, MiniMuff noise attenuators (Natus Medical Inc., San Carlos, CA, USA) were used to cover the dental putty, and a set of paediatric MR-compatible piezoelectric headphones (MR Confon, Magdeburg, Germany) were placed on top. As soon as the infant was fully prepped (Figure 2.2), the MR table was moved into the scanning room and the infant

was transferred from the portable table onto the scanning bed. A pulse oximeter was secured on the infant's toe, to enable monitoring of the heart rate and blood oxygen saturation levels during the scan. Furthermore, both a researcher and parent (if willing) remained inside the scanning room to observe the infant's behaviour throughout. If the infant awoke or showed any signs of distress, the session was immediately stopped.

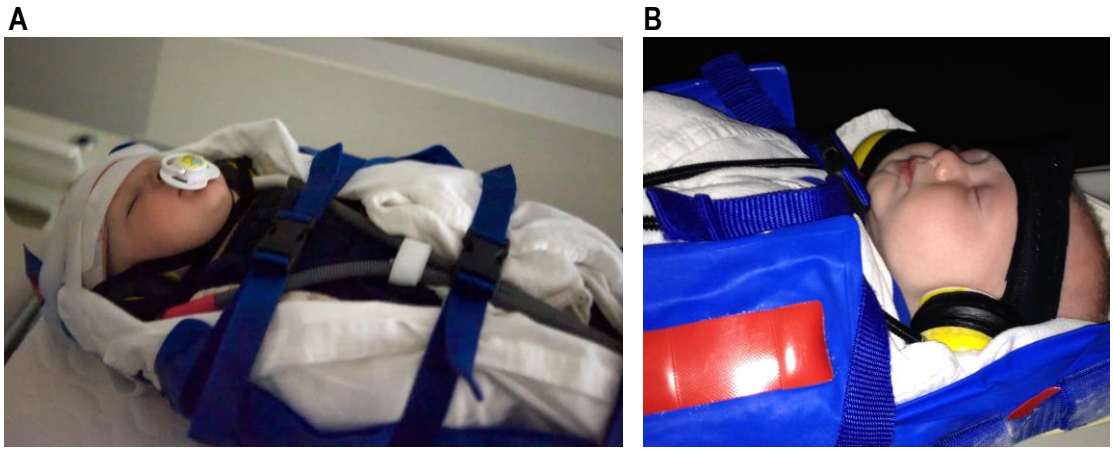

Figure 2.2: A 4 month-old infant prepped for scanning.
(A) The infant is comfortably swaddled in a cotton sheet and wrapped in an infant immobilisation bag. **(B)** The infant's ears are protected with dental putty, MiniMuffs, and headphones, with a headband used to secure these in place. As shown in image **(A),** dummies were allowed in the MRI scanner so long as they had been metal-checked by a radiographer.

The entire scanning protocol lasted for approximately 40 minutes, and involved the acquisition of structural and functional sequences. For the purpose of this thesis, analysis was based solely on the structural T2-weighted sequence. However, analyses of the functional datasets have already been published (Blasi et al., 2011, 2015).

2.2.5.2. Image acquisition

A T2-weighted fast spin echo sequence (T2w) with the following imaging parameters was acquired: TR = 3000/4500 ms, TE = 115 ms, slice thickness = 4 mm, slice gap = 2 mm, FOV = 180 mm, flip angle = 90°, and a 256 x 224 matrix.

2.2.5.3. Radiologic review

A neuroradiologist who was unaware of risk group reviewed all scans to screen for any obvious incidental abnormalities. In the eventuality of an identified anomaly, the neuroradiologist contacted the participant's general practitioner to inform them of the concern.

2.2.5.4. Image post-processing and volumetric segmentation

The T2w images (Figure 2.3A) were volumetrically segmented following an automated protocol, developed-in-house. First, the T2w images were skull-stripped using label propagation and decision fusion of three manually segmented brain masks (Heckemann et al., 2006). Subsequent to this, volumetric segmentations of the masked images were performed using an atlas-based approach, which adapted the Statistical Parametric Mapping software (SPM version 8), and used a 4D probabilistic neonatal brain atlas (Kuklisova-Murgasova et al., 2011) as the input. SPM's segmentation model unified tissue classification, image bias correction, and non-linear atlas registration (Ashburner and Friston, 2005). An Expectation-Maximisation algorithm (Dempster et al., 1977) and a Levenberg-Marquardt algorithm (Marquardt, 1963) were used to estimate the Gaussian Mixture Model (GMM) parameters. Then, in order to optimise these GMM parameters for tissue intensity distribution, bias field, and atlas deformation, Iterated Conditional Modes were employed. As a final step, the CSF segmentation was refined. This was done by thresholding the masked T2w image based on the mean intensity of the CSF, as calculated by SPM's posterior probability map. Partial volume misclassifications were particularly prominent at CSF boundaries. As a result, these misclassifications were corrected using second-order Markov Random Fields, which enabled spatial constraints to be imposed (Ledig et al., 2012).

Once the automated protocol had been applied to all T2w images, any errors of the automated segmentation were manually corrected by a single rater, who used the ITK-SNAP tool (version 2.2; Yushkevich et al., 2006) and a pen-tablet interface (Intuos Pro, Wacom, Japan) to produce the final segmentations (Figure 2.3B). All segmentations were carried out by investigators who were blind to infant risk group, and when necessary, blind to any relevant

behavioural measure. The final segmentation produced brain volumes (in cm^3) of the following regions: total grey and white matter tissue, extracerebral CSF (including third and fourth ventricles), lateral ventricles, subcortical region (including caudate nucleus, putamen, globus pallidus, thalamus, and internal capsule), midbrain (including cerebral peduncle, substantia nigra, brainstem, and pons), and cerebellum. Due to ongoing myelination, tissue contrast in 3-6 month-old brains does not easily allow for a reliable differentiation of grey and white matter. Therefore, similar to others (Hazlett et al., 2012), grey and white matter tissue classes were not further segmented.

In addition, the following global measures were calculated: intracranial volume (the sum of all regions), total brain tissue (including all brain matter but excluding CSF-filled spaces), and total CSF (comprising extracerebral CSF and lateral ventricles).

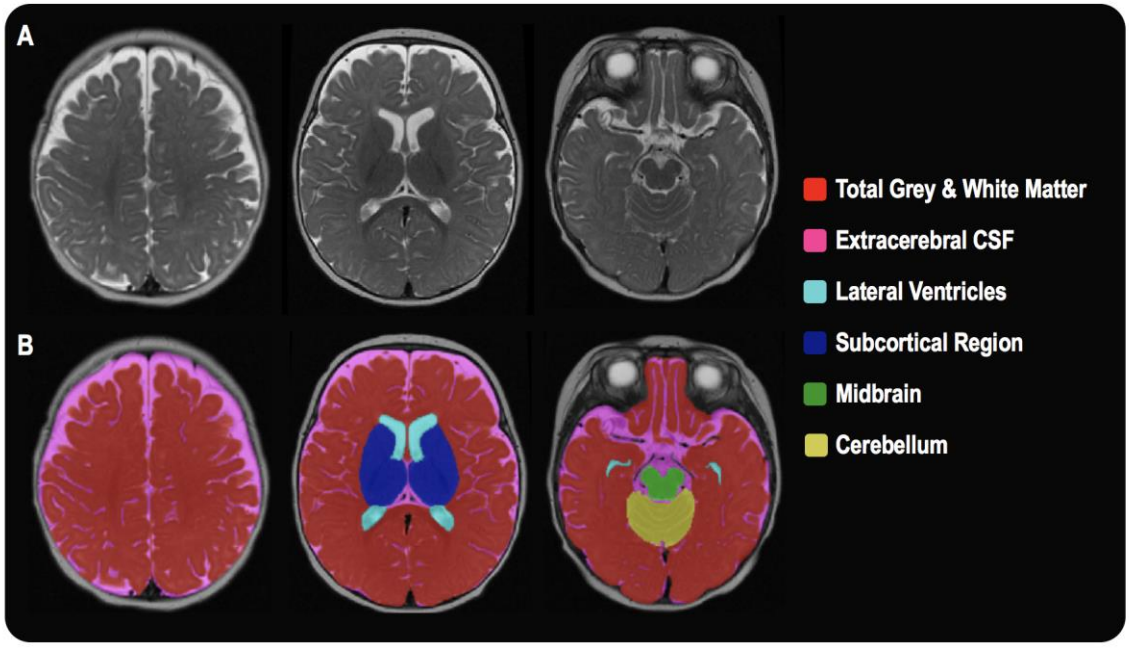

Figure 2.3: Volumetric segmentation of a 4-month infant brain acquired at 1.5T
(A) A transverse T2-weighted fast spin echo sequence acquired from a 4 month-old brain. **(B)** The output of the final segmentation, obtained after manual editing of the automated segmentation. Abbreviations: CSF = cerebrospinal fluid.

2.2.5.4.1. Validation of the automated technique, and reliability of the manual editing

The validity of the automated segmentation protocol was assessed by comparing its output with the output of manually segmented ('gold standard') brains, randomly selected from n=10

individuals (mean age = 60.00 corrected weeks; n = 3 male). All of the manual segmentations were completed on ITK-SNAP and performed by the same rater. The inter-rater intraclass correlation (ICC) for the total intracranial volume was 0.989 ($p < 0.001$), suggesting negligible variability between the two methods of segmentation. Similar results were obtained for the individual ICCs of each brain region, with values as follows: total grey and white matter (0.981, $p < 0.001$), extracerebral CSF (0.976, $p < 0.001$), lateral ventricles (0.953, $p < 0.001$), subcortical region (0.903, $p < 0.001$), midbrain (0.823, $p < 0.001$), and cerebellum (0.932, $p < 0.001$).

Intra-rater reliability of the manual corrections applied to the automated segmentations was also excellent, with ICC values ranging between 0.918 and 0.998. For the total intracranial volume, the ICC of the intra-rater variability was 0.998 ($p < 0.001$), indicating excellent reproducibility. Similar results were found for the individual correlations of each brain region: total grey and white matter (0.984, $p < 0.001$), extracerebral CSF (0.989, $p < 0.001$), lateral ventricles (0.965, $p = 0.001$), subcortical region (0.923, $p < 0.001$), midbrain (0.918, $p = 0.001$), and cerebellum (0.948, $p < 0.001$).

2.2.6. Clinical and behavioural procedures

2.2.6.1. Mother-infant interactions at 3/4-6 months

Within two weeks of the MRI scan, but usually on the same day, observed mother-infant interactions were video-recorded using a standard assessment protocol that can be applied to infants aged 2-6 months (Murray et al., 1996a). In a face-to-face play session that lasted for 5 minutes, mothers were asked to play with and talk to their infant as they normally would, but without the use of any toys or objects, and with the infant seated facing towards the mother. Maternal and infant behaviours were coded by two trained raters, experienced with the Global Rating Scales (GRS; Murray et al., 1996) and blind to infant risk group.

According to the GRS, maternal and infant behaviours are coded on a 5-point rating scale (1-5), with higher scores indicating more positive behaviours (for example, increased levels of

maternal sensitivity) and lower scores indicating inadequate interactions (for example, low levels of infant communication). Once the items have been scored, an average of the individual scores that constitute a given behavioural dimension is calculated in order to generate a composite score, also ranging from 1-5. The dimensions examined in this thesis were based on those commonly reported in the current parent-infant literature (Halligan et al., 2013; Stein et al., 2012), and comprised: maternal sensitivity, maternal affect, infant communication, and infant fretfulness (Table 2.1).

Table 2.1: A description of the behavioural dimensions examined as part of the mother-infant interaction assessment

Dimensions	Individual Items	Definition
Maternal		
Sensitivity	• Warm/Positive • Accepting/Rejecting • Responsive/Unresponsive • Demanding/Non-demanding • Sensitive/Insensitive	Maternal response to the infant's communication cues; the extent to which it is contingent and appropriate to the infant's needs and experiences. Includes attitudes and feelings towards the infant.
Affect	• Happy/Sad • Much energy/Low energy • Absorbed in the Infant/Self-Absorbed	Maternal display of affective state, including positive and negative affectivity (for example, depressive-like expressions).
Infant		
Communication	• Attentive/Avoidant • Active communication/No communication • Positive vocalisations/No positive vocalisations	Infant's level of engagement and communication, including positive vocal and non-vocal behaviour directed towards the mother.
Fretfulness	• Happy/Distressed • Non-fretful/Fretful	Infant's affective state, including positive and negative affectivity.

Note: Individual items are scored on a rating scale of 1-5, with higher scores indicating more positive behaviours. Composite dimension scores comprise an average of the individual items that make up each dimension, and hence, also range from of 1-5.

Inter-rater ICCs were measured on a randomly selected 20% of the interactions, and ranged between 0.741-0.993, indicating very good inter-rater reliability. In cases where there were discrepancies between raters, these were discussed, and final consensus ratings were obtained in collaboration with members of the research unit who helped develop the scale.

The reason for choosing the GRS over any other measure was partly a logistical one, as the scale was already being used in the department and by collaborators. However, the GRS is reliant on only a brief 5-minute mother-infant interaction, which may limit its generalizability. In addition, although it provides global measures of maternal and infant interactive behaviours, there are some aspects of early interactions that are not captured with the GRS, but that may have been relevant to study. These include aspects of tactile stimulation and verbal content, as well as dimensions that may be more relevant to a population at risk of ASD; for example, features which tap into the social behavioural deficits potentially present in the dyad. Finally, because the GRS is based on a face-to-face play session where participants are not allowed to use any toys or objects, the scale is not able to pick up on other dimensions of play which are dependent on the use of toys. For example, in a floor mat play session conducted with toys, a range of different behaviours would have been elicited, hence requiring a coding scheme which is able to capture maternal control and negativity, as well as the infant's ability to share.

Despite some of these weaknesses, there are many more reasons that make the GRS both a valid and reliable tool for assessing mother-infant interactions in the context of infants at risk of ASD. First, the GRS is sensitive to impaired interactions even amongst low-risk samples (Cohn et al., 1986; Gunning et al., 2004; Murray et al., 1996a), which suggests that it may be equally sensitive to interactions involving infants with and without a familial risk of ASD. Second, the GRS has been applied cross-culturally, in Africa, South America, and Europe (Cooper et al., 1999; Gunning et al., 2004; Sepulveda et al., 1999), which suggests that it is reliable for use in this study, which encompasses families from a range of distinct cultures and ethnicities. Third, the scales have good discriminant validity, having already been used with a

range of clinical groups, including mothers with depression (Murray et al., 1996a, 1996b), schizophrenia (Riordan et al., 1999), and borderline personality disorder (Crandell et al., 2003). The scale has also been recently used with mothers of infants at risk of ASD (Blasi et al., 2015), and although other studies examining this population have chosen to use an alternative measure (Wan et al., 2012), there is substantial overlap between the two. In fact, the measure used by Wan et al., (2012) was built on the fundamentals of the GRS, and modified to suit the study's sample population in terms of age and ASD risk-status. Although this would have been an interesting approach to use, it was felt that the modified measure was not necessarily as well-validated and reliable as the GRS; therefore, and also due to limited time and resources, the GRS was chosen instead. Fourth, maternal and infant ratings, as acquired using the GRS, have been shown to predict infant and child cognitive outcomes at a later stage in development (Murray et al., 1996b), and as such, were suited for the objectives of this study. The scale was also chosen for use in this study because it is not overly time-consuming to administer or to rate, and yet, allows for very sensitive data to be acquired with high levels of reliability and perceptiveness.

Finally, the mother-infant interactions obtained in this study also complement the brain measures used. While information on brain volume and chemistry may provide details on a potential biological basis for behaviours observed, they do not in themselves reveal anything about behaviour. For that, we need other measures such as observed mother-infant interactions, especially since these measures provide a window into the parenting environment of the infant, which may itself shape brain biology.

2.2.6.2. Outcome assessments at 36 months

At 36 months of age, all infants in the high-risk group were invited back for a follow-up behavioural assessment, which included the ADOS-2, the ADI-R, and the MSEL. The MSEL is a standard instrument for the evaluation of cognitive ability and development; it is administered directly with the child and is appropriate for use between birth and 68 months of age. The assessment yields a standardised score (mean = 100, SD = 15) of overall

intellectual ability (Early Learning Composite; ELC). The ADOS-2 is a standard and semi-structured play-based assessment, used to examine autism-related behavioural characteristics. For the ADOS-2, either module 1 (designed for non-verbal children or children with only single words) or module 2 (designed for children with consistent phrase speech) was administered at 36 months of age. However, to facilitate comparisons of symptom severity across different modules and ages, total algorithm scores were converted into standardised calibrated severity scores, which range from 1 to 10 (Gotham et al., 2009). The observations from the ADOS-2 were complemented with a parent-report of the infant's behaviours, administered by a standard structured interview – the ADI-R.

In common with other research groups studying infants at risk of ASD (Zwaigenbaum et al., 2007), a 'best estimate clinical consensus' approach to diagnosis was taken. That is, outcome classifications were defined by a group of experienced clinical researchers (TC, GP, CC), who took into account all available information (the MSEL, ADOS-2, ADI-R, and any informal observations), and agreed on a consensus ASD outcome. Children were characterised as 'high-risk ASD' if they met the DSM-5 criteria for ASD (American Psychiatric Association, 2013); in contrast, they were considered as 'high-risk non-ASD' if they did not meet the specified criteria.

2.2.7. Work done by others

The infant imaging data was acquired with the help of researchers (AB, VS, and MG) and radiographers at the Institute of Psychiatry, Psychology, and Neuroscience. In addition, SW completed the image post-processing and automated segmentation steps. Behavioural assessments were administered and coded by members of the BASIS team (TC, GP and CC), with the exception of the mother-infant interactions, which were conducted by VLS, VS, AS, and LB.

2.2.8. Power considerations and sample size estimation

The design of this project was based on evidence suggesting that approximately 20% of infants who have a sibling with ASD, will themselves be diagnosed with the condition (Constantino et al., 2010; Ozonoff et al., 2011; Sandin et al., 2014). Moreover, previous MRI studies using the infants at risk design to examine differences in infants as young as 6 months, have reported significant results with sample sizes of less than 20, but up to at least 30, per group (Blasi et al., 2015; Lloyd-Fox et al., 2013; Shen et al., 2013). A minimum sample size of 25 participants per group was therefore thought to provide sufficient power for the identification of preliminary differences ($p \leq 0.05$).

Post-hoc power calculations for the main finding(s) of each study are included in Appendix 1. Effect sizes are also reported, using partial eta squared (η_p^2), which measures the proportion of variance of the dependent variable that is accounted for by the independent variable (Portney et al., 2009). The effect sizes were interpreted using Cohen's (1988) criteria, where $\eta_p^2 \geq 0.01$, 0.06, and 0.14 are respectively considered small, medium, and large effects. For further details on the results of these calculations, please refer to Appendix 1 on page 255.

2.3. Project 2: prospective serial imaging study at 3T

This research project built upon the pilot findings of project 1. Besides having access to optimised infant MRI protocols, acquired at 3T, this project was also able to accommodate for scanning at even younger ages.

2.3.1. Ethical approval

This project was granted ethical approval by the UK National Research Ethics Service committee of Dulwich and Riverside (REC 12/LO/2017 and 14/LO/1169). Written informed consent was obtained from all participants, and when appropriate, parents consented on behalf of their infants.

2.3.2. Recruitment strategy

Participants were referred to this project from antenatal US departments and postnatal wards in hospitals across South London. The following hospitals were actively involved in the recruitment process: King's College Hospital, St. George's Hospital, St. Thomas' Hospital, Medway Maritime Hospital, Croydon University Hospital, and the South London and Maudsley Trust. Some participants were recruited from the local community (for example, from breastfeeding cafes and prenatal yoga classes), and some contacted the team voluntarily, having heard of the study from family, friends, and colleagues. Alternatively, participants with a familial risk of ASD were recruited more strategically from ASD charities, special needs schools, and the BASIS network.

Prior to enrolment in the project, all participants who had given permission for their contact details to be passed to the research team were contacted for an initial screening interview. The objective of this interview was to determine eligibility, as well as to safety screen for any MRI contraindications. Only then and if eligible to take part, did participants become formally enrolled. In order to accommodate for as many participants as possible, there was flexibility with the timing of enrolment; participants were allowed to enrol at any stage between pregnancy and up until early infancy, around 3-4 months of age.

2.3.3. Study population

2.3.3.1. Low-risk group

Participants were considered to be at low-risk if they did not have a first-degree biological relative with a diagnosis of ASD and/or a known genetic risk of ASD (for example, the 22q11.2 deletion syndrome).

2.3.3.2. High-risk group

Participants were characterised as high-risk if they had at least one biological (full or half) sibling with a clinical diagnosis of ASD. The diagnostic status of the sibling was verified by a copy document of the clinical diagnosis or any other relevant medical correspondence.

2.3.3.3. Inclusion criteria

The classification of participants into low-risk and high-risk groups was based solely on the presence of a familial risk of ASD. Therefore, participants with additional risk factors were included in both groups. For example, infants with cerebellar abnormalities and/or ventriculomegaly, which are commonly but not only associated with ASD outcome, were incorporated into either group (Courchesne et al., 1994; Gilmore et al., 2001; Limperopoulos et al., 2007; Palmen et al., 2005). Furthermore, since there is now a growing body of evidence to suggest that antenatal depression may be an important environmental risk factor for ASD (Rai et al., 2013), infants born to mothers with a clinical diagnosis of major depressive disorder were allowed to remain in the study. Similarly, late-preterm infants, classified as born between 34-37 gestational weeks, were also included. Indeed, preterm infants are currently being involved in other early ASD studies (Padilla et al., 2015; Ure et al., 2015), since they too provide an additional risk factor for a later diagnosis (Goldin and Matson, 2016; Guy et al., 2015; Pritchard et al., 2016).

This approach, of including participants with additional risk factors to both risk groups, ensured that the groups were fairly equally matched for risks of ASD other than familial. Thus,

if there were any significant differences between groups, these would more confidently be attributed to the genetic risk, present only in the high-risk group.

2.3.3.4. Exclusion criteria

The exclusion criteria for both low-risk and high-risk groups included: (i) preterm infants born at < 34 gestational weeks, with (ii) structural brain abnormalities identified at a routine antenatal US (with the exception of mild cerebellar abnormalities and/or mild to moderate ventriculomegaly), and (iii) contraindications for MRI (for example, metallic implants). Participants were also excluded if there was a (iv) major complication in pregnancy (such as perinatal asphyxia) and/or delivery (resulting in abnormal neurological signs as evidenced by an Apgar score of < 7 at five minutes), as well as any (v) serious incidental findings (such as cystic infarcts) on fetal, neonatal, and/or infant MRI examinations. Finally, infants born to mothers (vi) with serious medical conditions (such as epilepsy), (vii) any current or past major psychiatric illness (with the exception of major depressive disorder), (viii) exposed to illicit drugs and/or alcohol consumption (of more than 7 units per week) during pregnancy, and (ix) with poor working knowledge of the English language (precluding informed consent), were also excluded.

2.3.4. Experimental design

As part of this research project, all participants were offered the opportunity to take part in fetal, neonatal, and infant assessments (Figure 2.4). MRI acquisition occurred at all three timepoints, and in each scanning session the data acquired comprised of structural, functional, diffusion, and spectroscopic sequences. However, for the purpose of this thesis, only the structural and spectroscopic datasets were analysed. Specifically, spectroscopy was analysed at all three timepoints, while the structural data was only analysed at fetal and neonatal timepoints. In addition, basic demographic data on both the infant and the parents was collected. Physical measures including head circumference and body weight were also obtained, starting from birth up until the period of early infancy.

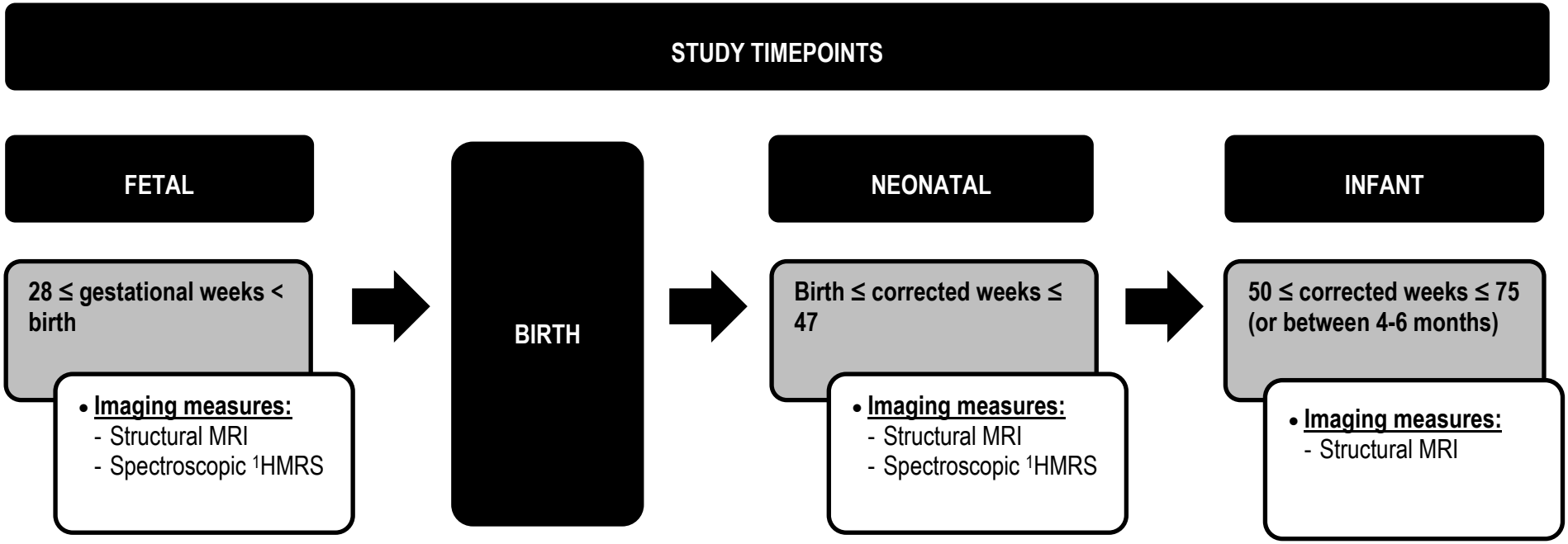

Figure 2.4: Schematic diagram illustrating the experimental design of project 2.
Low-risk and high-risk participants were assessed at several timepoints. At fetal, neonatal, and infant timepoints, all participants underwent an MRI scan, with structural and spectroscopic sequences acquired.

2.3.5. Imaging procedures

Fetuses, neonates, and infants were scanned at the Centre for the Developing Brain at St. Thomas' Hospital. All image acquisition took place on a 3T Phillips Achieva MRI scanner (Philips Healthcare, Best, The Netherlands).

2.3.5.1. Fetal imaging

Expectant mothers enrolled in the research project and willing to take part in fetal MRI were screened, to ensure that they were safe to be scanned. At this stage, the main concern was to determine whether the participant had a metallic implant and/or a BMI ≥ 35, as either of these conditions would prohibit the scan from taking place. Once eligibility had been established, a fetal MRI appointment was scheduled after 28 weeks gestation. This limit on gestational age was chosen since it ensured that fetuses were large enough that there was a restricted amount of fetal motion (Hayat et al., 2011), allowing for images of better quality to be acquired. Prior to their appointment, expectant mothers were also provided with an information sheet detailing the purpose of the research project and the practicalities of the scanning procedure.

On the day of the scan upon arrival to the centre, the maternity records of the expectant mother were checked to ensure that the correct EDD was known. Subsequently, written informed consent was obtained from the mother, and the possibility of incidental findings was discussed. The participant was then asked to remove all jewellery and to change into hospital scrubs, so as to ensure optimal comfort and metal-free clothing. A detailed metal check was also conducted to safety screen for any MRI contraindications. Prior to entry in the scanning room, the expectant mother's body temperature and weight were recorded. In instances where the maternal temperature was ≥ 37.5°C, the scan was postponed. Alternatively if all was well, the mother's temperature was measured at the end of the scan, to ensure that both maternal and fetal body temperatures had remained within a normal range during the MR examination. As a precautionary measure, the temperature inside the scanning room was set to 18°C, with air-conditioning inside the bore of the magnet providing additional cooling.

Once in the scanning room, the participant was asked to lie on the MRI table, feet first, in a lateral tilt position to avoid compression of the inferior vena cava. A 32-channel cardiac-thoracic coil was placed around the abdominal area proximal to the fetal head, and pregnancy pillows were placed around the mother to position her as comfortably as possible. Earplugs and headphones were provided to protect maternal hearing, allow for the radiographers to communicate with the mother, and enable her to listen to music. In addition, the expectant mother was given a "buzzer", which she was advised to use if feeling unwell or uncomfortable. Once pressed, this would alert the radiographers and depending on the issue of concern, a consensus was reached on whether to stop or continue scanning. A pulse oximeter was also attached to the mother's toe in order to enable monitoring of heart rate and blood oxygen saturation levels throughout the scan.

In total, the entire scanning procedure lasted for approximately 60 minutes. Due to fetal motion, image acquisition was intermittent throughout, with each imaging sequence requiring some geometrical pre-planning.

2.3.5.1.1. Image acquisition

The fetal MRI assessment involved a set protocol of sequences. Initial sequences were run for radiologic reporting purposes and to ensure that normal brain appearances could be confirmed, while subsequent sequences were acquired solely as part of the research protocol. Irrespective of this, all sequences have been described in detail below, with imaging parameters included in Table 2.2.

Survey: The survey is a quick 48-second acquisition, which enables the radiographers to identify the fetus's presentation; that is, whether cephalic or breech. Depending on this, the mother's positioning within the scanner and/or the position of the coil may need to be adjusted, so that the fetal brain is placed as close to the overlying coil as possible, to allow for maximum SNR.

Balanced Fast Field Echo Cine Soft Tone Sequence (BBFE Cine): The cine is a balanced fast field echo sequence; it is based on a cardiac sequence and is effective in observing fetal movement with near full-body coverage (Hayat et al., 2011). The sequence has proven to be particularly useful in research studies designed to assess fetal movement patterns. For this study, it was mainly obtained as a visual acknowledgement to the parents, and as a confirmation that their baby was healthy and mobile.

T2-weighted Single Shot Turbo Spin Echo of Uterus (T2ssTSE UTERUS): This is another rapidly acquired sequence, mainly used for the radiologic reporting of the intrauterine environment, including the placenta and the amniotic fluid. Each image is acquired in less than a second, and therefore, it is usually free from any motion artefacts. These sequences were acquired in the transverse, coronal, and sagittal planes.

T2-weighted Dynamic Single Shot Fast Spin Echo (T2ssFSE): This sequence was designed and optimised in the department to allow for a snapshot to volume reconstruction, used to overcome motion artefacts (Jiang et al., 2007). Multiple single shot acquisitions (4 transverse, 2 coronal, and 2 sagittal) with overlapping thin slices were obtained (Figure 2.5). Then, the T2ssFSE sequences were processed offline to enable production of a dataset suitable for volumetric analysis (see section 2.3.5.1.4.1 for a description of the reconstruction process).

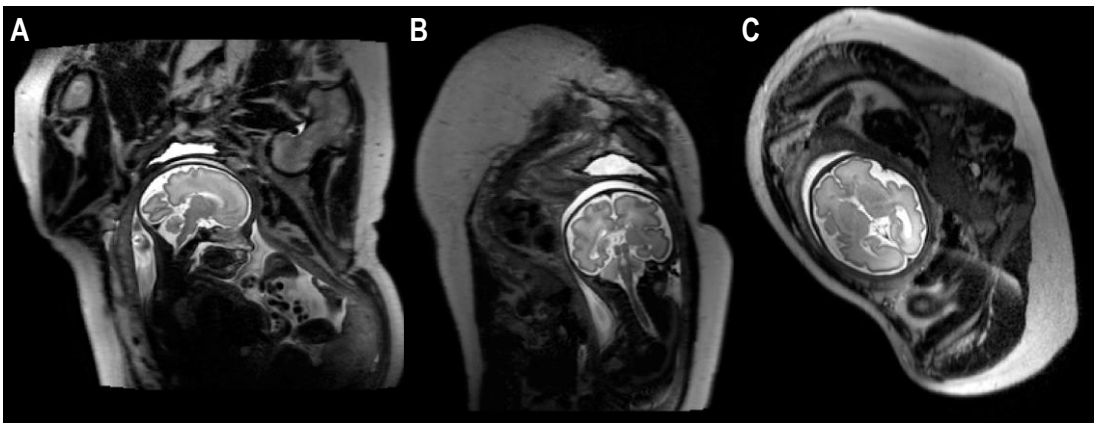

Figure 2.5: A T2-weighted dynamic single shot fast spin echo sequence (T2ssFSE)
This T2ssFSE sequence was acquired from an expectant mother at 31^{+6} gestational weeks. The image shows the T2ssFSE sequence acquired in the **(A)** sagittal, **(B)** coronal, and **(C)** transverse plane. As is evident there is a slight inhomogeneity in the contrast of the image, likely due to 3T heterogeneity artefacts, but which can be improved with image reconstruction.

T1-weighted Snapshot Inversion-Recovery (SNAPIR): In contrast to conventional T1-weighted sequences, this SNAPIR sequence (Figure 2.6), designed and developed in the department (Malamateniou et al., 2011), provides a much better delineation of the fetal brain, even in the presence of motion. The sequence was acquired in the transverse plane and mainly used for clinical reporting, as it allows for a very good visualisation of haemorrhage, fat and myelination.

Figure 2.6: T1-weighted snapshot inversion-recovery (SNAPIR) sequence. This is an image of a SNAPIR sequence acquired in the transverse plane from an expectant mother at 34^{+1} weeks gestation.

Point Resolved Spectroscopy (PRESS): Spectroscopic ^{1}HMRS was obtained using the PRESS sequence. To enable quantification of different metabolites, the sequence was acquired at two distinct echo times: 55 ms and 144 ms. Prior to data acquisition, a 20x20x20mm voxel was placed in the region of the left basal ganglia, avoiding any CSF-filled spaces (Figure 2.7). All spectroscopic acquisitions were performed using water suppression.

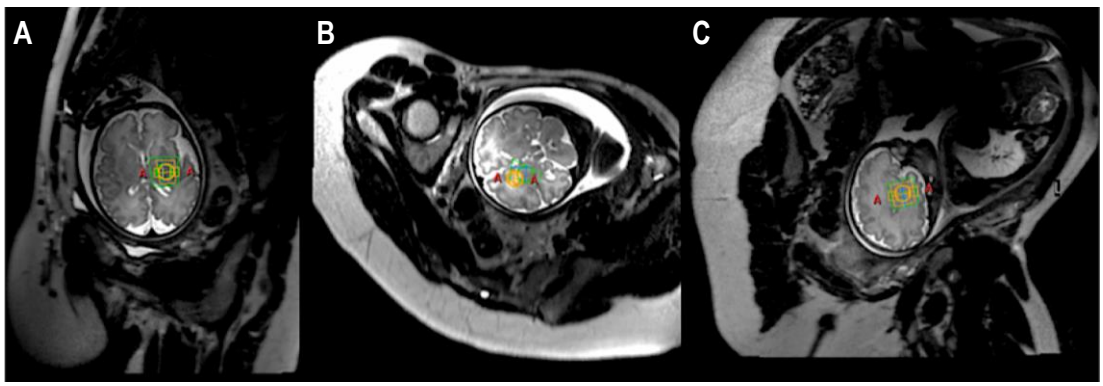

Figure 2.7: Voxel placement in a fetal ^{1}HMRS PRESS sequence.
This image was acquired from a fetus at 31^{+6} gestational weeks. The 20x20x20 mm voxel, indicated by the green box, was placed in the fetal brain region of the left basal ganglia. Voxel placement is shown in the **(A)** transverse, **(B)** coronal, and **(C)** sagittal planes.

Table 2.2: Fetal imaging parameters

Parameters	Survey	BBFE Cine	T2ssTSE UTERUS	T2ssFSE	SNAPIR	PRESS 55	PRESS 144
TE (ms)	87	2.4	140	180	12	55	144
TR (ms)	8000	4.9	1022	35000	35000	1500	1500
Flip angle (deg.)	90	60	90	90	180	90	90
Acquisition voxel size (mm)	3.03x3.01x10	2.19x2.21x30	1.08x1.98x4	1.25x1.25x2.50	1.00x1.01x4	-	-
Slice gap (mm)	3	0	0	-1.25	0	-	-
Reconstructed voxel size (mm)	0.93x0.93x10	1.25x1.25x30	0.84x0.84x4	1.18x1.18x2.50	0.96x0.97x4	-	-
FOV (mm)	400x400	500x500x30	430x430x160	320x340x100	320x340x128	-	-
SAR (W/Kg)	0.4	0.7	0.7	0.7	0.6	0.4	0.4

Note: The Survey is a rapidly acquired sequence, which ensures that the fetal brain is within field of view. The T2-weighted single shot Turbo Spin Echo of the Uterus (T2ssTSE UTERUS) and the T1-weighted Snapshot Inversion-Recovery (SNAPIR) are mainly used for radiologic reporting. The Balanced Fast Field Echo Cine Soft Tone (BBFE Cine) sequence is useful for confirming fetal and cardiac motion, but here, it was mainly acquired for the parents. As part of this thesis, volumetric analysis was completed using a 3D reconstruction of the transverse, coronal, and sagittal T2-weighted dynamic single shot Fast Spin Echo (T2ssFSE) sequences. Spectroscopic analysis was based on the point resolved spectroscopy (PRESS) sequences acquired at 55 ms and 144 ms, with a 20x20x20 mm voxel placed in the fetal region of the left basal ganglia. Abbreviations: TE = echo time; TR = repetition time; FOV = field of view; SAR = specific absorption weight.

2.3.5.1.2. Radiologic review

At the end of each scanning session, a neuroradiologist (MR, OC, KP, and SA) reviewed all of the acquired images in order to assess fetal development and to screen for any potential incidental findings. The radiologic review included assessment of brain structures, but also of the orbits (including the lenses and optic nerve), teeth, ears, and pituitary stalk. Apart from assessing the general appearance of these regions, the following measurements were also taken: biparietal diameter, transcerebellar diameter, vermis height, pons diameter, post horn diameter of lateral ventricles, cavum septum pellucidum width, and globe diameter. Normal measurements were considered to be between the 5th and 95th centile for any given gestational age (to access the Departmental fetal centile calculator, please visit https://www.developingbrain.co.uk/fetalcentiles/). In cases where abnormalities were identified, the expectant mother was informed; her general practitioner and/or obstetrician was also contacted directly by the clinician responsible for the case.

2.3.5.1.3. Spectroscopic analysis

^{1}HMRS data was analysed in precisely the same manner for all three imaging timepoints, and therefore, it will be described in detail later on (please see section 2.3.5.4 on page 142).

2.3.5.1.4. Structural analysis

2.3.5.1.4.1 Image post-processing

Before the structural T2ssFSE images could be segmented, a 3D volumetric reconstruction of the acquired scans was produced using the Snapshot MRI with Volume Reconstruction (SVR) technique, developed in the department (Kuklisova-Murgasova et al., 2012). Since fetal motion poses a major challenge in imaging, the acquisition time of the T2ssFSE images was set at less than one second per slice. This allowed for the freezing of motion in time and ensured, as much as possible, that movement could only be observed between slices. In addition, acquisition was also performed with overlapping slices, in order to oversample and ensure full coverage of the fetal brain. In total, a series of eight T2ssFSE sequences were

acquired across all three orthogonal planes (Figure 2.8A), with imaging parameters as previously described (see Table 2.2).

Once acquisition was complete, an automated script split the acquired sequences into their constituent loops, with each sequence typically comprised of two loops. Then, in order to ensure adequate image quality, all individual loops were manually reviewed on the Image Registration Toolkit (IRTK). Image loops that had been seriously corrupted by motion artefacts or where the anatomical detail had been lost were removed from subsequent post-processing steps. For each of the remaining loops, four landmarks were manually selected on IRTK; these included the top of the brainstem, bottom of the brainstem, left eye, and right eye. Subsequent to this, an image loop with full brain coverage and with the least motion corruption was selected as a template. Transformations that adjusted the orientation of the individual loops to the template loop were calculated using the previously selected landmarks. Then, the region of the fetal brain was manually segmented on the template loop using ITK-SNAP, to create a brain mask that excluded most of the maternal tissue.

Next, the selected loops, transformations aligning these loops to the template loop, and the fetal brain mask, were used as an input to the reconstruction software (Kuklisova-Murgasova et al., 2012). Registration was performed under the assumption that the fetal brain underwent unknown motion during scanning, but did not change in shape or size, and so could only experience rigid body motion. Initially, a volumetric registration of the individual loops to the template loop was performed, so that the manually created template mask could be used to crop the loops and remove the maternal tissue. At this time, an initial estimate of the volume was also reconstructed.

Although T2ssFSE sequences tend to freeze fetal motion in time, it is possible that a few slices may exhibit artefacts due to sudden fetal motion. This is evident especially at earlier gestations when the fetus is still able to move freely because of a disproportionate amount of amniotic fluid relative to fetal size. Hence, the reconstruction algorithm ensured that all slices

with motion artefacts were automatically identified using robust statistics, and excluded from the reconstruction process. Then, the algorithm interleaved slice-to-volume registration with volumetric reconstruction for a fixed number of iterations, while increasing the number of free registration parameters at each iteration. This meant that motion correction was performed by slice-to-volume registration of the acquired slices to the latest estimate of the reconstructed volume. During the last iteration, each acquired slice was registered to the reconstructed volume separately, in order to fully recover inter-slice motion. Altogether, the algorithm performed interleaved motion-correction, rejection of slices corrupted by motion, intensity correction, and volumetric reconstruction of fetal brain T2ssFSE images.

At times, the final reconstruction result was not perfectly orientated. In these instances, manual input using IRTK was required to minimally orientate the fetal brain, so that the final volume was appropriately displayed in the orthogonal plane – with transverse, coronal, and sagittal projections (Figure 2.8B). Ensuring a correct orientation was particularly important in order to achieve high reproducibility and homogeneity between subjects.

The final step in post-processing was to resample the reconstructed brain. The voxel size of the final reconstructed brain (0.75x0.75x0.75 mm) was far too large for an accurate volumetric segmentation, mainly because the analysis would be prone to errors driven by partial volume misclassifications. Therefore, the voxel size of the reconstructed and oriented image was converted from 0.75x0.75x0.75 mm to 0.20x0.20x1.00 mm (Figure 2.8C). This specific voxel size was chosen as it provided high image resolution and a feasible number of slices for manual segmentation (that is, approximately 100 slices in the transverse plane).

Image post-processing of a single participant (including registration, reconstruction, orientation, and resampling) took, on average, two hours to complete. The final product of the volumetric reconstruction yielded a 3D fetal brain of full coverage, with high resolution and SNR. This allowed for the fetal brain to be viewed with equal detail and quality in all three orthogonal planes, ensuring an optimal starting point for a reliable volumetric segmentation.

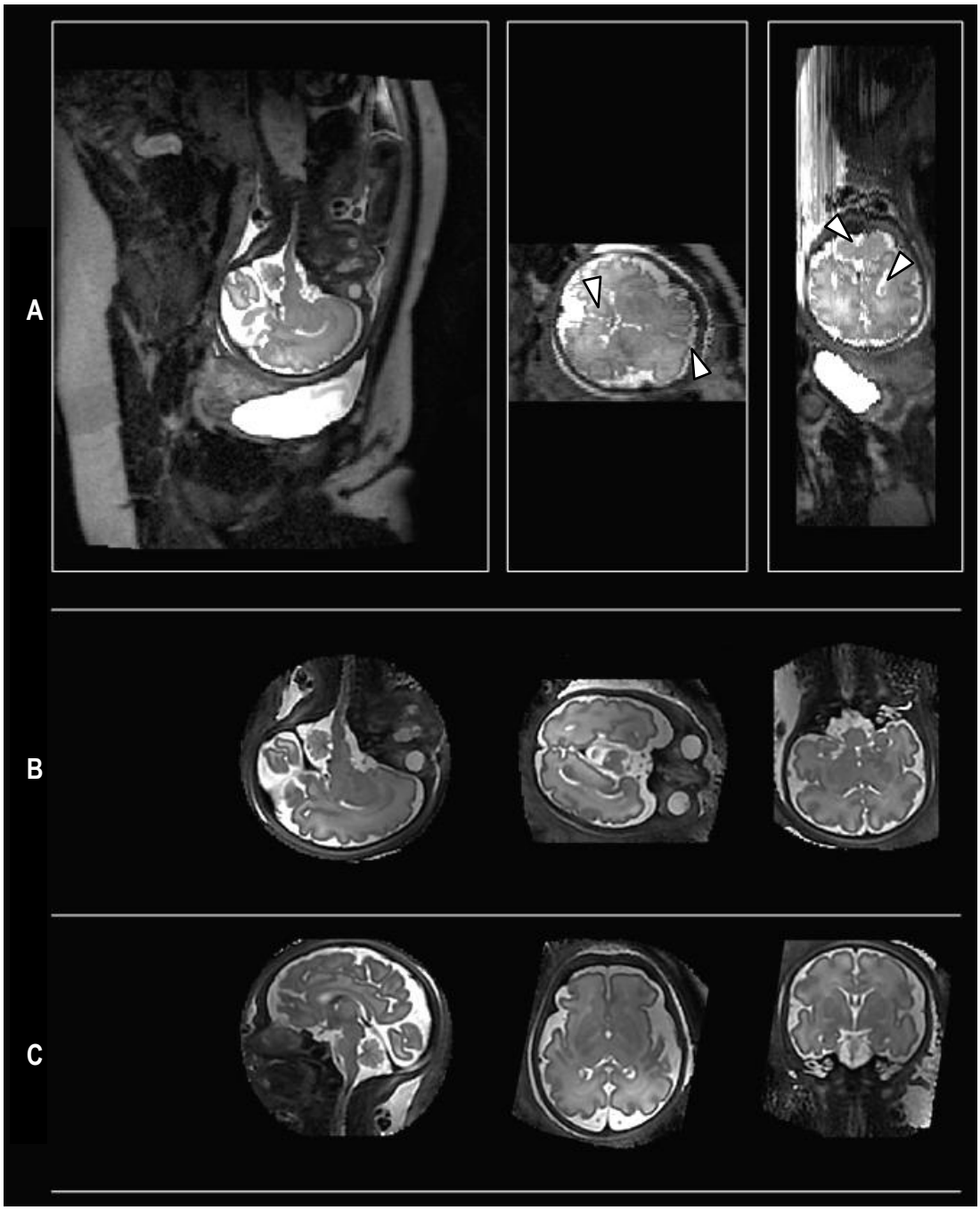

Figure 2.8: Post-processing of fetal T2-weighted images

Section **(A)** presents a single loop of a T2ssFSE sequence acquired in the sagittal plane from a fetus at 31^{+4} gestational weeks. Notice how the slices are corrupted by fetal motion, with missing data represented by a series of dark lines in both the transverse and coronal planes (see arrowheads). In **(B)** the panel below, a reconstructed image of a 3D fetal brain, oriented in the orthogonal plane, is shown. The final panel **(C)** illustrates the oriented brain, which has been resampled to a voxel size of 0.2x0.2x1.0 mm, and is optimal for volumetric segmentation.

2.3.5.1.4.2 Volumetric segmentation

Once the full reconstruction was complete (Figure 2.9), volumetric segmentations were performed on ITK-SNAP (Yushkevich et al., 2006), which enables all three orthogonal planes to be segmented simultaneously. Although the software was originally designed for adult medical images, an analysis protocol was developed-in-house to ensure that the fetal brain would be segmented reliably (Kyriakopoulou et al., 2014, 2016; Vatansever et al., 2013).

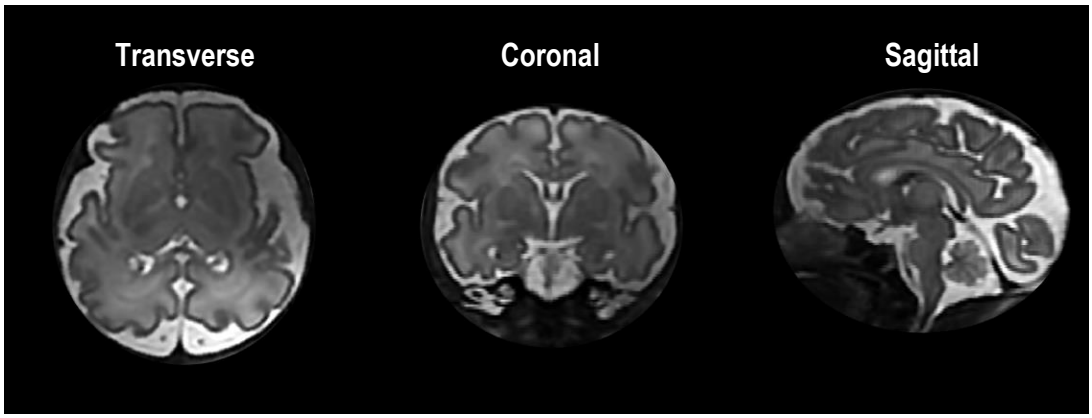

Figure 2.9: The 3D reconstructed brain of a fetus at 34^{+1} gestational weeks.

Manual segmentations are still the 'gold-standard' in fetal brain imaging; however, by making use of ITK-SNAP's semi-automated technique, the developed protocol attempted to minimise manual labour as much as possible. This was feasible through the active contour evolution of ITK-SNAP, which relies on the fact that different brain structures have different contrast intensities. First, by visually assessing the image, upper and lower intensity thresholds were established and manually defined for each region-of-interest. Once the threshold parameters had been set, active 'bubbles' were placed on strategic location within the region. Then, by making use of the active contour evolution, it was possible to visualise the automatic expansion of the bubbles evolve from a rough estimate to a very close approximation of the region-of-interest.

Contour evolution is governed by the velocity of expansion, which depends on the shape and size of the bubbles created, as well as on the intensities of the neighbouring voxels. The ITK-SNAP software allows for the user to define the velocity of the contour evolution. It also

enables for the process to be viewed in real-time, which ensures a greater control of the segmentation, compared to more fully automated techniques in which only the end-result is available to the user. According to the fetal segmentation protocol, once the process of contour evolution had been stopped, any errors of the semi-automated technique were corrected in order to optimise accuracy. Editing of the segmentation was performed manually using a pen-tablet interface (Intuos Pro, Wacom, Japan), with the rater amending any erroneously segmented voxels in order to arrive at the final segmentation (Figure 2.10).

The entire segmentation process was conducted on the transverse plane by investigators who were blind to infant risk group. More details on workload distribution and rater reliability are provided later on (please see pages 126-127). The transverse plane was chosen because it provided the highest image quality and contrast resolution, as well as the best delineation of the anatomy. Accuracy of the segmentations was confirmed on both sagittal and coronal planes. Once complete, the volume of the region-of-interest was automatically calculated in cm^3 on ITK-SNAP, through multiplication of the segmented area by the thickness of each slice. The following regions were segmented: lateral ventricles, third ventricle, fourth ventricle, cerebellum, pons, extracerebral CSF, supratentorial brain tissue, and cortex (see Table 2.3 for a detailed description of the anatomical boundaries).

As was done at the infant timepoint, some additional measures were also calculated. These included: intracranial volume (defined as the sum of all regions), total brain tissue (which included all brain matter but excluded CSF-filled spaces), and total CSF (comprising extracerebral CSF and ventricles). Moreover, since the subcortical region (including basal ganglia and thalami) is consistently implicated in ASD (Calderoni et al., 2014; Estes et al., 2011), but was not segmented at the fetal timepoint, I subtracted the volume of the cortex from the volume of the supratentorial tissue, to calculate a composite measure of the supratentorial white matter and subcortical grey matter tissue. Although not perfect, this index was used as an approximation of the subcortical volume, to try and assess the development of the subcortical region.

Table 2.3: A description of the anatomical boundaries used for fetal segmentation

Brain region	Description of anatomical boundaries
Lateral ventricles	Aside from both right and left lateral ventricles, the volume of this region also included the choroid plexuses. It excluded the cavum septum pellucidum and cavum vergae, which are anatomically separated from the lateral ventricles by the septal leaves.
Third ventricle	This region was delimited longitudinally by the anterior and posterior commissures, laterally by the thalami, and superiorly by the cavum septum pellucidum.
Fourth ventricle	The fourth ventricle was defined superiorly by the superior medullary velum, and inferiorly by the obex. The circumferential boundaries of the fourth ventricle were defined anteriorly by the pons, laterally by the middle cerebellar peduncles, and posteriorly by the vermis.
Cerebellum	The CSF surrounding the cerebellum defined its posterior, inferior, and lateral boundaries, while the superior boundary was determined by the inferior extent of the cerebrum. The cerebellar hemispheres and the vermis were included in the segmentation.
Pons	The pons was anteriorly defined by the pre-pontine cistern, and posteriorly by the inferior cerebellar peduncles and fourth ventricle. The superior and inferior boundaries were based on visualisation of the pontine bulge, most easily identified on the sagittal plane.
Extracerebral CSF	This region included all of the intracranial CSF space surrounding the supratentorial brain tissue and cerebellum; it also included the interhemispheric fissure space. It excluded the cavum septum pellucidum and the cavum vergae. The CSF borders were marked by the difference in intensity between the CSF and the skull, as well as the CSF and the cortex. The cisterna magna (included in the segmentation) and the spinal cord canal defined the inferior boundary of this region.
Supratentorial tissue	The volume of this region included grey and white matter brain tissue, but it excluded the intracerebral CSF, choroid plexuses, cerebellum, and brainstem structures below that of the pons.
Cortex	All cortical grey matter between the outer cortical border (at the boundary of the CSF and cortex) and the inner cerebral cortex (at the boundary of the cortex and the white matter) was included.

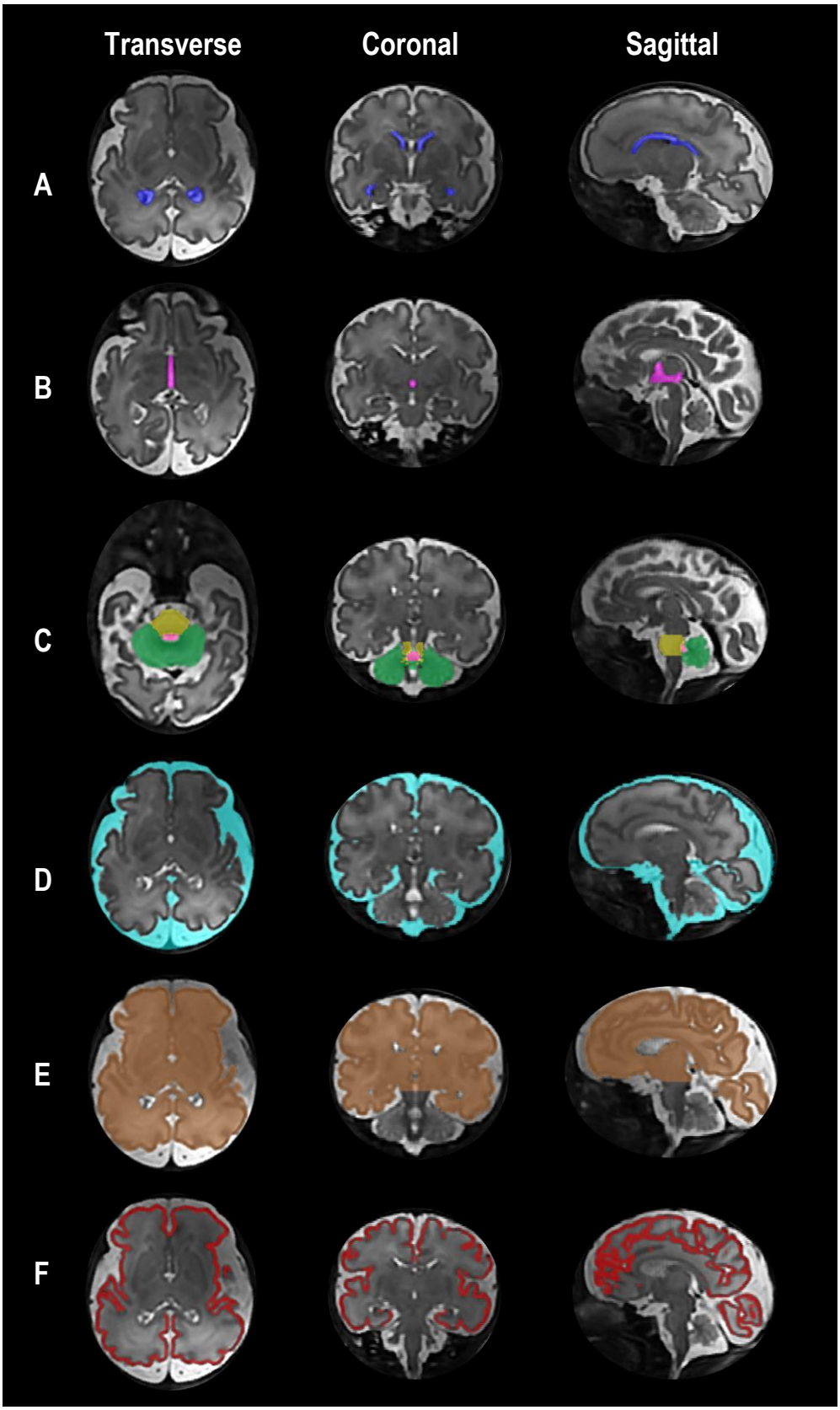

Figure 2.10: Volumetric segmentation of a 3D reconstructed fetal brain at 34^{+1} gestational weeks. (A-F) Volumetric segmentations of the **(A)** lateral ventricles, **(B)** third ventricle, **(C)** posterior fossa, including cerebellum (in green), pons (in yellow), and fourth ventricle (in pink), **(D)** extracerebral CSF, **(E)** supratentorial brain tissue, and **(F)** cortex.

The region of the cortex was the hardest to segment, largely due to its convoluted appearance. Furthermore, not all cortical areas were clearly visualised in all fetal images, either due to the reconstructed image quality, or because the limits surrounding the developing structures were unclear. As a result, a specific segmentation protocol was designed to ensure consistent segmentations, irrespective of the reconstructed image quality and fetal gestational age. Specifically, the protocol defined strict rules of what to do when dealing with uncertain cortical areas.

The following rules were applied:

(i) The cingulate gyrus was segmented up until the first convolution from the corpus callosum (Figure 2.11A).

(ii) The cortical regions surrounding the interhemispheric fissure were segmented, even in the presence of low-signal intensity (Figure 2.11B).

(iii) The parieto-occipital sulcus was segmented up until the medial aspect of the hippocampus isthmus (Figure 2.11C).

(iv) The calcarine sulcus was segmented in its entirety, including the deep convolutions present in fetuses of older gestational ages (Figure 2.11D).

(v) The cortex surrounding the inferior part of the frontal lobes was not included in the segmentation due to a consistently compromised visualisation of this region, driven by partial volume of the frontal lobes, orbits, and nasal cavity (Figure 2.11 E and F).

Owing to the design of this segmentation protocol, some cortical areas had to be excluded despite being visualised. As a result, the cortical volumes provided in this thesis are most likely an underestimation of the true value. Nonetheless, whatever underestimation error does exist is present equally in both groups, and therefore, should not affect the results.

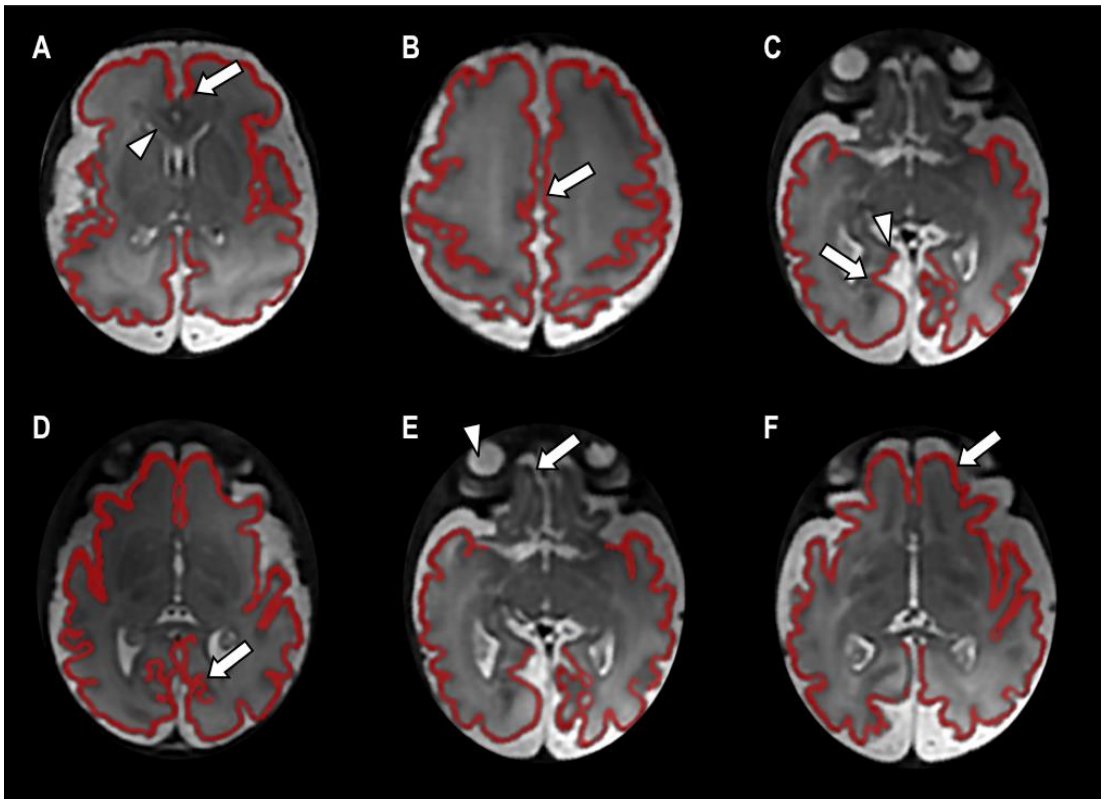

Figure 2.11: A representation of the cortical segmentation rules used when segmenting a reconstructed fetal brain. (A) The cingulate gyrus (arrow) was segmented up until the first convolution from the corpus callosum (arrowhead). **(B)** The cortical regions surrounding the interhemispheric fissure (arrow) were segmented. **(C)** The parieto-occipital sulcus (arrow) was segmented up until the medial aspect of the hippocampus isthmus (arrowhead). **(D)** The calcarine sulcus (arrow) was segmented in its entirety. **(E)** The cortex surrounding the inferior part of the frontal lobes was not included in the segmentation (arrow), due to partial volume from the orbits (arrowhead); however, **(F)** slices with no partial volume, such as those immediately above, were included (arrow).

Duration of volumetric segmentations:

The duration of the volumetric segmentations varied and was largely dependent on the gestational age of the fetal brain, as well as the quality of the reconstructed image. For example, a reconstruction of poor image quality, involving a fetus of advanced gestational age, resulted in longer segmentation times. On average, the time required to segment each brain region was as follows: lateral ventricles = 30 minutes, third ventricle = 10 minutes, posterior fossa (including pons, cerebellum, and fourth ventricle) = 2 hours, extracerebral CSF = 3 hours, supratentorial tissue = 5 hours, and cortex = 6-8 hours.

Inter-rater and intra-rater reliability of volumetric segmentations:

Manual segmentation is an extremely laborious task. As a result, the fetal segmentations were performed with the help of research assistants (AD and AN) and students that I supervised (AF, CDR, JM and JS). In total there were 7 raters, including myself (IP). Some regions were segmented by a single rater while others, particularly those encompassing larger volumes, were split between two. IP segmented the lateral and third ventricles, JM and AN segmented the posterior fossa, CDR and AF segmented the supratentorial brain tissue, AD and JS segmented the cortex, and CDR and AD segmented the extracerebral CSF.

Volumetric segmentations were validated to ensure both reliability and accuracy. Hence, each rater obtained inter-rater reliability with the team, and intra-rater reliability with themselves. For inter-rater reliability, volumetric results from a test series of n = 5 cases (mean gestational age = 30.49 weeks), completed by the rater in question, were compared to the measurements obtained by an experienced member of the team. The inter-rater ICCs of each brain region suggested negligible variability between the raters and the team, with individual values as follows: lateral ventricles (IP: 0.999, $p < 0.001$), third ventricle (IP: 0.905, $p < 0.001$), fourth ventricle (JM: 0.823, $p = 0.001$; AN: 0.803, $p = 0.001$), cerebellum (JM: 0.985, $p < 0.001$; AN: 0.986, $p = 0.001$), pons (JM: 0.863, $p < 0.001$; AN: 0.934, $p = 0.016$), extracerebral CSF (CDR: 0.988, $p < 0.001$; AD: 0.999, $p < 0.001$), supratentorial tissue (CDR: 0.999, $p < 0.001$; AF: 1.000, $p < 0.001$), and cortex (AD: 0.999, $p < 0.001$; JS: 0.982, $p < 0.001$).

Then, intra-rater ICCs were also calculated from a random selection of n = 5 cases, with values confirming excellent reproducibility of segmentation by the same rater. The intra-rater ICC values of each brain region were as follows: lateral ventricles (IP: 0.987, $p < 0.001$), third ventricle (IP: 0.975, $p < 0.001$), fourth ventricle (JM: 0.983, $p < 0.001$; AN: 0.995, $p < 0.001$), cerebellum (JM: 0.981, $p < 0.001$; AN: 0.999, $p < 0.001$), pons (JM: 0.977, $p < 0.001$; AN: 0.976, $p = 0.001$), extracerebral CSF (CDR: 0.993, $p < 0.001$; AD: 0.997, $p < 0.001$), supratentorial tissue (CDR: 0.999, $p < 0.001$; AF: 0.989, $p < 0.001$), and cortex (AD: 0.997, $p < 0.001$; JS: 0.982, $p < 0.001$).

2.3.5.1.5. Other data collected at this timepoint

During the fetal timepoint, either prior to or after the MRI scan, mothers were interviewed to obtain the family's demographic information as well as the expectant mother's obstetric, medical, and psychiatric history. With permission from the mother, antenatal notes were also reviewed to confirm details.

2.3.5.1.6. Work done by others

Fetal imaging was only possible with help from the BIBS team, the radiographers at the Centre for the Developing Brain (MF and JA), and the research nurses (JK and DH). Volumetric segmentations were performed with the support of research assistants and students (AD, AN, AF, CDR, JM, and JS).

2.3.5.2. Neonatal imaging

All participants enrolled in this project by the time of the neonatal timepoint were offered an MRI scan. Eligible families who agreed to take part were booked in for an appointment within the infant's first postnatal month, and at less than 47 corrected weeks. Prior to their appointment, families were sent an information sheet re-iterating the purpose of the research and providing specific details on the practicalities of scanning at this time. On the day of the scan upon arrival to the centre, written informed consent was obtained from one of the parents on behalf of the child, and the possibility of incidental findings was discussed. A detailed metal check was also conducted to safety screen for any MRI contraindications. Then, to ensure that the infant was fit for scanning, an experienced clinician (usually a paediatrician or neonatologist) conducted a physical examination. At this point, the neonate was also weighed and his head circumference measured. He was then changed into a metal-free gown and left to feed in a darkened quiet room with his parents. Electrocardiogram electrodes were also placed on the infant's chest and a pulse oximeter was attached to his toe. These devices allowed for the heart rate, oxygen saturation, and body temperature to be recorded throughout the scan. In addition, both a research nurse and experienced clinician were present to supervise the examination at all times (Pennock, 2002).

Although neonatal scanning as part of this research project began on August 2014, due to the start of the developing Human Connectome Project (dHCP), all neonatal imaging protocols at the Centre for the Developing Brain – including that of this project – were changed in May 2015. Consequently, this thesis includes neonatal imaging data acquired from both the pre-dHCP and dHCP protocols. Moreover, since implementation of the dHCP also included optimisation of pre-scan patient preparation, two distinct preparation processes were used. Both are outlined below.

Neonatal scanning was conducted during natural sleep. If the baby awoke or showed any signs of distress, the session was immediately stopped. The entire scanning protocol lasted for approximately 60-90 minutes, and involved the acquisition of structural, spectroscopic, functional, and diffusion sequences. For the purpose of this thesis, however, only the structural and spectroscopic sequences were analysed and therefore only those will be discussed.

2.3.5.2.1. Pre-dHCP pre-scan preparation

Once asleep, neonates were swaddled in a cotton sheet and comfortably positioned in a Med-Vac Infant Immobilisation Bag (CFI Medical Solutions, Fenton, MI, USA), which provided neck support and ensured that the head was immobilised during scanning. In addition, to ensure ear protection, all neonates were fitted with mouldable earplugs made of silicone-based dental putty (President Putty, Mahwah, NJ, USA) and adhesive MiniMuff noise attenuators (Natus Medical Inc., San Carlos, CA, USA). Preparation took place on a portable MR table, and as soon as the baby was fully prepped, the table was moved into the scanning room and the neonate was transferred onto the scanning bed. In order to minimise further acoustic noise, the scanner bore was also insulated with sound attenuating foam (Ultra Barrier, American Micro Industries, Chambersburg, PA, USA). As part of the pre-dHCP, all neonates were scanned with a 32-channel adult head coil.

2.3.5.2.2. dHCP pre-scan preparation

The objective of the dHCP protocol was to obtain the best possible neonatal imaging data. Adult coils are suboptimal for scanning the neonatal brain and therefore a dedicated imaging system was developed-in-house (Hughes et al., 2016). This imaging system included a 32-channel neonatal head coil and a baby transport/positioning device (Figure 2.12). The device was designed to withstand vibrations from high gradient scans but also to be light, safe, and permitting of acoustic protection, immobilisation, and appropriate physiological monitoring.

Once asleep, neonates scanned under dHCP were placed on the transport/positioning device, which consisted of a V-shaped base (Figure 2.12A) attached to a headpiece (Figure 2.12B). Neonates were wrapped in a specially designed cotton sheet that incorporated a head extension and pull tag. The attached tag was passed through a designated hole in the headpiece and pulled to guide the head into position, with minimal disruption to the baby (Figure 2.12C; red arrow). As before, in order to ensure acoustic protection, all neonates were fitted with mouldable earplugs (President Putty, Mahwah, NJ, USA) and adhesive MiniMuffs (Natus Medical Inc., San Carlos, CA, USA). Then, three immobilisation cushions conforming to the shape of the baby's head were positioned over the ears and under the base of the head, in order to reduce further motion (Figure 2.12D).

Once the baby's head was securely positioned as confirmed by visual inspection through the two additional holes in the headpiece (Figure 2.12B), the Med-Vac Immobilisation Bag (CFI Medical Solutions, Fenton, MI, USA) was adjusted to the baby's body using vacuum air removal. To prevent lateral movement of the body independent of the head, the Med-Vac was locked into the V-shaped base. Finally, the 32-channel neonatal head coil was slid over the baby's head. An acoustic hood (Ultra Barrier, American Micro Industries, Chambersburg, PA, USA), which allowed for circulation of air to the baby, was placed on top.

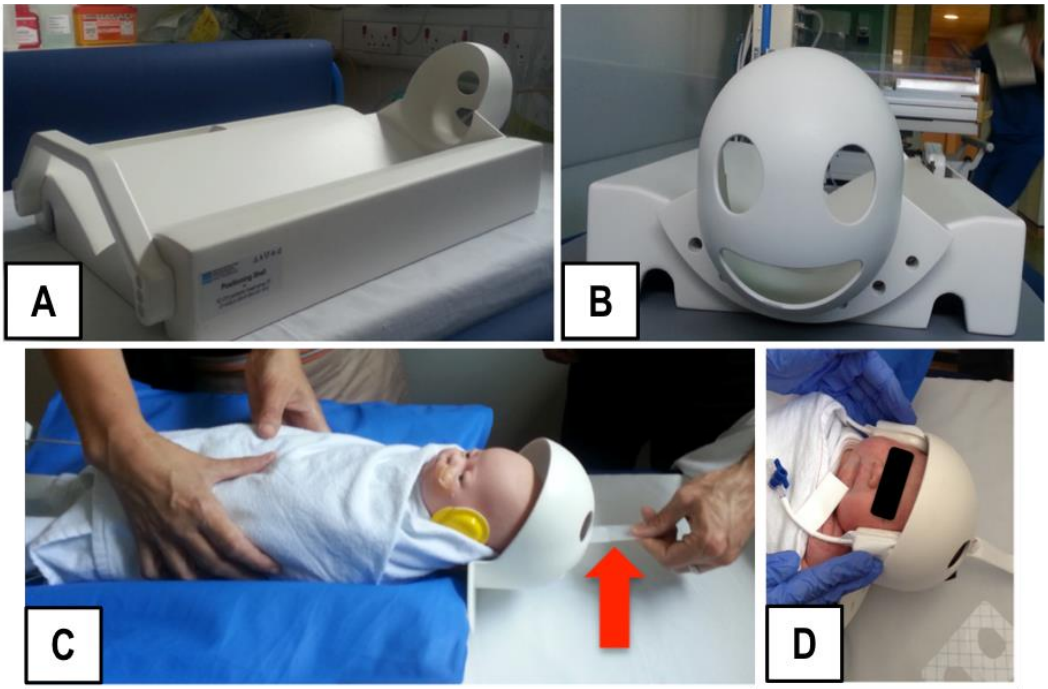

Figure 2.12: The dHCP neonatal imaging system. The system includes a 32-channel neonatal head coil and a transport/positioning device, consisting of **(A)** a V-shaped base and **(B)** a headpiece. Neonates are wrapped in a specialised cotton sheet, which is attached to a pull tag. The pull tag is passed through a hole in the headpiece and **(C)** pulled to guide the neonatal head into position, as shown by the red arrow. **(D)** Three immobilisation cushions are positioned to ensure minimal head movement. Image adapted from Hughes et al., (2016).

2.3.5.2.3. Image acquisition

A detailed description of the structural and spectroscopic sequences, for both pre-dHCP and dHCP protocols, are included below.

T1- and T2-weighted Structural Sequences: A T1-weighted inversion recovery turbo spin echo (T1 IR-TSE) and a T2-weighted multishot turbo spin echo (T2 TSE) sequence was acquired for both pre-dHCP and dHCP protocols. These sequences were obtained in both transverse and sagittal planes – with the exception of the T1 IR-TSE sequence, which when conducted under pre-dHCP, was only acquired in the transverse plane. Imaging parameters also differed slightly between the two protocols and therefore these have been provided in separate tables (Table 2.4 and 2.5). The T2-weighted sequences were reconstructed and used for volumetric segmentation, whilst the T1-weighted sequences were mainly used for radiologic assessment.

Table 2.4: Neonatal pre-dHCP structural imaging parameters

Parameters	T1 IR-TSE (transverse)	T2 TSE (transverse)	T2 TSE (sagittal)
TE (ms)	8.0	156	156
TR (ms)	4795	10000	10000
Flip angle (deg.)	90	90	90
Acquisition voxel size (mm)	1.01x1.01x2.00	1.01x1.01x2.00	1.01x1.01x2.00
Slice gap (mm)	-1.00	-1.00	-1.00
Number of slices	100	100	112
Reconstructed voxel size (mm)	0.45x0.45x2.00	0.45x0.45x2.00	0.45x0.45x2.00
FOV (mm)	145X120.8X101	145x120.8x101	145x145x113
SENSE factor	1.1300	1.3200	1.2500
TSE factor	7	12	12
SAR (W/Kg)	0.1	0.2	0.2

Note: The T2-weighted sequences were reconstructed and used for volumetric segmentation, whereas the T1-weighted sequences were mainly used for radiologic assessment. Abbreviations: T1 IR-TSE IR = T1-weighted inversion recovery turbo spin echo; T2 TSE = T2-weighted multishot turbo spin echo; TE = echo time; TR = repetition time; FOV = field of view; SENSE = SENSitivity Encoding; TSE = turbo spin echo; SAR = specific absorption rate.

Table 2.5: Neonatal dHCP structural imaging parameters

Parameters	T1 IR-TSE (transverse)	T1 IR-TSE (sagittal)	T2 TSE (transverse)	T2 TSE (sagittal)
TE (ms)	8.7	8.7	156	156
TR (ms)	4795	4795	12000	12000
Flip angle (deg.)	90	90	90	90
Acquisition voxel size (mm)	0.81x0.81x1.60	0.81x0.81x1.60	0.81x0.81x1.60	0.81x0.81x1.60
Slice gap (mm)	-0.80	-0.80	-0.80	-0.80
Number of slices	125	134	125	134
Reconstructed voxel size (mm)	0.43x0.43x1.60	0.43x0.43x1.60	0.45x0.45x1.60	0.45x0.45x1.60
FOV (mm^3)	144x121.6x100	144x144x107.2	144x116.8x100	144x144x107.2
SENSE factor	2.1714	2.5714	2.0278	2.5999
TSE factor	7	7	12	12
SAR (W/Kg)	0.1	0.1	0.2	0.2

Note: The T2-weighted sequences were reconstructed and used for volumetric segmentation, whereas the T1-weighted sequences were mainly used for radiologic assessment. Abbreviations: T1 TSE IR = T1-weighted inversion recovery turbo spin echo; T2 TSE = T2-weighted multishot turbo spin echo; TE = echo time; TR = repetition time; FOV = field of view; SENSE = SENSitivity Encoding; TSE = turbo spin echo; SAR = specific absorption rate.

Point Resolved Spectroscopy (PRESS): To enable quantification of different metabolites and to allow for comparison with data acquired at the fetal timepoint, neonatal ^{1}HMRS was obtained with PRESS sequences acquired at two separate echo times: 55 ms and 144 ms. Prior to data acquisition, a 20x20x20 mm voxel was placed on the region of the left basal ganglia, avoiding any CSF-filled spaces (Figure 2.13). Imaging parameters were exactly the same for both pre-dHCP and dHCP protocols, as follows: TR = 1500 ms, TE = 55 or 144 ms, flip angle = 90°, and SAR = 0.0 W/Kg. Acquisitions were performed using water suppression.

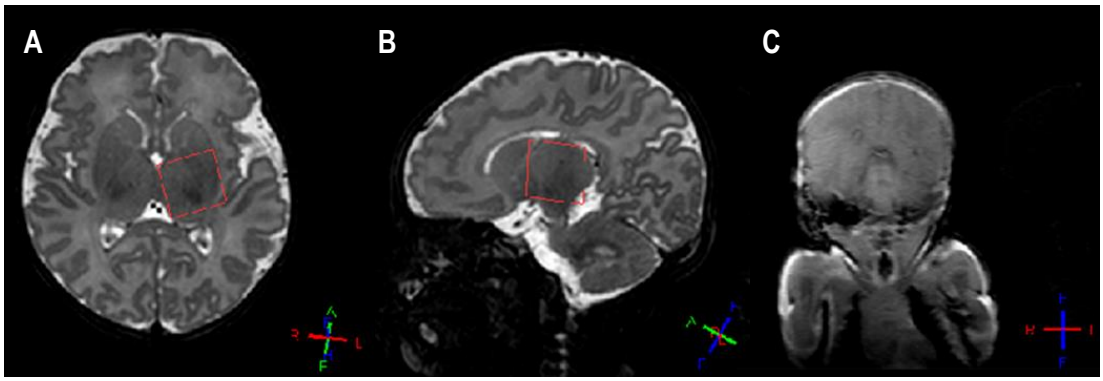

Figure 2.13: Voxel placement in a spectroscopic neonatal PRESS sequence.
This image was acquired from a neonate scanned at 43^{+4} corrected weeks. The 20x20x20 mm voxel, indicated by the red box, was placed on the region of the left basal ganglia. Voxel placement is shown in the **(A)** transverse and **(B)** sagittal planes, with the neonate lying in a **(C)** fixed supine orientation.

2.3.5.2.4. Radiologic review

At the end of each scanning session, a neuroradiologist (MR, OC, KP, and SA) reviewed all of the acquired images to assess brain development and screen for any potential incidental findings. The neonatal review was conducted in much the same way as the fetal one, but due to the timepoint in question, there was a greater focus on assessing the progress of myelination. If any incidental findings were identified, the participant's parents and general practitioner were contacted directly by the clinician responsible for the case.

2.3.5.2.5. Spectroscopic analysis

A full description of the ^{1}HMRS data analysis will be provided later on (please see section 2.3.5.4 on page 142).

2.3.5.2.6. Structural analysis

2.3.5.2.6.1 Image post-processing and volume reconstruction

Although neonatal imaging was conducted during natural sleep, it was common for sporadic movements to occur, even if the neonate was deeply settled. Moreover, multislice multishot imaging as was acquired at this timepoint, tends to be particularly vulnerable to motion artefacts (Andre et al., 2015). In an uncorrected image (Figure 2.14A), for example, motion artefacts and signal variations are frequently observed from slice-to-slice. Therefore, before the structural T2 TSE images could be segmented, a 3D motion corrected reconstruction was applied to the acquired images (Cordero-Grande et al., 2016). This reconstruction process estimated the motion states corresponding to the acquired shots and slices to ensure that both within-plane and through-plane motion were dealt with (Cordero-Grande et al., 2016). As part of the methodological pipeline, motion corrected reconstructions were first applied to the transverse and sagittal views independently. Upon successful reconstruction, artefacts tended to be fully or almost fully resolved, and the quality of the overall image was substantially improved without introducing any major side effects (Figure 2.14B).

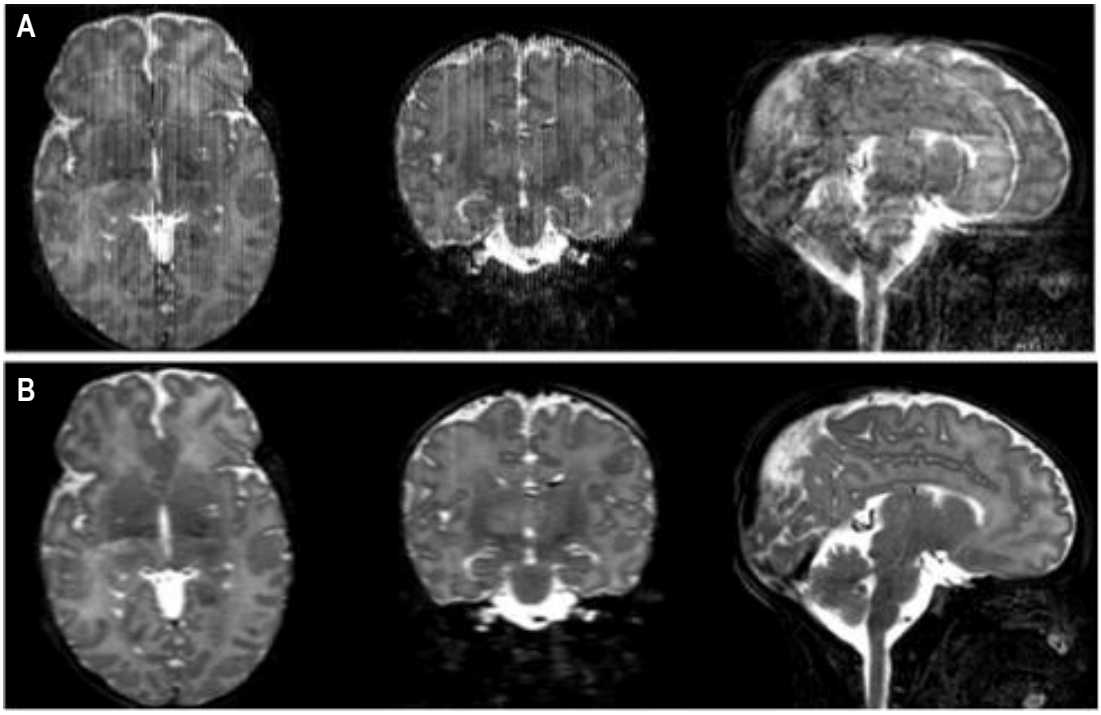

Figure 2.14: Applying motion corrected reconstruction to a sagittal T2 TSE neonatal volume. (A) Uncorrected versus **(B)** motion corrected reconstruction of a T2 TSE sagittal volume, with all three orthogonal views (transverse, coronal, and sagittal) shown from left to right. This image has been obtained from Cordero-Grande et al., (2016).

Once each view had been independently reconstructed, the two views were assembled by slice-to-volume registration (Kuklisova-Murgasova et al., 2012), based on the methodology applied at the fetal timepoint. By correcting for rigid motion within structural scans, the final result yielded a motion-free reconstruction with high resolution and SNR (Figure 21.5), allowing for optimal tissue segmentation. The reconstruction process was conducted in the exact same way for both pre-dHCP and dHCP images. Depending on the extent of motion present in the original images, the process could take between 30 minutes to 3 hours of computational time.

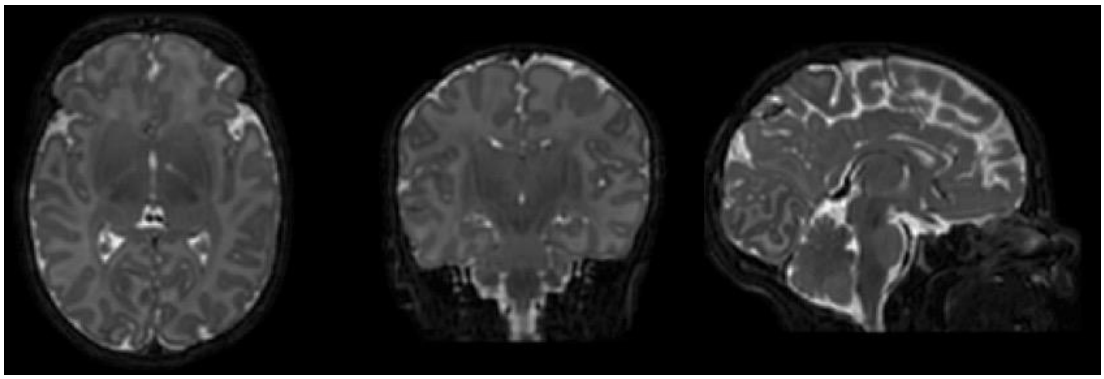

Figure 2.15: Final reconstruction of a neonatal brain acquired at 42^{+2} corrected weeks. Once the transverse and sagittal views had been independently reconstructed, the two views were assembled by slice-to-volume registration. The final reconstruction is displayed above, with all three orthogonal views (transverse, coronal, and sagittal) shown from left to right.

2.3.5.2.6.2 Volumetric segmentation

Once the 3D motion corrected reconstruction was complete, the neonatal images were segmented. Segmentation was performed using Draw-EM (Developing Brain Region Annotation with Expectation-Maximisation; https://github.com/MIRTK/DrawEM) – an open-source software for neonatal brain segmentation developed-in-house based on methods proposed by Makropoulos et al. (2014).

As part of the segmentation process, the first step was to conduct a brain-extraction of the T2 reconstructed image to remove any non-brain tissue (Smith, 2002). Only then was the reconstructed image corrected for intensity inhomogeneity (Tustison et al., 2010). After this, in

order to compute a GMM probability map of the image, initial tissue segmentation was performed. Then, predefined atlases were registered to the subject's target image by using a multi-channel registration that incorporated the image intensity and the GMM probability map. The atlas labels were transformed and averaged according to the similarity between the atlas and the target image. Draw-EM utilises manually segmented atlases (Gousias et al., 2012), incorporating multiple labels and spanning an age-range of 36 to 44 corrected weeks. After registering theses atlases to the individual target images, a spatial prior probability of the different brain structures was computed, based on the local similarity of the transformed atlases and the input target image. The final segmentation was performed with an Expectation-Maximisation algorithm, which included a spatial prior term and an intensity model of the image. The intensity model of the image was approximated with a GMM, and the spatial dependency between the brain structures was modelled with Markov Random Field regularisation. The Draw-EM pipeline also incorporated model averaging, to limit the influence of intensity in the delineation of structures with very similar contrasts. In addition, the pipeline corrected for any partial volume misclassifications, particularly prominent at CSF boundaries.

After the Draw-EM pipeline had been applied, two different segmentation outputs (with grey and white matter parts merged) were produced: the 'label' segmentation and the 'tissue' segmentation. In order to examine similar brain regions to those obtained at fetal and infant timepoints, a decision was made to focus on the tissue segmentation output, which consisted of 8 labels: white matter, cortex, subcortical grey matter (encompassing the thalamus, caudate nucleus, subthalamic nucleus, lentiform nucleus, and internal capsule), hippocampi and amygdala (segmented together), brainstem, cerebellum, lateral ventricles, and extracerebral CSF (including third and fourth ventricles) (Figure 2.16). However, since the neonatal segmentation software also produced a more detailed segmentation (the 'label' segmentation), specific brain structures commonly implicated in ASD were also selected for analysis. These included the hippocampus, amygdala, insula, thalamus, subthalamic nucleus, lentiform nucleus, caudate nucleus, and corpus callosum (Figure 2.17).

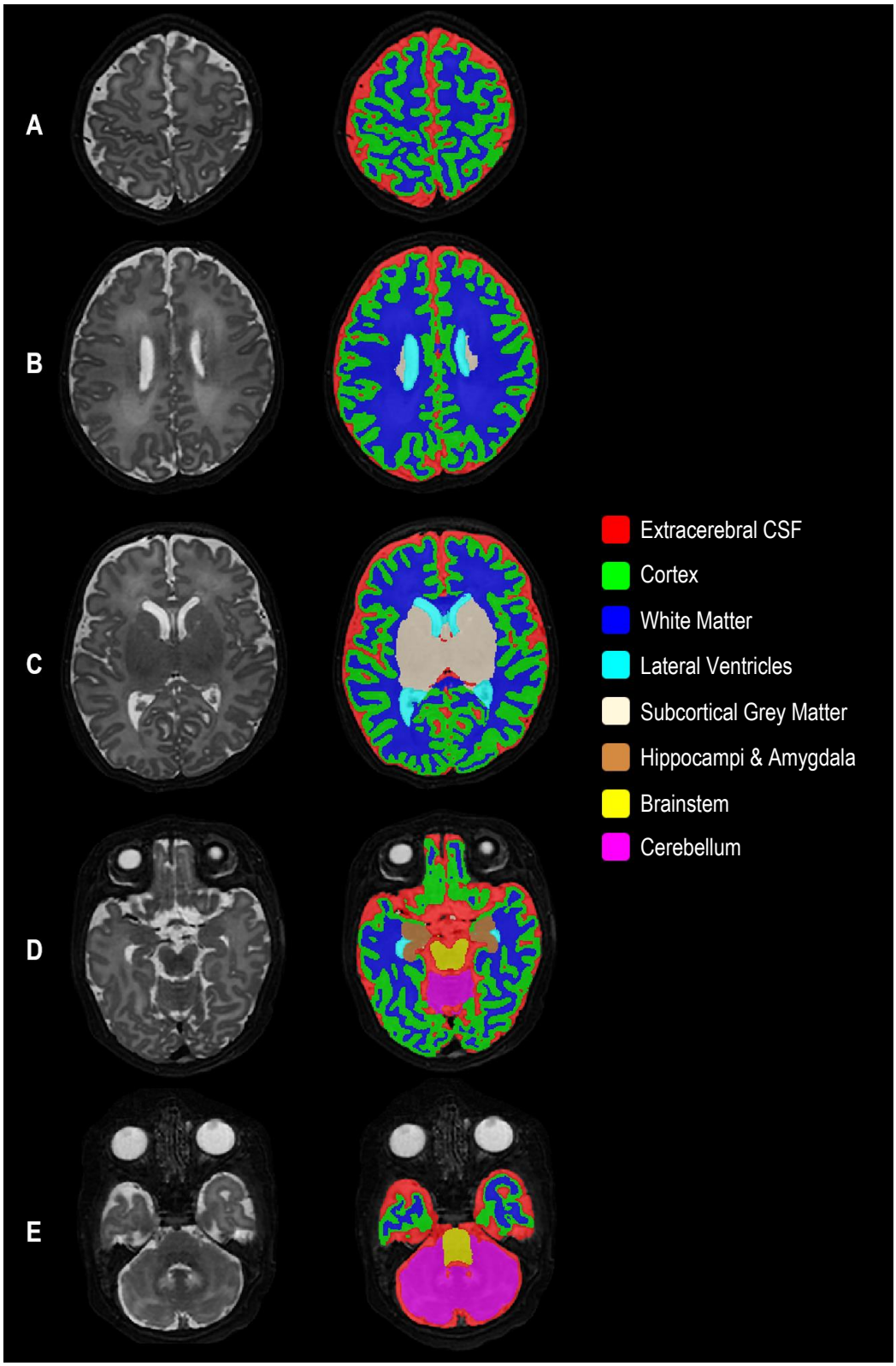

Figure 2.16: Volumetric tissue segmentation of a 3D reconstructed neonatal brain. The panel on the left includes the T2-weighted reconstructed volume, and the panel on the right includes the corresponding tissue segmentation. As we move from the anterior to the posterior brain **(A-E)**, only transverse sections are shown. **(A)** Shows extracerebral CSF, cortex, and white matter, while **(B)** exhibits the lateral ventricles and **(C)** the subcortical grey. The hippocampus, amygdala, and brainstem are shown in **(D)**, and **(E)** is mainly cerebellum.

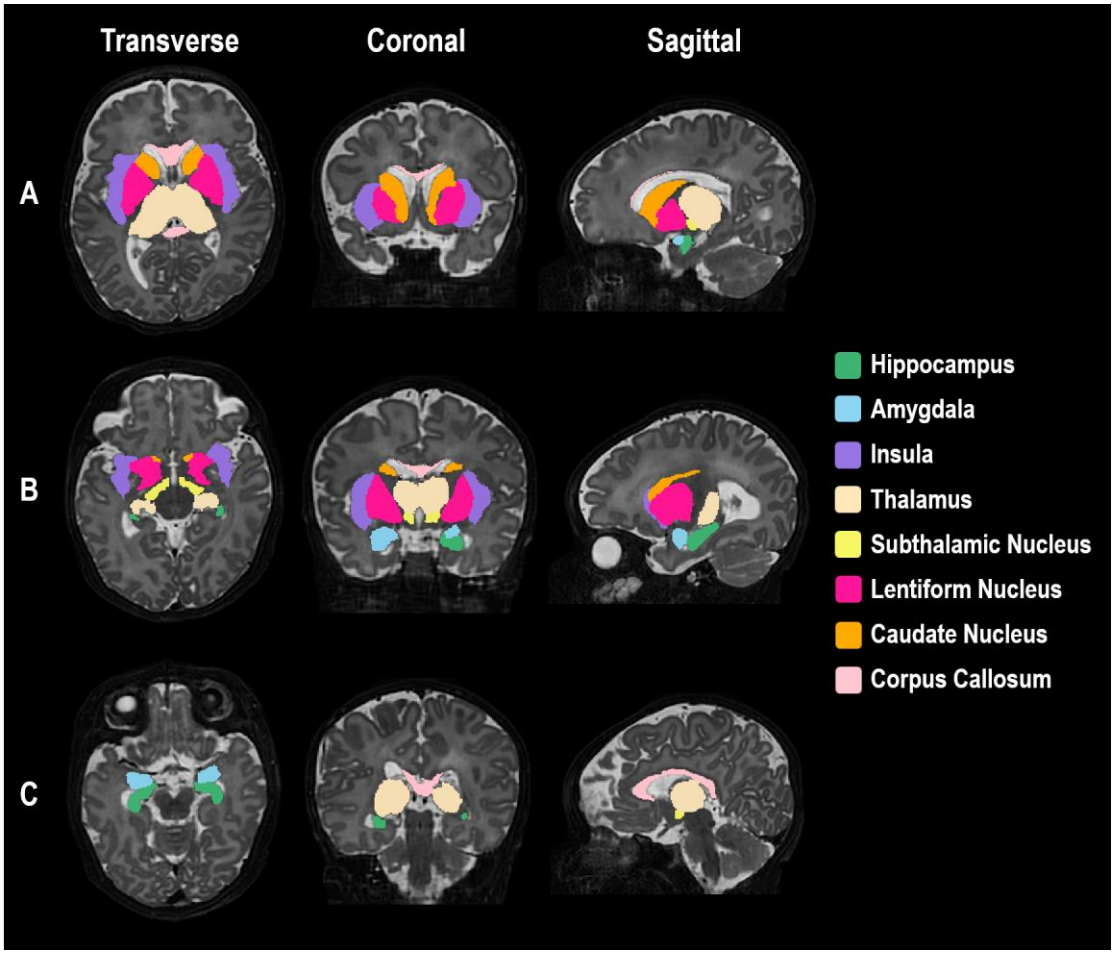

Figure 2.17: Volumetric segmentation of selected structures obtained from a 3D reconstructed neonatal brain. In this image, transverse, coronal, and sagittal views are shown. **(A)** Comprises the corpus callosum, caudate nucleus, lentiform, insula, and thalamus. **(B)** Also shows the subthalamic nucleus, while **(C)** includes the hippocampus and amygdala.

These segmentations were utilised to extract volumetric measures (in cm^3) of the tissues and specified structures of interest. As before, additional brain measures were calculated, including the volume of the intracranium, total brain tissue, and total CSF. These calculations were based on the values obtained from the tissue segmentation output. The intracranium was defined as the sum of all regions, while the total brain tissue included all brain matter but excluded CSF. The measure for total CSF included extracerebral CSF and lateral ventricles.

2.3.5.2.7. Comparison between pre-dHCP and dHCP measures

Volumetric measures: T2 image reconstruction and segmentation was performed using the exact same pipelines, for both pre-dHCP and dHCP protocols. The original images, however, were acquired using slightly different imaging parameters and different coils. As a result, small differences in volumetric measures could have arisen from the distinct methodologies. Therefore, once these measures had been quantified, an independent samples t-test was run to compare the values obtained from n = 5 neonates scanned under pre-dHCP (mean age = 43.20 corrected weeks; 2 male) and n = 5 scanned under dHCP (mean age = 43.32 corrected weeks; 3 male), with both groups matched for age (t = -0.18, p = 0.864). Since no differences were found between the regional brain volumes obtained from the two protocols (all p > 0.05), the results were merged and analysed together.

Spectroscopic measures: Despite equal pre-dHCP and dHCP PRESS parameters, the different coils used for the separate protocols meant that small differences could have arisen in the acquired spectra. Therefore, once spectroscopic analysis had been conducted (please see section 2.3.5.4 on page 142 for a detailed description of the process), an independent samples t-test was run to compare the metabolite ratios obtained from n = 5 neonates scanned under pre-dHCP (mean age = 43.23 corrected weeks; 4 male) and n = 5 scanned under dHCP (mean age = 43.20 corrected weeks; 3 male), with both groups matched for age (t = 0.05, p = 0.963). As with the volumetric measures, there were no significant differences between the metabolite ratios obtained from the two protocols (all p > 0.05). Consequently, the results from both protocols were merged and analysed together.

2.3.5.2.8. Other data collected at this timepoint

Prior to the neonatal scan, delivery summaries were reviewed to obtain more specific details not always known to the mother, but of relevance to the research. These measures included Apgar scores at 1 and 5 minutes, mode of delivery, as well as body weight and head circumference at birth.

2.3.5.2.9. Work done by others

Neonatal imaging data was acquired with the help of the BIBS team, radiographers at the Centre for the Developing Brain (MF, JA, and EH), research nurses (JW, MS, JBC, and PW), and specified clinicians (NT, CK, MK, DC, and MB). LC completed the volumetric reconstructions, whilst the automated segmentations were conducted by AM.

2.3.5.3. Infant imaging

All participants enrolled in the research project by the time of the infant timepoint were offered an MRI scan. Eligible families who agreed to take part were booked in for an appointment when the infant was aged between 50-75 corrected weeks (or at approximately 4-6 months). At this age infants are very aware of their surroundings, which makes it incredibly difficult to get them to settle down in a new environment. Therefore, the usual protocol for imaging these infants at the Centre for the Developing Brain, involves the optional use of a low dose of chloral hydrate – a very mild sedative which helps to promote sleep. To ensure that the families were given sufficient time to consider this, research nurses discussed the use of sedation prior to booking. On the day of scanning, the assigned paediatrician also discussed this option with the parents yet again. Nonetheless, as part of this study, all of the families who participated in infant imaging agreed to the use of sedation.

As at other timepoints, families were sent an information sheet re-iterating the purpose of the research and providing specific details on the practicalities of scanning at the infant timepoint. Then, upon arrival to the centre on the day of the scan, written informed consent was obtained from one of the parents on behalf of the child, and the possibility of incidental findings was discussed. A detailed metal check was also conducted to safety screen for any MRI contraindications. At this time, the parents were once again briefed on how the sedation would be administered. Although chloral hydrate has an extremely safe profile, side effects can still occur; therefore, parents were informed of the potential adverse effects, which include nausea, vomiting, and mild respiratory depression (Delgado et al., 2014; Finnemore et al., 2014). Afterwards, a routine physical examination was conducted by the case assigned

clinician, who ensured that the infant was fit for scanning and for administration of chloral hydrate. The infant was also weighed and his head circumference measured. He was then changed into a metal-free gown and left to feed with his parents.

Once ready, usually 1 hour after feeding, chloral hydrate was orally administered to the infant in a weight-dependent dose of 30-50 mg/kg. Since the medication has a bitter aftertaste, which infants find unpleasant, it was always administered alongside sucrose. Importantly, chloral hydrate is classified as a sedative rather than an anaesthetic, meaning that it merely predisposes infants to fall into natural sleep more easily. Usually, this takes approximately 15-20 minutes to take effect; therefore, as soon as the medication was administered, the parents were given some time alone to let the infant settle. Once asleep, the infant was prepped according to pre-dHCP guidelines (please refer back to section 2.3.5.2.1 on page 128). This included the fitting of electrocardiogram electrodes and a pulse oximeter, which allowed for the infant's heart rate, oxygen saturation levels, and body temperature to be monitored throughout the scan. As was done at the neonatal timepoint, both a research nurse and a clinician were present to supervise the examination. In addition, because the effect of chloral hydrate usually only lasts for 40-60 minutes, there was a chance that the infant could wake up during the scan. If this occurred, the scanning session was immediately stopped.

The entire scanning protocol lasted for approximately 60 minutes and involved the acquisition of structural, spectroscopic, and functional sequences. Post-scan, infants were monitored for 30 minutes. Parents were given a post-sedation care leaflet and were contacted 24 hours after the administration of the sedative to ensure that all was well.

For the purposes of this thesis, only the infant spectroscopic sequences were analysed and therefore only the imaging parameters of those sequences will be provided.

2.3.5.3.1. Image acquisition

Infants were scanned with a 32-channel adult head coil. Spectroscopic data was acquired in the exact same manner as it was done at the neonatal timepoint, with PRESS sequences obtained at two separate echo times: 55 ms and 144 ms. All acquisitions were performed using water suppression, and with a 20x20x20 mm voxel placed in the region of the left basal ganglia. Imaging parameters were as follows: TR = 1500 ms, TE = 55 or 144 ms, flip angle = 90°, and SAR = 0.0 W/Kg.

2.3.5.3.2. Radiologic review

Radiologic review of the acquired images was conducted in much the same way as was done at the neonatal timepoint (please refer back to section 2.3.5.2.4 on page 133 for more details). In the case of an incidental finding, the infant's' parents and general practitioner were contacted.

2.3.5.3.3. Other data collected at this timepoint

If the infant under examination had not participated in the neonatal timepoint, delivery summaries were reviewed here, to obtain all relevant information pertaining to the birth.

2.3.5.3.4. Work done by others

The imaging data collected as part of the infant timepoint would not have been possible without the help of the BIBS team, the radiographers at the Centre for the Developing Brain (MF, JA, and EH), the research nurses (JW, MS, JBC, and PW), and the relevant clinicians (NT, CK, MK, DC, and MB).

2.3.5.4. Spectroscopic analysis

Irrespective of the timepoint of acquisition (that is, fetal, neonatal, or infant), all ^{1}HMRS spectra were acquired using identical imaging parameters. This allowed for all spectroscopic data to be analysed and processed in the exact same manner, which rendered the comparisons between timepoints more accurate. The first step was to visually assess each ^{1}HMRS

spectrum in order to ensure adequate SNR and no obvious artefacts. Then, the data was analysed in a fully automated manner using the TARQUIN software version 4.3.6 (Wilson et al., 2011).

TARQUIN is a novel algorithm used to quantify ^{1}HMRS data; it is particularly suitable for the analysis of sequences acquired at short echo times. The algorithm uses a least squares approach to estimate signal amplitudes, and imposes a method of soft constraints on the projection to reduce errors associated with overfitting. In addition, baseline interference is reduced by point truncation and water peak removal in a fully automated process. Point truncation eliminates the very early points of the free induction decay, which contain very broad signals that are difficult to model; it also removes the last few points, which tend to only contain noise. Given its automated quantitation, TARQUIN ensures that user variability is eliminated (Scott et al., 2016), which made it a particularly useful tool for the analysis of the ^{1}HMRS data acquired in this thesis. Another important aspect of the TARQUIN software is that it is a robust tool for the analysis of clinical data of variable quality, having been compared favourably to other automated processes such as LCModel (Wilson et al., 2011).

When defining the quantitation settings, TARQUIN asks that a reference metabolite be chosen in order to produce appropriate phase adjustments of the data. Since the ^{1}HMRS spectrum changes considerably between the prenatal and early postnatal periods, these settings were therefore input in a slightly different manner depending on the timepoint in question. For example, given that Cho is the most abundant peak at the fetal timepoint, it was selected as the reference metabolite when analysing fetal spectra. Conversely, when analysing neonatal and infant spectra, a combination of metabolites was chosen as the reference, including NAA, Cho, and Cr. TARQUIN also provides basis sets of predefined models; however, for this analysis, the same internal basis set was used to analyse data collected at different timepoints and using different echo times.

After the automated quantitation has been concluded, TARQUIN produces a processed signal of the ^{1}HMRS spectra. A residual line is also created, with visual inspection of the line allowing for adequate SNR to be confirmed; ideally, the residual should represent a fairly homogenous line. In addition, the ^{1}HMRS signal is superimposed with a model signal from which the metabolite peaks are fitted (Figure 2.18). Only metabolites that met a reliable fit, with a standard deviation of < 25%, were included in further analyses.

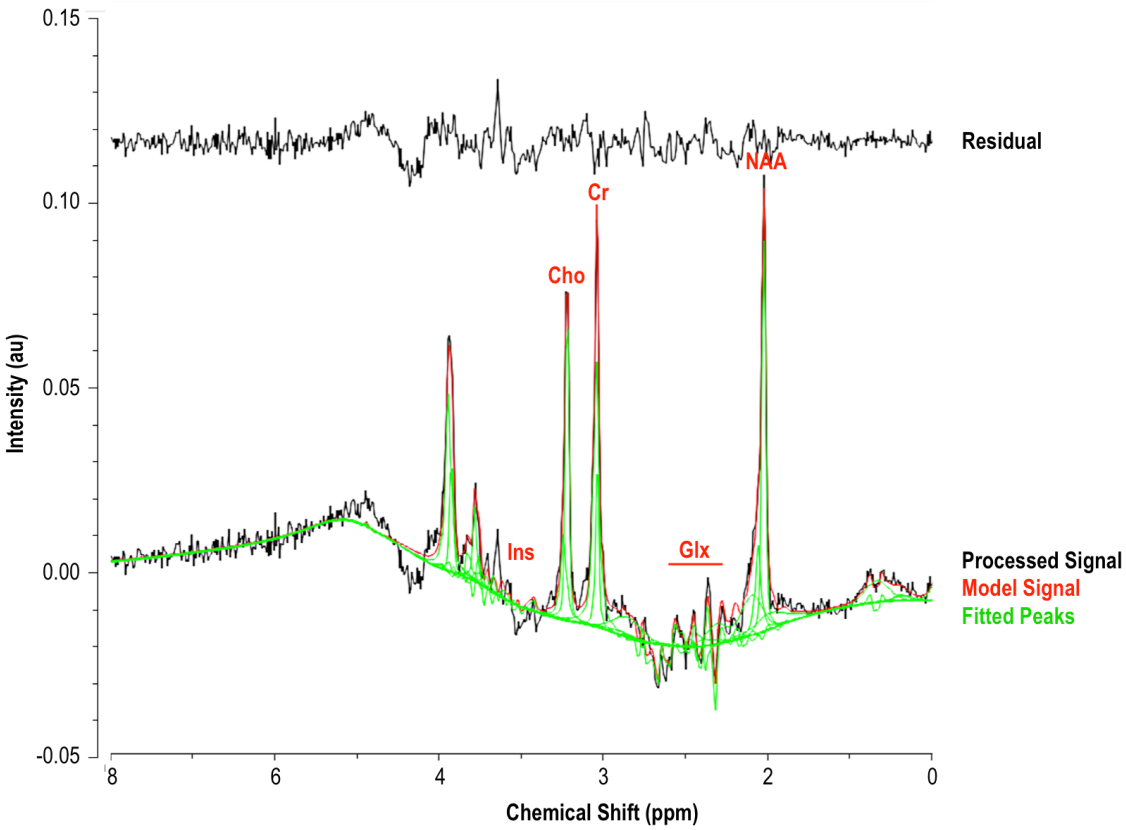

Figure 2.18: Spectroscopic analysis performed using the TARQUIN software. In this example, a 55 ms PRESS sequence acquired at the infant timepoint has been analysed. As is shown, TARQUIN has created a processed signal from the original spectra and superimposed it with a model signal, allowing for metabolites to be reliably fitted. The residual line created also enables visual inspection of SNR. Abbreviations: Ins = myo-inositol; Cho = choline; Cr = creatine; Glx = glutamate and glutamine; NAA = N-acetylaspartate.

As part of the spectroscopic analysis, the following metabolites were assessed: N-acetylaspartate and N-acetylaspartylglutamate (NAA); creatine and phosphocreatine (Cr); free choline, glycerophosphocholine, and phosphocholine (Cho); myo-inositol (Ins); and glutamate

and glutamine (Glx). Since all ^{1}HMRS acquisitions were performed using water suppression, metabolite concentrations were reported as relative ratios, expressed in relation to Cho and Cr, as follows: Cho/Cr, Ins/Cho, Ins/Cr, Glx/Cho, Glx/Cr, NAA/Cho, and NAA/Cr.

2.3.6. Power considerations and sample size estimation

As with project 1, the design of research project 2 was based on evidence suggesting that there is a 20% chance that individuals born to a sibling with ASD will themselves be diagnosed with the condition (Constantino et al., 2010; Ozonoff et al., 2011; Sandin et al., 2014). Previous studies using MRI to examine brain volume differences in 6 month-old infants at risk of ASD have reported significant results with sample sizes of 20-30 subjects per group (Blasi et al., 2015; Lloyd-Fox et al., 2013; Shen et al., 2013). However, the data acquired as part of project 2 included individuals of younger ages, scanned at fetal and neonatal timepoints. Project 2 also included ^{1}HMRS data, which has not been previously used in studies of individuals at risk. Therefore, the issue of sample size estimations was a difficult one to address here. Nonetheless, based on other studies carried out at the fetal and neonatal timepoints, examining different clinical groups (such as individuals with intrauterine growth restriction and isolated ventriculomegaly), significant group differences in brain volume and chemistry were identified with approximately 20 subjects per group (Damodaram et al., 2012; Lockwood Estrin et al., 2016). In a study more akin to the present, significant differences were identified in the brain volumes of preterm neonates with and without a later ASD diagnosis, and there were only 11 and 22 subjects in each group respectively (Padilla et al., 2015). Consequently, a minimum sample size of 15 participants per group was deemed sufficient to identify preliminary differences ($p \leq 0.05$).

Post-hoc power calculations for the main finding(s) of each study are included in Appendix 1. Effect sizes are also reported, using partial eta squared (η_p^2), and interpreted using Cohen's (1988) criteria, where $\eta_p^2 \geq 0.01$, 0.06, and 0.14 reflect small, medium, and large effects. For further details on the results of these calculations, please refer to Appendix 1 on page 255.

2.4. Analytic approach

All statistical analyses were performed using IBM SPSS (Statistical Package for the Social Sciences) Software Package version 21 (IBM Corp, Armonk, NY). Unless otherwise stated, the statistical threshold was set at $p \leq 0.05$. In cases where transformations were utilised, statistical analysis was run on the transformed data. However, for ease of interpretation, both descriptive and visual displays depict untransformed data.

A detailed description of the analytic approach carried out in each study is described in the individual experimental chapters to come.

Chapter 3: Mother-infant interactions and regional brain volumes in infancy: an MRI study

Brain Struct Funct
DOI 10.1007/s00429-016-1347-1

ORIGINAL ARTICLE

Mother–infant interactions and regional brain volumes in infancy: an MRI study

Vaheshta Sethna[1] · Inês Pote[1] · Siying Wang[2] · Maria Gudbrandsen[1] · Anna Blasi[3] · Caroline McCusker[1] · Eileen Daly[1] · Emily Perry[1] · Kerrie P. H. Adams[1] · Maria Kuklisova-Murgasova[4] · Paula Busuulwa[1,9] · Sarah Lloyd-Fox[3] · Lynne Murray[5,6] · Mark H. Johnson[3] · Steven C. R. Williams[7,8] · Declan G. M. Murphy[1] · Michael C. Craig[1] · Grainne M. McAlonan[1]

Received: 5 August 2016 / Accepted: 25 November 2016

Abstract It is generally agreed that the human brain is responsive to environmental influences, and that the male brain may be particularly sensitive to early adversity. However, this is largely based on retrospective studies of older children and adolescents exposed to extreme environments in childhood. Less is understood about how normative variations in parent–child interactions are associated with the development of the infant brain in typical settings. To address this, we used magnetic resonance imaging to investigate the relationship between observational measures of mother–infant interactions and regional brain volumes in a community sample of 3- to 6-month-old infants ($N = 39$). In addition, we examined whether this relationship differed in male and female infants. We found that lower maternal sensitivity was correlated with smaller subcortical grey matter volumes in the whole sample, and that this was similar in both sexes. However, male infants who showed greater levels of positive communication and engagement during early interactions had smaller cerebellar volumes. These preliminary findings suggest that variations in mother–infant interaction dimensions are associated with differences in infant brain development. Although the study is cross-sectional and causation cannot be inferred, the findings reveal a dynamic interaction between brain and environment that may be important when considering interventions to optimize infant outcomes.

Keywords Mother–infant interaction · Infant brain structure · MRI · Infancy · Sex differences · Maternal sensitivity · Infant cerebellum

Introduction

Parent–infant interactions are critical for child development. For instance, sensitive and responsive early care is linked to optimal behavioural and cognitive outcomes

V. Sethna, I. Pote, D. G. M. Murphy, M. C. Craig and G. M. McAlonan contributed equally.

✉ Vaheshta Sethna
vaheshta.sethna@kcl.ac.uk

[1] Department of Forensic and Neurodevelopmental Sciences, Sackler Institute for Translational Neurodevelopment, Institute of Psychiatry, Psychology and Neuroscience, King's College London, PO 50, 16 De Crespigny Park, London SE5 8A, UK

[2] Department of Engineering Science, Institute of Biomedical Engineering, University of Oxford, Oxford, UK

[3] Centre for Brain and Cognitive Development, Birkbeck, University of London, London, UK

[4] Division of Imaging Sciences and Biomedical Engineering, Centre for the Developing Brain, King's College London, London, UK

[5] School of Psychology and Clinical Language Sciences, University of Reading, Reading, UK

[6] Stellenbosch University, Stellenbosch, South Africa

[7] Department of Neuroimaging, Institute of Psychiatry, Psychology and Neuroscience, King's College London, London, UK

[8] NIHR Biomedical Research Centre for Mental Health at the South London and Maudsley NHS Foundation Trust and King's College London, London, UK

[9] GKT School of Medical Education, King's College London, London, UK

Published online: 03 December 2016

(Cabrera et al. 2011; Lugo-Gil and Tamis-LeMonda 2008); in contrast, parental insensitivity increases the risk of children developing psychopathology in later life (Murray et al. 2010). Although the biological mechanisms mediating these associations are not entirely understood, it is generally agreed that the human brain is most vulnerable to environmental influences (De Bellis et al. 2001; Schore 2001)—including parent–infant interactions (Rifkin-Graboi, et al. 2015)—early in development.

For example, elevated levels of stress hormones stemming from early-life adversity are thought to lead to altered brain development through the accelerated loss of neurons, disrupted pruning, inhibition of neurogenesis (Teicher et al. 2006; Tupler and De Bellis 2006), and perhaps also altered anatomical 'connectivity' (Sarkar et al. 2014). Prior reports also suggest that early childhood maltreatment is associated with later fronto-limbic abnormalities (Belsky and de Haan 2011; Hart and Rubia 2012); smaller corpus callosum and total brain volumes, and increased ventricular volumes (De Bellis et al. 2002; Teicher et al. 2004). It has also been suggested that the male brain is particularly vulnerable to such insults (De Bellis and Keshavan 2003; Tupler and De Bellis 2006). For example, smaller cerebral volumes have been reported in older male children exposed to childhood maltreatment (Belsky and de Haan 2011).

However, existing studies in humans mainly document outcomes following extreme adversity in infancy (i.e., institutional rearing or severe maltreatment), and are retrospective in design. Also, the high prevalence of psychopathology (72%) in these retrospective analyses of older cohorts (De Bellis et al. 2001) makes it difficult to determine whether the structural brain differences observed explain the aetiology of psychopathology or are caused by it and/or its treatment [for example, medication exposure may confound interpretation (Tupler and De Bellis 2006)]. Thus, the results of these high-risk samples do not reveal how normative variations in early parent–child interactions influence child brain structure in the early postnatal period.

This is an important omission, considering the compelling evidence that an early sensitive caregiving environment likely provides an optimal emotional context for children's early brain maturation and subsequent cognitive abilities (Bernier et al. 2010). Furthermore, the postnatal period is characterized by rapid brain development. Specifically, the first year of life is the period of greatest brain volume growth in typical children—total brain volume at 2–4 weeks of age is approximately 36% of adult volume, and by 1 year it is approximately 72% of adult volume (Knickmeyer et al. 2008). Brain plasticity during this period makes the infant brain particularly sensitive to environmental influence, especially the social-affective environment (Schore 2001). Variations in maternal care are thought to help shape neural structures and circuits, and subsequently psychological outcomes (Roth and Sweatt 2011); and there is reasonable consensus that maternal sensitivity in the first year of life has a key impact on development (de Wolff and van Ijzendoorn 1997). Defined as the timely and accurate response to the infant's communicative cues, maternal sensitivity predicts positive social relationships and enhanced cognitive abilities in the infant (Wade et al. 2015); and sensitive caregiving during the first year is critical for the maturation of the infant's stress response system (Gunnar and Cheatham 2003; Hane and Fox 2006).

Therefore, the relationship between normative variations in parenting and brain structure in children has now started to be examined (Kok et al. 2015; Moutsiana et al. 2015; Rao et al. 2010; Rifkin-Graboi, et al. 2015; Whittle et al. 2014). For example, higher levels of parental sensitivity in early childhood have been linked with larger total brain and grey matter volumes in children at 8 years of age (Kok, et al. 2015). In another study, insecure attachment at 18 months was associated with greater amygdala volumes at 22 years (Moutsiana et al. 2015). In contrast, a study of structural MRI data from twenty 6-month-old infants, has demonstrated a link between maternal sensitivity and hippocampus volume (Rifkin-Graboi et al. 2015)—specifically, reduced maternal sensitivity was associated with larger volumes. While these studies are important first steps, some had a lengthy period between caregiving measures and brain MRI acquisition (Kok et al. 2015; Moutsiana et al. 2015), and others used adolescent samples (Whittle et al. 2014). In infancy and childhood, the changes in brain volume over time occur in parallel to maturation of cognitive, motor and socio-emotional processes (Shulman 2016; van Soelen et al. 2012). By examining the brain and the factors that influence it at the same time, we can begin to identify possible causes of altered brain growth and behaviour, as well as potential treatment targets and biomarkers that are predictive of outcomes.

In the current study, we used magnetic resonance imaging (MRI) to investigate whether mother–infant interactions observed in a community sample of mothers and their 3- to 6-month-old infants, are related to variations in regional brain volumes. In addition to studying an association between maternal behaviours and infant brain volume, it is important to know whether—or not—infant behaviours are related to brain volumes as this may help us understand what brain systems drive infant behaviour and/or respond to infant behaviour changes. Such information may eventually help us develop objective predictive tools to identify infants who might benefit from early intervention to improve outcomes. Moreover, since there is a bidirectional link between maternal sensitivity and infant behaviours (Beebe et al. 2016; Feldman 2007; MacLean et al. 2014), it is also possible that infant behaviours relate

to brain development indices. Therefore, we predicted that there would be a relationship between both maternal and infant behaviours and regional brain volumes. Owing to limited prior information in infancy, with both larger and smaller regional brain volumes reported in relation to early caregiving, and no previous evidence in relation to infant behaviours, the direction of this relationship was not a priori predicted.

Finally, where an association between brain regions and mother–infant interactions was observed, we conducted an exploratory examination of potential sex differences in these relationships. As preclinical and clinical studies of adverse rearing conditions (i.e., exposure to childhood maltreatment) indicate that the male brain is influenced more by the early environment (Belsky and de Haan 2011; Glaser 2000), we predicted that any relationship between maternal and/or infant behaviour and brain would be stronger in males.

Methods

Participants

Participants were 43 mother–infant dyads recruited from the local community in London. The aim was to capture data from infants aged around 4 months. For logistical reasons, infants were eligible for the study if they were aged between 3 and 6 months, born at term (gestational age >36 weeks) with no congenital abnormalities. Mothers had to have a working knowledge of the English language, and be free of any current or past major psychiatric illness, or any antenatal or obstetric complications potentially altering infant development (for example, perinatal asphyxia). Exclusion criteria included contraindications for MRI scanning (for example, metallic implants or pacemakers). Written informed consent was obtained from mothers for the protocol approved by the UK National Research Ethics Committee (REC 08/H0718/76, 06/MRE02/73 and 12/LO/2017).

A total of four MRI scans were excluded from the analysis due to poor image quality driven by motion artefacts ($n = 3$), and an incidental brain anatomical anomaly ($n = 1$). Hence, the final sample included 39 infants (mean age = 4.83 months, SD = 1.15 months; 51.3% male) with data on both measures, i.e., mother–infant interactions and brain volumes from MRI scans. Of the total sample, 51.3% ($n = 20$) were male, and there was no difference in infant age at scan between the sexes ($p = 0.577$). Maternal and infant demographic characteristics for the total sample, and split by infant sex, are presented in Table 1.

Procedures

Mother–infant interactions

Observations of mother–infant interactions were video-recorded for 5 min using a standard assessment protocol of face-to-face play (Murray et al. 1996b)—with the infant placed in an infant seat. Mothers were instructed to play with and talk to their infant as they normally would, but without using any toys or objects. Maternal and infant behaviours were coded by two trained raters using the Global Rating Scales (GRS, Murray et al. 1996b), which are sensitive to impaired interactions even in low-risk samples (Gunning et al. 2004).

The first five uninterrupted continuous play minutes of videotaped mother–infant interaction were coded as in previous studies (Halligan et al. 2013). Maternal communication modalities coded were sensitivity and affect. These dimensions were included since maternal sensitivity is known to predict infant and child cognitive outcomes, and high levels of negative affectivity disrupt the infant's regulatory capacity and quality of parent–infant relationships, leading to maladaptive child outcomes (Murray et al. 1996a; Murray and Trevarthen 1986). Additionally, two infant dimensions were included—communication and affective state—both of which are critical for shaping cognitive outcomes (Cates et al. 2012).

In line with previous work, the dimensions were scored on a standard five-point scale, where 1 corresponds to "poor" interactive maternal or infant behaviour and 5 to most "optimal" behaviour. Dimensions of mother–infant interactions were derived as per standard use in previous studies (Murray et al. 1996a; Stein et al. 2012).

(1) *Sensitivity* Maternal response to the infant's communication cues; the extent to which it is contingent and appropriate to the infant's needs and experiences; also including attitude and feelings towards the infant. Maternal sensitivity was characterized by warmth, acceptance, non-demanding, and non-intrusive behavioural dimensions.

(2) *Affect* Maternal demonstration of affective state, including positive and negative affectivity (i.e., depressive-like expressions). Affective state was characterized by level of maternal enjoyment, effort and vitality, degree of self-consciousness, and the extent of anxiety in the interaction.

(3) *Communication* Infant's level of engagement and communication (i.e., positive vocal and non-vocal behaviour directed towards the mother). Communication included the amount of visual contact, and positive vocalizations, in addition to other forms of

Table 1 Maternal and infant demographic characteristics for the whole sample and by infant sex

	Whole sample ($N = 39$)	Males ($n = 20$)	Females ($n = 19$)	Sex difference statistic (p value)
Infant demographics				
Age at MRI (months); mean (SD)	4.83 (1.15)	4.73 (1.20)	4.94 (1.11)	$t = -0.563$, $p = 0.577$
Gestational age at birth (weeks); mean (SD)	39.71 (1.95)	39.85 (1.83)	39.57 (2.11)	$t = -0.445$, $p = 0.659$
Birth weight (g); mean (SD)	3390.51 (527.48)	3490.50 (424.05)	3285.26 (612.19)	$t = -1.22$, $p = 0.229$
Weight at MRI (g); mean (SD)	7105.30 (1302.95)	7262.51 (1172.48)	6939.81 (1440.83)	$t = -0.77$, $p = 0.450$
Maternal demographics				
Age (years); mean (SD)	33.82 (4.45)	33.90 (4.48)	33.74 (4.53)	$t = -1.13$, $p = 0.911$
Ethnicity; n (%)				$\chi^2 = 4.47$, $p = 0.214$
White	32 (82.1)	18 (90.0)	14 (73.7)	
Asian	4 (10.3)	1 (5.0)	3 (15.8)	
Black	1 (2.6)	1 (5.0)	0 (0.0)	
Mixed race	2 (5.1)	0 (0.0)	2 (10.5)	
Educational level; n (%)				$\chi^2 = 1.25$, $p = 0.536$
GCSE and A-levels	2 (5.1)	1 (5.0)	1 (5.3)	
Vocational college	4 (10.3)	1 (5.0)	3 (15.8)	
Higher education	33 (84.6)	18 (90.0)	15 (78.9)	

SD standard deviation, *GCSE* General Certificate of Secondary Education, *A-Levels* General Certificate of Education Advanced Level, *Higher education* undergraduate and postgraduate degree

communication (for example, mouthing, movement of limbs).

(4) *Fretfulness* Infant's affective state and level of distress.

Inter-rater intraclass correlations (Shrout and Fleiss 1979) were measured on a randomly selected 20% of the interactions, and ranged from 0.741 to 0.993, indicating good-to-excellent inter-rater reliability. Discrepancies between raters were discussed, and final ratings were determined in collaboration with members of the Winnicott Research Unit who were involved in the development of the scale. ICCs stated for the GRS scales utilized absolute scores and were calculated prior to adjustments to ratings—that is, they include the original values by raters.

MRI data acquisition

MRI data were acquired on a 1.5-T General Electric scanner (GE Medical Systems, Milwaukee, WI, USA), equipped with an 8-channel head coil. Infants were scanned in natural sleep; further details can be found in Blasi et al. (2011). A T2-weighted fast spin echo (T2w) sequence with the following imaging parameters was acquired: number of slices = 20; slice thickness = 4 mm; slice gap = 2 mm; repetition time = 3000/4500 ms; echo time = 115 ms; field of view = 180 mm; flip angle = 90°; matrix size = 256 × 224. The structural sequence used for this study was necessarily a short scan acquired alongside functional MRI. All images were analysed blind to mother–infant interaction ratings.

Image processing and volumetric segmentation

The T2w MR images were first skull-stripped using label propagation and decision fusion of three manual brain masks (Heckemann et al. 2006). Segmentations of the masked images were then performed using an atlas-based method, which adapted the Statistical Parametric Mapping (SPM v.8) software, and a probabilistic neonatal brain atlas (Kuklisova-Murgasova et al. 2011) as an input to the SPM software. The SPM segmentation model unifies tissue classification, image bias correction and non-linear atlas registration (Ashburner and Friston 2005). Iterated Conditional Modes were employed to optimize the Gaussian mixture model (GMM) parameters for the tissue intensity distributions, the bias field parameters and the atlas deformation parameters. The GMM parameters were estimated using an expectation–maximization algorithm (Fombonne 2009) and a Levenberg–Marquardt algorithm (Courchesne et al. 2000), to obtain the bias field and deformation parameters. Subsequently, the segmentation of cerebrospinal fluid (CSF) was refined by thresholding the masked T2w image based on the mean of the intensity distribution calculated using the SPM posterior probability map of CSF. The partial volume misclassifications by this intensity-based SPM segmentation model were corrected using second order Markov random fields, which enabled

spatial constraints to be imposed by configuring a three-dimensional connectivity tensor (Erskine et al. 2013). Following this automated protocol, one rater examined all images in a final manual editing process using ITK-SNAP (v.2.2) (Yushkevich et al. 2006).

This process yielded volumes of the following brain regions (Fig. 1): (a) CSF (including both CSF, third ventricle and fourth ventricle); (b) lateral ventricles (including the cavum septum pellucidum and vergae); (c) midbrain (including the cerebral peduncle, substantia nigra, brainstem and pons); (d) cerebellum; (e) subcortical grey matter (including the caudate, putamen, globus pallidus and thalamus), and the remaining (f) total grey and white matter. Further grey and white matter segmentation was not conducted given the difficulty in accurately classifying these tissue classes at this age (Hazlett et al. 2012). Finally, a measure of (g) intracranial volume was also obtained by summing all regions (a–f). All regional brain volumes were expressed as proportions of intracranial volume, and these 'corrected' measures were used in the analyses.

Volumetric segmentations: intra-rater reliability

The reliability of the volumetric segmentations was confirmed by intra-rater intraclass correlations between the final segmentations, and a repeat measurement of a random 20% selection of the automatically segmented images. For the intracranial volume, the intraclass correlation of the intra-rater variability was 0.998 ($p < 0.001$), indicating excellent reproducibility. Similar results were found for the individual correlations of each brain region: CSF (0.989, $p < 0.001$), lateral ventricles (0.965, $p < 0.001$), midbrain (0.918, $p < 0.001$), cerebellum (0.948, $p < 0.001$), subcortical grey matter (0.923, $p < 0.001$), and total grey and white matter (0.984, $p < 0.001$). The ICCs stated were derived from absolute measurements.

Statistical analysis

Data were analysed using the IBM SPSS (Statistical Package for the Social Sciences) Software Package (v.22) (SPSS Chicago, IL, USA). We examined the relationships between mother–infant interactions and brain volumes across the entire cohort; when these were present we then examined the relationship in male and female infants separately.

First, descriptive data were examined to confirm that these conformed to assumptions of normality. Regional brain volume measures were 'corrected' (expressed as proportions of intracranial volume) and the sexes compared. Next, a set of planned bivariate correlation analyses between the maternal and infant interaction indices and brain volumes was calculated. A threshold of at least a moderate effect size ($r > 0.3$) with the significance level set to $p < 0.05$ was selected as preliminary evidence for a relationship between behaviour and brain volume (Cohen 2013; Kotrlik and Williams 2003). Second, after a

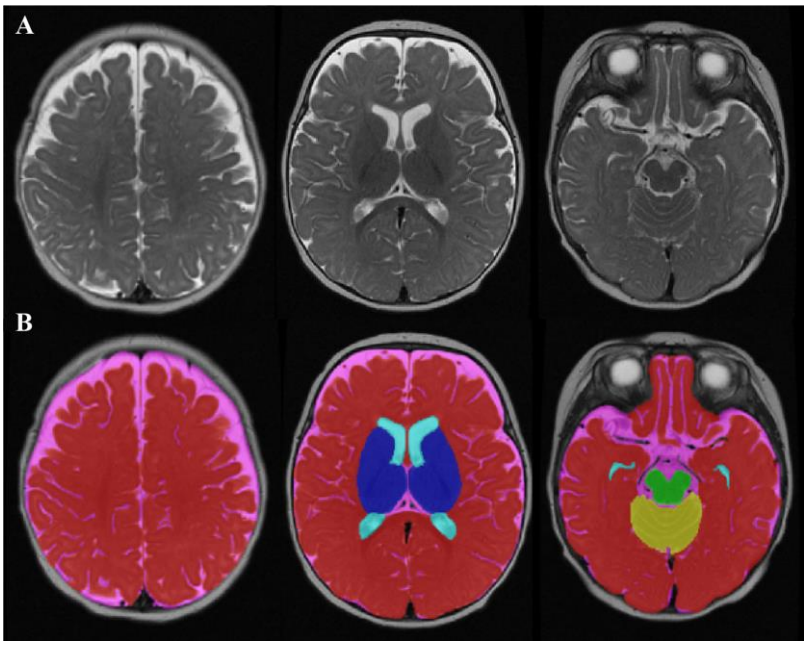

Fig. 1 Volumetric segmentation of a 4-month-old brain. **a** T2-weighted axial MRI image of a 4-month-old infant brain. **b** The final result of the volumetric segmentation, with label maps for CSF (*pink*), lateral ventricles (*light blue*), midbrain (*green*), cerebellum (*yellow*), subcortical grey matter (*dark blue*), and total grey and white matter (*red*)

Bonferroni correction for multiple correlations, where a significant association emerged, the association between interaction dimension and brain volume was further examined using the PROCESS macro tool (Hayes 2013). We estimated whether the interaction term between each mother and infant behaviour and sex (i.e., maternal interaction dimension × sex and infant behaviour × sex) was associated with brain structure volume. Infant age and weight at time of scan were included as covariates, to adjust for age and weight differences in brain volume (Parikh et al. 2013). We also controlled for maternal education (an index of socio-economic status), which has been linked to brain structure (Brito and Noble 2014). PROCESS applies bias-corrected bootstrapping intervals to probe the interaction term and make inferences about indirect effects, rather than relying on the normality assumption. The number of bootstrap samples used to determine 95% bias-corrected bootstrap confidence intervals was 10,000. PROCESS also produces the conditional effects of the independent variable at the two values of a binary moderator (sex: male = 0, female = 1).

Results

Table 2 shows the means, standard deviations, and sex differences for mother–infant interaction dimensions and brain volumes. Significant sex differences were found in the raw measures of the subcortical grey and intracranial volumes; in both instances, male infants had larger volumes than females—subcortical grey: (males: mean = 36.17, SD = 4.16; females: mean = 33.05, SD = 2.36; t (37) = 2.89, $p = 0.007$), and intracranial volume (males: mean = 888.56, SD = 88.54; females: mean = 825.20, SD = 102.68; t (37) = 2.07, $p = 0.046$).

Relationship between mother–infant interaction dimensions and brain volumes

Maternal affect

Maternal affect was positively correlated with total grey and white matter volume, and negatively correlated with CSF volume ($r = 0.33$, $p = 0.042$; $r = -0.33$, $p = 0.039$, respectively). Thus, infants exposed to negative affect (i.e., depressive-like expressions) had smaller total grey and white matter volumes, and larger CSF volumes. However, these associations did not survive correction for multiple testing.

Maternal sensitivity

Furthermore, a positive association of moderate effect size was found between maternal sensitivity and subcortical grey matter volume ($r = 0.54$, $p < 0.001$) in the whole sample—i.e., infants interacting with less sensitive mothers had smaller subcortical grey volumes. The association survived correction for multiple comparisons (Bonferroni corrected p value =0.001). When adjusting for covariates (infant age, weight and maternal education) the association remained statistically significant ($B = 0.002$, $p = 0.046$), and there was no evidence that infant sex moderated the association between maternal sensitivity and subcortical grey matter volume, as the interaction term (maternal sensitivity × sex) was not significant ($p = 0.806$). Furthermore, none of the covariates were associated with the outcome (i.e., subcortical volume) in the model tested.

Infant communication

There was a significant negative correlation of moderate effect size between infant communication and cerebellar volume ($r = -0.48$, $p = 0.002$) in the whole sample—i.e., greater infant communication and engagement during mother–infant interactions was associated with smaller cerebellum volumes. This association also survived correction for multiple comparisons (Bonferroni corrected p value =0.020), and remained significant when adjusting for covariates ($B = -0.01$, $p = 0.003$). Covariates associated with the outcome (i.e., cerebellum volume) in the model tested included infant age ($p < 0.001$) and sex ($p = 0.019$)—implying larger cerebellum, in older, male infants. Furthermore, the interaction term (infant communication × sex) in this model was significant ($B = 0.01$, $p = 0.017$), indicating that infant sex moderated the association between infant communication and cerebellum volume (R^2 increase due to the interaction = 0.09, $F = 6.32$, $p = 0.017$). While the conditional association between infant communication and cerebellum volume was significant in male infants ($B = -0.05$, $p = 0.003$), suggesting smaller cerebellar volumes with increased communication; there was no such evidence in female infants ($B = 0.00$, $p = 0.762$).

Infant fretfulness

Infant fretfulness was not significantly correlated with regional brain volumes

Discussion

In this cross-sectional exploratory study, we show that variations in typical mother–infant interactions are associated with differences in infant brain volumes. Specifically, we found that lower maternal sensitivity was correlated with smaller subcortical grey matter volumes in

Table 2 Mother–infant interaction dimensions and brain volumes: whole group descriptive statistics and comparisons by infant sex

	Whole sample ($N = 39$)	Males ($n = 20$)	Females ($n = 19$)	Sex difference	
	Mean (SD)	Mean (SD)	Mean (SD)	t	p value
Interaction dimensions[a]					
Maternal dimensions					
Sensitivity	3.48 (0.54)	3.51 (0.52)	3.45 (0.56)	−0.30	0.765
Affect	4.25 (0.53)	4.26 (0.54)	4.23 (0.52)	−0.21	0.836
Infant dimensions[a]					
Communication	3.52 (0.91)	3.76 (0.86)	3.28 (0.91)	−1.70	0.098
Fretfulness	4.11 (0.69)	4.06 (0.66)	4.15 (0.74)	0.40	0.695
Brain volumes, cm^3					
Total grey and white matter	586.12 (69.66)	603.53 (69.35)	567.80 (66.92)	1.64	0.110
Midbrain	13.90 (1.91)	14.42 (1.83)	13.35 (1.89)	1.79	0.082
Subcortical grey	34.65 (3.71)	36.17 (4.16)	33.05 (2.36)	2.89	0.007
Cerebellum	74.83 (11.91)	77.11 (12.51)	72.43 (11.06)	1.24	0.224
Lateral ventricles	14.27 (4.58)	15.01 (4.54)	13.49 (4.62)	1.03	0.308
Cerebrospinal fluid	133.94 (40.70)	142.36 (44.95)	125.07 (34.68)	1.34	0.189
Intracranium	857.71 (99.72)	888.58 (88.54)	825.20 (102.68)	2.07	0.046

[a] Low scores indicate poor interactions (for example, lower levels of sensitivity, increased depressive affect, fewer communication attempts and increased infant fretfulness)

both sexes. In contrast, male infants with higher levels of communication during early interactions had smaller cerebellar volumes.

Prior studies of extreme neglect, leading to paediatric post-traumatic stress disorder, have reported that childhood maltreatment is associated with smaller total grey and white matter volumes, and larger frontal lobe CSF volumes, especially in males (De Bellis and Keshavan 2003; De Bellis et al. 2002). A more recent investigation of normal variations in parental care and brain structure (at 8 years of age) has revealed a similar relationship between early childhood parental sensitivity and total brain and grey matter volumes (Kok et al. 2015). More specifically, and when compared to other brain regions, the subcortical grey matter appears to be particularly 'responsive' to early environmental influences. For example, the basal ganglia and thalami (which comprise the subcortical grey) are very sensitive to hypoxic events in utero (Okereafor et al. 2008; du Plessis and Volpe 2002; Shalak and Perlman 2004); and infants so exposed, tend to have poor neurodevelopmental outcomes.

Our work extends these findings to show that a relationship between maternal sensitivity and infant brain development is present from as early as 3 months. However, these findings are correlational and do not necessarily indicate a causative link between early care and infant brain structure. Also, we cannot say firmly whether this relationship has 'positive' or 'negative' developmental implications. Neither can we be certain whether smaller regional brain volumes are a consequence of poorer parenting quality, or whether infants with smaller regional brain volumes influence their mothers' interactions. It is also possible that since infant and mother are closely genetically related, the associations observed could be mediated through shared genetic variants, including an inherited brain volume and behavioural style.

We do suggest, however, that the infant stress response system, which undergoes rapid development in the first year of life, is likely to be involved. For example, in the early postnatal period when the hypothalamic–pituitary–adrenal (HPA) axis of infants is labile, sensitive parenting is associated with either smaller increases or less prolonged activations of the infant HPA axis, when subjected to mild stress (Albers et al. 2008). Therefore, exposure to negative (for example, insensitive or intrusive) parental behaviours may constitute a source of stress for the infant, and activate the infant's adrenocortical axis (Atkinson et al. 2013). The subsequent elevation in cortisol may influence brain volume and 'connectivity' in the growing child (Sarkar et al. 2014). Furthermore, mothers who are more sensitive in the postnatal period have been reported to demonstrate secure mental representations of attachment during pregnancy, which in turn may impact upon the HPA axis and the intrauterine environment (Kinsella and Monk 2009). Hence, associations between maternal behaviours and infant brain volume may have their origins even earlier in development,

but future studies including objective measures of the HPA axis and a comprehensive characterization of maternal psychopathology during pregnancy are needed to better understand the mechanisms involved. In addition, as maternal sensitivity is thought to be a stable trait over time (Feldman 2010), follow-up of these dyads would help to determine whether the relationship we observed between maternal sensitivity and the infant brain persists or shifts as children grow.

An important aspect of our study design was that it also permitted examination of a possible link between infant behaviour (for example, communication and fretfulness) and brain volume. We found that a smaller cerebellum volume is associated with better infant communication, and this relationship was particularly evident in male infants. Again, we emphasize that the causal direction of this relationship is not known—i.e., does cerebellar development drive communication, or vice versa? Regardless, a link between cerebellar development and communication is not surprising given its key role in emotion processing and executive functioning (Schmahmann et al. 2007). For example, the cerebellum has been proposed to have a key role in the temporal processing of events and in allocating attentional resources in 'real-time' to guide or prepare behaviour (Schwartze and Kotz 2016). In addition, the cerebellum responds to auditory stimulation including spoken language (Buckner 2013). Together, these attributes likely make a key contribution to organizing effective communication during face-to-face interaction, and our data suggest that the link between cerebellum and communication is present from early infancy. Furthermore, that our results reveal a relationship primarily in males might also have been expected, as the developmental trajectory of the cerebellum is sexually dimorphic. The male cerebellum develops more slowly than the female (Tiemeier et al. 2010), potentially making the former more vulnerable to early adverse environments. Consistent with this, cerebellar pathology is a hallmark of neurodevelopmental disorders, such as ASD, which also shows marked sex differences (Wang et al. 2014). Finally, our sample size and current study design precludes an in-depth analysis of potential processes which might explain the link between infant behaviour and brain volume; including, for example, the role of maternal sensitivity which could be considered in future research.

Our study has a number of limitations. First, as noted above, our results are correlational and causality cannot be inferred. Second, although in line with the current literature (Rifkin-Graboi et al. 2015), our sample size was modest and replication in larger samples will be necessary. Third, the infants in our study were mainly from white European 'middle-class' families, educated to degree level, and therefore, we cannot be certain that these results generalize to families of different ethnicities and educational backgrounds. Fourth, we did not define a priori regions of interest since we do not yet have extensive knowledge of all brain areas affected by normative variations of parenting in infancy. Fifth, our primary goal in this initial study was to establish if there were brain regions linked to mother-infant interactions across the group, and then, having done that, to explore if there were sex differences in those specific regions. This approach helped us avoid type 1 error when running multiple tests. However, it risked generating type 2 errors of incorrectly retaining a false-negative finding. Therefore, we cannot exclude the possibility that there are sex differences in regions without main effects; and in our ongoing studies we are recruiting much larger cohorts in order to look at each sex separately across multiple brain regions. We hope this will provide adequate power to explore regional associations with sex and parent–child interactions in detail. Finally, there were also technical constraints to our study. The scanning of very young infants is challenging and the structural sequences used were of relatively low resolution. Hence, our overall volumetric measurement may miss the fine-grained structural differences that might be detectable in larger samples, or through higher resolution scanning protocols. Furthermore, and in line with previous studies of this age range (Hazlett et al. 2012), another limitation was the inability to differentiate between grey and white matter volume, due to ongoing myelination in these young infants.

Nonetheless, the current analyses provide a Proof of Principle that early mother–infant interactions are associated with variations in infant brain development. If correct, our finding that early sensitivity (a modifiable factor) is linked to the development of brain regions (known to impact upon emotional and cognitive development), opens up the potential to influence infant developmental trajectories.

Acknowledgements This paper represents independent research part funded by the National Institute for Health Research (NIHR) Biomedical Research Centre at South London and Maudsley NHS Foundation Trust and King's College London. The views expressed are those of the author(s) and not necessarily those of the NHS, the NIHR or the Department of Health. The work was conducted as part of the EU-AIMS IMI programme to identify biomarkers for Autism. DGMM and GMM receive support from the Sackler Centre for Translational Neurodevelopment at King's College London. MHJ, AB and SLF are additionally supported by the UK Medical Research Council. The authors gratefully acknowledge the contribution of Laura Bozicevic, MSc, from the University of Reading, UK, for help with coding mother–infant interactions. We would also like to thank parents and their infants for their invaluable contribution.

Compliance with ethical standards

Conflict of interest No conflicts declared.

References

Albers EM, Marianne Riksen-Walraven J, Sweep FC, Weerth CD (2008) Maternal behavior predicts infant cortisol recovery from a mild everyday stressor. J Child Psychol Psychiatry 49(1):97–103

Ashburner J, Friston KJ (2005) Unified Segmentation. NeuroImage 26:839–851

Atkinson L, Gonzalez A, Kashy DA, Santo Basile V, Masellis M, Pereira J et al (2013) Maternal sensitivity and infant and mother adrenocortical function across challenges. Psychoneuroendocrinology 38(12):2943–2951

Beebe B, Messinger D, Bahrick LE, Margolis A, Buck KA, Chen H (2016) A systems view of mother–infant face-to-face communication. Dev Psychol 52(4):556

Belsky J, de Haan M (2011) Annual research review: parenting and children's brain development: the end of the beginning. J Child Psychol Psychiatry 52(4):409–428

Bernier A, Carlson SM, Whipple N (2010) From external regulation to self-regulation: early parenting precursors of young children's executive functioning. Child Dev 81(1):326–339

Blasi A, Mercure E, Lloyd-Fox S, Thomson A, Brammer M, Sauter D et al (2011) Early specialization for voice and emotion processing in the infant brain. Curr Biol 21(14):1220–1224

Brito NH, Noble KG (2014) Socioeconomic status and structural brain development. Front Neurosci 8:276

Buckner Randy L (2013) The cerebellum and cognitive function: 25 years of insight from anatomy and neuroimaging. Neuron 80(3):807–815

Cabrera NJ, Fagan J, Wight V, Schadler C (2011) Influence of mother, father, and child risk on parenting and children's cognitive and social behaviors. Child Dev 82(6):1985–2005

Cates CB, Dreyer BP, Berkule SB, White LJ, Arevalo JA, Mendelsohn AL (2012) Infant communication and subsequent language development in children from low income families: the role of early cognitive stimulation. J Dev Behav Pediatr 33(7):577–585

Cohen J (2013) Statistical power analysis for the behavioral sciences. Academic press, New York

Courchesne E, Chisum HJ, Townsend J, Cowles A, Covington J, Egaas B et al (2000) Normal brain development and aging: quantitative analysis at in vivo MR imaging in healthy volunteers. Radiology 216(3):672–682

De Bellis MD, Keshavan MS (2003) Sex differences in brain maturation in maltreatment-related pediatric posttraumatic stress disorder. Neurosci Biobehav Rev 27(1):103–117

De Bellis MD, Hall J, Boring AM, Frustaci K, Moritz G (2001) A pilot longitudinal study of hippocampal volumes in pediatric maltreatment-related posttraumatic stress disorder. Biol Psychiatry 50(4):305–309

Du Plessis AJ, Volpe JJ. Perinatal brain injury in the preterm and term newborn. Curr Opin Neurol 15:151–157. doi:10.1097/00019052-200204000-00005

De Bellis MD, Keshavan MS, Shifflett H, Iyengar S, Beers SR, Hall J et al (2002) Brain structures in pediatric maltreatment-related posttraumatic stress disorder: a sociodemographically matched study. Biol Psychiatry 52(11):1066–1078

de Wolff MS, van Ijzendoorn MH (1997) Sensitivity and attachment: a meta-analysis on parental antecedents of infant attachment. Child Dev 68(4):571–591

Erskine HE, Ferrari AJ, Nelson P, Polanczyk GV, Flaxman AD, Vos T et al (2013) Research Review: epidemiological modelling of attention-deficit/hyperactivity disorder and conduct disorder for the Global Burden of Disease Study 2010. J Child Psychol Psychiatry 54(12):1263–1274

Feldman R (2007) Parent–infant synchrony and the construction of shared timing; physiological precursors, developmental outcomes, and risk conditions. J Child Psychol Psychiatry 48(3–4):329–354

Feldman R (2010) The relational basis of adolescent adjustment: trajectories of mother–child interactive behaviors from infancy to adolescence shape adolescents' adaptation. Attach Hum Dev 12(1–2):173–192

Fombonne E (2009) Epidemiology of pervasive developmental disorders. Pediatr Res 65(6):591–598

Glaser D (2000) Child abuse and neglect and the brain—a review. J Child Psychol Psychiatry 41(01):97–116

Gunnar MR, Cheatham CL (2003) Brain and behavior interface: stress and the developing brain. Infant Mental Health J 24(3):195–211

Gunning M, Conroy S, Valoriani V, Figueiredo B, Kammerer MH, Muzik M et al (2004) Measurement of mother–infant interactions and the home environment in a European setting: preliminary results from a cross-cultural study. Br J Psychiatry 184(46):s38–s44

Halligan SL, Cooper PJ, Fearon P, Wheeler SL, Crosby M, Murray L (2013) The longitudinal development of emotion regulation capacities in children at risk for externalizing disorders. Dev Psychopathol 25(2):391–406

Hane AA, Fox NA (2006) Ordinary variations in maternal caregiving influence human infants' stress reactivity. Psychol Sci 17(6):550–556

Hart H, Rubia K (2012) Neuroimaging of child abuse: a critical review. Front Hum Neurosci 6:52. doi:10.3389/fnhum.2012.00052

Hayes AF (2013) Introduction to mediation, moderation, and conditional process analysis: a regression-based approach. Guildford Press, New York

Hazlett HC, Gu H, McKinstry RC, Shaw DWW, Botteron KN, Dager S et al (2012) Brain volume findings in six month old infants at high familial risk for Autism. Am J Psychiatry 169(6):601–608

Heckemann RA, Hajnal JV, Aljabar P, Rueckert D, Hammers A (2006) Automatic anatomical brain MRI segmentation combining label propagation and decision fusion. NeuroImage 33:115–126

Kinsella MT, Monk C (2009) Impact of maternal stress, depression and anxiety on fetal neurobehavioral development. Clin Obstet Gynecol 52(3):425–440

Knickmeyer RC, Gouttard S, Kang C, Evans D, Wilber K, Smith JK et al (2008) A structural MRI study of human brain development from birth to 2 years. J Neurosci 28:12176–12182. doi:10.1523/jneurosci.3479-08.2008

Kok R, Thijssen S, Bakermans-Kranenburg MJ, Jaddoe VW, Verhulst FC, White T et al (2015) Normal Variation in Early Parental Sensitivity Predicts Child Structural Brain Development. J Am Acad Child Adoles Psychiatry 54(10):824–831 **(e821)**

Kotrlik JWKJW, Williams HAWHA (2003) The incorporation of effect size in information technology, learning, information technology, learning, and performance research and performance research. Inform Technol Learn Perform J 21(1):1

Kuklisova-Murgasova M, Aljabar P, Srinivasan L, Counsell SJ, Doria V, Serag A et al (2011) A dynamic 4D probabilistic atlas of the developing brain. NeuroImage 54:2750–2763

Lugo-Gil J, Tamis-LeMonda CS (2008) Family resources and parenting quality: links to children's cognitive development across the first 3 years. Child Dev 79(4):1065–1085

MacLean PC, Rynes KN, Aragon C, Caprihan A, Phillips JP, Lowe JR (2014) Mother–infant mutual eye gaze supports emotion regulation in infancy during the still-face paradigm. Infant Behav Dev 37(4):512–522. doi:10.1016/j.infbeh.2014.1006.1008

Moutsiana C, Johnstone T, Murray L, Fearon P, Cooper PJ, Pliatsikas C et al (2015) Insecure attachment during infancy predicts greater amygdala volumes in early adulthood. J Child Psychol Psychiatry 56(5):540–548

Murray L, Trevarthen C (1986) The infant's role in mother–infant communications. J Child Lang 13(01):15–29

Murray L, Fiori-Cowley A, Hooper R, Cooper P (1996a) The impact of postnatal depression and associated adversity on early mother–infant interactions and later infant outcome. Child Dev 67(5):2512–2526

Murray L, Hipwell A, Hooper R, Stein A, Cooper P (1996b) The cognitive development of 5-year-old children of postnatally depressed mothers. J Child Psychol Psychiatry 37(8):927–935

Murray L, Halligan S, Cooper P (2010) Effects of postnatal depression on mother–infant interactions, and child development. In: Bremner JG, Wachs TD (eds) The Wiley-Blackwell Handbook of Infant Development. Applied and Policy Issues, vol II, 2nd edn. Wiley, pp 192–220. ISBN 9781405178747

Okereafor A, Allsop J, Counsell SJ, et al (2008) Patterns of brain injury in neonates exposed to perinatal sentinel events. Pediatrics 121:906–914. doi:10.1542/peds.2007-0770

Parikh NA, Lasky RE, Kennedy KA, McDavid G, Tyson JE (2013) Perinatal factors and regional brain volume abnormalities at term in a cohort of extremely low birth weight infants. PLoS One 8(5):e62804

Rao H, Betancourt L, Giannetta JM, Brodsky NL, Korczykowski M, Avants BB et al (2010) Early parental care is important for hippocampal maturation: evidence from brain morphology in humans. Neuroimage 49(1):1144–1150

Rifkin-Graboi A, Kong L, Sim LW, Sanmugam S, Broekman BFP, Chen H et al (2015) Maternal sensitivity, infant limbic structure volume and functional connectivity: a preliminary study. [Original Article]. Transl Psychiatry 5:e668

Roth TL, Sweatt JD (2011) Annual research review: epigenetic mechanisms and environmental shaping of the brain during sensitive periods of development. J Child Psychol Psychiatry 52(4):398–408

Sarkar S, Craig MC, Dell'Acqua F, O'Connor TG, Catani M, Deeley Q et al (2014) Prenatal stress and limbic-prefrontal white matter microstructure in children aged 6–9 years: a preliminary diffusion tensor imaging study. World J Biol Psychiatry 15(4):346–352

Schmahmann JD, Weilburg JB, Sherman JC (2007) The neuropsychiatry of the cerebellum—insights from the clinic. Cerebellum 6:254–267

Schore AN (2001) Effects of a secure attachment relationship on right brain development, affect regulation, and infant mental health. Infant Mental Health J 22(1–2):7–66

Schwartze M, Kotz SA (2016) Contributions of cerebellar event-based temporal processing and preparatory function to speech perception. Brain Lang 161:28–32

Shalak L, Perlman JM (2004) Hypoxic-ischemic brain injury in the term infant-current concepts. Early Hum Dev 80:125–141. doi:10.1016/j.earlhumdev.2004.06.003

Shrout PE, Fleiss JL (1979) Intraclass correlations: uses in assessing rater reliability. Psychol Bull 86(2):420

Shulman C (2016). Social and emotional development in infant and early childhood mental health research and practice in infant and early childhood mental health (vol. XIII, pp. 226). Springer International Publishing, Switzerland

Stein A, Craske MG, Lehtonen A, Harvey A, Savage-McGlynn E, Davies B et al (2012) Maternal cognitions and mother–infant interaction in postnatal depression and generalized anxiety disorder. J Abnorm Psychol 121(4):795–809

Teicher MH, Dumont NL, Ito Y, Vaituzis C, Giedd JN, Andersen SL (2004) Childhood neglect is associated with reduced corpus callosum area. Biol Psychiatry 56(2):80–85

Teicher MH, Tomoda A, Andersen SL (2006) Neurobiological consequences of early stress and childhood maltreatment: are results from human and animal studies comparable? Ann N Y Acad Sci 1071(1):313–323

Tiemeier H, Lenroot RK, Greenstein DK, Tran L, Giedd JN, Pierson R et al (2010) Cerebellum development during childhood and adolescence: a longitudinal morphometric MRI study. NeuroImage 49(1):63–70

Tupler LA, De Bellis MD (2006) Segmented hippocampal volume in children and adolescents with posttraumatic stress disorder. Biol Psychiatry 59(6):523–529

van Soelen IL, Brouwer RM, Peper JS, van Leeuwen M, Koenis MM, van Beijsterveldt TC et al (2012) Brain SCALE: brain structure and cognition: an adolescent longitudinal twin study into the genetic etiology of individual differences. Twin Res Human Genet 15(03):453–467

Wade M, Moore C, Astington JW, Frampton K, Jenkins JM (2015) Cumulative contextual risk, maternal responsivity, and social cognition at 18 months. Dev Psychopathol 27(01):189–203

Wang SSH, Kloth AD, Badura A (2014) The cerebellum, sensitive periods, and autism. Neuron 83(3):518–532

Whittle S, Simmons JG, Dennison M, Vijayakumar N, Schwartz O, Yap MB et al (2014) Positive parenting predicts the development of adolescent brain structure: a longitudinal study. Dev Cogn Neurosci 8:7–17

Yushkevich PA, Piven J, Hazlett HC, Smith RG, Ho S, Gee JC et al (2006) User-guided 3D active contour segmentation of anatomical structures: significantly improved efficiency and reliability. NeuroImage 31:1116–1128

Aside from what was mentioned in the concluding remarks of this paper, the findings of this study also have implications for understanding the relative vulnerability of males to neurodevelopmental problems, and for considering potential (possibly parent-mediated) interventions.

Based on these results, the next study incorporated observational measures of mother-infant interactions in the analysis of infants genetically predisposed to ASD. The objective of the study was to compare total and regional brain volumes in infants with and without a familial risk of ASD, and to explore whether any differences in brain volume were associated with subsequent ASD severity and/or clinical diagnostic status. Finally, the study also sought to examine whether mother-infant interactions moderated the extent of differences in brain volume and/or severity of subsequent ASD symptoms.

Chapter 4: Regional brain volumes and behavioural outcomes in infants with a familial risk of ASD

Part of this study is currently under review with Psychological Medicine: Pote et al., "Familial risk of autism alters brain anatomy in infants and predicts the emergence of autistic behaviours in early childhood".

4.1. Introduction

As outlined in the main introduction of this thesis, the majority of studies investigating structural brain differences in ASD, relative to unaffected controls, have been carried out in adults, adolescents, and older children. Among the most consistently observed findings in studies of younger ASD populations, is that affected individuals may undergo a pattern of abnormal early brain development (Lange et al., 2015). For instance, a number of groups have reported a postnatal period of accelerated brain growth, leading to an increase in total brain volume (of up to 10%) by the age of 2 (Courchesne et al., 2001; Hazlett et al., 2011; Redcay and Courchesne, 2005; Schumann et al., 2010; Sparks et al., 2002). Also, evidence for larger head sizes at 4-6 months in children who later developed ASD has been reported by some (Courchesne et al., 2003; Dawson et al., 2007; Lainhart et al., 1997; Nordahl et al., 2011), but not all (Surén et al., 2013; Zwaigenbaum et al., 2014), and suggests that underlying differences in brain structure may precede the onset of clinical symptoms.

In recent years, prospective studies of infants at risk of ASD have made some crucial first steps in understanding the early biological signs of the disorder. As more of these studies arise, they may help to identify neural markers that predate the emergence of symptoms. Thus far, MRI studies comparing brain structure in 6 month-old siblings of infants with ASD, relative to those with typically developing siblings, have reported differences in white matter

microstructure as well as extracerebral CSF and corpus callosum (Shen et al., 2013; Wolff et al., 2012, 2015). Specifically, increased area and thickness of the corpus callosum (Wolff et al., 2015), as well as increased volume of subarachnoid CSF (Shen et al., 2013) correlated with subsequent ASD symptom severity at 24 months (Shen et al., 2013; Wolff et al., 2015). There is therefore preliminary evidence to suggest that infants at high-risk of ASD have early differences in brain structure by 6 months, which are associated with the subsequent development of ASD symptoms. However, it is still unclear whether differences in brain volume can be identified in high-risk infants at younger ages and/or in other brain regions.

Moreover, as reported in the first experimental study of this thesis (chapter 3), variations in early mother-infant interactions are associated with differences in brain volume. Hence, the early caregiving environment may have the ability to impact upon later behavioural and cognitive outcomes (Cabrera et al., 2011; Lugo-Gil and Tamis-LeMonda, 2008). In addition, prior studies of infants at risk of ASD have reported that differences in early parent-infant interactions are evident by 6 months of age. For instance, parents of high-risk infants have shown increased directiveness and lower levels of sensitive responding, compared to low-risk controls. High-risk infants also appear less lively (Doussard-Roosevelt et al., 2003; Wan et al., 2012, 2013). To date, however, no studies of infants at risk of ASD have related variations in parenting style to differences in infant brain volume. It is therefore unknown whether any putative differences in brain development are influenced by early mother-infant interactions. Nonetheless, just as early identification of ASD has become a priority, so has the search for how parent-infant interactions can modulate outcome.

In summary, there is initial evidence that infants at high-risk of ASD have early differences in brain development and in parent-infant interactions. However, it is not yet known if infants with a familial risk of ASD have differences in brain volume that can be detected before 6 months of age. Neither is it known whether the early caregiving environment influences any such putative differences.

As a result, this prospective longitudinal study used MRI to (i) investigate total and regional brain volume differences in 4-6 month-old infants at high familial risk of ASD, relative to a group of infants at low-risk. Since larger volumes of extracerebral CSF in 6 month-old infants at risk of ASD have been reported in comparison to infants at low-risk (Shen et al., 2013), the CSF was specifically examined. Next, (ii) I examined whether any observed group differences were associated with subsequent ASD symptom severity and/or clinical diagnostic status at 36 months. Finally, (iii) the possibility that early mother-infant interactions moderated the extent of differences in brain volume and/or severity of ASD symptoms was also explored.

Given the pre-existing evidence implicating extracerebral CSF in ASD, a group difference in CSF volume was predicted. All other brain regions remained exploratory. In addition, based on the findings from the prior study (chapter 3), it was hypothesised that mother-infant interactions would moderate the association between risk group and infant brain volume. However, as no previous volumetric study has examined high-risk infants younger than 6 months of age, no *a priori* hypothesis regarding the direction of these differences was constructed.

4.2. Materials and methods

4.2.1. Participants

For this particular study, both high-risk and low-risk infants were included, and participants were categorised based on the criteria previously described in the methodology section of this thesis (please see section 2.2.3 on page 95). A total of 59 infants originally participated in this study. Of the 59 cases, 9 were excluded from the main analysis: 8 due to poor image quality and motion artefacts, and 1 low-risk participant because they subsequently received an ASD diagnosis. Hence, the final sample size consisted of 50 infants: 26 low-risk (n = 12 male; mean corrected age at scan = 60.54 corrected weeks, SD = 4.17) and 24 high-risk (n = 11 male; mean corrected age at scan = 60.73 corrected weeks, SD = 3.20).

4.2.2. Experimental procedures

Infants were scanned within an age-range of 50-70 corrected weeks (between approximately 4-6 months of age). Within two weeks of the MRI acquisition, but usually on the same day, mother-infant interaction dimensions were obtained. Behavioural measures of observed mother-infant interactions were available for only n = 23 of the 26 infants in the low-risk group, and n = 21 of the 24 infants in the high-risk group. At 36 months of age, all infants in the high-risk group were invited back for a follow-up behavioural assessment; n = 23 of the 24 infants scanned returned. All experimental procedures were conducted as described earlier in the main methodology of this thesis (see sections 2.2.4-2.2.6, starting on page 96). By the time of analysis, however, the segmentation protocol had been further refined, so that the volumetric measure for lateral ventricles included here did not incorporate the cavum septum pellucidum.

4.2.3. Statistical analysis

Normality of data distribution was assessed visually using box-plots, and statistically using the Shapiro-Wilk Test. Group differences in infant characteristics and mother-infant interaction dimensions were tested using the Independent Samples t-test, the Mann-Whitney U-test, and the Pearson's Chi-Square test, as appropriate.

4.2.3.1. Baseline differences in regional brain volumes

Brain volumes were not normally distributed; hence, logarithmic transformations were performed on all volumes to adjust for skew and achieve normal distribution. An analysis of co-variance (ANCOVA) on the log-transformed data was used to examine cross-sectional differences in regional brain volumes between the two risk groups (low-risk vs. high-risk). The dependent variables of interest included: total grey and white matter, subcortical region, midbrain, cerebellum, total brain tissue, lateral ventricles, extracerebral CSF, total CSF, and intracranial volume. The proportion of extracerebral CSF over total CSF volume was also compared between risk groups. Infant age and intracranial volume were included as co-variates, and sex was included as a (between subjects) fixed factor, mainly because males and females are known to have different developmental trajectories (Lenroot et al., 2007),

4.2.3.2. Regional brain volumes and outcome measures within the high-risk group

In regions where the high-risk group had shown significant differences in brain volumes at 4-6 months, the associations between these early volumes and ASD outcome measures at 36 months were examined. Dimensional analyses were run using non-parametric (Spearman's rank) correlations. These analyses explored the association between regional brain volumes at 4-6 months and observable autistic behaviours at 36 months, as assessed using the ADOS-2 calibrated severity scores. Statistical significance was set at $p \leq 0.05$ (one-tailed).

Following assessment at 36 months, n = 4 male infants in the high-risk group received a diagnosis of ASD. Analyses were thus repeated to determine if the results were representative of the high-risk group as a whole, or whether driven by individuals with an ASD diagnosis.

4.2.3.3. Moderation by mother-infant interactions

Moderation analyses were conducted to examine whether mother-infant interactions (that is, maternal and/or infant behaviours) influenced brain regions with significant group differences in volume at 4-6 months of age. The PROCESS macro tool (Hayes, 2012) was applied to test whether the interaction between risk group and maternal behaviour (Group x Maternal Behaviour) predicted infant brain volume. This was then repeated to test the interaction between risk group and infant behaviour (Group x Infant Behaviour). In this analysis, infant age, sex, and intracranial volume were included as co-variates. PROCESS applies bias corrected bootstrapping intervals to probe the interaction term and make inferences about indirect effects, rather than relying on the normality assumption. The number of bootstrap samples used to determine 95% bias-corrected bootstrap confidence intervals was 1000. For continuous moderators, PROCESS produces the conditional effects of the independent variable at the sample mean of the moderator, and at plus and minus one standard deviation from the mean. A Bonferroni correction for multiple comparisons was applied to these results. Where a significant interaction term emerged, the association between behaviour and brain volume was further examined using simple correlations within each risk group.

Finally, further moderation analyses were conducted within the high-risk group only, to examine whether the behaviours found to moderate the association between risk group and brain volume at 4-6 months (that is, the impact of maternal sensitivity on the subcortical region), moderated the association between brain volume and infant outcome at 36 months. Again, the PROCESS macro tool was applied to test whether the interaction between maternal sensitivity and early brain volume (Subcortical Volume x Maternal Sensitivity) predicted infant outcome at 36 months. Infant outcome was assessed by both the ADI-R and the ADOS-2, but since the scores were not normally distributed, logarithmic transformations were performed to obtain normality, and the transformed values were used instead. As before, infant age, sex, and intracranial volume were included as co-variates. A Bonferroni correction for multiple comparisons was also applied to the results.

4.3. Results

4.3.1. Sample characteristics

The characteristics of the total sample, and split by risk group, are presented in Table 4.1. Infants (n = 50; 26 low-risk, 24 high-risk) were scanned at a mean age of 60.63 corrected weeks (SD = 3.70, range = 53.00-68.00 corrected weeks; Figure 4.1), and risk groups did not differ significantly in age (at birth and at MRI), body weight (at birth and at MRI), head circumference (at MRI), or sex. There were also no significant group differences in observed mother-infant interactions for any of the dimensions examined at 4-6 months. The range in the quality of behaviours was also comparable between groups (Table 4.2).

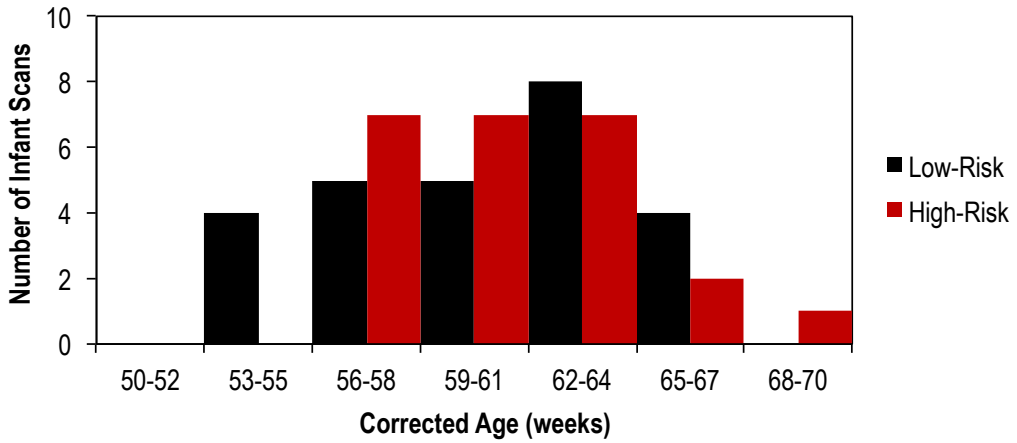

Figure 4.1: Distribution of the participants' age at the infant timepoint.
A histogram of the participants' corrected age at the time of the infant MRI is shown.
The total sample comprised of 50 infants, with 26 low-risk (in black) and 24 high-risk (in red).

Table 4.1: Infant characteristics stratified by risk group

Infant Characteristics	Total Sample (N = 50)	Low-Risk Group (n = 26)	High-Risk Group (n = 24)	Group Difference Statistic (*p*-value)
Gestational age at birth (weeks); mean (SD)	39.63 (1.45)	39.68 (1.72)	39.59 (1.18)	U = 281.00, $p = 0.537$
Corrected age at MRI (weeks); mean (SD)	60.63 (3.70)	60.54 (4.17)	60.73 (3.20)	$t = -0.18$, $p = 0.857$
Sex (male); n (%)	23 (46.00)	12 (46.15)	11 (45.83)	$\chi^2 = 0.00$, $p = 0.982$
Body weight at birth (kg); mean (SD)	3.44 (0.52)	3.34 (0.49)	3.54 (0.54)	$t = -1.40$, $p = 0.167$
Body weight at MRI (kg); mean (SD)	7.16 (0.92)	7.00 (0.95)	7.34 (0.87)	$t = -1.32$, $p = 0.195$
Head circumference at MRI (cm); mean (SD)	42.42 (1.54)	42.50 (1.69)	42.33 (1.39)	$t = 0.39$, $p = 0.700$

Abbreviations: SD = standard deviation; MRI = magnetic resonance imaging; U = Mann-Whitney U-statistic; *t* = Independent samples t-statistic; χ^2 = Pearson's Chi-Square.

Table 4.2: Maternal and infant interaction dimensions stratified by risk group

	Total Sample (N = 44)		Low-Risk Group (n = 23)		High-Risk Group (n = 21)		Group Difference	
Interaction Dimensions	**Mean**	**SD**	**Mean**	**SD**	**Mean**	**SD**	***t***	***p*-value**
Maternal Dimensions								
Sensitivity	3.58	0.69	3.70	0.75	3.44	0.59	1.24	0.223
Affect	4.24	0.51	4.37	0.44	4.11	0.55	1.78	0.083
Infant Dimensions								
Communication	3.33	0.84	3.36	0.83	3.28	0.87	0.89	0.745
Fretfulness	4.11	0.71	4.09	0.73	4.13	0.71	0.76	0.886

Note: Interaction dimensions are scored on a scale from 1-5; low scores indicate poor interactions (for example, lower levels of sensitivity, increased depressive affect, fewer communication attempts, and increased infant fretfulness). Abbreviations: *t* = Independent Samples *t*-statistic; SD = standard deviation.

Following assessment at 36 months, infants in the high-risk group were subdivided by outcome classification as follows: high-risk non-ASD (n = 19), and high-risk ASD (n = 4). When stratified by outcome group, participants did not differ significantly in age (p = 0.896) or MSEL (p = 0.105); but please see Table 4.3 for a complete description of behavioural scores.

4.3.2. Group differences in total brain matter and intracranial volume at 4-6 months

There was no significant difference in the volume of total brain matter [F(1,45) = 0.36, p = 0.549] or intracranium [F(1,45) = 0.33, p = 0.569], between infants in the high-risk and low-risk groups (Table 4.4).

4.3.3. Group differences in regional brain volumes at 4-6 months

Infants in the high-risk group had a significantly larger volume of the cerebellum [F(1,44) = 6.92, p = 0.012] and the subcortical region [F(1,44) = 4.64, p = 0.037], when compared to those in the low-risk group (Table 4.4, Figure 4.2). Results did not differ when the analysis was co-varied for total brain tissue, as opposed to intracranial volume. No other brain region or calculated proportion showed significant differences between groups (Table 4.4).

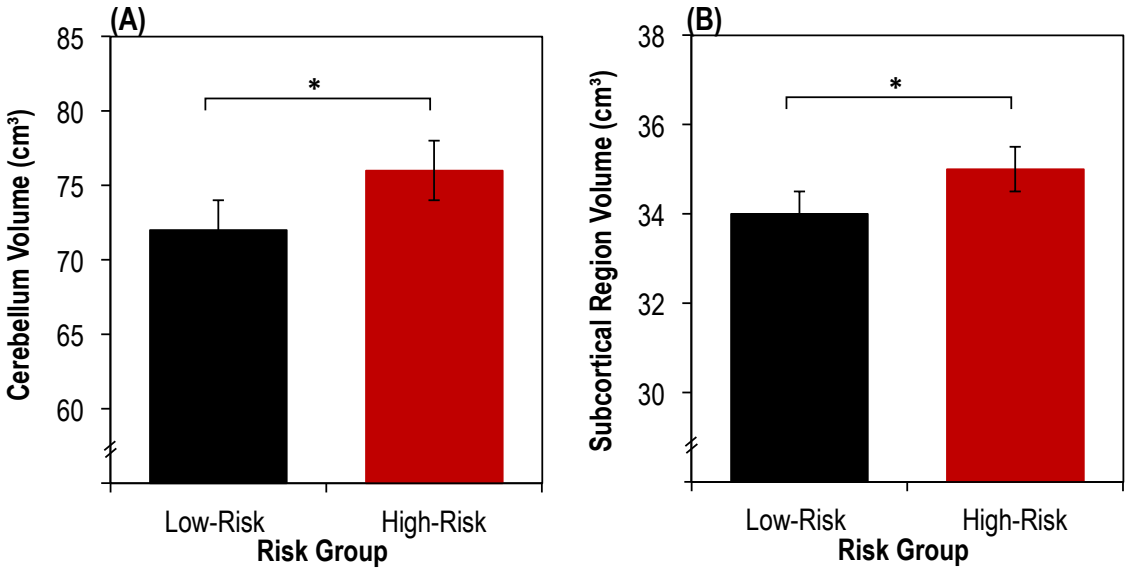

Figure 4.2: Mean cerebellar and subcortical volumes in 4-6 month-old infants at low and high-risk of ASD. Infants in the high-risk group had a significantly larger volume of the **(A)** cerebellum and **(B)** subcortical region, when compared to low-risk controls. Error bars represent one standard error of the mean, *p ≤ 0.05.

Table 4.3: Infant clinical and behavioural measures stratified by outcome group

	High-Risk Non-ASD Group (n = 19)		High-Risk ASD Group (n = 4)	
Measure	**Mean**	**SD**	**Mean**	**SD**
Age at Assessment Visit (months)	38.97	1.54	38.86	0.89
Mullen ELC SS*	107.89	22.66	81.00	34.07
ADOS-2 Domains				
Social Affect CSS	2.58	1.81	6.00	3.56
Restricted & Repetitive Behaviours CSS	3.53	2.57	7.25	1.71
Total CSS	2.11	1.73	6.00	4.24
ADI-R Domains*				
Social	1.63	1.34	16.00	6.68
Communication	2.37	2.97	13.50	3.70
Repetitive Behaviours & Interests	0.53	0.96	6.00	0.82

Note: *Mullen and ADI-R measures were only available for n = 3 of the 4 infants in the high-risk ASD group. Abbreviations: Mullen ELC SS = Mullen Scale of Early Learning Composite Standard Score; ADOS-2 = Autism Diagnostic Observation Schedule – Second Edition; CSS = Calibrated Severity Score; ADI-R = Autism Diagnostic Interview – Revised; SD = standard deviation.

Table 4.4: Group differences in infant brain volumes and proportions of volumes, between low-risk and high-risk groups

	Low-Risk Group (n = 26)		High-Risk Group (n = 24)		Group Difference	
	Mean	**SD**	**Mean**	**SD**	**F**	***p*-value**
Brain Volumes (cm^3)						
Total Grey & White Matter	584.47	61.47	590.02	59.30	0.29	0.593
Subcortical Region	**33.59**	**2.99**	**35.27**	**3.34**	**4.64**	**0.037**
Midbrain	13.35	1.89	13.17	1.57	0.84	0.364
Cerebellum	**71.15**	**8.91**	**75.83**	**8.09**	**6.92**	**0.012**
Total Brain Tissue	702.56	71.55	714.29	69.03	0.36	0.549
Lateral Ventricles	14.22	5.67	13.34	3.73	0.59	0.448
Extracerebral CSF	122.90	27.23	125.30	31.75	0.03	0.857
Total CSF	137.12	29.21	138.64	33.34	0.12	0.727
Intracranium[a]	839.68	86.23	852.93	80.05	0.33	0.569
Brain Proportions (au.)						
Extracerebral CSF/Total CSF	0.90	0.04	0.90	0.03	0.50	0.483

Note: In this analysis of co-variance, infant age and intracranial volume were included as co-variates, and sex was included as a fixed factor; hence, F = F(1,44). [a]In this analysis, only infant age and sex were corrected for; hence, F = F(1,45). Significant results are shown in **bold.** Abbreviations: CSF = cerebrospinal fluid; F = F-statistic; SD = standard deviation.

When the 4 participants who received a diagnosis of ASD were excluded from the analyses, the cerebellum remained significantly larger in the high-risk group [$F(1,40) = 8.79$, $p = 0.005$]. However, there was no significant difference in cerebellar volume between high-risk infants who received an ASD diagnosis, relative to those who did not [$F(1,18) = 1.07$, $p = 0.315$]. In contrast, the subcortical region was no longer significantly enlarged in the high-risk group [$F(1,40) = 1.60$, $p = 0.213$], most likely because the high-risk infants who received an ASD diagnosis had significantly larger subcortical volumes than the high-risk group without a later diagnosis [$F(1,18) = 8.39$, $p = 0.010$]. Results did not differ when co-varied for total brain tissue, as opposed to intracranial volume.

4.3.4. Associations between regional brain volumes at 4-6 months and ASD symptoms at 36 months

Within the high-risk group, there was a significant positive correlation between the volume of the subcortical region at 4-6 months and restricted and repetitive autistic behaviours at 36 months ($r = 0.52$, $p = 0.011$) (Figure 4.3A). There was also a strong trend to significance in social affect ($r = 0.38$, $p = 0.071$) and total autistic symptoms ($r = 0.40$, $p = 0.061$). When the 4 children who received a diagnosis of ASD at 36 months were excluded from the analyses, the correlation between subcortical volume and the ADOS-2 score for repetitive behaviour still approached, but did not reach, significance ($r = 0.36$, $p = 0.066$).

There was a significant correlation between cerebellar volume at 4-6 months and restricted and repetitive behaviours at 36 months, as measured by the ADOS-2 ($r = 0.44$, $p = 0.017$) (Figure 4.3B). Correlations between cerebellar volume and social affect ($r = 0.347$; $p = 0.052$), as well as total ADOS-2 score ($r = 0.315$; $p = 0.071$) also approached significance. When the 4 children who received a diagnosis of ASD at 36 months were excluded from the analyses, correlations between cerebellar volume and ADOS-2 scores remained highly significant across all behavioural domains (restricted and repetitive: $r = 0.64$, $p = 0.001$; social affect: $r = 0.51$, $p = 0.014$; total: $r = 0.55$, $p = 0.007$).

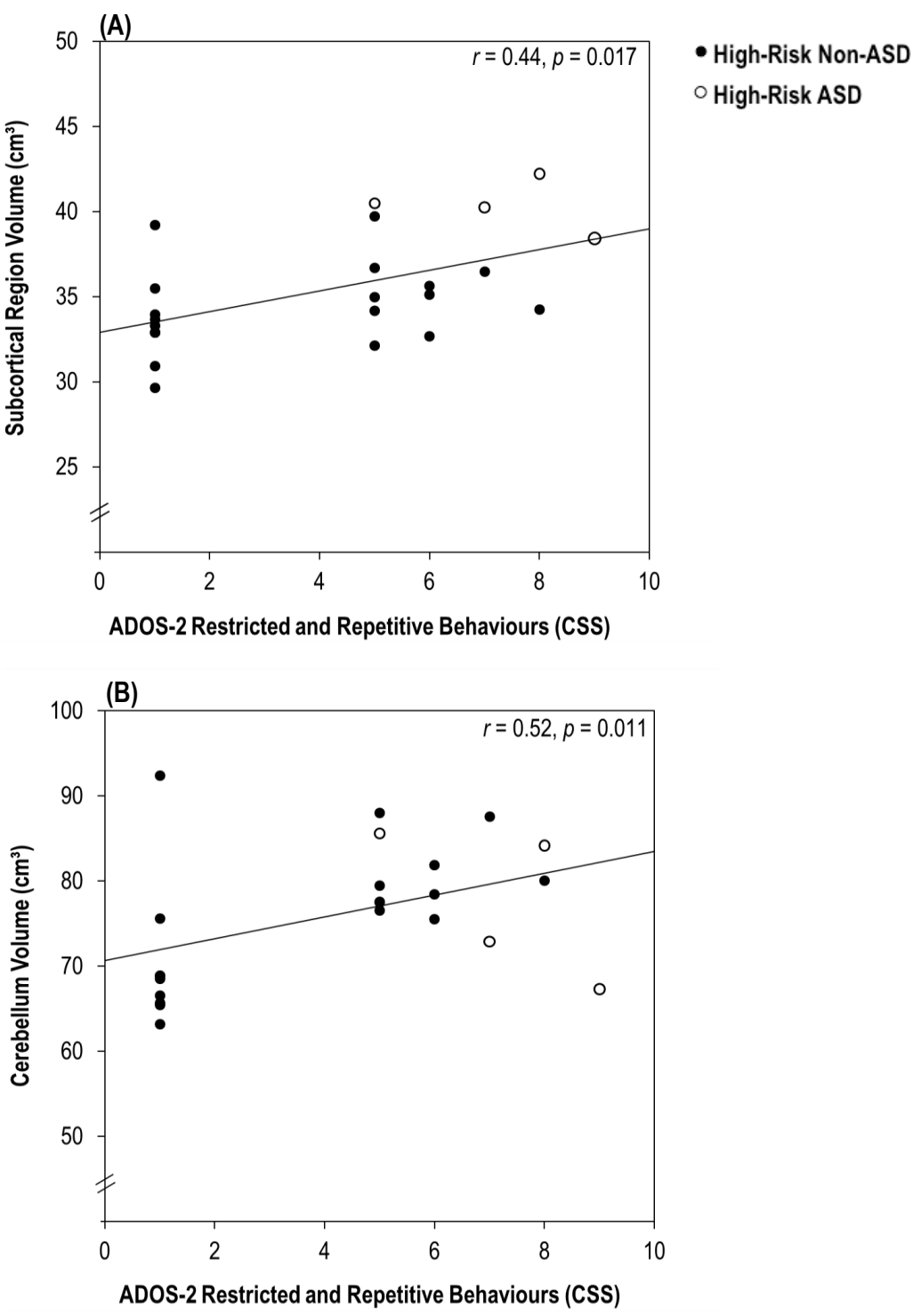

Figure 4.3: Scatter plots of the correlations between infant regional brain volumes at 4-6 months of age, and restricted and repetitive behaviours at 36 months in high-risk infants. (A) Subcortical and **(B)** cerebellar volumes are shown. The linear trendline indicates the correlation for all high-risk infants, but those who received an ASD diagnosis at 36 months are highlighted in clear circles. Abbreviations: ADOS-2 = Autism Diagnostic Observation Schedule – Second Edition; CSS = Calibrated Severity Scores; r = Spearman's rank correlation coefficient.

4.3.5. Moderation of regional brain volumes by mother-infant interactions at 4-6 months

Maternal sensitivity moderated the association between infant risk group and volume of the subcortical region, suggesting that there was an interaction between risk group and maternal sensitivity [Group x Maternal Sensitivity: Unadjusted (β = -0.05, p = 0.016, CI = -0.08, -0.01)] (Figure 4.4). This interaction term (Group x Maternal Sensitivity) survived Bonferroni correction (p = 0.032), and remained significant at trend level after adjusting for infant age, sex, and intracranial volume [Group x Maternal Sensitivity: Adjusted (β = -0.03, p = 0.059, CI = -0.06, 0.00)].

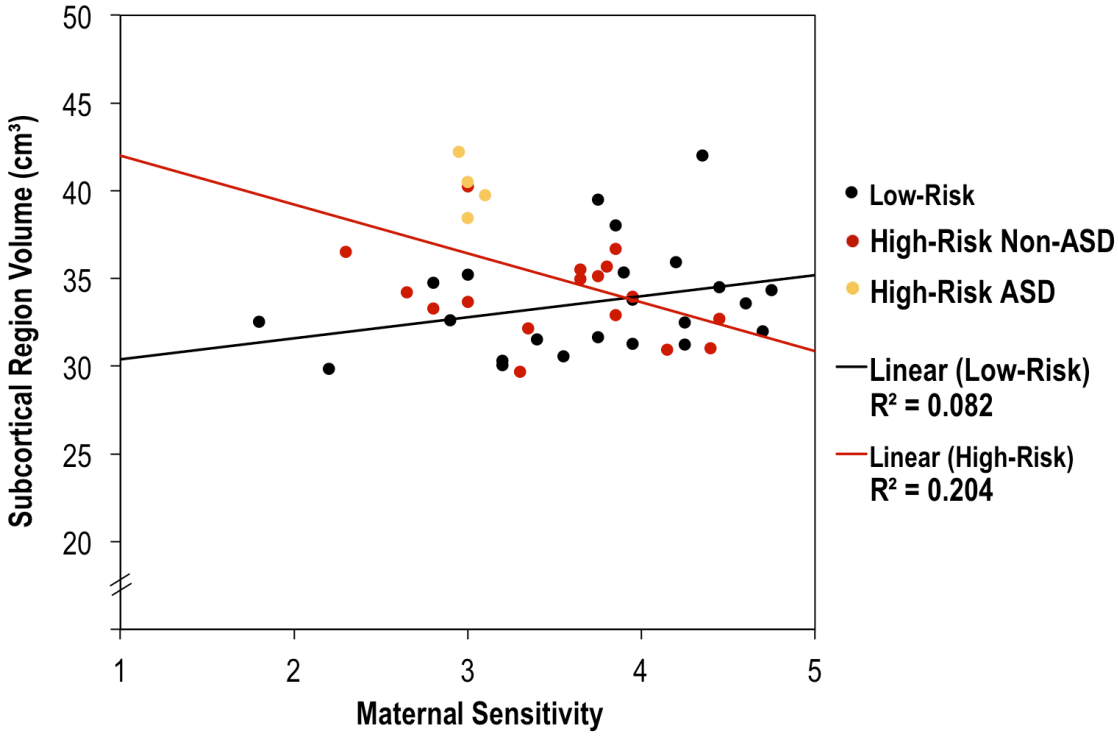

Figure 4.4: A representation of the interaction between maternal sensitivity and risk group on infant subcortical volume. High-risk infants are shown in red, whilst low-risk infants are shown in black. However, high-risk infants who received a diagnosis of ASD at 36 months are highlighted in yellow. Note: linear trendlines have been fitted to the risk groups, and not the outcome groups.

In light of this finding, the association between subcortical volume and maternal sensitivity was examined within each risk group separately. In the high-risk group, there was a significant negative correlation between the degree of sensitivity displayed by mothers and the infants'

subcortical volume (r = -0.45, p = 0.045). In contrast, maternal sensitivity was not significantly correlated with infant subcortical volume in the low-risk group (r = 0.29, p = 0.187). The difference between these correlation coefficients was significant (z = 2.37, p = 0.018). Thus, infants in the high-risk group whose mothers demonstrated higher levels of 'sensitivity' tended to have subcortical volumes more similar to those of the low-risk ('typical') infants.

No other maternal or infant behaviour moderated the association between risk group and infant subcortical volume. In addition, no maternal or infant behaviour moderated the difference in cerebellar volume.

4.3.6. Moderation of infant outcome at 36 months by maternal sensitivity at 4-6 months

Within the high-risk group, maternal sensitivity moderated the association between subcortical volume at 4-6 months and infant outcome at 36 months, as assessed by the ADI-R score on social affect [Subcortical Volume x Maternal Sensitivity: Adjusted (β = -37.55, p = 0.032, CI = -71.31, -3.79)]. The interaction term survived Bonferroni correction at trend level (p = 0.096). This suggests that there was an interaction between subcortical volume and maternal sensitivity, which was predictive of ASD symptom severity at a later timepoint. The model explained 53.0% of the outcome and of this, 23.0% was explained by the interaction term (Subcortical Volume x Maternal Sensitivity). In addition, 33.1% was explained by the subcortical volume alone and 2.4% by maternal sensitivity.

Maternal sensitivity did not moderate the association between subcortical volume at 4-6 months and any other observed measure of infant behaviour at 36 months.

4.4. Discussion

In this longitudinal MRI study, brain volumes were compared between young infants with and without a familial risk of ASD. The study also examined whether any such differences were associated with subsequent ASD severity and/or clinical diagnostic status at 36 months. Whether early mother-infant interactions moderated the extent of differences in brain volume

and/or severity of ASD symptoms was also explored. There were no significant differences between high-risk and low-risk groups in either total brain tissue volume or head size (that is, intracranial volume). However, infants in the high-risk group had larger cerebellum and subcortical volumes at 4-6 months of age. These early differences in volume were also associated with the extent of autistic behaviours at 36 months. Moreover, preliminary evidence of a negative correlation between maternal sensitivity and subcortical volume within the high-risk group was identified, and the interaction between brain and parenting was predictive of ASD symptom severity at 36 months within the social domain.

4.4.1. Cerebellum findings

Cerebellar abnormalities are among the most consistently reported findings in ASD literature (for review see Becker and Stoodley, 2013; Fatemi et al., 2012; Rogers et al., 2013). Most prior investigations, however, were carried out in adolescents and adults with ASD, and mainly report hypoplasia rather than overgrowth (Courchesne et al., 1988; Levitt et al., 1999; McAlonan et al., 2002; Rojas et al., 2006). In contrast, studies of younger children have found enlargement of the cerebellum. For example, in studies of 2-5 year-olds, children with ASD were reported to have significantly larger total cerebellum (Sparks et al., 2002) and cerebellar white matter volume (Courchesne et al., 2001), as compared to typically developing controls. The results of this study extend these findings in children to younger ages, and indicate that a familial risk of ASD may alter cerebellar development by as early as 4-6 months of age. Although the underlying cause(s) of this early enlargement (and subsequent lower size) remain to be established, it most likely reflects an abnormal regulation of growth (Courchesne et al., 2001; Sparks et al., 2002). Some have suggested that this may involve an initial excess in synaptic proliferation, myelination, and neurogenesis, as well as enlarged glia, premature dendritic/axonal growth, and incomplete synaptic pruning (for review see Bauman and Kemper, 2005; Palmen et al., 2004), which is then followed by compensatory apoptotic and/or excitotoxic processes (Courchesne et al., 2001).

Unlike the subcortical region, enlargement of the cerebellum did not reach significance in the subgroup of infants who received an ASD diagnosis at 36 months. In contrast, across the entire high-risk group, there was a significant association between cerebellum volume and subsequent severity of repetitive behaviours. Moreover, when high-risk infants with ASD were excluded from the outcome correlation analyses, the associations between cerebellum volume, repetitive behaviours, and other autistic symptoms remained significant. Thus, the relationship between larger cerebellar volumes at 4-6 months and poorer behavioural outcomes at 36 months did not depend on those relatively few high-risk infants who received a diagnosis of ASD. However, since ASD diagnoses are more commonly made around 2-3 years of age, 36 months is an early diagnosis. The possibility that other infants in this study will be diagnosed at an older age cannot therefore be excluded, and so, these infants will continue to be followed-up.

A relationship between cerebellar volume and repetitive behaviours in ASD has been previously documented in older cohorts, with both smaller (D'Mello et al., 2015; Rojas et al., 2015) and larger (D'Mello et al., 2015) volumes linked with repetitive and stereotyped behaviours. The measures of repetitive behaviours obtained in this study at 36 months may be particularly sensitive to motor stereotypies. Indeed, motor features appear to be one of the earliest infant manifestations of the disorder (Esposito et al., 2011; Focaroli et al., 2016; Zwaigenbaum et al., 2013), and findings from this study suggest that they could partly be explained by differences in the early development of the cerebellum. Similarly, a relationship between the cerebellum and social communication has been reported in ASD before. Studies of older individuals with ASD, however, found that smaller grey matter volumes of cerebellum lobules VIII were associated with more severe ratings on social communication scores (D'Mello et al., 2015; Rojas et al., 2006). In the present study, findings were in the opposite direction, but the entire cerebellum was measured. It is therefore not possible to say which sub-region(s) of the cerebellum might be driving the results. Further studies will be needed to map the trajectory of cerebellar development in infants at risk of ASD who go on to be diagnosed.

4.4.2. Subcortical findings

In this study, the subcortical region was significantly larger in infants at risk of ASD compared to low-risk controls. Although high-risk infants who later received a diagnosis of ASD had the largest volumes, the size of the subcortical region at 4-6 months correlated with repetitive behaviours at 36 months, regardless of diagnostic classification. The caveat is that this study was not powered to identify diagnostic markers of ASD, as this would require a much larger sample size of high-risk infants. However, the observation that subcortical enlargement at 4-6 months may be a feature of high-risk infants who receive a diagnosis, is worthy of follow-up.

Although there are no published studies examining subcortical volume in infants at risk of ASD, there are many reports that older individuals diagnosed with ASD have significant differences in the anatomy of subcortical structures. For example, the caudate nucleus has been reported to be larger in children, adolescents, and adults (Estes et al., 2011; Haznedar et al., 2006; Herbert et al., 2003; Hollander et al., 2005; Langen et al., 2007; Rojas et al., 2006; Sears et al., 1999). Caudate overgrowth has even been proposed as a core abnormality of ASD (Stanfield et al., 2008). Other regions such as the globus pallidus and putamen have also been reported to be enlarged in individuals with ASD (Estes et al., 2011; Herbert et al., 2003; Hollander et al., 2005; Langen et al., 2007; Sato et al., 2014; Turner et al., 2016), although some of these findings may be confounded by differences in total brain volume (Estes et al., 2011; Herbert et al., 2003). Results from studies of the thalamus in ASD are less clear-cut, with reports of no difference (Haznedar et al., 2006), larger volumes (Herbert et al., 2003), and smaller volumes (Hardan et al., 2006a; Tsatsanis et al., 2003).

Subcortical volume differences have also been linked to ASD symptoms in older cohorts, although the direction of the relationship varies. For example, larger volume of the caudate in adolescents and adults with ASD has been reported to be both positively (Hollander et al., 2005; Rojas et al., 2006) and negatively (Sears et al., 1999) correlated with severity of repetitive and stereotyped behaviours. Caudate volume in these individuals has also been positively correlated with social and communication scores (Rojas et al., 2006). In contrast,

studies of younger individuals (aged 3-4 years) found that more repetitive and stereotyped behaviours were linked to smaller volumes of several subcortical regions, including the left thalamus, right globus pallidus, putamen, and striatum (Estes et al., 2011). Therefore, regardless of the direction of the association, work to date clearly implicates abnormalities of the subcortical region with ASD symptoms, and especially repetitive behaviours.

The findings of the present study extend current knowledge, and suggest that the subcortical region is already enlarged by 4-6 months of age in infants at high-risk of ASD who go on to develop a clinical diagnosis at 36 months. Results also suggests that, even when children who receive an ASD diagnosis are excluded from the analysis, larger subcortical volumes in early development are indicative of more repetitive behaviours at a later age.

4.4.3. Non-significant CSF findings

In contrast to what had been *a priori* predicted based on the findings documented in a recent study of infants at risk of ASD (Shen et al., 2013), this study did not identify any evidence of greater extracerebral CSF volume in the high-risk group. It also did not find differences in CSF proportions between groups. There are several reasons that could explain the divergent results in studies. First, this study focussed on infants aged 4-6 months, whereas the other examined infants aged 6-9 months, and it could be that enlarged extracerebral CSF volume is only present in individuals slightly older than 6 months. Second, the study by Shen et al., (2013) drew a horizontal slice through the anterior commissure in order to define a ventral boundary for the region of the extracerebral CSF. The present study did not, and therefore, this slight difference in the anatomical delineation of the region may have driven the non-significant results. Finally, and although the study by Shen et al., (2013) had a similar sample size to that of the present study (high-risk: n = 33 vs. n = 24; low-risk: n = 22 vs. n = 26), the possibility of a false negative error in this study (or a false positive in the other) cannot be excluded.

4.4.4. The impact of mother-infant interactions on early brain volume and severity of later autistic symptoms

Finally, although this study reported that high-risk infants had larger subcortical volumes than low-risk controls, there was also preliminary evidence of a negative association between maternal sensitivity and subcortical volume within the high-risk group. That is, infants in the high-risk group exposed to more 'sensitive' mothers tended to have subcortical brain volumes more comparable to the low-risk ('typical') group. Maternal sensitivity also moderated the association between the volume of the subcortical region at 4-6 months and infant social affect at 36 months, suggesting that the interaction between brain and behaviour may be predictive of social difficulties at a later timepoint. Thus, not only do these results indicate that the subcortical region is altered in infants with a familial risk of ASD who go on to develop a clinical diagnosis, but also that this region may be responsive to the early parent-child environment.

Others have shown that normative variations in early parenting may influence brain development. For example, higher levels of parental sensitivity have been associated with markers of more optimal brain development in 8 year-old children, including larger total brain and grey matter volumes, as well as more rapid cortical thinning (Kok et al., 2015). The findings of this study imply a similar protective effect of exposure to more 'sensitive' mothers. Sensitive parenting may reduce a child's experience and perception of stress (Kertes et al., 2009; Luijk et al., 2010), facilitating more appropriate brain and behavioural development. To be clear, however, the present study does not support the suggestion that differences in maternal behaviour cause their infant to develop ASD. Since infant and mother are closely genetically related, it is possible for instance that the associations observed in this study could be mediated through shared genetic variants, including an inherited brain volume and/or behavioural style (Klahr and Burt, 2014). Other factors, such as the infant's behaviour, the presence of an older ASD sibling, and the parent's own approach may also be playing a role here, influencing the mother-infant interaction. For example, mothers may unconsciously detect subtle behavioural differences in the social interactions of infants at risk of ASD, which

precede the onset of clinical symptoms (Jones et al., 2014), and are likely to cause the mother to adjust her behaviour in response to the infant's affect and attention. Similarly, in families with an older sibling diagnosed with ASD, the strategies developed by parents to interact with the autistic child may be inadvertently transferred to the interaction with the later born infant. In line with this, high-risk infants may also pick-up on behaviours exhibited by the older sibling, and which to some extent, may mould the infant's own behaviour. Finally, parents of high-risk infants may also demonstrate characteristics of the BAP themselves, and thus be less sensitive to their infant's' mental state (Bolton et al., 1998; Gerdts and Bernier, 2011), which may negatively impact upon the mother-infant interaction.

4.4.5. Study limitations

This study has several limitations. First, given the modest sample size and the need to understand the dimensional nature of ASD, this study focused on a comparison of high and low-risk infants at 4-6 months, rather than their behavioural outcomes. The comparison of high-risk infants with and without a diagnosis of ASD at 36 months should be considered exploratory only. Also given the small sample size and tentative nature of this study, no correction for multiple comparisons was conducted when examining mean volumetric differences between groups. The possibility of a false positive (type I) error cannot therefore be excluded. Second, outcome data was only collected for high-risk infants. If outcome measures for both risk groups had been obtained, this would have enabled a better classification of the cohort, and would have allowed for different questions to be asked. For example, how many low-risk infants developed ASD, and how did their regional brain volumes compare to that of high-risk infants who also received an ASD diagnosis? With this in mind, outcome measures for project 2 (conducted at 3T, and including both fetal and neonatal timepoints) are currently being collected for individuals enrolled in either risk group. Third, but in line with what has been reported by others (Hazlett et al., 2012), the differentiation of grey and white matter was not possible due to ongoing myelination at this age. Fourth, the images included in this study were acquired with a large slice gap of 2 mm, which may have affected the accuracy of the volumetric segmentation. Also owing to the low resolution of the images,

the cerebellum and the subcortical region could not be separated into their individual components. Specifically, the cerebellum was not partitioned into cerebellar hemispheres and vermis lobules, while the subcortical region was not subdivided into caudate nucleus, putamen, globus pallidus, thalamus, and internal capsule. Last, the parent-child interactions included in this study were limited to observations with only the mothers, and further research would benefit from the inclusion of paternal interactions.

4.4.6. Conclusions

To the best of my knowledge, this is the first MRI study to report that regional brain volume differences in infants at risk of ASD are present prior to 6 months of age, and correlate with subsequent ASD severity. Thus, this study adds to the existing evidence that a familial risk of ASD causes differences in brain structure which are associated with the subsequent development of autistic behaviours. Building on the findings from the prior study, which reported significant associations between maternal sensitivity and subcortical volume, this study extends this finding further by providing preliminary evidence of an association between maternal sensitivity and subcortical volume within the high-risk sample. This suggests that the subcortical region may be responsive to both genetic and environmental exposures from early on in infancy. Further investigation is warranted to establish the utility of the cerebellum and subcortical region as potential 'risk' markers. Finally, the possibility that the development of the subcortical region may be modifiable through parenting style should also be tested, with the ultimate goal of encouraging future parent-mediated intervention trials.

To extend these results and given the evidence suggesting that ASD begins in prenatal life, the next step was to examine even earlier brain development, and to compare brain volumes between fetuses at high and low-risk of ASD. As such, the main aim was to investigate whether a familial risk of ASD can already show differences in brain volume *in utero*.

Chapter 5: Brain volumes in fetuses with and without a familial risk of ASD

5.1. Introduction

The previous experimental study made novel, albeit preliminary, contributions to our understanding of early brain development in infants genetically predisposed to ASD. As far as I am aware, it was the first MRI study to report that regional brain volume differences are present in high-risk infants prior to 6 months of age, and that brain volumes correlate with subsequent autistic behaviours. In order to explore whether a familial risk of ASD is also associated with differences in brain volume at an earlier time in development, the present study – aimed at investigating differences in fetal life – was carried out.

The fetal period is a time of dynamic change during which the human brain undergoes extensive growth and development. Particularly important are the final weeks of gestation, as this is when a volumetric expansion of the brain is accompanied by folding of the cerebral cortex. This process of cortical development follows a co-ordinated sequence of steps, and is crucial for the establishment of appropriate connectivity across brain networks (Kostović and Jovanov-Milošević, 2006; Sur and Rubenstein, 2005). As described earlier in the introduction of this thesis, several cellular mechanisms underlie this important stage of development, including cell proliferation, differentiation, and migration. Errors in many of these processes have now been implicated in neurodevelopmental disorders like ASD. In addition, these errors are thought to result from multifactorial genetic and environmental risk factors, many of which manifest in the prenatal period. For example, some of the genes that regulate prenatal processes such as neurogenesis, cortical patterning, and neuronal differentiation, are reportedly deregulated in individuals with ASD (Chow et al., 2012; Pinto et al., 2010). Moreover, epidemiological evidence has associated ASD with environmental risk factors, such as high levels of maternal stress (Kinney et al., 2008; Rai et al., ,2013) and prenatal exposure

to anticonvulsants and/or antidepressants (Boukhris et al., 2015; Christensen et al., 2013; Croen et al., 2011; Williams et al., 2001).

Considering these risk factors and the early postnatal brain differences observed in individuals exposed to a familial risk of ASD, previous attempts have been made to establish whether brain/head differences are already present amongst genetically predisposed individuals *in utero*. While retrospective studies using prenatal US found no significant difference in fetal head growth between individuals with and without ASD (Hobbs et al., 2007; Whitehouse et al., 2011), other subtle differences have been identified. For example, there is evidence of enlarged fetal biparietal diameter relative to head circumference in individuals with ASD, as compared to controls (Hobbs et al., 2007). In addition, other retrospective evidence suggests that abnormalities in the development of the fetal ventricular system and cerebellum, both of which can be identified on US, may predate a later ASD diagnosis (for review see Gamliel et al., 2012).

As such, prospective studies of fetuses with a familial risk of ASD have started to emerge. In the first published study of prenatal growth in siblings of individuals with and without ASD (Unwin et al., 2016), US scans were conducted at three separate timepoints in pregnancy. Fetal biometric measures, growth rates, and head-to-body ratios were compared between risk groups, but no significant differences were reported (Unwin et al., 2016). A serious limitation of this study was that measures of head circumference were used as a proxy measure of brain size. While the two are strongly correlated, especially at young ages (Bartholomeusz et al., 2002), this indirect approach limits the interpretation of results. Furthermore, although US is a reliable tool for measuring the macrostructure of the fetal brain, it does not allow for the analysis of specific sub-regions potentially implicated in ASD, such as the cerebellum. Instead, to explore subtle differences in brain regions between groups, fetal MRI may be a more suitable technique.

Thus, this study used fetal MRI to (i) first characterise the volumetric growth of brain regions between 28-38 gestational weeks, in a mixed sample of fetuses with and without a familial risk of ASD. Specifically, growth trajectories were constructed to qualitatively inspect whether there were any obvious outliers and/or deviations in brain growth between fetuses at high and low-risk of ASD. In addition, relative growth rates were calculated in order to compare with normative rates reported by others. Then, in order to formally assess volumetric differences between risk groups, the study (ii) compared total and regional brain volumes in fetuses with and without a familial risk of ASD. Based on the results of the previous infant study, subcortical and cerebellum volumes were a specific focus. Moreover, because the subcortex drives cortical development at this timepoint, (iii) the volumetric relationship between the cortex and subcortex was explored in each risk group separately.

Owing to the limited information on prenatal brain development in fetuses at risk of ASD, no firm predictions were made regarding the direction of any differences observed.

5.2. Materials and methods

5.2.1. Participants

This study included both high-risk and low-risk groups, with participants categorised based on the inclusion criteria previously described in the main methodology of this thesis (please see section 2.3.3 on page 108). Of the 89 participants enrolled in the study prenatally, 64 agreed to take part in the fetal MRI scan. The remaining 25 participants did not take part: 20 did not wish to participate at this time, and 5 could not be scanned (4 due to a high BMI, and 1 because of a metallic implant). Of the 64 participants that did agree to take part, scanning was unsuccessful for 2 participants who began to experience anxiety once prepped in the scanning bed. Data was therefore successfully collected from a total of 62 participants. However, a further 9 participants were excluded from the main volumetric analysis due to poor image quality driven by fetal motion, which precluded an accurate fetal reconstruction. Hence, the final sample size consisted of 53 fetuses: 35 low-risk (n = 20 male; mean gestational age

at scan = 32.30 weeks, SD = 1.71) and 18 high-risk (n = 9 male; mean gestational age at scan = 32.33 weeks, SD = 2.03).

5.2.2. Experimental procedures

Participants taking part in the fetal timepoint were scanned between 28-38 gestational weeks. All experimental procedures were conducted as previously described in the methodology of this thesis (please see section 2.3.5.1 on page 111).

5.2.3. Statistical analysis

Normality of data distribution was assessed visually using box-plots, and statistically using the Shapiro-Wilk Test. Group differences in sample characteristics were tested using the Independent Samples t-test, the Mann-Whitney U-test, the Person's Chi-Square test, or the Fisher's exact test, as appropriate. Where regional brain volumes were not normally distributed, logarithmic transformations were performed.

5.2.3.1. Effects of gestational age on regional brain volumes

The effects of gestational age on regional brain volumes were assessed for the whole sample (that is, for low-risk and high-risk groups combined). Depending on the data distribution, correlations between fetal gestational age and regional brain volumes were tested with either Pearson's or Spearman's rank correlation. Then, for each specific brain region, the curve of best fit was selected, and the mean volume of that region at 28, 33, and 38 gestational weeks was calculated. Growth trajectories for each brain region were plotted with the curve of best fit, and lines representing two standard deviations (±2SD) from the mean were included in these plots. Low-risk and high-risk fetuses were also labelled on these plots to allow visual inspection of any obvious outliers and/or deviations in growth between groups. To facilitate comparisons with other published studies, relative growth rates were calculated and expressed as the percentage volume increase per week.

5.2.3.2. Group differences in regional brain volumes

To test for any potential effect of risk group on regional brain volumes, an ANCOVA was run on the normally distributed data, with risk group (low-risk vs. high-risk) input as the fixed factor. The dependent variables of interest included: volume of supratentorial tissue, supratentorial white matter and subcortical grey matter tissue, cerebellum, pons, cortex, total brain tissue, lateral ventricles, third ventricle, fourth ventricle, extracerebral CSF, total CSF, and intracranium, as well as the proportion of extracerebral CSF to total CSF. Gestational age and intracranial volume were included as co-variates, whilst sex was included as a (between subjects) fixed factor. Although maternal and paternal education differed between risk groups (Table 5.1), a decision was made to only co-vary for biological factors rather than 'over-control' for variables in this small sample.

Finally, to examine the volumetric relationship between the cortex and the subcortex (using the volume of the supratentorial white matter and subcortical grey matter as an index for the subcortex), correlation analyses were run between these two measures in the high-risk and low-risk group separately.

5.3. Results

5.3.1. Sample characteristics

The characteristics of the total sample, and split by risk group, are presented in Table 5.1. Fetuses (n = 53; 35 low-risk, 18 high-risk) were scanned at a mean gestational age of 32.31 weeks (SD = 1.81, range = 28.29-38.29 weeks; Figure 5.1), and risk groups did not differ significantly in age or sex. In addition, risk groups did not differ significantly in most parental characteristics, including age at conception, ethnicity, marital status, or maternal smoking and alcohol consumption. However, both maternal and paternal education differed significantly between groups (p = 0.010 and p = 0.001, respectively), with high-risk parents being less well educated than those in the low-risk group.

The quality of some fetal reconstructions did not allow for cortical segmentation to be complete. Therefore, the volume of the cortex as well as the supratentorial white matter and subcortical grey matter tissue (which was calculated using the cortical volume) was available for only n = 41 fetuses, comprising 27 low-risk (n=18 male; mean gestational age at scan = 32.13 weeks, SD = 1.79) and 14 high-risk (n=8 male; mean gestational age at scan = 31.67 weeks, SD = 1.39). As before, there were no group differences in age (p = 0.413) or sex (p = 0.548) in this sub-sample of fetuses.

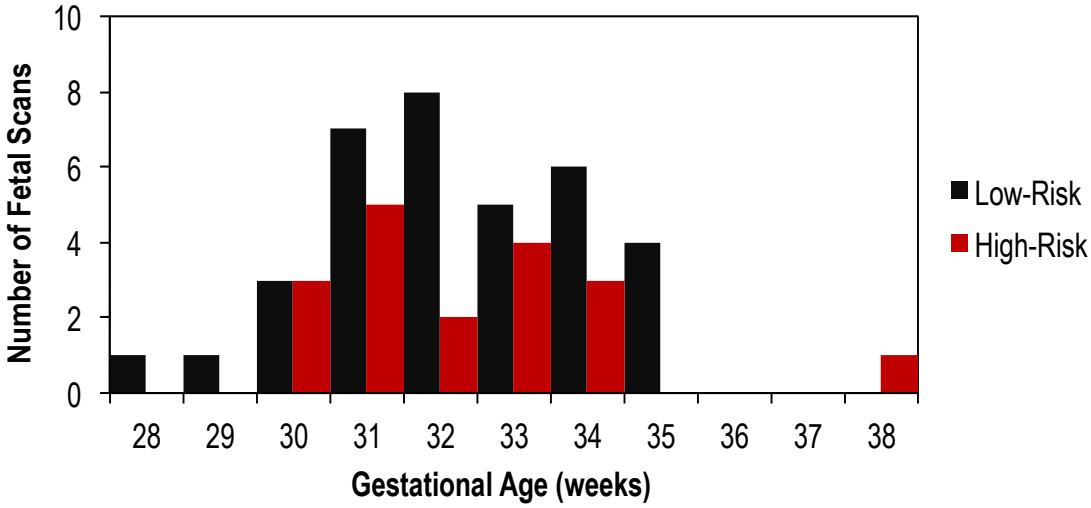

Figure 5.1: Distribution of the participants' gestational age at the fetal timepoint.
A histogram of fetal gestational age at the time of MRI acquisition is shown.
The total sample comprised of 53 fetuses: 35 low-risk (in black) and 18 high-risk (in red).

Table 5.1: Fetal and parental characteristics stratified by risk group

	Total Sample (N = 53)	Low-Risk Group (n = 35)	High-Risk Group (n = 18)	Group Difference Statistic (*p*-value)
Fetal characteristics				
Gestational age at MRI (days); mean (SD)	32.31 (1.81)	32.30 (1.71)	32.33 (2.03)	U = 293.00; p = 0.679
Sex (male); n (%)	29 (54.71)	20 (57.14)	9 (50.00)	χ^2 = 0.25; p = 0.621
Parental characteristics				
Maternal age at conception (years); mean (SD)	32.52 (4.38)	32.79 (3.76)	31.94 (5.58)	t = 0.51, p = 0.614
Paternal age at conception[a] (years); mean (SD)	34.52 (6.01)	34.97 (5.08)	33.56 (7.75)	t = 0.77, p = 0.446
Maternal alcohol intake during pregnancy; n (%)				p = 0.113
Never	26 (49.06)	16 (45.71)	10 (55.56)	
Weekly	2 (3.77)	2 (5.71)	0 (0.00)	
Monthly or less	17 (32.08)	14 (40.00)	3 (16.67)	
Not answered	8 (15.09)	3 (8.57)	5 (27.78)	
Maternal smoking during pregnancy; n (%)				p = 0.476
Yes	1 (1.89)	1 (2.86)	0 (0.00)	
No	15 (28.30)	8 (15.09)	7 (38.89)	
Not answered	37 (69.81)	26 (74.29)	11 (61.11)	
Marital status (married); n (%)	39 (73.58)	28 (80.00)	11 (61.11)	p = 0.159
Maternal ethnicity (white); n (%)	38 (71.70)	27 (77.14)	11 (61.11)	p = 0.152
Paternal ethnicity (white); n (%)	44 (83.02)	31 (88.57)	13 (72.22)	p = 0.250
Maternal education (higher education); n (%)	**44 (83.02)**	**33 (94.29)**	**11 (61.11)**	***p* = 0.009**
Paternal education (higher education); n (%)	**34 (64.15)**	**29 (82.86)**	**5 (27.78)**	***p* = 0.001**

Note: [a]Paternal age was only available for 50 participants (34 low-risk; 16 high-risk). The Fisher's exact test does not have an associated statistic; thus, only *p*-values were reported. Significant results are in **bold**. Abbreviations: MRI = magnetic resonance imaging; Higher Education = undergraduate and/or postgraduate degree; SD = standard deviation; U = Mann-Whitney *U*-statistic; t = Independent samples *t*-statistic; X^2 = Pearson's Chi-Square.

5.3.2. The effect of fetal gestational age: growth trajectories of regional brain volumes

Correlations between fetal gestational age and regional brain volume are presented in Table 5.2. This table also displays the mean volume (in cm^3) of each region at 28, 33, and 38 gestational weeks, as well as their relative growth rate (expressed as the % change in volume per week).

Across risk groups, most brain regions showed evidence of a strong, positive, and statistically significant correlation between gestational age and brain volume (Table 5.2). However, for the lateral ventricles, extracerebral CSF, and total CSF, volumes appeared to remain relatively stable with advancing gestation [lateral ventricles: (r = 0.09, p = 0.501); extracerebral CSF: (r = -0.02, p = 0.911); total CSF: (r = 0.00, p = 0.978)]. The fastest growing region in this latter stage of gestation was the cortex, with a relative growth rate of 10.86% per week, from an average of 23.62 cm^3 at 28 weeks gestation to 71.67 cm^3 at 38 weeks. Not far behind was the cerebellum, increasing at a relative rate of 7.51%, followed by the supratentorial white matter and subcortical grey matter tissue, total brain tissue, supratentorial tissue, and pons – with growth rates ranging between 5.26% and 7.23%. The fourth ventricle was the fastest growing CSF-filled space, increasing at a relative rate of 5.60% per week, from an average of 0.04 cm^3 at 28 weeks to 0.12 cm^3 at 38. In contrast, the slowest growing region was the third ventricle, with a growth rate of 2.74%. All other regions of the ventricular system decreased in volume from 28-38 gestational weeks, with values ranging between -4.72% and -5.62%.

Linear and quadratic equations explained the growth trajectory of each region equally well, as shown in Figure 5.2 and 5.3. However, mean volumes were calculated based on quadratic equations, which best described the data according to the goodness-of-fit measure. An exception was the growth of the fourth ventricle, which followed an exponential trajectory (Figure 5.3C). Visual inspection of growth plots revealed little difference between groups, and no obvious outliers and/or deviations in growth within the high-risk group. High-risk fetuses mainly stayed within ±2SD of the mean, and in brain regions where outliers did exist, they were equally distributed between groups.

Table 5.2: Correlations between brain volumes and fetal gestational age, presented for the total sample (n=53)

	Correlation with Gestational Age		Mean Volume (cm^3)			Relative Growth Rate
Brain Region	**r**	***p*-value**	**28 GW**	**33 GW**	**38 GW**	**(% Per week)**
Supratentorial Tissue	**0.83**	**<0.001**	117.91	211.92	306.47	5.35
Cerebellum	**0.82**	**<0.001**	4.86	11.42	17.28	7.51
Pons	**0.76**	**<0.001**	1.19	1.96	2.67	5.26
Cortex[a]	**0.78**	**<0.001**	23.62	43.07	71.67	10.86
Supratentorial White Matter & Subcortical Grey Matter Tissue[a]	**0.79**	**<0.001**	118.19	164.96	300.45	7.23
Total Brain Tissue	**0.83**	**<0.001**	124.08	225.46	326.64	5.45
Lateral Ventricles	0.09	0.501	4.87	6.36	5.21	-5.62
Third Ventricle	**0.35**	**0.010**	0.16	0.34	0.30	2.74
Fourth Ventricle	**0.54**	**<0.001**	0.04	0.07	0.12	5.60
Extracerebral CSF	-0.02	0.911	66.06	85.93	59.09	-4.68
Total CSF	0.00	0.978	71.04	92.63	64.62	-4.72
Intracranium	**0.75**	**<0.001**	194.42	317.1	389.93	3.22

Note: The relative growth rate (% per week) represents the percent volume increase relative to the mean volume of the structure. [a]These regional volumes were only available for 41 fetuses (27 low-risk; 14 high-risk). Significant results ($p \leq 0.05$) are shown in **bold**. Abbreviations: CSF = cerebrospinal fluid; GW = gestational age in weeks; r = (Spearman's rank or Pearson's) correlation coefficient.

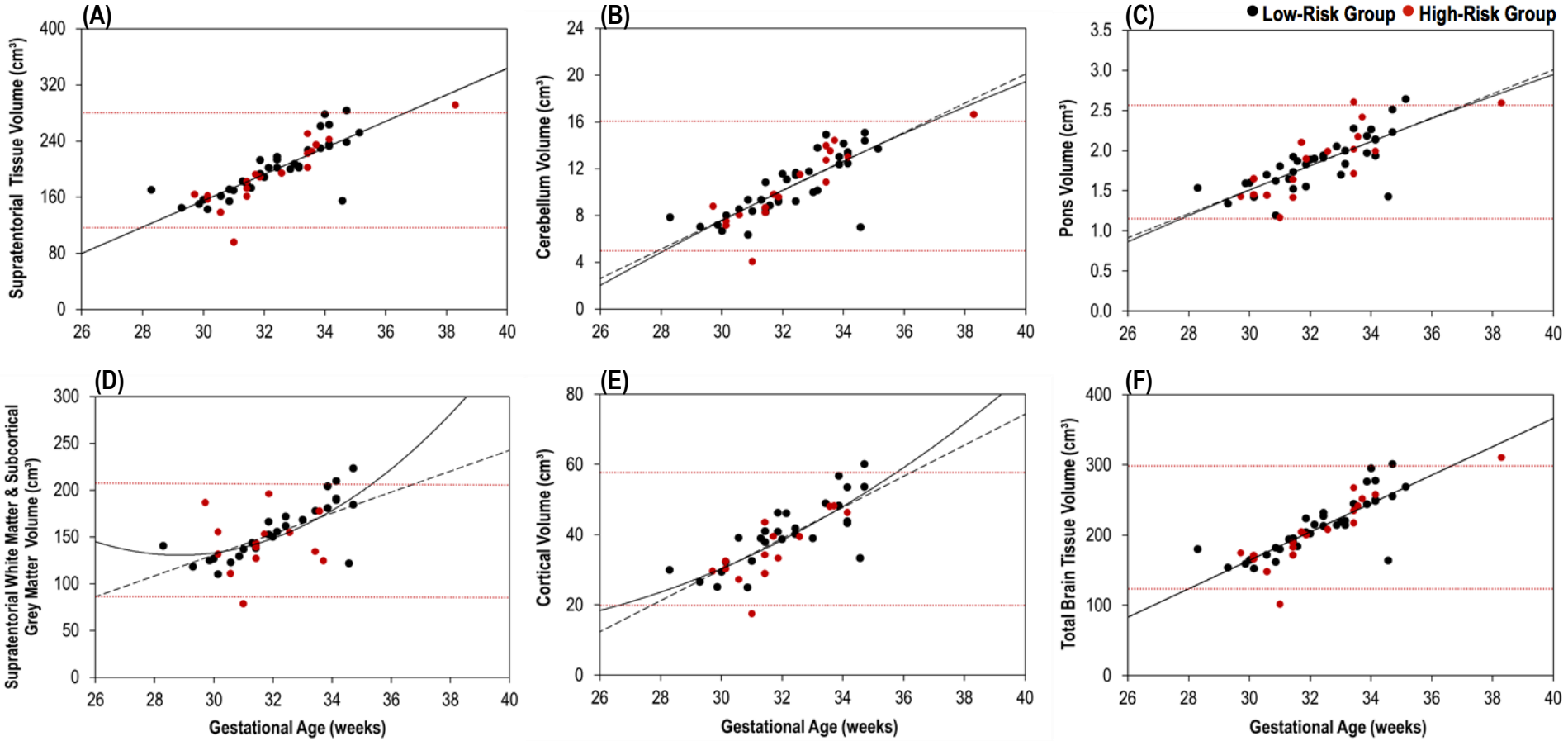

Figure 5.2: Growth trajectories of total and regional brain volumes acquired for the whole sample (low-risk and high-risk groups combined).
(A) Supratentorial tissue, **(B)** cerebellum **(C)** pons, **(D)** supratentorial white matter and subcortical grey matter tissue, **(E)** cortex, and **(F)** total brain tissue. The trendlines (in black) indicate the correlation between gestational age and volume for the whole sample, and although a quadratic model provided the best fit, both linear (dashed line) and quadratic (solid line) curves are shown. The two horizontal red dotted lines represent ±2 SD from the mean.

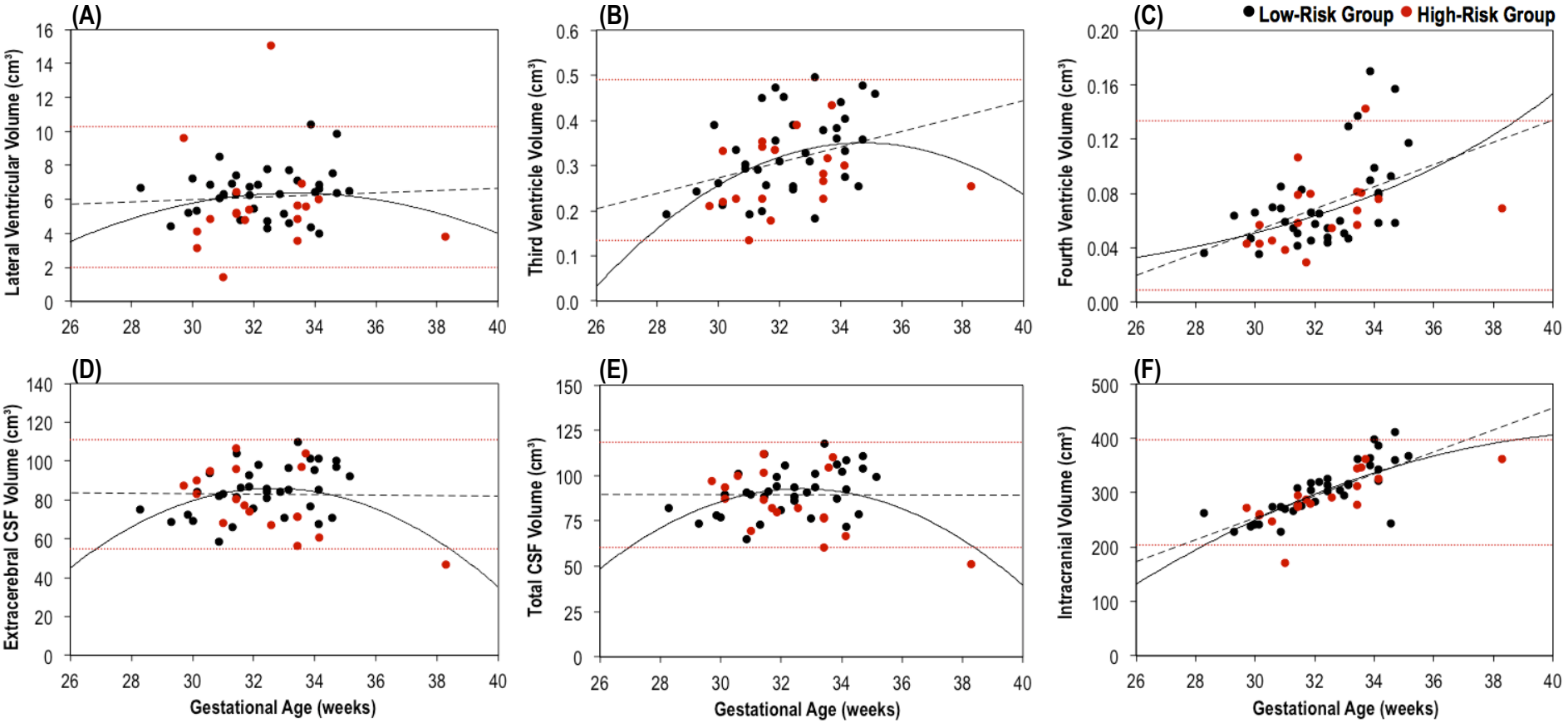

Figure 5.3: Growth trajectories of the CSF spaces and intracranium, as acquired for the whole sample (low-risk and high-risk groups combined). **(A)** Lateral ventricles, **(B)** third ventricle, **(C)** fourth ventricle, **(D)** extracerebral CSF, **(E)** total CSF, and **(F)** intracranium. The trendlines (in black) indicate the correlation between gestational age and volume for the whole sample, and although a quadratic model provided the best fit, both linear (dashed line) and quadratic (solid line) curves are shown. The two horizontal red dotted lines represent ±2 SD from the mean.

5.3.3. Group differences in fetal brain volumes

Significant group differences were identified for the cortex [$F(1,35) = 5.21$, $p = 0.029$], with high-risk fetuses having smaller cortical volumes than low-risk controls (Figure 5.4). No other brain region showed significant differences between groups (Table 5.3).

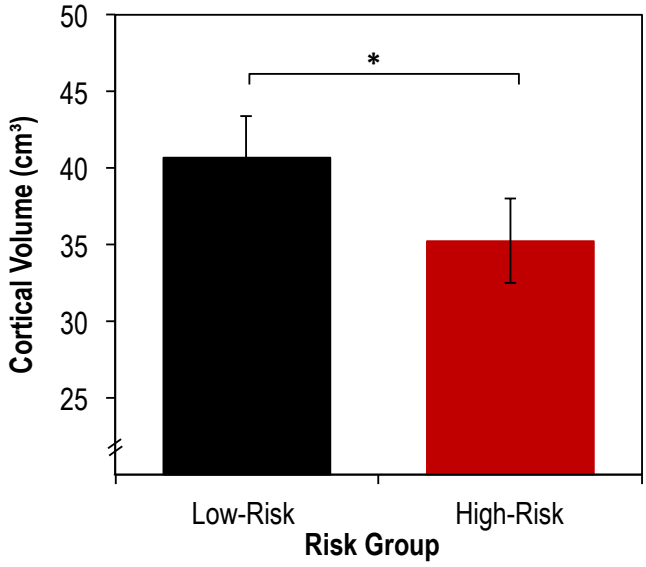

Figure 5.4: Mean cortical volume in fetuses at low and high-risk of ASD.
Fetuses in the high-risk group had a significantly smaller volume (cm^3) of the cortex, when compared to low-risk controls. Error bars represent one standard error of the mean, *$p \leq 0.05$.

In both risk groups there was a strong positive correlation between the volume of the cortex and that of the supratentorial white matter and subcortical grey matter tissue, which was statistically significant [high-risk group: ($r = 0.93$, $p < 0.001$); low-risk group: ($r = 0.87$, $p < 0.001$)]. There was no significant difference in correlation coefficients between groups (one-tailed test: $z = 0.88$, $p = 0.189$).

Table 5.3: Group differences in fetal brain volumes (cm^3) and in proportions of volumes (au.) between low-risk and high-risk groups

	Low-Risk Group (n = 35)		High-Risk Group (n = 18)		Group Difference	
	Mean	**SD**	**Mean**	**SD**	**F**	***p*-value**
Brain Volumes (cm^3)						
Supratentorial Tissue	201.37	38.57	193.38	46.17	0.10	0.749
Cerebellum	10.58	2.58	10.39	3.17	1.14	0.292
Pons	1.86	0.32	1.86	0.42	1.07	0.307
Cortex[a]	**40.68**	**9.45**	**35.23**	**8.70**	**5.21**	**0.029**
Supratentorial White Matter & Subcortical Grey Matter Tissue[a]	157.35	30.60	144.29	30.70	0.38	0.543
Total Brain Tissue	213.80	41.15	205.63	49.59	0.19	0.666
Lateral Ventricles	6.41	1.47	5.63	2.90	2.42	0.126
Third Ventricle	0.33	0.09	0.28	0.08	2.23	0.142
Fourth Ventricle	0.07	0.03	0.07	0.03	0.40	0.532
Extracerebral CSF	84.68	12.41	79.54	16.7	0.08	0.782
Total CSF	91.49	12.79	85.52	17.07	0.19	0.666
Intracranium[b]	305.30	49.26	291.15	46.65	2.50	0.121
Brain Proportions (au.)						
Extracerebral CSF/Total CSF	0.92	0.02	0.93	0.03	0.26	0.611

Note: In this analysis of co-variance, gestational age and intracranial volume were included as co-variates, whilst sex was included as a fixed factor; hence, F = F(1, 47). [a]These regional volumes were only available for 41 fetuses (27 low-risk; 14 high-risk), therefore F = F(1, 35). [b]In this analysis, only gestational age and sex were corrected for; hence, F = F(1, 48). Significant results are in **bold**. Abbreviations: F = F-statistic; CSF = cerebrospinal fluid; SD=standard deviation.

5.4. Discussion

To the best of my knowledge, this was the first MRI study to examine regional brain maturation in fetuses with and without a familial risk of ASD. Across both groups, the volume of all brain regions (with the exception of some CSF-filled spaces) increased significantly from 28-38 gestational weeks. Visual inspection revealed little difference between groups, and no obvious outliers and/or deviations in growth within the high-risk group. Still, high-risk fetuses had significantly smaller cortical volumes than low-risk controls.

5.4.1. Volumetric growth trajectories of fetal brain regions

This study confirmed previous indications that a quadratic model best describes the fetal growth of most brain regions (Gholipour et al., 2011; Kyriakopoulou et al., 2014, 2016; Vatansever et al., 2013). When examining the full cohort, the cortex was the fastest growing region between 28 and 38 gestational weeks, with volumes increasing at a relative rate of 10.86% per week. Only a small number of prior studies have measured cortical volumes using fetal MRI, but those that have report growth rates broadly in agreement with the present study [13.15% (Kyriakopoulou et al., 2014), 14.78% (Kyriakopoulou et al., 2016), and 18.00% (Scott et al., 2011)]. Within this timepoint, the second fastest growing region was the cerebellum, with a relative growth rate of 7.51%. Other studies using similar methodologies have observed slightly higher growth rates for this region, ranging between 12.87% and 17.31% (Clouchoux et al., 2012; Kyriakopoulou et al., 2016; Vatansever et al., 2013). However, these studies included fetuses of younger gestational ages than those included in the present study (< 28 weeks), which could explain the difference in results.

The rates of supratentorial and total brain tissue growth observed here (of 5.35% and 5.45% per week, respectively) were slower, compared to other studies reporting growth rates ranging between 10.22% and 17.00%; although again, these studies included measures from the second trimester (Clouchoux et al., 2012; Kyriakopoulou et al., 2014, 2016; Rajagopalan et al., 2011; Scott et al., 2011). However, since the mean volume of total brain tissue obtained in this study (225 cm^3) was well within the range of that reported at equivalent ages by others

[for example, 200-250 cm^3 at 32 weeks gestation (Clouchoux et al., 2012; Gholipour et al., 2011)], it is likely that if the age-range of this study had been extended to second trimester fetuses, the growth rates observed here would be more closely aligned to those reported by others.

All CSF-filled spaces, with the exception of the fourth ventricle, were only weakly correlated with gestational age. Moreover, upon visual inspection of the data (please refer back to Figure 5.3 on page 190), the volumetric growth trajectories of these spaces appeared to follow more of an inverted U-shaped curve, as volumes decreased towards the end of gestation. In this study, lateral ventricular volumes decreased at a relative growth rate of -5.62% per week between 28-38 gestational weeks, in agreement with another study of a similar age-range, which reported a growth rate of -4.18% (Clouchoux et al., 2012). Others, however, have reported that the lateral ventricular volume both increases (Kyriakopoulou et al., 2014, 2016; Scott et al., 2011) or remains stable (Grossman et al., 2006) throughout gestation, and the inconsistency in results is likely due to the difference in ages examined. For example, post-mortem studies have described a pattern whereby the volume of lateral ventricles gradually increases from 9-23 weeks, peaks at around 23-26 weeks, and decreases thereafter (Kinoshita et al., 2001; Lan et al., 2000). Hence, depending on what age-range is being examined, it is reasonable to expect different patterns of growth. Nonetheless, the decrease in lateral ventricular volume identified in studies examining the latter half of gestation, as was the case of the current study, is in agreement with post-mortem findings.

In contrast, both the volume of the third and fourth ventricles increased with gestational age at corresponding growth rates of 2.74% and 5.60% per week. The only other study that has examined the third ventricle also observed a small increase in its volume, with a relative growth rate of 0.10% per week (Kyriakopoulou et al., 2014). In addition, volumetric studies examining the growth rate of the fourth ventricle have reported very distinct rates of 0.13% (Kyriakopoulou et al., 2014) and 12.00% (Vatansever et al., 2013), despite having assessed fetuses of the same gestational age-range. Thus, there appears to be considerable variability

in the growth rate of this region, most likely due to its small size and its reliance on the morphological changes of the surrounding tissue (Scott et al., 2012; Vatansever et al., 2013).

To summarise, the fetal brain growth observed here was in line with what has been reported in the literature.

5.4.2. Group differences in fetal brain volumes

In the only other study of fetuses with and without a familial risk of ASD, US was used, and no group differences were identified on a range of biometric measurements, including occipitofrontal and biparietal distance (Unwin et al., 2016). Due to the limitations of US, this latter study was unable to directly examine brain volumes. Therefore, the use of MRI in the present study was a considerable advantage. Qualitatively, there were no obvious outliers and/or deviations in brain growth amongst fetuses with and without a familial risk of ASD. However this study revealed, albeit in a small cohort, that fetuses at risk of ASD have smaller cortical volumes than low-risk controls. This locus of potential pathology is in line with mounting evidence from older age groups implicating the cortex in the neuropathology of ASD. Nonetheless, variations in cortical volume may arise from alterations in cortical surface area, cortical thickness, or both, and my future analyses will examine these component indices.

Some clues about the relative importance of different indices of cortical morphology in ASD come from studies of older cohorts. For example, individuals with ASD have been reported to have greater cortical thickness in some regions (Ecker et al., 2013b; Hardan et al., 2006b), but also cortical thinning (Hadjikhani et al., 2006; Wallace et al., 2010), enlarged surface areas (Hazlett et al., 2011; Ohta et al., 2016), and anomalies in cortical folding (Hardan et al., 2004; Jou et al., 2010; Nordahl et al., 2007; Wallace et al., 2013). Similarly, opposite abnormalities in cortical surface, such as polymicrogyria (multiple small gyri leading to excessive gyrification, thought to arise in prenatal life) and macrogyria (enlarged gyri) have been reported in

individuals with ASD, more often than in age-matched controls (Piven et al., 1990; Ritvo et al., 1986; Schifter et al., 1994).

Despite the complexity of cortical differences in ASD, there is consensus that cortical volume is greater in young children (aged 1-5 years) with ASD (Hazlett et al., 2011; Schumann et al., 2010). However, here, in fetuses at risk of ASD, the cortex is smaller rather than larger. Therefore, it is critically important to note the key distinctions between this study and previous studies, specifically: (i) the timepoint of assessment and (ii) the sample population. For example, the current study did not measure brain volumes in *young children with* ASD; it measured brain volumes in *fetuses at risk of* ASD.

Although not entirely comparable, several retrospective studies have shown that, at birth, individuals who later go on to develop ASD have head circumferences that are no different (Dawson et al., 2007; Hazlett et al., 2005; Surén et al., 2013), or smaller (Courchesne et al., 2003; Mraz et al., 2007; Redcay and Courchesne, 2005), than those who do not receive a diagnosis. In contrast, at 6-14 months, head circumferences are significantly larger in individuals with ASD, relative to age-matched controls (Courchesne et al., 2003). Based on this evidence and on the findings of the present study, there appears to be an overshoot in head size during the early postnatal period, which is preceded by a prenatal period of delayed and/or abnormal maturation, especially of the cortex.

The mechanisms underpinning these observations are not fully understood. Post-mortem studies have reported that individuals with ASD, compared to those unaffected, have more minicolumnar abnormalities (Buxhoeveden et al., 2006; Casanova et al., 2002, 2006; McKavanagh et al., 2015), focal patches of abnormal laminar cytoarchitecture (Stoner et al., 2014), and irregularities in cell patterning at the cortical–white matter boundary (Avino and Hutsler, 2010). This evidence points towards a deregulation of cortical development in ASD, which could be explained by prenatal errors in neuron migration, layer-specific differentiation, and subplate dissolution (Avino and Hutsler, 2010; Stoner et al., 2014). In support of this,

many of these processes have now been implicated in genetic studies of ASD (Chow et al., 2012; Pinto et al., 2010).

Another possible cause of the disruption in cortical development may be differences in prenatal hormones. For example, elevated levels of steroid hormones, such as testosterone, have been identified in the amniotic fluid of males who later received an ASD diagnosis (Baron-Cohen et al., 2015). Steroid hormones are essential for normal neurodevelopment. However, elevated levels of these hormones are thought to alter gene expression via epigenetic programming, which may modify neurodevelopmental processes. In addition, evidence suggests that high levels of testosterone can exert neuronal damage, both directly by the induction of the apoptotic cascade (Estrada et al., 2006), as well as indirectly via the exacerbation of glutamate neurotoxicity (Yang et al., 2002). However, steroid hormones were not measured in this study, and therefore this suggestion remains speculative.

ASD risk did not measurably affect the volume of any other brain region examined in this study, including the cerebellum and subcortical region. However, as shown in Table 5.3, the mean volume of all brain regions was smaller in high-risk fetuses, relative to low-risk controls. There may be several reasons why no significant differences were identified in regions other than the cortex. For example, the analysis may have been underpowered to identify any differences that actually do exist (reflective of a false negative error), or there may actually be no differences in the volume of other brain regions at this time. Alternatively, the volume measures used may not have been sensitive enough to detect subtle differences. This may be especially true for the subcortical region, given that the specificity of the measurement was hugely limited by the fact that it also incorporated the volume of the supratentorial white matter. Thus, the possibility that subcortical differences were present, but undetected, cannot be ruled out.

In fetal life there is also evidence that the subcortical region drives the development of cortex (Kostović and Jovanov-Milošević, 2006; Sur and Rubenstein, 2005), and therefore, it is

possible that the small cortical volumes identified in fetuses at risk of ASD are reflective of an underlying subcortical abnormality. That being said, the relationship between subcortical and cortical volumes was preserved in the high-risk group, and stronger, although not significantly different from low-risk controls (p = 0.189). In a recent study, individuals with ASD showed increased functional connectivity between subcortical and cortical brain regions, when compared to typically developing controls. This subcortico-cortical connectivity also decreased significantly with age amongst individuals in the ASD group (Cerliani et al., 2015). Future work should therefore focus on segmenting the fetal subcortical region in detail, to elucidate whether or not there is a disrupted relationship between cortical and subcortical regions, in individuals genetically predisposed to ASD at this time.

5.4.3. Study limitations

This study has a number of limitations. First, there was a small sample size in each risk group, which limited group comparisons in growth trajectories, and only allowed for comparisons in volumetric means. The small sample size also adds to the possibility of false negatives; hence, replications with larger samples will be necessary. In line with this, and partly due to the exploratory nature of this study, the statistical threshold was not corrected for the total number of comparisons, increasing the risk of false positives. Second, only biological co-variates were used in the analysis, and factors such as socioeconomic status, likely to be important, were not controlled for. Third, cortical segmentations were only performed in a subset of the fetuses incorporated in this study. This was largely due to the poor image of some reconstructions, which limited the ability to obtain an accurate and detailed manual segmentation of this convoluted structure. In addition and as already mentioned, this study used a measure for the subcortex which included the supratentorial white matter, and hugely limited the specificity of the region under consideration. The team is currently working towards the development of an automated protocol for fetal brain segmentation (Wright et al., 2012), which will include a detailed parcellation of the subcortical region, and will facilitate and accelerate the quantification of fetal brain volume. Alongside this, a protocol for the 3D reconstruction of fetal cortical surfaces is also being developed (Wright et al., 2014, 2015).

Once fully validated, implementation of this protocol will allow for measures of cortical surface area, thickness, curvature, and gyrification to be obtained in a precise and reproducible manner. In future, characterisation and quantification of cortical surface development in fetuses at risk of ASD will be an important next step, as it may provide valuable insight into the cortical development of these fetuses, including subtle deviations from the norm that may help disentangle the findings of the present study.

At the time of writing, the postnatal outcome data is not yet available; however, behavioural follow-up is currently underway. Hence, once the scanned fetuses reach a postnatal age at which autistic symptoms can be appraised, outcome data will help to elucidate on the clinical significance and specificity – if any – of these results.

5.4.4. Conclusions

In conclusion, this is the first study to provide preliminary evidence suggesting that brain differences (i.e. smaller cortical volumes) between individuals with and without a familial risk of ASD may already be evident *in utero*. If confirmed, these findings provide an important observation at a critical time in development, which may in future inform our understanding of the aetiological pathways to ASD.

Based on these results, my next step was to compare total and regional brain volumes between neonates with and without a familial risk of ASD. The objective was to determine whether cortical abnormalities persist into neonatal life. In addition, I wished to determine whether any other brain regions linked to ASD in infancy and beyond, including the subcortical and cerebellar regions, are also affected in the neonate.

Chapter 6: Brain volumes in neonates with and without a familial risk of ASD

6.1. Introduction

In the previous experimental study, the first to directly compare total and regional brain volumes in fetuses with and without a familial risk of ASD, no significant group differences were identified in the subcortex or cerebellum (chapter 5) – regions with group differences in infants aged 4-6 months (chapter 4). However, fetuses at risk of ASD had smaller cortical volumes when compared to low-risk controls. Whether or not there are cortical volume differences between ASD risk groups at 4-6 months remains unknown, mainly because image quality did not allow for cortical segmentation. To establish the trajectory of brain maturation in individuals at low and high-risk of ASD, measurements between these two quite distinct developmental periods (i.e. between the fetal and infant period) are needed. The next step was therefore to investigate whether regional brain volume differences – especially in the cortex, subcortex, and/or cerebellum – are present in the neonatal period, shortly after birth.

Birth is a critical time in development, as it is when the neonate first comes into contact with the environment outside the womb. As a result, there is an increasing interest in potential exposures and/or events occurring immediately prior to, during, and after birth, which could influence neurodevelopment. Thus far, factors such as a breech presentation, induced labour, premature birth, congenital malformation, and low Apgar score, have all been proposed to play a contributory role in the emergence of ASD (Gardener et al., 2011; Guinchat et al., 2012). However, it is unlikely that any of these factors are specific to ASD, as some also seem to influence the risk of other neurodevelopmental disorders such as ADHD, intellectual disability, and epilepsy (Atladóttir et al., 2015). Moreover, there is currently insufficient evidence to implicate any one risk factor in a definite causal pathway to ASD. For example, being born with congenital malformations may not in itself cause ASD, but it may indicate that

fetal development has been abnormal and that the infant is on a trajectory towards atypical development (Bolton et al., 1997). Despite this, what is clear is that many of the risk factors associated with ASD, come into play at and around the time of birth. As such, birth has been suggested as a key stage in the divergence from typical neurodevelopment (Ben-Ari, 2015).

This study therefore aimed to examine brain development in the critical period after birth. First, MRI was used to (i) characterise the growth of total and regional brain volumes within the first month of life, in a mixed sample of individuals with and without a familial risk of ASD. As before, growth trajectories allowed for a qualitative assessment of whether there were any obvious outliers and/or deviations in brain growth between individuals at high and low-risk of ASD. Relative growth rates were also calculated to extend information obtained from the fetal period, as well as to compare with other studies conducted at this age. Finally, this study also aimed to (ii) compare total and regional brain volumes in neonates with and without a familial risk of ASD. Specifically, it sought to determine whether cortical abnormalities, evident *in utero*, persisted in neonatal life. In addition, the study explored whether any other brain regions were affected at this time, particularly those commonly implicated in ASD, such as the cerebellum and subcortex.

For this component of the thesis, it was possible to access more sophisticated neonatal MRI protocols, developed as part of the dHCP. This enabled a more detailed parcellation of subcortical (and other) structures, which was not possible at fetal and infant timepoints. Thus, this study also examined the caudate, subthalamic, and lentiform nucleus, as well as the thalamus, hippocampus, amygdala, and insula.

In the present study, I tested the hypothesis that any differences in the neonatal brains of individuals with and without a familial risk of ASD would be localised to one or more of these subcortical structures and/or the cerebellum. Also, given findings from the fetal study and the emerging evidence implicating cortical abnormities in older cohorts with ASD, I also tested if there were differences in cortical volume at this age.

6.2. Materials and methods

6.2.1. Participants

As in prior experimental chapters, participants were assigned to either the high-risk or low-risk group, based on the criteria described in the methodology section of this thesis (please refer to section 2.3.3 on page 108). Of the 113 participants enrolled in the study postnatally, 71 agreed to take part in assessment at the neonatal timepoint. The remaining 42 did not wish to participate at this time, either because it was too soon after the birth of the baby, or because the family was still recovering from minor complications associated with delivery. Of the 71 participants that did agree to take part, scanning was unsuccessful for 10 of these: 8 did not settle to sleep, and 2 could not be scanned due to scheduling problems. Data was successfully collected from a total of 61 participants. However, a further 8 participants were excluded from the main volumetric analysis: 7 due to poor image quality driven by motion artefacts, and 1 due to an incidental neuroanatomical finding. Hence, the final sample size consisted of 53 neonates (22 of which were also scanned at the fetal timepoint), including 35 low-risk (n = 18 male; mean corrected age at scan = 42.60 weeks, SD = 1.86) and 18 high-risk (n = 11 male; mean corrected age at scan = 42.16 weeks, SD = 2.57).

6.2.2. Experimental procedures

Participants taking part in the neonatal timepoint were scanned as soon as possible after birth, and at no more than one month of age. Some babies were born after 40 gestational weeks; therefore, even if scanned within the first month of postnatal life, their corrected age at scan would still be over 44 weeks. Thus, the ages included in this study ranged from 35-47 corrected weeks. All experimental procedures were conducted as described earlier in the main methodology of this thesis (see section 2.3.5.2 on page 127).

6.2.3. Statistical analysis

Normality of data distribution was assessed as usual. Where regional brain volumes were not normally distributed, logarithmic transformations were performed. Group differences in sample characteristics were examined using the most appropriate test.

6.2.3.1. Effects of age on regional brain volumes

Contingent on the data distribution, correlations between neonatal age and regional brain volumes were assessed for the whole sample (that is, for low-risk and high-risk groups combined), using either Pearson's or Spearman's rank correlations. Then, for each specific brain region, the curve of best fit was selected, and the mean volume of that region at 38, 42, and 46 corrected weeks was calculated using the equation for the best-fit curve. Growth trajectories for each brain region were plotted with the curve of best fit, as well as with lines representing ±2 SD from the mean. In addition, low-risk and high-risk groups were labelled distinctly on these plots, to allow for visual inspection of any obvious outliers and/or deviations in growth between groups. Relative growth rates were also calculated in order to compare with growth rates reported at the fetal timepoint, as well as with normative rates reported in other neonatal studies.

6.2.3.2. Group differences in total and regional brain volumes

In this analysis, the first priority was to determine whether total brain tissue and intracranial volume (i.e. brain and head size, respectively) varied significantly between groups. Therefore, an initial ANCOVA was run with risk group (low-risk vs. high-risk) as a fixed factor, and with total brain and intracranial volume as the dependent variables of interest. Since both age and sex are known to affect brain volume, and neonatal body weight was significantly different between groups (Table 6.1), these variables were all included as co-variates. Any significant findings were explored post-hoc, including any group difference in the relationship between intracranial volume and body weight. Although some socioeconomic factors were significantly different between groups (for example, maternal and paternal education), a decision was made to only co-vary for biological factors rather than 'over-control' for multiple variables.

To assess group differences in regional brain volumes, an ANCOVA was run with risk group was entered as a fixed factor, and with sex, age, intracranial volume, and body weight input as co-variates. In addition, because prematurity is an independent risk factor for neurodevelopmental disorders like ASD (Goldin and Matson, 2016; Guy et al., 2015; Johnson

et al., 2010; Kuzniewicz et al., 2014), late-preterm neonates (born between 34-37 gestational weeks) were also included in this study. However, to determine if a late-preterm birth influenced the direction of findings, the analysis was repeated post-hoc after excluding these preterm neonates (n = 4 high-risk; no low-risk).

6.2.3.2.1. Supplementary work: exploratory longitudinal analysis

An exploratory analysis of the available longitudinal data was conducted using a repeated measures mixed model analysis with unstructured co-variance matrices. This analytic approach was chosen as it allows for different patterns of missing data, and accommodates an unbalanced design. Timepoint (fetal vs. neonatal) and risk group (high-risk vs. low-risk) was input as a fixed factor, and the dependent variables of interest included all of the examined brain regions that were common to individuals scanned at both timepoints. Age and intracranial volume were included as co-variates, and sex as a (between subjects) fixed factor.

6.3. Results

6.3.1. Sample characteristics

The characteristics of the total sample and of each risk group are presented in Table 6.1. Neonates (n = 53; 35 low-risk, 18 high-risk) were scanned at a mean corrected age of 42.45 weeks (SD = 2.11, range = 35.14-46.57 corrected weeks; Figure 6.1), and risk groups did not differ significantly in age (at birth or at MRI). They also did not differ significantly in sex, head circumference (at birth and at MRI), ethnicity, mode of delivery, or Apgar scores (at 1 and 5 minutes). Moreover, whilst body weight was not significantly different at birth, risk groups differed in body weight at MRI (p = 0.019), with the high-risk group weighing significantly more than the low-risk. Regarding parental characteristics, although marital status and parental age were not significantly different between groups, parental education was. Specifically, the parents of low-risk neonates were educated to a higher degree than those in the high-risk group (maternal education: p = 0.005; paternal education: p = 0.002).

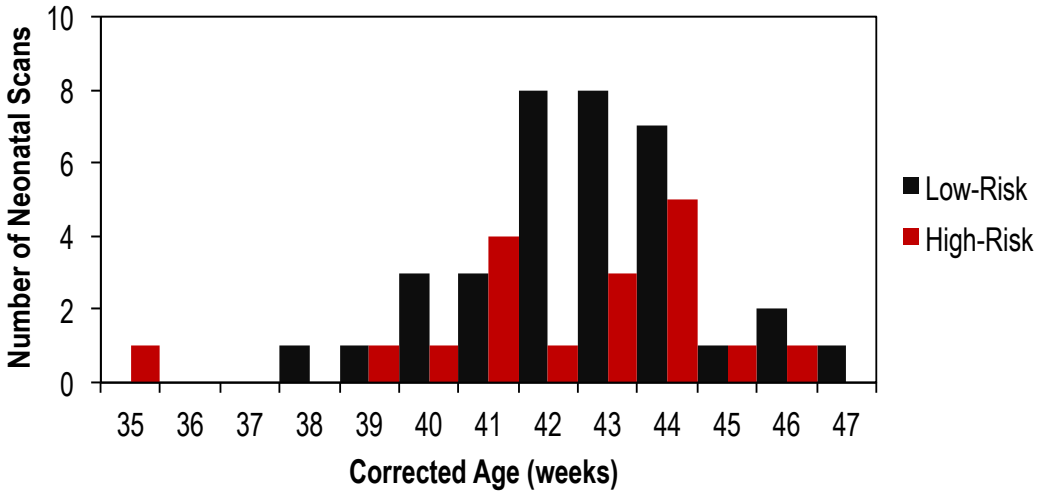

Figure 6.1: Distribution of the participants' age at the neonatal timepoint.
A histogram of the participants' corrected age at the time of neonatal MRI is shown. The total sample comprised of 53 neonates: 35 low-risk (in black) and 18 high-risk (in red).

Table 6.1: Neonatal and parental characteristics stratified by risk group

	Total Sample (N = 53)	Low-Risk Group (n = 35)	High-Risk Group (n = 18)	Group difference Statistic (*p*-value)
Neonatal characteristics				
Gestational age at birth (weeks); mean (SD)	39.64 (1.63)	39.96 (1.24)	39.02 (2.10)	U = 257.50, p = 0.279
Corrected age at MRI (weeks); mean (SD)	42.45 (2.11)	42.60 (1.86)	42.16 (2.57)	t = 0.71, p = 0.480
Sex (male); n (%)	29 (54.72)	18 (51.43)	11 (61.1)	χ^2 = 0.45, p = 0.502
Ethnicity (white); n (%)	33 (62.26)	24 (68.57)	9 (50.00)	p = 0.163
Body weight at birth (kg); mean (SD)	3.35 (0.45)	3.37 (0.48)	3.33 (0.40)	t = 0.30, p = 0.765
Body weight at MRI (kg); mean (SD)	**3.87 (0.62)**	**3.73 (0.48)**	**4.15 (0.77)**	***t* = -2.41, *p* = 0.019**
Head circumference at birth[a] (cm); mean (SD)	34.39 (1.47)	34.50 (1.60)	34.19 (1.20)	t = 0.62, p =0.536
Head circumference at MRI (cm); mean (SD)	36.10 (1.47)	36.05 (1.39)	36.08 (1.66)	t = -0.08, p = 0.936
Mode of delivery (caesarean section); n (%)	13 (24.53)	8 (22.86)	5 (27.78)	p = 0.178
Apgar score at 1 minute[b]; mean (SD)	8.41 (1.83)	8.27 (2.16)	8.60 (0.86)	U = 165.50, p = 0.901
Apgar score at 5 minute[b]; mean (SD)	9.46 (0.72)	9.42 (0.81)	9.54 (0.52)	U = 166.50, p = 0.933
Parental characteristics				
Maternal age at infant's birth (years); mean (SD)	33.35 (4.41)	33.26 (5.27)	32.94 (3.26)	t = 0.23, p = 0.819
Paternal age at infant's birth[c] (years); mean (SD)	35.73 (7.14)	35.03 (7.15)	37.12 (7.12)	U = 242.00, p = 0.345
Marital status[d] (married); n (%)	37 (72.55)	25 (75.76)	12 (66.67)	p = 0.880
Maternal education (higher education); n (%)	**33 (62.26)**	**27 (77.14)**	**6 (33.33)**	***p* = 0.005**
Paternal education[c] (higher education); n (%)	**23 (45.10)**	**21 (61.76)**	**2 (11.76)**	***p* = 0.002**

Note: [a]This measure was only available for 41 neonates (27 low-risk; 14 high-risk) and [b]39 neonates (26 low-risk; 13 high-risk). [c]These measures were missing for 2 participants (1 low-risk and 1 high-risk), as was [d]this measure (both low-risk). The Fisher's exact test does not have an associated statistic; thus, only p-values were reported. Significant results are shown in **bold**. Abbreviations: MRI = magnetic resonance imaging; Higher Education = undergraduate and/or postgraduate degree; SD = standard deviation; U = Mann-Whitney *U*-statistic; t = Independent samples *t*-statistic; X^2 = Pearson's Chi-Square.

6.3.2. The effect of neonatal age: growth trajectories of regional brain volumes

Correlations between neonatal age and brain volumes are presented in Table 6.2. This table also displays the mean volume (in cm^3) of each brain region at 38, 42, and 46 corrected weeks, as well as their relative growth rate (expressed as the % change in volume per week). Linear and quadratic equations explained the growth trajectory of each region equally well, as is shown in Figure 6.2 and 6.3. However, mean volumes were calculated based on quadratic equations, which best described the data according to the goodness-of-fit measures. Visual inspection of these plots also indicated that there was no obvious difference in growth between risk groups. The majority of neonates stayed within ±2 SD of the mean, and in brain regions where outliers did exist, they were equally distributed between groups.

Across risk groups, all brain regions showed evidence of a strong, positive, and statistically significant correlation with age. The cerebellum and the cortex showed the strongest correlations [cerebellum: (r = 0. 85, p < 0.001); cortex: (r = 0.84, p < 0.001)], suggesting that these were amongst the fastest growing regions of all those examined. Specifically, the cortex increased at a relative growth rate of 51.54% per week, whilst the cerebellum increased at a rate of 63.63%, from a mean volume of 19.51 cm^3 at 38 corrected weeks to 34.10 cm^3 at 46. The corpus callosum also demonstrated a strong correlation with age (r = 0.68, p < 0.001), as well as a high growth rate of 53.54% – well above that of the total brain and intracranial volume (with relative rates of 34.21% and 34.57%, respectively). Most subcortical regions were strongly correlated with age, increasing in volume at relative growth rates ranging between 27.92% and 38.55%, with the latter representing the growth rate of the lentiform nucleus. In contrast, the volume of the lateral ventricles exhibited the weakest correlation of all (r = 0.32, p = 0.022). Its relative growth rate was the highest though, with a 68.86% increase per week, likely due to the large spread of the data – evident by comparing the mean volume of the lateral ventricles (5.71 cm^3) with its standard deviation (2.54 cm^3). The slowest growing region of all was the white matter, demonstrating both a weak correlation with age (r = 0.46, p = 0.001) and a relative growth rate of only 15.29% per week. Contrary to what was reported at the fetal period, there was no region with negative growth rates at this time (Table 6.2).

Table 6.2: Correlations between brain volume and neonatal age, presented for the total sample (n=53)

	Correlation with Age		Mean Volume (cm^3)			Relative Growth Rate
Brain Region	***r***	***p*-value**	**38 CW**	**42 CW**	**46 CW**	**(% Per week)**
Cortex	**0.84**	**0.001**	119.63	161.16	205.91	51.54
White Matter	**0.46**	**0.001**	145.00	158.99	173.84	15.29
Subcortical Grey Matter	**0.69**	**<0.001**	23.62	28.87	32.95	29.71
Thalamus	**0.69**	**<0.001**	7.93	9.60	11.14	31.18
Caudate Nucleus	**0.53**	**<0.001**	3.26	4.00	4.25	27.92
Subthalamic Nucleus	**0.54**	**<0.001**	0.42	0.50	0.65	37.28
Lentiform Nucleus	**0.78**	**<0.001**	5.42	7.03	8.44	38.55
Hippocampus	**0.63**	**<0.001**	1.33	1.54	1.89	29.20
Amygdala	**0.60**	**<0.001**	0.86	1.07	1.19	28.85
Insula	**0.51**	**<0.001**	7.81	9.10	10.78	31.83
Corpus Callosum	**0.68**	**<0.001**	2.26	2.83	3.59	53.54
Brainstem	**0.68**	**<0.001**	5.77	6.79	7.78	34.00
Cerebellum	**0.85**	**<0.001**	19.51	27.49	34.10	63.63
Total Brain Tissue	**0.76**	**<0.001**	315.72	385.90	457.66	34.21
Lateral Ventricles	**0.32**	**0.022**	3.97	5.25	8.14	68.86
Extracerebral CSF	**0.51**	**<0.001**	71.45	82.77	107.57	34.34
Total CSF	**0.53**	**<0.001**	75.42	88.02	115.71	36.08
Intracranium	**0.75**	**<0.001**	391.13	473.91	573.37	34.57

Note: The relative growth rate (% per week) represents the percent volume increase relative to the mean volume of the structure. Significant results are shown in **bold**. Abbreviations: *r* = Correlation Coefficient (Pearson's or Spearman's rank), CW = Corrected age in weeks.

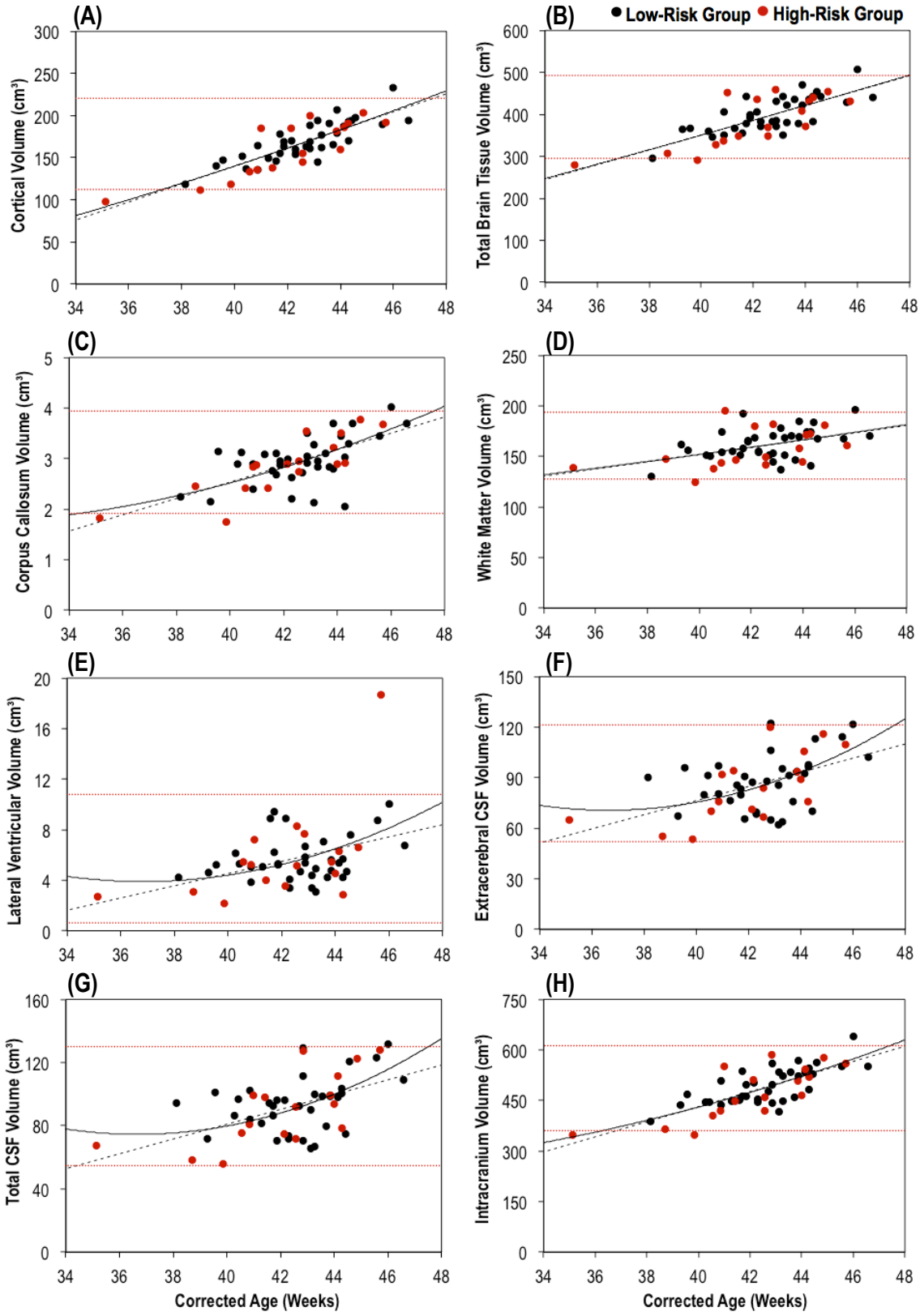

Figure 6.2: Growth trajectories of total and regional brain volumes acquired for the whole sample (low-risk and high-risk groups combined).

(A) Cortex, **(B)** total brain tissue, **(C)** corpus callosum, **(D)** white matter, **(E)** lateral ventricles, **(F)** extracerebral CSF, **(G)** total CSF, and **(H)** intracranium. The trendlines (in black) indicate the correlation between volume and age for the whole sample, and although a quadratic model provided the best fit for the data, both linear (dashed line) and quadratic (solid line) curves are shown. The two horizontal red dotted lines represent ±2 SD from the mean.

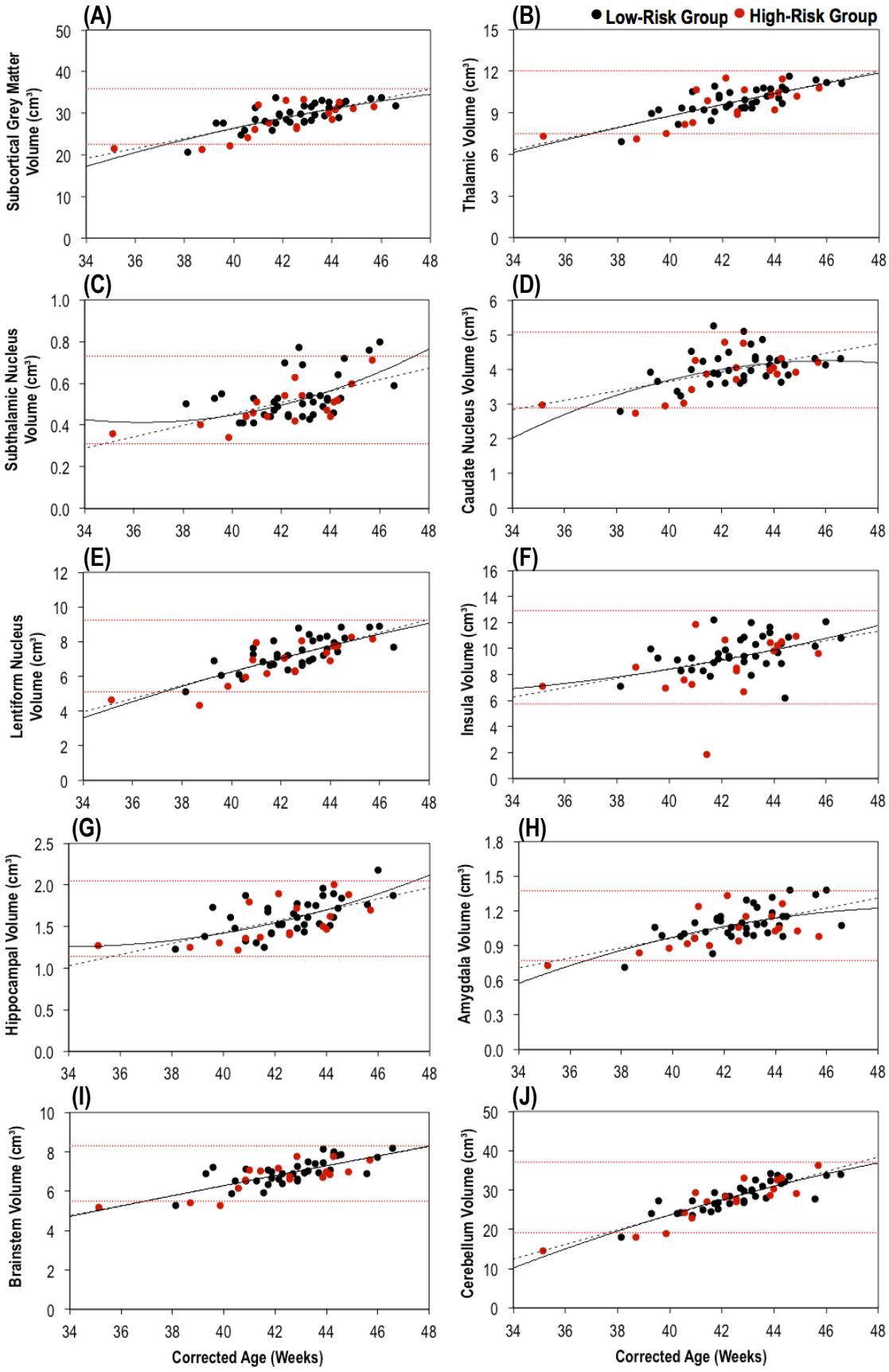

Figure 6.3: Growth trajectories of cortical and subcortical regions acquired for the whole sample (low-risk and high-risk groups combined).

The trendlines (in black) indicate the correlation between volume and age for the whole sample, and although a quadratic model provided the best fit for the data, both linear (dashed line) and quadratic (solid line) curves are shown. The two horizontal red dotted lines represent ±2 SD from the mean.

6.3.3. Group differences

6.3.3.1. In total brain tissue and intracranial volume

There were significant group differences in both brain and head size. High-risk neonates had a significantly smaller volume of the total brain tissue [$F(1,47) = 4.76$, $p = 0.034$] and intracranium [$F(1,47) = 5.40$, $p = 0.024$], when compared to low-risk controls (Table 6.3).

6.3.3.2. In head-to-body proportions

At the neonatal timepoint, the high-risk group weighed considerably more than the low-risk (mean body weight: high-risk = 4.15 kg, low-risk = 3.73 kg; $p = 0.019$), but had significantly smaller intracranial volumes (mean intracranial volume: high-risk = 476.29 cm^3, low-risk = 491.76 cm^3; $p = 0.024$). In addition, the head-to-body proportion (calculated as the intracranial volume over body weight) was significantly different between groups [$F(1, 48) = 14.87$, $p < 0.001$]. Neonates in the high-risk group had significantly smaller head-to-body proportions, when compared to those in the low-risk group (Table 6.3, Figure 6.4), which suggests that high-risk neonates generally have smaller head sizes despite increased body weights.

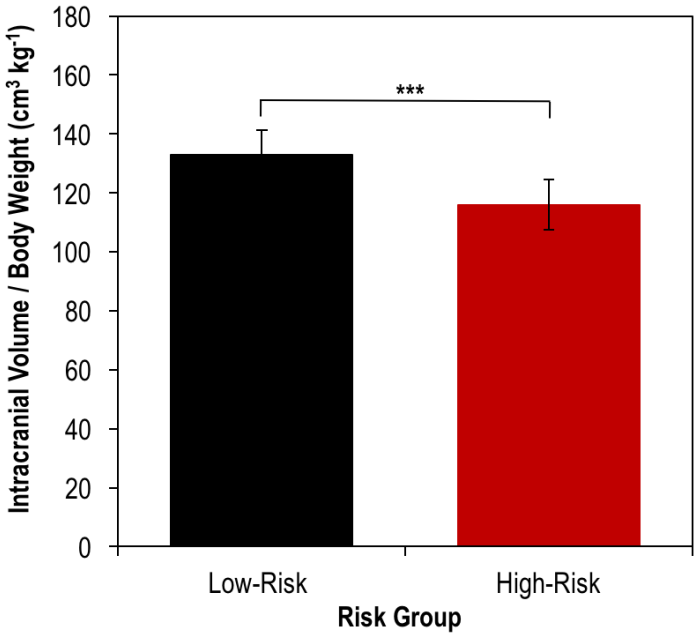

Figure 6.4: Mean head-to-body proportion in neonates at low and high-risk of ASD. Neonates in the high-risk group had a significantly smaller head-to-body proportion, when compared to low-risk controls. This suggests that high-risk neonates generally have smaller head sizes, despite increased body weights. Error bars represent one standard error of the mean, ***$p \leq 0.001$.

6.3.3.3. In regional brain volumes

There was a significant group difference in the volume of the lentiform nucleus [F(1, 46) = 4.62, p = 0.037], with high-risk neonates having significantly smaller volumes than low-risk controls (Table 6.3, Figure 6.5). Results did not differ when the analysis was co-varied for total brain tissue, as opposed to intracranial volume. There were no other regional brain volumes or proportions with significant group differences at this time (Table 6.3).

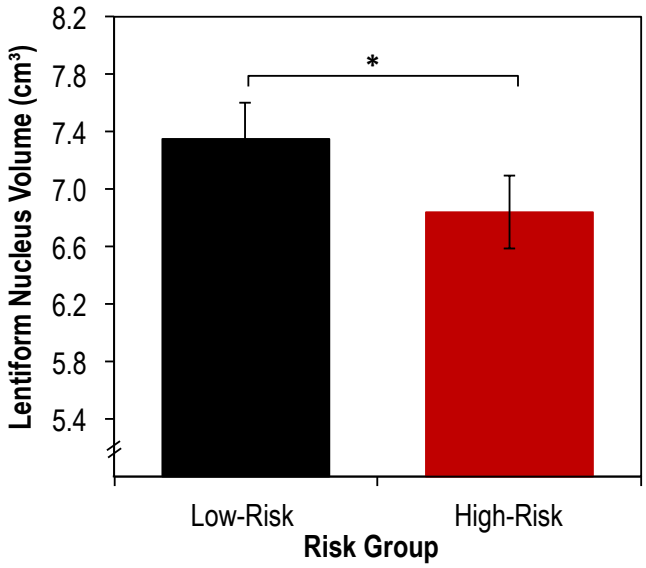

Figure 6.5: Mean lentiform volume in neonates at low and high-risk of ASD.
Neonates in the high-risk group had a significantly smaller lentiform volume (cm^3), when compared to low-risk controls. Error bars represent one standard error of the mean, *$p \leq 0.05$.

Supplementary analyses uncorrected for intracranial volume confirmed that group differences were mainly restricted to the cortical and subcortical regions. For example, the subcortical grey matter, subthalamic nucleus, lentiform nucleus, amygdala, and cortex were all significantly smaller in high-risk neonates, as compared to low-risk controls. The insula and caudate nucleus were also smaller in high-risk individuals, but these differences just failed to reach statistical significance (Table 6.3).

6.3.3.4. Post-hoc analysis: excluding late-preterm neonates

When the analysis was re-run to exclude late-preterm neonates (n = 4, all high-risk; 3 male; mean corrected age at scan = 40.11 weeks, SD = 3.40), this did not alter the results. Group differences remained for the total brain tissue volume [$F(1,43) = 7.32$, $p = 0.010$], intracranial volume [$F(1,43) = 8.75$, $p = 0.005$], and head-to-body proportions [$F(1,44) = 10.82$, $p = 0.002$], with high-risk neonates consistently reporting smaller values than low-risk controls. In addition, the lentiform nucleus remained significantly smaller for the high-risk group, when compared to the low-risk [$F(1,42) = 5.25$, $p = 0.027$]. All other brain regions showed no significant differences, as before.

6.3.3.5. Supplementary results: exploratory longitudinal analysis

Where volumetric data at both fetal and neonatal timepoints was available (n = 22; 14 low-risk, 8 high-risk), an exploratory longitudinal analysis was run to test whether there was a significant main effect of timepoint (fetal vs. neonatal) and risk group (high-risk vs. low-risk) on total and regional brain volumes. Only brain regions that were common to both timepoints were assessed (i.e. lateral ventricles, extracerebral CSF, total CSF, supratentorial tissue, cerebellum, cortex, total brain tissue, and intracranium).

Results showed a significant main effect of timepoint for all the brain regions examined, with larger volumes at the neonatal timepoint compared to the fetal. While there was no main effect of risk group for any of the brain regions examined, there was an indication of a possible interaction effect between timepoint and risk group (Timepoint x Risk Group), which was in line with results from the main cross-sectional analyses. For example, fetuses at high-risk of ASD had a smaller volume of the total brain tissue compared to those at low-risk; however, by the neonatal timepoint, the opposite was true ($p = 0.074$). To examine these questions more thoroughly in future, larger sample sizes will be necessary.

Table 6.3: Group differences in neonatal brain volumes and in brain and body proportions between low-risk and high-risk groups

	Risk Group				Group Difference			
	Low-Risk (n = 35)		High-Risk (n = 18)		[a]Unadjusted		[b]Adjusted	
	Mean	**SD**	**Mean**	**SD**	**F**	***p*-value**	**F**	***p*-value**
Brain Volumes (cm^3)								
Cortex	**168.80**	**23.37**	**161.87**	**33.38**	**5.00**	**0.030**	0.08	0.781
White Matter	161.98	14.95	158.29	19.51	3.04	0.088	0.16	0.691
Subcortical Grey Matter	**29.65**	**2.85**	**28.38**	**4.08**	**6.72**	**0.013**	1.70	0.199
Thalamus	9.86	0.97	9.56	1.41	2.57	0.116	0.10	0.759
Caudate Nucleus	4.06	0.51	3.84	0.61	3.05	0.087	0.62	0.436
Subthalamic Nucleus	**0.54**	**0.11**	**0.49**	**0.09**	**4.91**	**0.032**	1.63	0.209
Lentiform Nucleus	**7.35**	**0.91**	**6.84**	**1.19**	**10.11**	**0.003**	**4.62**	**0.037**
Hippocampus	1.61	0.21	1.56	0.26	2.56	0.117	0.16	0.692
Amygdala	**1.10**	**0.14**	**1.02**	**0.15**	**4.73**	**0.035**	1.34	0.253
Insula	9.63	1.39	8.74	2.33	3.33	0.074	0.93	0.339
Corpus Callosum	2.96	0.48	2.87	0.57	0.91	0.345	0.31	0.581
Brainstem	6.97	0.64	6.76	0.81	3.33	0.074	0.54	0.465
Cerebellum	28.49	3.73	27.36	5.73	2.44	0.125	0.14	0.710
Total Brain Tissue	**398.61**	**42.64**	**385.25**	**60.81**	**4.76**	**0.034**	0.02	0.877
Lateral Ventricles	5.67	1.79	5.81	3.65	0.48	0.493	0.24	0.625
Extracerebral CSF	87.49	16.09	85.23	19.93	1.98	0.166	0.00	0.965
Total CSF	93.15	17.13	91.04	22.29	1.63	0.208	0.02	0.877
Intracranium	**491.76**	**53.58**	**476.29**	**79.07**	**5.40**	**0.024**	-	-
Proportions								
Intracranium/Body Weight[c]	**132.86**	**14.73**	**115.96**	**12.62**	**14.87**	**<0.001**	-	-
Extracerebral CSF/Total CSF	0.94	0.02	0.94	0.03	0.00	0.972	0.72	0.402

Note: [a]In this analysis, only age and body weight were included as co-variates, with sex as a fixed factor; hence, F = F(1,47). [b]Here, intracranial volume was added as a co-variate, and so F = F(1,46). [c]In order to compare group differences in head-to-body proportions (units = $cm^3\ kg^{-1}$), only age and sex were corrected for, and so F = F(1,48). Significant results are in **bold.** Abbreviations: CSF = cerebrospinal fluid; SD = standard deviation.

6.4. Discussion

As far as I am aware, this was the first study to quantify brain volumes within the first month of postnatal life in individuals with and without a familial risk of ASD. Across risk groups, the volume of all brain regions increased significantly with age. High-risk neonates had significantly heavier body weights, but significantly smaller volumes of the intracranium, total brain tissue, and lentiform nucleus, when compared to low-risk controls.

6.4.1. Volumetric growth trajectories of neonatal brain regions

Compared to the fetal brain, much more is currently known about volumetric brain growth in the neonatal period. In agreement with other studies examining growth trajectories in the first few weeks after birth (Holland et al., 2014; Makropoulos et al., 2015), all of the brain volumes examined in this study were significantly and positively correlated with age. The relative growth rates reported here were considerably higher than those calculated at the fetal timepoint (chapter 5), and suggest that brain growth is more rapid in the first month of postnatal life, as compared to earlier during the third trimester of pregnancy. Nonetheless, both cerebellum and cortex were amongst the fastest growing regions in neonatal life, comparable to what was observed in the fetal period.

Moreover, the regional growth rates observed here were in broad agreement with other studies carried out shortly after birth. For example, others have reported the cerebellum as the fastest growing region in the early postnatal period (Holland et al., 2014; Knickmeyer et al., 2008), doubling in volume within the first three months of life (Holland et al., 2014). This is most probably due to the cerebellum's role in early development, particularly regarding motor co-ordination and control – both of which are crucial outcomes of early brain maturation. Aside from its motor function the cerebellum has also been implicated in cognitive function (Schmahmann and Sherman, 1998), and the reciprocal connections that it shares with specific cortical regions via cortico-cerebellar circuits, are thought to mediate these 'high-order' skills (Makris et al., 2005; Schmahmann, 2001). It has even been suggested that the rapid growth of the cerebellum in the first months of life is a prerequisite for adequate cortical development

(Knickmeyer et al., 2008), and as evident in this study, the cortex also undergoes a steep growth trajectory in neonatal life.

Relative to the cerebellum (increasing in volume at a rate of 63.63% per week), the hippocampus was amongst one of the slowest growing regions within the first postnatal month (increasing at a relative rate of 29.20%). This finding corroborates that of others, which have also reported a similarly low growth rate for the hippocampus (Holland et al., 2014). The disparity in regional growth rates observed in this and other studies may be due to the relative developmental importance of the abilities each region oversees. For example, spatial and episodic memory (skills largely overseen by the hippocampus) are potentially not as important in the first few months of life as motor skills (regulated by the cerebellum) are (Holland et al., 2014; Knickmeyer et al., 2008).

In other studies using MRI to examine brain development in the neonatal period and in the first 2 years after birth, brain maturation appears to be mainly driven by grey matter, as opposed to white matter growth (Gilmore et al., 2007; Knickmeyer et al., 2008). This too was evident in the present study, with white matter having the slowest growth rate of all (increasing in volume by 15.29% per week). Although it is poorly understood what the different developmental trajectories in grey and white matter tissue may signify, it could simply be that the slow growth rate of the white matter is a reflection of the protracted period of myelination, which persists well into postnatal life.

In summary, this study identified volumetric growth trajectories in line with what is commonly reported in the neonatal literature. Visual inspection of growth plots also did not indicate any gross deviation from the established norm amongst individuals in the high-risk group. However, a direct comparison of brain volumes revealed significant differences between the two groups.

6.4.2. Group differences in neonatal head size and in total and regional brain volumes

This study reported significant group differences in both brain and head size, with high-risk neonates having smaller total brain and intracranial volumes compared to low-risk controls. In addition, contrary to what is commonly reported in the literature (Gardener et al., 2011; Limperopoulos et al., 2008; Schieve et al., 2015), individuals in the high-risk group weighed significantly more than those considered to be at low-risk. Neonates at risk of ASD also had smaller head-to-body proportions, which implies a disproportionately smaller head size relative to body size, and suggests that the factors governing body and head growth are uncoupled in these high-risk individuals.

To date, there have been no studies carried out in individuals genetically predisposed to ASD within the first month of postnatal life; therefore, direct comparisons with other studies are limited. However, as mentioned in the previous chapter, several retrospective studies have shown that at birth, individuals who later develop ASD, have head circumferences that are either smaller (Courchesne et al., 2003; Mraz et al., 2007; Redcay and Courchesne, 2005) or no different (Dawson et al., 2007; Hazlett et al., 2005; Surén et al., 2013) than typically developing controls. In some of these studies, individuals who later developed ASD also had a rapid increase in head circumference, when compared to controls. This started at 1-2 postnatal months, and resulted in significant enlargements at 6, 10, and 14 months (Courchesne et al., 2003; Mraz et al., 2007). Smaller head circumferences at birth, and increased growth rates thereafter, were significantly associated with a greater number and greater severity of autistic symptoms (Courchesne et al., 2003). Hence, the initial trajectory of head (and perhaps brain) growth is abnormal in individuals with ASD. This early postnatal period of accelerated growth may reflect a protective and/or compensatory mechanism, in response to prior atypical neurodevelopmental processes (Courchesne et al., 2003; Dementieva et al., 2005; Mraz et al., 2007). Nonetheless, it is important to bear in mind that head circumference is not a direct measure of current brain size. In the present neonatal study, for example, although differences in intracranial and total brain volume were identified (and correspond to differences in head and brain size, respectively), there were no differences

in head circumference between risk groups at birth or in neonatal life. Recent reports have also suggested that many of the head circumference studies previously mentioned may have been influenced by biases in population norms (Raznahan et al., 2013), and so we cannot be entirely sure of the validity of their results.

Studies like the present one that directly measure brain volume (as opposed to head size) and compare it with age-matched controls (as opposed to normative averages), avoid the risk of the biases associated with using historical population 'norms'. They also provide stronger evidence for potential differences between groups, allowing for more reliable conclusions to be drawn. Thus far, however, there have been few studies reporting on neonatal brain volumes in individuals predisposed to ASD. The few studies that do exist have focussed on prematurity, rather than family history, as a risk factor for ASD (Padilla et al., 2015; Ure et al., 2015). Still, the results of these studies are broadly in line with those of the current investigation. For example in one of these prior studies, poor brain growth was also identified; except that in this case it was observed at term-equivalent age in preterm neonates before the onset of ASD, and was localised to the temporal, occipital, insular, and limbic regions (Padilla et al., 2015). In another study, preterm infants who later developed ASD also had smaller brain volumes at term-equivalent age, compared to those who did not receive a diagnosis. This finding, however, was restricted to the cerebellum (Ure et al., 2015). Nonetheless, when placed together, these results suggest that preterm infants, who were subsequently diagnosed with ASD, had smaller regional brain volumes in neonatal life, when compared to preterm infants who did not go on to develop the disorder. Although outcome data is not yet available for the neonates included in the present study, a similar pattern of results was identified here, in neonates genetically predisposed to ASD. In conclusion, this suggests that small brain volumes around the time of birth may be associated with a later ASD diagnosis.

Preterm born infants are at an increased risk of developing ASD (Johnson et al., 2010; Kuzniewicz et al., 2014; Pritchard et al., 2016); therefore, neonates born prematurely were also allowed in this study. However, compared to the studies previously described, which

focused on prematurity as a main risk factor for ASD and included infants born at < 30 gestational weeks (Padilla et al., 2015; Ure et al., 2015), the present study only included late-preterm neonates, born between 34-37 gestational weeks. In addition, preterm infants commonly show reduced brain volumes at term-equivalent age (Ball et al., 2012; Inder et al., 2005; Peterson et al., 2003). Therefore, to assess the extent to which prematurity was a major contributing factor to the smaller brain volumes observed within the high-risk group of this study, the analysis was repeated after excluding these preterm infants. Findings remained unchanged suggesting that prematurity did not drive the results, and that neonates genetically predisposed to ASD have smaller brain volumes than low-risk controls.

Besides the small volumes in intracranium and total brain tissue, individuals with a familial risk of ASD also had significantly smaller volumes of cortical and subcortical grey matter structures, when compared to age-matched controls. However, when this analysis was corrected for intracranial volume, the lentiform nucleus was the only region to remain significantly smaller in high-risk neonates. As a result, this finding cannot easily be explained by generalised influences acting on the whole brain.

The lentiform nucleus encompasses the globus pallidus and putamen. Both these regions have been extensively implicated in ASD, and possibly also in 4-6 month-old infants at risk of the disorder (chapter 4). It is important to note, however, that according to the findings described in chapter 4, the entire subcortical region was affected in high-risk infants, with no way of determining what subcortical structure was driving the results. Nonetheless, the majority of studies published thus far have specifically identified enlarged lentiform nuclei in individuals with ASD. For example, in both children and adults with ASD, the globus pallidus and putamen are reportedly enlarged, compared to age-matched controls (Herbert et al., 2003; Hollander et al., 2005; Langen et al., 2007; Sato et al., 2014; Turner et al., 2016). Similarly, greater lentiform volumes have been identified in children with ASD as young as 3-4 years (Estes et al., 2011). In contrast, the results of the present study indicate that the lentiform nuclei is smaller in individuals at risk of ASD within the first month of postnatal life,

and that this region is more severely impacted than the whole brain. When taken in conjunction with the findings of older cohorts, it is therefore proposed that the lentiform nucleus may undergo an aberrant developmental trajectory in individuals with and at risk of ASD.

Finally, this neonatal study did not identify any differences in cortical or cerebellar volumes between risk groups. Although cortical volumes were smaller in fetuses at risk of ASD, compared to low-risk controls (chapter 5), these differences were not present early in postnatal life. This suggests that they may have been temporarily resolved, or that only more subtle differences in cortical thickness, surface area, and/or curvature are identifiable at this time. Aside from the cortex, the cerebellum had also been *a priori* hypothesised to be altered in neonates at risk of ASD. The fact that no differences were found in neonatal life was therefore surprising, particularly given the evidence implicating the cerebellum at term-equivalent age in preterm infants who later developed ASD (Limperopoulos, 2009; Ure et al., 2015). Several reasons could explain why no differences were identified in the cerebellum at the neonatal timepoint. For example, although the cerebellum was enlarged in 4-6 month-old infants at risk of ASD (chapter 4), aside from no differences in neonatal life, there were also no observed differences at the fetal timepoint (chapter 5). Thus, it may be that alterations to the cerebellum are only present in infants genetically predisposed to ASD at and after 4-6 months. Alternatively, since cerebellum enlargement correlated with ASD symptoms, but did not predict diagnostic outcome (chapter 4), its enlarged volume in infant life could be a consequence rather than a cause of atypical development. If true, this could also explain why no differences were observed in younger individuals at risk of ASD. Furthermore, as evident in this and other studies, the cerebellum is amongst one of the fastest growing regions in early prenatal and postnatal life. It may therefore be considerably more difficult to identify volumetric differences in this region using a cross-sectional design, and thus, my future work will address this by using thorough longitudinal analyses.

6.4.3. Study limitations

This study has a number of limitations that need to be acknowledged. First, the sample size was small, which increases the risk of false negatives. In addition, since correction for multiple comparisons was not conducted, there is also increased risk of false positives. Second, socioeconomic status was not included as a co-variate because I did not want to 'over-control' for variables in this small sample-sized analysis. This may be viewed as problematic, given the significant difference in parental education between risk groups, and the growing body of evidence indicating the powerful effect of socioeconomic status on infant brain structure (Brito and Noble, 2014; Hackman and Farah, 2009; Noble et al., 2012, 2015). However, in an exploratory analysis including maternal education (an index of socioeconomic status) as an additional co-variate, results were not significantly different from those reported here. This is likely to be because infant weight, commonly associated with socioeconomic status (Gould and LeRoy, 1988; Parker et al., 1994; Wijlaars et al., 2011), was controlled for in this study. Third, and although there was a marked improvement in the quality of images acquired at this time (allowing for segmentation of brain regions not examined at the fetal and infant timepoints), the parcellation of the lentiform nucleus into its constituents (that is, the globus pallidus and putamen) was still not possible. With continued optimisation of measurement protocols, this situation may change in future. Last, while a supplementary exploratory analysis was conducted to assess the longitudinal trajectory of brain volume in individuals with and without a familial risk of ASD, the fact that only 8 high-risk participants were scanned at both fetal and neonatal timepoints, limited the analysis and interpretation of results. Nonetheless, there was some indication of a possible interaction effect between timepoint and risk group, which should encourage a formal longitudinal analysis to be conducted once more high-risk participants have been scanned.

6.4.4. Conclusions

In conclusion, the present study suggests that in the first few weeks after birth, individuals with a familial risk of ASD have altered brain growth, relative to those at low-risk. Specifically, high-risk neonates had smaller intracranial and total brain volumes. They also had a reduced

volume of the lentiform nucleus, which could not be explained by the overall small brain and head sizes. Hence, the findings of this study indicate that an increased genetic risk of ASD is associated with an early alteration in brain growth. Further work will be needed to clarify if this atypical pattern of neurodevelopment predicts a later ASD diagnosis, and neonates included in this study are currently being followed-up to establish this.

Considering the difference in lentiform volumes identified in this study, as well as the subcortical enlargement in 4-6 month-old infants at risk of ASD (chapter 4), it may be that the subcortical region is important in the underlying development of the disorder. The next step was therefore to explore this region in more detail, by examining whether there are subcortical neurochemical abnormalities in individuals genetically predisposed to ASD.

Chapter 7: Subcortical biochemistry from prenatal to early postnatal life, and metabolic differences in infants with and without a familial risk of ASD

7.1. Introduction

Thus far, I have presented evidence that the brain volume of individuals at risk of ASD differs from that of low-risk controls. During the fetal and neonatal timepoints, brain regions were smaller in high-risk individuals; the cortex was implicated in fetal life, while the intracranium, total brain tissue, and lentiform nucleus were affected in the first postnatal month (chapters 5 and 6). In contrast, both the subcortical and cerebellar regions were enlarged in 4-6 month-old infants at risk of ASD (chapter 4). Therefore, although some brain regions were only altered at one timepoint, the subcortex (encompassing basal ganglia and thalami) was affected in both neonatal and infant timepoints, suggesting that it may be an important region in the early pathology of ASD. Brain metabolites, especially glutamate (but also GABA), are crucial to normal developmental processes (Coyle et al., 2002; Gallo and Ghiani, 2000; Yuan et al., 1998). In addition, it is thought that differences in neurochemistry could predate, or even drive, subsequent structural alterations (Fayed et al., 2006). The deregulation of perinatal shifts in excitatory-to-inhibitory balance may also be a critical pathophysiological step in ASD (Tyzio et al., 2014). Yet, no one has compared subcortical glutamate levels in individuals with and without a familial risk of ASD.

[1]HMRS is an invaluable tool for safely studying the typical and atypical metabolic development of the human brain *in vivo*. According to the current literature (discussed in section 1.2.7 on page 48), dynamic changes in brain metabolite concentrations are present in early life, but begin to stabilise by about three years of age. NAA, for example, is reported to increase with

postnatal age during these first few years of life, whilst the concentrations of both Ins and Cho are found to decrease (Blüml et al., 2013; Girard et al., 2006a, 2006b; Huppi et al., 1995; Kok et al., 2002; Kreis et al., 1993). In addition, there is evidence that Cr may increase during the first 2 years of postnatal life, rather than remain stable as previously thought (Blüml et al., 2013; Degnan et al., 2014; Evangelou et al., 2016; Girard et al., 2006a; Huppi et al., 1995; Kreis et al., 1993, 2002). Glx has also been detected in the brain as early as 24 weeks gestation (Girard et al., 2006b), but there is limited information on its prenatal development. In contrast, there is preliminary evidence to suggest that Glx increases with postnatal age (Blüml et al., 2013; Degnan et al., 2014; Kornhuber et al., 1993; Kreis et al., 2002), but further research is required to confirm this.

Aside from its application in studies of typical brain development, recent ^{1}HMRS findings have begun to shed some light on the neurochemical differences potentially underpinning some of the developmental differences in ASD (for review see Baruth et al., 2013; Ford and Crewther, 2016; Ipser et al., 2012). Despite discrepancies in the literature, spectroscopic studies mainly report that children with ASD have low levels of NAA, Cr, and Ins, when compared to age-matched controls. The evidence from ASD studies assessing Cho and Glx is less clear. For example, children with ASD have reportedly exhibited lower (Corrigan et al., 2013; DeVito et al., 2007; Kubas et al., 2012), higher (Bejjani et al., 2012; Doyle-Thomas et al., 2014), and no significant differences in Glx levels (Friedman et al., 2003, 2006), when compared to age-matched controls. Studies assessing Cho in children with ASD are just as inconsistent (for review see Ford and Crewther, 2016). Moreover, although these studies have focused on paediatric populations, the neurochemistry of ASD has not been examined in individuals younger than 3-4 years. In addition, no studies have used ^{1}HMRS to assess the neurometabolic properties of infants genetically predisposed to the disorder.

Consequently, the main aims of this study were to: (i) characterise the subcortical levels of key metabolites across fetal, neonatal, and infant life, and (ii) investigate whether 4-6 month-old infants at high familial risk of ASD have differences in the levels of subcortical metabolites,

when compared to low-risk controls. For (i), because the typical maturational profile of major metabolites (NAA, Cr, Cho, and Ins) has already been described in early life, this study first aimed to replicate previous findings (Blüml et al., 2013; Evangelou et al., 2016; Girard et al., 2006a; Kreis et al., 2002). However, since the typical developmental trajectory of glutamate (or Glx) is still largely unknown, part of aim (i) was to extend understanding of its early maturational profile. For (ii), as this was the first study to compare brain metabolites in infants at low and high-risk of ASD, no definite *a priori* hypotheses were made regarding group differences. However, it was postulated that if any group differences did exist, an E/I imbalance in the ASD risk group would be reflected by differences in Glx (Nelson and Valakh, 2015; Rubenstein and Merzenich, 2003).

7.2. Materials and methods

7.2.1. Participants

High-risk and low-risk participants, scanned at least once in the fetal, neonatal, and/or infant timepoints, were included in this study. Participants were characterised by risk group based on the inclusion criteria previously described in the methodology of this thesis (please see section 2.3.3 on page 108).

[1]HMRS data was acquired for as many participants as possible (fetal: n = 60, neonatal: n= 29, and infant: n = 33), but the data was not available for all of those scanned. This was because the spectroscopic sequence came at the end of the acquisition protocol, and there were times in which the scanning session had to be stopped before the spectroscopic sequence was even started. This was mainly due to fetal motion, or because the neonate/infant awoke and could no longer be settled. In addition, while the majority of neonatal and infant spectra were suitable for analysis (neonatal: n = 28, 99.55%; infant: n = 33, 100%), only n = 25 (41.67%) of the fetal spectra could be quantified, as the rest were disrupted by fetal motion. A low-risk neonatal participant was also excluded from the analysis due to an incidental neuroanatomical finding. Hence, a total of 25 fetal (5 high-risk, 20 low-risk), 27 neonatal (5 high-risk, 22 low-

risk), and 33 infant (14 high-risk, 19 low-risk) ^{1}HMRS datasets were included in this study, with some participants contributing to more than one timepoint.

7.2.2. Experimental procedures

^{1}HMRS data was obtained using PRESS sequences sampled from the region of the left basal ganglia, and acquired at an echo time of 55 ms and 144 ms. All experimental procedures were conducted as described in the methodology section of this thesis, and spectroscopic analysis was performed using TARQUIN (as outlined in section 2.3.5.4 on page 142).

In older age groups not assessed in this study, Cr is the most commonly used reference metabolite. However in the developing brain, Cr is not as stable as originally thought, having recently been reported to increase with age (Blüml et al., 2013; Degnan et al., 2014). According to the largest fetal ^{1}HMRS study carried out to date, Cho appears more stable than Cr (Evangelou et al., 2016), suggesting that it may be a more appropriate metabolite to use as a reference at this age. Expressing the results relative to Cr may thus help to place them in the context of existing studies in older cohorts, whereas expressing them relative to Cho may provide a more accurate profile. Metabolites were therefore expressed in relation to both Cr and Cho, as follows: Cho/Cr, Ins/Cho, Ins/Cr, Glx/Cho, Glx/Cr, NAA/Cho, and NAA/Cr.

7.2.3. Statistical analysis

Normality of data distribution was verified as usual, using box-plots and the Shapiro-Wilk Test.

7.2.3.1. The effect of timepoint on brain metabolite ratios

Brain metabolite ratios were not normally distributed; hence, logarithmic transformations were performed. Then, using a repeated measures mixed model analysis, the longitudinal trajectories of these metabolite ratios were analysed across timepoints for the whole sample (that is, for low-risk and high-risk groups combined). As part of this analysis, an unstructured co-variance matrix was applied, given that it allows for different patterns of missing data and accommodates an unbalanced design. Timepoint (fetal vs. neonatal vs. infant) was input as a

fixed factor, and the dependent variables of interest included all of the examined metabolite ratios: Cho/Cr, Ins/Cho, Ins/Cr, Glx/Cho, Glx/Cr, NAA/Cho and NAA/Cr. Age was included as a co-variate, and sex as a (between subjects) fixed factor. Following significant results, Bonferroni corrected pairwise comparisons were performed.

7.2.3.2. Group differences in brain metabolite ratios at 4-6 months of age

The next question to examine was whether there was any effect of infant risk group on brain metabolite ratios at 4-6 months of age. Firstly, group differences in parental and infant demographic characteristics were assessed. Then, an ANCOVA was run on the normally distributed data, with infant risk group (low-risk vs. high-risk) input as a fixed factor. The dependent variables of interest included all of the measured metabolite ratios. Infant age was included as a co-variate, and sex as a (between subjects) fixed factor. Other control variables included any biological factors that were significantly different between groups, and which in this case included infant mode of delivery (Table 7.2). Although some socioeconomic factors were significantly different between groups (for example, marital status and parental education), as these were expected to influence biological factors, a decision was made to only co-vary for the biological factors rather than 'over-control' for variables.

Group differences in brain metabolite ratios were not examined for the fetal or neonatal timepoints. This was due to the small number of high-risk participants (n = 5) at both these timepoints, which also precluded a longitudinal analysis from being conducted.

7.3. Results

7.3.1. The effect of timepoint on brain metabolite ratios

There was a significant main effect of timepoint for all the metabolite ratios examined (Table 7.1). Whilst Cho/Cr, Ins/Cho, and Ins/Cr all decreased significantly from the fetal to the infant timepoint, NAA/Cho and NAA/Cr increased across all three timepoints. In contrast, there was a significant decrease in the ratio of Glx/Cho and Glx/Cr from the fetal to the neonatal timepoint, followed by an increase from there up until early infancy (Figure 7.1).

Table 7.1: Mean differences in brain metabolite ratios across fetal, neonatal, and infant timepoints

Echo Time	Metabolite Ratio	Mean (SD) Brain Metabolite Ratio			Main Effect of Timepoint		Pairwise Comparisons
		Fetal	Neonatal	Infant	F-statistic	*p*-value	
55 ms	Cho/Cr	0.43 (0.16)	0.33 (0.06)	0.29 (0.03)	**858.57**	**<0.001**	F > I***, N > I***
	Ins/Cho	3.83 (3.83)	1.47 (0.58)	0.81 (0.33)	**27.96**	**<0.001**	F > N***, F > I***, N > I***
	Ins/Cr	1.42 (1.24)	0.48 (0.16)	0.24 (0.09)	**1184.54**	**0.001**	F > N***, F > I***, N > I***
	Glx/Cho	4.49 (4.04)	1.89 (0.55)	3.16 (0.55)	**218.87**	**<0.001**	F > N***, F > I**, N < I***
	Glx/Cr	1.53 (1.26)	0.62 (0.19)	0.93 (0.18)	**36182.38**	**<0.001**	F > N***, F > I***, N < I***
144 ms	Cho/Cr	0.64 (0.19)	0.46 (0.13)	0.39 (0.03)	**155.32**	**<0.001**	F > N*, F > I***, N > I***
	NAA/Cho	0.88 (0.38)	1.60 (0.47)	2.90 (0.33)	**293.07**	**<0.001**	F < N**, F < I***, N < I***
	NAA/Cr	0.63 (0.29)	0.75 (0.27)	1.13 (0.11)	**35.44**	**0.001**	F < N*, N < I***

Note: Significant results are shown in **bold** or indicated by an asterisk (*), where *p ≤ 0.05, **p ≤ 0.01, ***p ≤ 0.001. Abbreviations: F = Fetal, N = Neonatal, and I = Infant Timepoint; NAA = N-acetylaspartate and N-acetylaspartylglutamate; Cr = creatine and phosphocreatine; Cho = free choline, glycerophosphocholine, and phosphocholine; Ins = myo-inositol; Glx = glutamate and glutamine; SD = standard deviation.

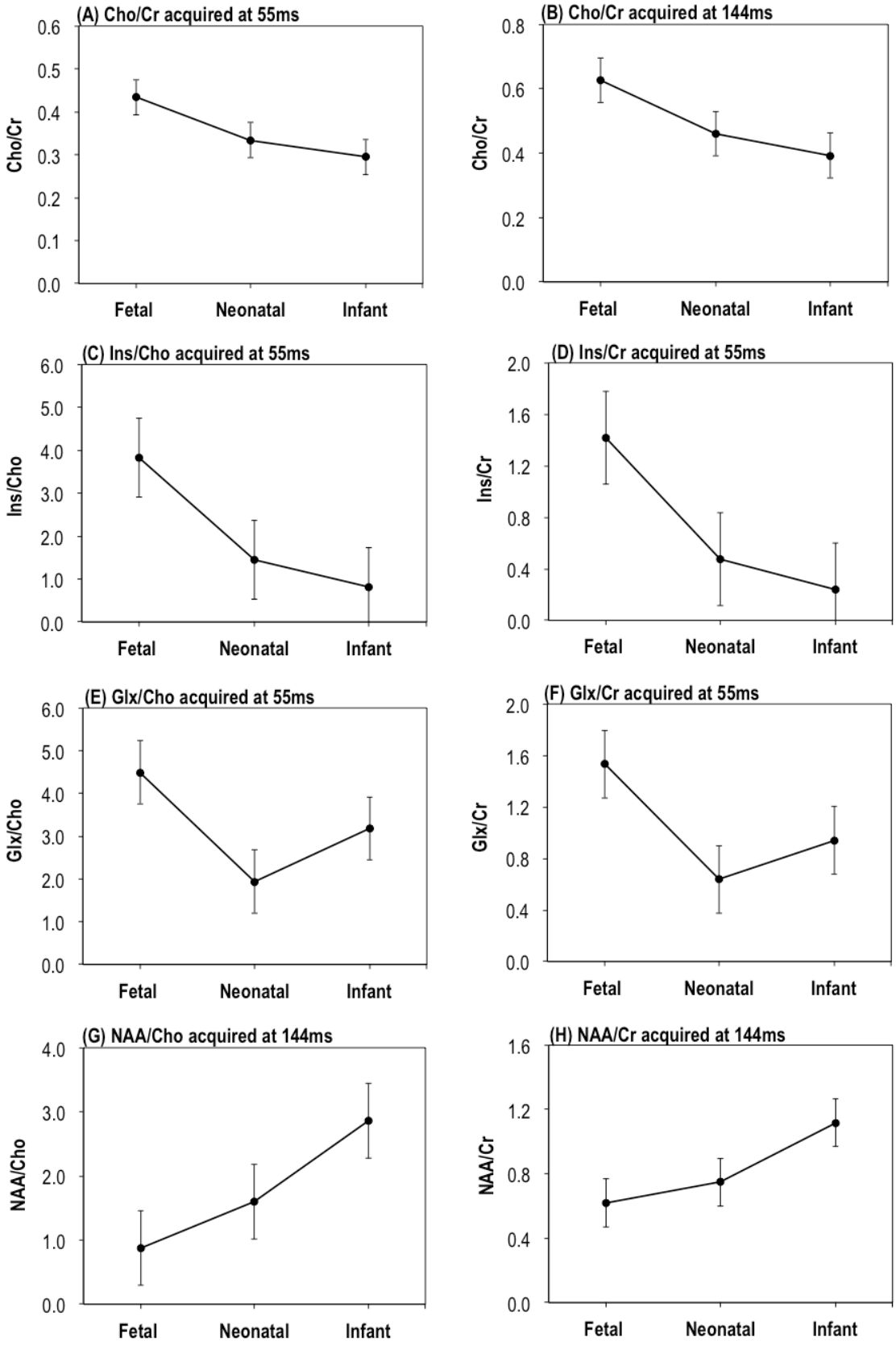

Figure 7.1: Longitudinal patterns of metabolic development from the fetal to the infant timepoint. These plots are representative of the whole sample (that is, low-risk and high-risk groups combined). **(A-B)** Cho/Cr, **(C)** Ins/Cho, **(D)** Ins/Cr, **(E)** Glx/Cho, **(F)** Glx/Cr, **(G)** NAA/Cho, and **(H)** NAA/Cr. Errors bars represent one standard error of the mean.

7.3.2. Group differences in brain metabolite ratios at 4-6 months of age

7.3.2.1. Sample characteristics

When stratified by risk group, infants did not differ significantly in age, sex, ethnicity, body weight (at birth and at MRI), head circumference (at birth and at MRI), or Apgar scores (at 1 and 5 minutes) (Table 7.2). However, they did differ significantly in mode of delivery (p = 0.024), with more low-risk infants being born via caesarean section. In addition, whilst maternal and paternal ages were not significantly different between groups, there were other parental characteristics that were. For instance, the parents of low-risk infants were educated to a higher level than those in the high-risk group (maternal education: p = 0.019; paternal education: p < 0.001). Also, there were slightly more parents in the low-risk group that were married, as compared to those in the high-risk group, although the difference was not entirely significant (p = 0.054).

7.3.2.2. Group differences

Infants in the high-risk group had significantly higher levels of Glx/Cho [F(1, 21) = 4.86, p = 0.039] and Glx/Cr [F(1, 21) = 6.04, p = 0.023], when compared to those in the low-risk group (Figure 7.2). No other metabolite ratios showed significant group differences (Table 7.3).

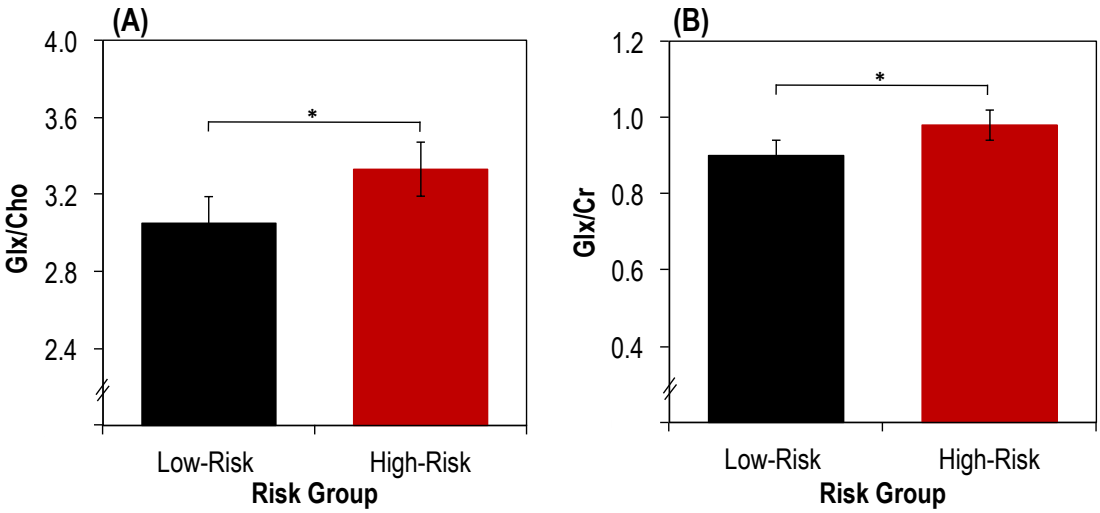

Figure 7.2: Mean differences in Glx ratios between infants at low-risk and high-risk of ASD. Infants at high-risk of ASD had elevated levels of **(A)** Glx/Cho and **(B)** Glx/Cr, when compared to low-risk controls. Error bars represent one standard error of the mean, *p≤0.05.

Table 7.2: Infant and parental characteristics stratified by risk group

	Total Sample (N = 33)	Low-Risk Group (n = 19)	High-Risk Group (n = 14)	Group difference Statistic (*p*-value)
Infant characteristics				
Gestational age at birth (weeks); mean (SD)	40.11 (1.17)	40.06 (1.23)	40.17 (1.12)	t = -0.27, p = 0.788
Corrected age at MRI (weeks); mean (SD)	66.43 (1.51)	66.68 (1.42)	66.09 (1.63)	t = 1.10, p = 0.280
Sex (male); n (%)	17 (51.52)	11 (57.89)	6 (42.86)	χ^2 = 0.73, p = 0.393
Ethnicity (white); n (%)	25 (75.76)	15 (78.95)	10 (71.43)	p = 0.134
Body weight at birth (kg); mean (SD)	3.44 (0.54)	3.47 (0.58)	3.37 (0.48)	t = 0.50, p = 0.622
Body weight at MRI (kg); mean (SD)	7.98 (1.05)	8.20 (1.00)	7.68 (1.07)	t = 1.43, p = 0.162
Head circumference at birth (cm); mean (SD)	34.74 (1.25)	34.62 (1.33)	34.53 (1.41)	t = 0.16, p = 0.875
Head circumference at MRI (cm); mean (SD)	43.56 (1.46)	43.89 (1.35)	43.42 (1.84)	t = 0.80, p = 0.433
Mode of delivery (caesarean section); n (%)	**12 (36.36)**	**10 (52. 63)**	**2 (14.29)**	***p* = 0.024**
Apgar score at 1 minute[a]; mean (SD)	8.24 (1.81)	8.23 (2.17)	8.25 (1.17)	U = 41.50, p = 0.384
Apgar score at 5 minute[a]; mean (SD)	9.57 (0.81)	9.54 (0.97)	9.63 (0.52)	U = 47.50, p = 0.681
Parental characteristics				
Maternal age at infant's birth (years); mean (SD)	34.39 (4.29)	34.95 (5.27)	4.03 (3.11)	t = 0.86, p = 0.397
Paternal age at infant's birth (years); mean (SD)	37.30 (8.60)	33.64 (7.15)	4.67 (6.20)	t = 0.37, p = 0.711
Marital status (married); n (%)	21 (63.64)	15 (78.95)	6 (42.86)	p = 0.054
Maternal education (higher education); n (%)	**19 (57.58)**	**15 (78.95)**	**4 (28.57)**	***p* = 0.019**
Paternal education (higher education); n (%)	**16 (48.48)**	**15 (78.95)**	**1 (7.14)**	***p* < 0.001**

Note: [a]Apgar scores were only available for 21 infants (13 low-risk and 8 high-risk). The Fisher's exact test does not have an associated statistic; thus, only p-values were reported. Significant results are shown in **bold**. Abbreviations: MRI = magnetic resonance imaging; Higher Education = undergraduate and/or postgraduate degree; U = Mann-Whitney *U*-statistic; t = Independent samples t-statistic; X^2 = Pearson's Chi-Square; SD = standard deviation.

Table 7.3: Group differences in brain metabolite ratios between infants in low-risk and high-risk groups

		Low-Risk Group		High-Risk Group		Group Difference	
Echo Time	**Metabolite Ratios**	**n**	**Mean (SD)**	**n**	**Mean (SD)**	**F-statistic**	***p*-value**
55 ms	Cho/Cr	19	0.29 (0.03)	13	0.29 (0.02)	1.10	0.305
	Ins/Cho	18	0.73 (0.24)	11	0.95 (0.42)	0.48	0.871
	Ins/Cr	18	0.21 (0.06)	11	0.27 (0.12)	0.72	0.408
	Glx/Cho	**19**	**3.05 (0.62)**	**13**	**3.33 (0.40)**	**4.86**	**0.039**
	Glx/Cr	**19**	**0.90 (0.20)**	**13**	**0.98 (0.13)**	**6.04**	**0.023**
144 ms	Cho/Cr	18	0.39 (0.03)	13	0.38 (0.04)	0.02	0.887
	NAA/Cho	18	2.79 (0.22)	13	3.05 (0.41)	0.96	0.339
	NAA/Cr	18	1.10 (0.10)	13	1.16 (0.12)	1.34	0.261

Note: In this analysis of co-variance, infant age at scan was included as a co-variate, whilst sex and mode of delivery were included as fixed factors. Significant results are shown in **bold.** Abbreviations: NAA = N-acetylaspartate and N-acetylaspartylglutamate; Cr = creatine and phosphocreatine; Cho = free choline, glycerophosphocholine, and phosphocholine; Ins = myo-inositol; Glx = glutamate and glutamine; F = F-statistic; SD = standard deviation.

7.4. Discussion

In this study, examining metabolic development from the fetal to the early postnatal period, Cho/Cr, Ins/Cho, and Ins/Cr all decreased with age, whilst NAA/Cho and NAA/Cr increased. In contrast, both Glx/Cho and Glx/Cr exhibited a more complex pattern of development; Glx ratios decreased from the fetal to the neonatal timepoint, but increased thereafter up until the period of early infancy. In addition, 4-6 month-old infants at high-risk of ASD had significantly higher levels of Glx when compared to low-risk controls.

7.4.1. Typical metabolic development across the fetal, neonatal, and infant brain

7.4.1.1. Cho

Between fetal and infant timepoints, Cho/Cr decreased significantly with age. These results are in accordance with other studies, which report that Cho levels are highest around 22-28 gestational weeks (Girard et al., 2006b), but rapidly decline from there up until 3-5 months of age, at which point they begin to plateau (Blüml et al., 2013; Kimura et al., 1995). Cho is considered as an essential component of cell membranes and is especially present in myelin. The overall decrease in Cho/Cr identified in both this and other studies, is therefore thought to correspond to the process of myelination, as well as the loss of immature myelin (Girard et al., 2006b; Kok et al., 2002; Story et al., 2011).

7.4.1.2. Cr

Given that Cho/Cr decreases during early brain development, it can be assumed that Cr/Cho increases within this same time frame. Indeed, although originally considered as a stable metabolite, recent studies have reported that Cr levels increase from fetal to early postnatal life, only stabilising at around 2 years of age (Blüml et al., 2013; Degnan et al., 2014; Evangelou et al., 2016). High levels of Cr are required for energy production during myelination; this explains why the metabolite is found in such high concentrations in early life when myelination is most prominent (Brighina et al., 2009; Huppi et al., 1995).

7.4.1.3. Ins

From the fetal to the infant period, both Ins/Cho and Ins/Cr ratios decreased significantly with age. More specifically and in agreement with the current literature (Blüml et al., 2013; Kok et al., 2001; Kreis et al., 1993), a dramatic drop in Ins ratios was evident between the fetal and neonatal period. This was followed by a less steep but still significant decrease between the first few months of postnatal life (for clarification, please see Figure 7.1C and D on page 229). Amongst its many roles, Ins is considered as an important glial marker (Brand et al., 1993; Kousi et al., 2013; Ross and Bluml, 2001). Thus, the high levels of Ins found between 22-28 gestational weeks, may reflect the high density of glial cells present in the brain at this time (Fisher et al., 2002; Girard et al., 2006a). The observation that Ins levels decay across early development also suggests that the proliferation and/or growth of glial cells is decreasing, and that the metabolite is being 'used up' as white matter maturation progresses (Blüml et al., 2013; Vigneron, 2006).

7.4.1.4. NAA

Perhaps the most consistent finding in the literature on typical metabolic development is that NAA increases with age (Degnan et al., 2014; Girard et al., 2006a, 2006b; Heerschap et al., 2003; Huppi et al., 1995; Kimura et al., 1995; Kok et al., 2002; Ross and Bluml, 2001). This study corroborates these findings as both NAA/Cho and NAA/Cr increased significantly across timepoints, from fetal up until early infant life. In addition, this finding was more pronounced for NAA/Cho as compared to NAA/Cr, possibly because as discussed earlier, Cho may be more stable than Cr in early development (Evangelou et al., 2016). Furthermore, since NAA is an important marker of both neuronal and glial cells, the increase in NAA across development, evident in both this and other studies, is reflective of appropriate brain maturation (Bhakoo and Pearce, 2000).

7.4.1.5. Glx

Compared to other metabolites, Glx has not been as extensively studied and little is known about how it changes with age. Thus far, Glx has been visualised *in utero* as early as 24

weeks gestation (Girard et al., 2006a), but the current study extends this finding further to suggest that the Glx signal is already present at 22 weeks. Moreover, of the few studies that have examined Glx during the fetal period, none has identified significant variations with age (Girard et al., 2006a, 2006b). However, there have been studies examining Glx changes in early infancy, and aside from one study suggesting that Glx does not vary with increasing postnatal age (Kreis et al., 1993), all others have reported postnatal increases in Glx, which are reflective of appropriate brain maturation (Blüml et al., 2013; Degnan et al., 2014; Kreis et al., 2002). In the present study, Glx ratios increased from neonatal to infant life, and are therefore in agreement with these latter studies. However before this postnatal increase, both Glx/Cho and Glx/Cr decreased from the fetal to the neonatal period, illustrating a 'dip' in Glx around the time of birth (please refer back to Figure 7.1E and F on page 229).

As the main excitatory neurotransmitter, glutamate (measured in this study as Glx) serves a multitude of functions in the developing human brain. One of its key functions is as the immediate precursor of GABA, which is largely involved in inhibitory neurotransmission. However, as described in the introduction of this thesis, early brain maturation is associated with a developmental switch in GABA, from excitatory to inhibitory (Ben-Ari, 2002). This is thought to occur during birth and implies that GABA exerts excitatory functions in early prenatal life. Overall, this switch is deemed crucial for normal brain development as it is partly responsible for the synchronisation of electrical activity, synaptic tuning, and neuronal wiring – all of which are necessary for appropriate neural connectivity and function (for review see Allene and Cossart, 2010; Khazipov and Luhmann, 2006).

Considering that both glutamate and GABA are excitatory up until the time of birth may help to explain why, in this study, Glx is present in such low levels in neonatal life. Potentially, the decrease in Glx from the fetal to the neonatal timepoint counter-balances what is happening to GABA at this time. During fetal life when GABA is excitatory, for example, there is less of a need for glutamate to be present in high amounts. This is because the combined efforts of Glx and GABA provide enough excitatory activity to allow for normal neurodevelopmental

processes to occur, but not enough (due to decreasing Glx) to cause pathological hyperexcitability. After birth, once GABA has switched to its inhibitory mode of transmission, more glutamate is needed. Therefore, Glx levels increase (as evidenced in this study), to ensure that an adequate level of excitability is maintained for neurodevelopmental processes to continue as usual. This proposed hypothesis is partly corroborated by the findings of a recent post-mortem study, which reported that human GABAergic neurons increase in density from mid-gestation to term, peaking at term, and decreasing thereafter (Xu et al., 2011). Although GABAergic neurons cannot be directly compared to GABA levels, this finding is in juxtaposition to what was identified for Glx, and adds to the existing evidence. Thus it is possible that the findings of this study provide the first *in vivo,* albeit indirect proof, for a GABA excitatory-to-inhibitory switch in humans.

In conclusion, the first aim of this study has been met; not only do these results replicate previous findings on the typical metabolic development of Cho, Cr, Ins, and NAA, they also extend our understanding of the maturational profile of glutamate (or Glx). Further work will be needed to replicate this finding, as well as to directly examine the human neurodevelopmental trajectory of GABA *in vivo.*

7.4.2. Group differences in brain metabolite ratios at 4-6 months of age

Infants at risk of ASD had significantly higher levels of Glx/Cho and Glx/Cr, when compared to low-risk controls. This suggests that absolute levels of Glx are elevated in these infants by 4-6 months of age. In addition and as far as I am aware, this was the first ^{1}HMRS study to examine the metabolic profile of infants genetically predisposed to ASD; therefore, direct comparisons with other studies were not possible. Moreover, the spectroscopic literature on young children and adolescents already diagnosed with ASD is inconsistent, with Glx levels reported to be higher (Bejjani et al., 2012; Doyle-Thomas et al., 2014), lower (Corrigan et al., 2013; DeVito et al., 2007; Kubas et al., 2012), and similar (Friedman et al., 2003, 2006; Hardan et al., 2008) in individuals with ASD compared to typically-developing controls. The discrepancy in these findings can be partly explained by the different brain regions examined.

Indeed, when focussing only on studies that have sampled from the same region as this study, the story becomes a little clearer. To date, of the six studies investigating Glx in the basal ganglia of children and adolescents with ASD, the majority have reported no significant differences when compared to age-matched controls (Corrigan et al., 2013; Friedman et al., 2003, 2006; Harada et al., 2011). However, studies reporting significant differences between groups have identified higher levels of putamen Glx/Cr (Doyle-Thomas et al., 2014), as well as blood and striatal glutamate (Hassan et al., 2013) in individuals with ASD. Thus, when placed together with the results of this study, it appears that an ASD risk status leads to elevated levels of subcortical Glx in infancy; levels which then either normalise or remain high in childhood.

The methods adopted in the current study make it impossible to discern whether the elevated levels of Glx identified are due to glutamate, glutamine, or both. However, previous studies have cautiously attributed Glx differences to glutamate, given that it is the most abundant transmitter in the nervous system (DeVito et al., 2007; Hardan et al., 2008; Page et al., 2006). Furthermore, reports of increased glutamate (Zheng et al., 2016) and decreased glutamine (Shimmura et al., 2011) in the blood plasma of individuals with ASD, relative to controls, supports this notion. Aside from this, there is also clinical (Tuchman et al., 2010), post-mortem (Fatemi et al., 2002; Purcell et al., 2001), and genetic evidence (Brune et al., 2008; Jamain et al., 2002; Ramoz et al., 2004; Serajee et al., 2003) to suggest that glutamatergic dysfunction is present in ASD, and that it may be of aetiological relevance to the disorder. For instance, elevated levels of glutamatergic transporters and receptors have been identified in the post-mortem brains of individuals with ASD (Purcell et al., 2001). Genetic studies have also reported associations between ASD and alleles encoding for genes involved in glutamatergic transmission (Jamain et al., 2002; Purcell et al., 2001; Serajee et al., 2003). Taken together, the findings of this and other studies support the hypothesis that the pathophysiology of ASD in early postnatal development may be characterised (at least partly) by an E/I imbalance, driven mainly by hyperglutamatergia (Fatemi, 2008; Polleux and Lauder, 2004; Rubenstein and Merzenich, 2003).

Glutamate is essential for several neurodevelopmental processes, including the proliferation and differentiation of oligodendrocytes, cell migration, plasticity, and synaptic pruning (Coyle et al., 2002; Gallo and Ghiani, 2000; Yuan et al., 1998). It is therefore not surprising that altered glutamatergic transmission, early in development, could result in neurodevelopmental abnormalities. In addition, since glutamate also facilitates neuronal synchronisation (Rodriguez et al., 2013), abnormalities of the glutamatergic system could impair typical brain function by impacting upon the formation of synapses and/or the functional connectivity of neural networks (Gatto and Broadie, 2010). Nonetheless, given the complementary action of glutamate and GABA, including the role they play in E/I balance, information about GABA in individuals with and at risk of ASD could augment our understanding of the underlying pathophysiology of the disorder.

To examine GABA using ^{1}HMRS is technically challenging, and therefore, only a few studies have been successful in quantifying this metabolite. Consequently, evidence for the involvement of GABA in ASD is still in its infancy. Thus far, the majority of studies have reported low levels of GABA in individuals with ASD, compared to controls (Cochran et al., 2015; Gaetz et al., 2014; Harada et al., 2011; Kubas et al., 2012; Port et al., 2016; Puts et al., 2016; Rojas et al., 2014). However, there have also been some studies reporting no significant differences in GABA levels between groups (Brix et al., 2015; Robertson et al., 2015). Moreover, a recent study has observed both lower GABA and higher glutamate levels in high-functioning adolescents with ASD (Drenthen et al., 2016). This finding strengthens the hypothesis of an E/I imbalance in ASD, largely driven by high glutamate and low GABA levels. In addition, low levels of GABA have been identified in unaffected siblings of children with ASD; thus, E/I imbalance may be a feature of the BAP and potentially even act as a heritable biomarker and/or endophenotype of the disorder (Rojas et al., 2014).

In summary, increased Glx ratios in 4-6 month-old infants at risk of ASD support the notion that an imbalance in E/I neurotransmission may partially underpin the pathophysiology of ASD. When the sample size permits, a key extension of the current study will be to examine

Glx differences in the fetal and neonatal period of individuals at high and low-risk of ASD. Future work will also seek to collect data on GABA simultaneously. This will allow for assessment of whether the GABA switch is disrupted in neurodevelopmental disorders like ASD, as recently proposed (Tyzio et al., 2014). Finally, proof that the glutamatergic pathway may be altered in individuals genetically predisposed to ASD, may incentivise the on-going search for pharmacological interventions targeting both glutamatergic and GABAergic systems (Chez et al., 2007; Erickson et al., 2014; Ghaleiha et al., 2013; Gürkan and Hagerman, 2012).

Aside from elevated Glx levels, there were no other significant differences in metabolite ratios between infants at high and low-risk of ASD. The ^{1}HMRS data acquired as part of this study was sampled solely from the region of the basal ganglia. Thus, it may be that other metabolites manifest differences in infants at risk of ASD only in other brain regions, such as the cerebellum, hippocampal-amygdala complex, and cortex (Chugani et al., 1999; DeVito et al., 2007; Fujii et al., 2010; Gabis et al., 2008; Otsuka et al., 1999; Vasconcelos et al., 2008). The present study may have also been underpowered due to its small sample size to detect subtle group differences in other metabolites. Also, the possibility of a false negative (type II) error cannot be excluded. This analysis will therefore be repeated once the sample size is larger. Future work will also extend this group comparison into younger populations, as we cannot rule out the possibility that other metabolites only show differences between risk groups at earlier (fetal and neonatal) timepoints.

7.4.3. Study limitations

The results of this study must be interpreted in the context of several limitations. First, the sample was of a modest size. This made it impossible to run risk group comparisons at fetal and neonatal timepoints; it also prohibited a longitudinal analysis, limiting our understanding of the trajectory and potential neurometabolic differences in individuals at risk of ASD younger than 4-6 months. Second, the presence of fetal motion meant that more than half (58.33%) of the acquired spectra could not be analysed, and so, the team is currently working to optimise

this. Third, the imaging protocol employed in this study did not allow for the resolution of Glx into its separate components (that is, glutamate and glutamine), nor did it allow for the quantification of GABA. Therefore, future studies employing optimised methods are needed to (i) confirm the results of this study, (ii) determine what specific metabolite is responsible for the changes in Glx, and (iii) examine any potential differences in GABA. Fourth, during ^{1}HMRS acquisition, a 20x20x20 mm voxel was placed in the region of the left basal ganglia, avoiding any CSF spaces, and ensuring adequate SNR. To maintain SNR, the same voxel size was used for all three timepoints, meaning that a relatively larger area of the fetal brain was sampled in comparison to that of the neonatal and infant brain. However, this limitation is unlikely to have affected results, as the longitudinal trajectory of Glx from the fetal to the infant timepoint was independent of the change in volume. Fifth, although essential to the successful completion of this study, a very low dose of chloral hydrate was used to encourage sleep during the scanning of infants aged 4-6 months, and represents a potential confounding factor. Other studies have also used this sedative (Kimura et al., 1995; Kreis et al., 1993) and their metabolite ratios, as well as those presented here, agree well with the values acquired without the use of sedation (Simões et al., 2015). In a recent fMRI study, the use of chloral hydrate also did not impact markedly upon functional activity within a number of neural networks (Doria et al., 2010). It is therefore unlikely that sedation affected the results, but caution in interpretation is advised. Sixth, this study reported relative ratios rather than absolute concentrations, which some argue is preferable especially in studies of development. However, metabolite ratios allow for comparison with other studies and therefore improve the interpretation of results. In future, unsuppressed water spectra will be acquired alongside the PRESS sequences used in this study, so that both absolute concentrations and relative ratios can be reported. Finally, this was a cross-sectional study that characterised infants in terms of high-risk and low-risk groups. Although not available at present, soon there will be data on the diagnostic outcomes of these infants, which will be useful to determine if the spectroscopic brain differences identified are linked with diagnostic outcome. Moreover, as undiagnosed siblings of children with ASD often develop the BAP, it would also be important to analyse this data in a dimensional manner.

7.4.4. Conclusions

Despite these limitations, this study offered preliminary evidence on the metabolic development of both the typical and potentially atypical brain. Aside from strengthening existing knowledge on the early maturation of Cho, Cr, Ins, and NAA, by reporting on how Glx develops from fetal to infant life, the study also provided indirect proof for a GABA excitatory-to-inhibitory switch in humans around the time of birth. In addition, this was the first study to report significant neurochemical differences in infants at risk of ASD, suggesting that increased levels of Glx may be an early biomarker and/or endophenotype of the disorder. Although in need of replication, these findings have implications for future pharmacological interventions, and for our understanding of the neural underpinnings of ASD. Finally, these preliminary results may incentivise longitudinal studies of infants at risk of ASD to incorporate spectroscopy within their study design.

Chapter 8: General Discussion

8.1. Summary of rationale and findings

With the advent of new imaging modalities, the past few years have hugely advanced our understanding of the human brain. Our knowledge of how the early prenatal and postnatal periods shape brain development, however, is limited. Furthermore, our understanding of how development may be disrupted in individuals predisposed to neurodevelopmental disorders is lacking. Hence, in an attempt to provide further insight into very early brain development, the studies included in this thesis examined the structure and chemistry of the fetal, neonatal, and infant human brain. By including individuals with a familial risk of ASD, the focus was also to investigate how genetic risk may disrupt typical neurodevelopment, and in so doing, compromise later behavioural outcomes pertaining to ASD and other related disorders.

In the first experimental study of this thesis (chapter 3), normative variations in mother-infant interactions were found to be associated with differences in regional brain volumes. The next study, therefore, also incorporated measures of mother-infant interactions into a comparison of regional brain volumes in infants at low and high-risk of ASD. This second experiment (chapter 4) revealed that subcortical and cerebellar enlargements were present in infants at risk of ASD by 4-6 months of age, and that larger volumes were associated with more autistic symptoms at 36 months. In addition, this study provided preliminary evidence of a negative association between maternal sensitivity and subcortical volume within the high-risk group, meaning that high-risk infants exposed to more 'sensitive' mothers tended to have subcortical brain volumes more comparable to that of the low-risk group. Based on the results from these infant studies, the next step was to examine even younger individuals. The objective was to establish the trajectory of typical brain development, and to determine, when differences between infants at low and high-risk of ASD might first appear.

Consequently, the following two studies assessed total and regional brain volumes at fetal and neonatal timepoints in individuals with and without a familial risk of ASD. Across risk groups, the cerebellum and cortex were amongst the fastest growing regions. However, in contrast to the results at 4-6 months, the brains of fetuses and neonates genetically predisposed to ASD were smaller in volume than low-risk controls. In the fetal period (chapter 5), this finding was restricted to the cortex, but in the first month of postnatal life (chapter 6), there was a more generalised restriction in growth amongst neonates at risk of ASD. This included smaller intracranial and total brain volumes, as well as a smaller lentiform nucleus, which could not be explained solely by the smaller head size. Given that the lentiform nucleus constitutes a major part of the subcortical region, altered in high-risk infants at 4-6 months of age, a familial risk of ASD appears to be particularly disruptive to the development of this region.

The subcortex was therefore selected as a region-of-interest in the final study (chapter 7), which examined metabolic maturation from the late prenatal to the early postnatal period. Across risk groups, Cho and Ins decreased significantly with age, whilst NAA and Cr increased. In contrast, glutamate (measured as Glx) decreased from fetal to neonatal life, with a marked 'dip' around the time of birth, before increasing in early infancy.

This last study also allowed for an exploration of potential neurochemical differences in infants at low and high-risk of ASD. It provided the first evidence that high-risk infants have significantly elevated levels of subcortical Glx at 4-6 months, when compared to low-risk controls. An ASD risk status is thus associated with both neurochemical and neuroanatomical abnormalities of the subcortical region, evident before 6 months of age.

Placed together, the results of the studies conducted here suggest that brain development in individuals genetically predisposed to ASD, begins to deviate from the typical neurodevelopmental tract *in utero* (Figure 8.1).

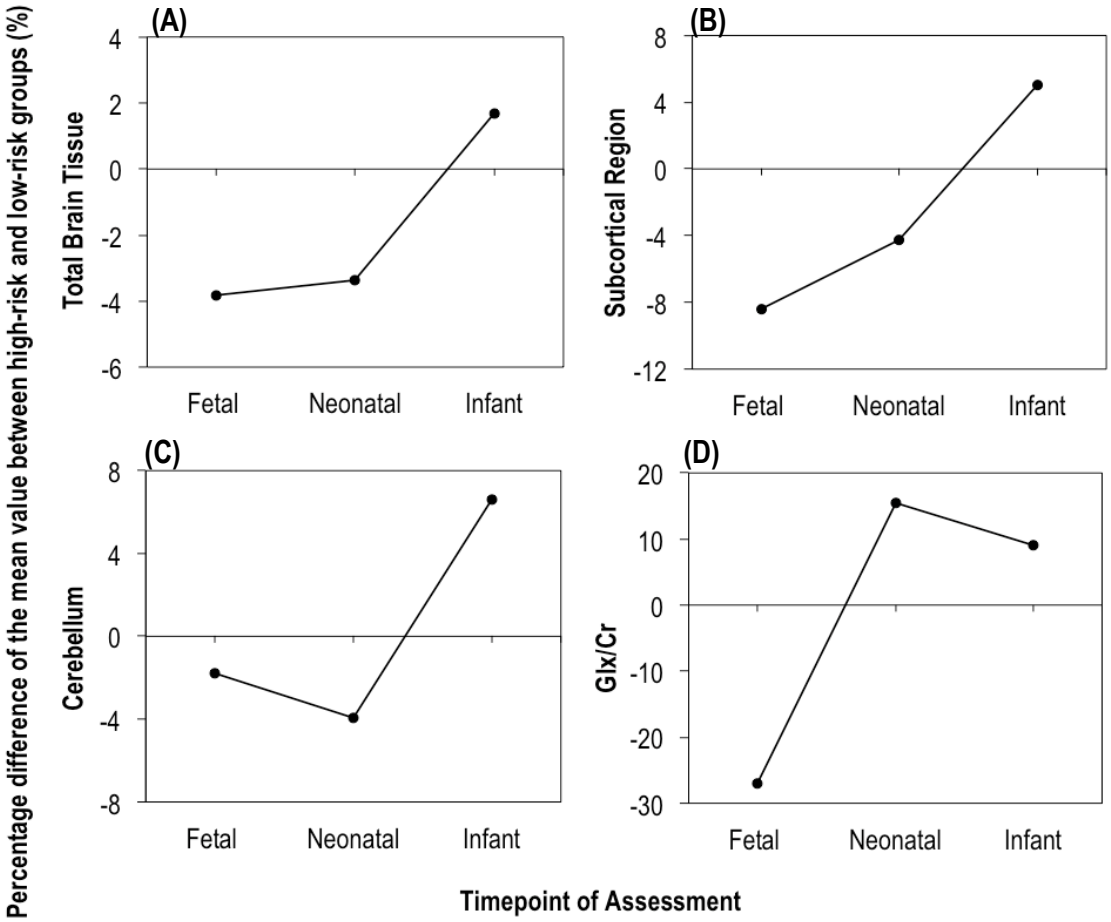

Figure 8.1: A graphical representation comparing brain development in individuals with and without a familial risk of ASD. Shortly prior to and after birth (during the fetal and neonatal periods, respectively), individuals at risk of ASD had smaller **(A)** total brain, **(B)** subcortical, and **(C)** cerebellar volumes, as well as lower **(D)** Glx/Cr ratios in fetal life, when compared to low-risk controls. In contrast, by 4-6 months of age, brain volumes were enlarged and Glx ratios elevated in high-risk individuals relative to controls. Although not all of these differences reached statistical significance, this graphical representation of the percentage difference of mean values between risk groups, attempts to demonstrate that individuals genetically predisposed to ASD show differences in typical brain development from the fetal period onwards. Abbreviations: Glx = glutamate/glutamine; Cr = creatine.

8.2. Potential pathways leading to aberrant development in ASD

Our understanding of brain development in ASD has improved significantly in recent years. However, since core symptoms of the disorder are usually already present in toddlers (aged 2-4 years), it is difficult to determine whether the brain abnormalities observed in these

individuals are a cause or consequence of the disorder. Studies of younger individuals prior to symptom manifestation are therefore needed to reveal causal pathways. Hence, by conducting early life studies of individuals genetically predisposed to ASD, the results of this thesis indicate that the genetic risk may be what constrains brain growth in the perinatal period, and what causes volumetric expansion of subcortical and cerebellar regions in early infancy. The alternative explanation is that a restriction of fetal and neonatal brain growth in individuals with a familial risk of ASD, triggers a compensatory overgrowth in brain volume that is measureable in infancy.

8.2.1. Cellular mechanisms

The perinatal period coincides with important neurodevelopmental processes, including neural proliferation, migration, and differentiation. One of the ways in which genetic pathways conferring risk for ASD might directly impact upon neurodevelopment, is by altering these processes. Evidence in support of this is now emerging (Casanova and Casanova, 2014; Chow et al., 2012; Voineagu et al., 2011). For example, in a study of individuals with and without ASD, an enrichment of CNVs disrupting gene-sets involved in cellular proliferation, projection, and motility, was identified in the ASD group (Pinto et al., 2010). Other biological processes, critical for development, such as chromatin remodelling, transcription, and splicing, also appear to be influenced by ASD genetic risk factors (Rubeis et al., 2014). In line with this, mutations in the ANKRD11 gene, encoding the Ankyrin repeat domain containing protein 11 (Ankrd11), have recently been linked to ASD (Iossifov et al., 2014; Willemsen et al., 2010). Ankrd11 is an important chromatin regulator that controls histone acetylation and gene expression during neural development. Targeting this protein in rodent mice by *in utero* electroporation of small hairpin RNAs resulted in decreased proliferation, errors in neuronal positioning, and ASD-like behaviours (Gallagher et al., 2015). Thus, there is strong evidence for a link between genetic mutations associated with ASD, abnormally regulated perinatal processes, and an ASD behavioural phenotype.

Further evidence for a perinatal disruption of neurodevelopmental processes in ASD stems from post-mortem studies. For example, irregular cell patterning has been observed at the cortical grey and white matter boundary, suggesting that the brains of affected individuals may undergo migratory deficits, abnormalities in neurogenesis, and/or a failed apoptosis of the subplate (Avino and Hutsler, 2010). In another more recent post-mortem study, focal patches of abnormal laminar cytoarchitecture were identified in the majority (91%) of young ASD brains, as opposed to only a minority (9%) of age-matched controls (Stoner et al., 2014). Aside from supporting a possible deregulation in cortical layer formation, these findings are also consistent with prenatal errors in neurogenesis, neural migration, and neural differentiation. Prenatal disruption of neurogenesis and cellular proliferation may result in a fewer number of neurons, and hence, contribute to the smaller total and/or regional brain volumes observed here, in individuals at risk of ASD during fetal and neonatal timepoints.

Finally, it is also possible that the large regional brain volumes observed in early infancy, are partly due to errors in proliferation. For example, recent work using induced pluripotent stem cells derived from a cohort of individuals with both ASD and brain overgrowth at 2-5 years of age, has shown that the neural stem cells of these individuals display abnormally rapid proliferation, when compared to the cells derived from unaffected controls (Marchetto et al., 2016). Thus, although further work is needed to untangle the mechanisms underlying smaller brain volumes in perinatal life and enlarged volumes in early infancy amongst high-risk individuals, errors in proliferation are most likely of causal relevance.

8.2.2. Biochemical mechanisms

Neurochemical abnormalities in ASD may precede and/or accompany the errors in cellular mechanisms that alter important neurodevelopmental processes. Results from both preclinical and clinical work, for example, propose that an E/I imbalance may be especially relevant to ASD. Specifically, evidence stemming from genetic, animal, post-mortem, and neuroimaging work, suggests that the glutamatergic system is altered in ASD (for review see Nelson and Valakh, 2015; Rubenstein and Merzenich, 2003).

The results reported in this thesis extend these findings further to propose that glutamatergic abnormalities in ASD emerge in early life. Since glutamate is crucial for a variety of neurodevelopmental processes – including proliferation, migration, and differentiation, as well as synaptogenesis and neuroplasticity (Gallo and Ghiani, 2000; Huttenlocher et al., 1982; Yuan et al., 1998) – this could have important implications for brain maturation. Indeed, too much glutamate can be detrimental to the brain, resulting in excitotoxicity, oxidative stress, mitochondrial damage, and apoptosis (Debanne et al., 2003; James et al., 2004; Kern, 2003). Moreover, hyperglutamatergia in early life appears to have worse consequences than if it were to be present in adulthood (Rosenberg et al., 2003; Yoshioka et al., 1996).

Hyperglutamatergia was clearly evident in the 4-6 month-old infants at risk of ASD studied here. In addition, although glutamate levels were not formally compared between fetuses and neonates at high and low-risk of ASD, there is a possibility that the glutamatergic system may already be aberrant in high-risk individuals during these earlier timepoints. As shown in Figure 8.1, fetuses at risk of ASD tended to have less glutamate than those at low-risk. However, by the neonatal timepoint, glutamate levels were already elevated in the high-risk group, consistent with the findings in early infancy. These observations coincide with a recognised perinatal 'shift' in GABA function, from excitatory prenatally to inhibitory postnatally. A delay in this switch has recently been implicated in neurodevelopmental disorders, including ASD (He et al., 2014; Tyzio et al., 2014). Thus, aside from continuing to acquire spectroscopic glutamate measures from very young individuals with and without a familial risk of ASD, there is also a plan to start measuring GABA, by including a MEGA-PRESS sequence into the existing ^{1}HMRS protocol (Mullins et al., 2014).

Future work will also examine the relationship between glutamate measures and brain structure in individuals genetically predisposed to ASD. High levels of glutamate have been reported in association with glial activation (Laurence and Fatemi, 2005; Vargas et al., 2005), and when activated, microglia can become enlarged (Morgan et al., 2010) and contribute to pruning deficits (Paolicelli and Gross, 2011). Therefore, it is possible that hyperglutamatergia

in the months after birth, as evident in high-risk individuals, could drive a compensatory increase in brain volume via glial activation. In support of this, human post-mortem studies have reported significantly increased activation of both astroglia and microglia in individuals with ASD, as compared to typically developing controls (Li et al., 2009; Morgan et al., 2010; Vargas et al., 2005).

8.3. Is the subcortical region core to aberrant neurodevelopment in ASD?

The subcortical region (encompassing basal ganglia and thalami) has been consistently implicated in the ASD literature (Calderoni et al., 2014; Estes et al., 2011; Hollander et al., 2005; Qiu et al., 2010; Sears et al., 1999). Moreover, this brain region was reported as abnormal in the individuals genetically predisposed to ASD studied in this thesis. For example, both the volume and biochemistry of the subcortex were observed to be different in neonates and infants at risk of ASD, relative to age-matched controls. A significant association between the early caregiving environment and the infant's subcortical volume was also present by 4-6 months of age in both low-risk and high-risk samples. Thus, the subcortical region is sensitive to genetic risk factors, but also to environmental risk factors that can alter neurodevelopment. This is consistent with other evidence suggesting that the subcortical region may be particularly vulnerable to early environmental influences, although prior work has tended to focus on extreme exposures such as perinatal hypoxia (Okereafor et al., 2008; du Plessis and Volpe, 2002; Shalak and Perlman, 2004).

Importantly, the subcortical region is thought to be crucial for normal brain development. For example, the subventricular zone within the subcortical region is a major locus for neuronal proliferation and migration. Aberrant development of this region may therefore be associated with some of the errors in prenatal processes frequently implicated in ASD. In addition, given that the subcortical region drives cortical development in fetal life (Kostović and Jovanov-Milošević, 2006; Sur and Rubenstein, 2005), abnormal maturation of this region could also

result in some of the cortical irregularities identified in ASD (Ecker et al., 2013b; Hazlett et al., 2011; Nordahl et al., 2007; Ohta et al., 2016; Wallace et al., 2013) and in fetuses at risk of ASD (chapter 5). It is possible, for instance, that the subcortical abnormalities reported in this thesis may contribute to the overall pattern of atypical neurodevelopment in ASD.

Since the subcortical region also plays a crucial role in motor co-ordination and control, the early dysfunctional development of this region could lead to the repetitive (often motoric) behaviours commonly observed in ASD. For example, in individuals genetically predisposed to ASD, a larger subcortical volume at 4-6 months was significantly correlated with a greater number and severity of restricted and repetitive behaviours at 36 months (chapter 4). These symptoms have been suggested to be amongst some of the earliest to manifest in individuals with and at risk of ASD (Mooney et al., 2006). Therefore, it would make sense for the subcortical region of these individuals to be aberrant from an early age, and potentially play a significant role in the underlying development of the disorder.

8.4. Implications for early therapeutic intervention

8.4.1. Parent-mediated interventions

According to the studies included in this thesis, by 6 months of age, individuals at risk of ASD have brain abnormalities that correlate with subsequent ASD-like symptoms. In addition, there is evidence indicating that the early caregiving environment is strongly associated with infant brain volume. With the caveat that the current work did not address therapeutic interventions, the results presented here suggest that parenting style is correlated with both infant brain and behaviour. Early parent-mediated interventions may therefore be beneficial for young infants with and at risk of ASD (for review see Oono et al., 2013). For example, in the first parent-mediated intervention trial aimed at high-risk infants within the first year of life, significant reductions in ASD-like behaviours were observed (Green et al., 2015). Although promising, before any definite conclusions can be drawn, further research is needed to replicate these findings in larger samples of high-risk individuals.

Moreover, the large regional brain volumes identified in 4-6 month-old infants at risk of ASD were significantly associated with several autistic traits at 36 months, but especially with restricted and repetitive behaviours (chapter 4). Yet, an improvement in these behaviours is rarely included as an outcome measure within intervention trials for children with ASD. This is an important omission, as early interventions should be focused on reducing *all* core behaviours. In addition, aside from being one of the first symptoms to manifest in ASD (Mooney et al., 2006), restricted and repetitive behaviours can be stigmatising and detrimental to the infant's consequent behavioural functioning by interfering with the acquisition of other skills (Gabriels et al., 2005; Lam et al., 2008; Loftin et al., 2008). As a result, recent work has focused on methods for reducing restricted and repetitive behaviours in infants with ASD; for instance, via environmental enrichment including exposure to multiple sensorimotor stimuli (Woo et al., 2015). Preliminary evidence suggests that these methods ameliorate restricted and repetitive symptoms in affected infants (Woo et al., 2015). Thus, this may be something worth including in future parent-mediated intervention trials, specifically those aimed at individuals with and at risk of ASD.

8.4.2. Pharmacological treatment

Although behavioural interventions should be viewed as the therapy of choice for young infants with and at risk of ASD, the possibility of early pharmacological interventions should not be excluded. However, since paediatric populations are rarely included in clinical trials, little is known about how infants and children respond to drugs (Bavdekar, 2013). When working towards the development of pharmacological agents with potential applicability to very young individuals, there is therefore a need (more so than usual) to conduct an appropriate risk-benefit assessment, and to carefully screen for any potential side effects.

According to the final study of this thesis (chapter 7), hyperglutamatergia may be implicated in some aspects of early ASD pathophysiology, and thus, should encourage the ongoing search for pharmacological interventions targeting the E/I balance. For example, $GABA_A$ and $GABA_B$ receptor agonists reverse ASD-like features in a range of animal models (Han et al., 2012,

2014; Henderson et al., 2012; Heulens et al., 2012). In contrast, metabotropic glutamate receptor 5 antagonists rescue ASD-like behaviours in mouse models of ASD (Michalon et al., 2014; Pop et al., 2013; Silverman et al., 2012). Translating these findings into the clinic, however, has been unsuccessful thus far (Berry-Kravis et al., 2009).

E/I balance in early life can also be modulated indirectly using the diuretic bumetanide, a selective NKCC1 chloride-importer antagonist, which can restore the inhibitory action of GABA and prevent ASD-like behaviours in the offspring (Tyzio et al., 2014). In translation, a 3 month bumetanide treatment administered to children with ASD, significantly ameliorated symptom manifestation (Lemonnier and Ben-Ari, 2010; Lemonnier et al., 2012). Moreover, since there have been no serious side effects reported in association with bumetanide (Lemonnier et al., 2012), this may be a promising new drug for ASD. Still, trials with larger sample sizes are necessary; for example, to determine whether there is an ASD subgroup population for whom this treatment would be most suitable.

It has also recently been demonstrated that the combination of pharmacological and behavioural interventions is more effective in reducing behavioural difficulties in children with neurodevelopmental disorders, as compared to medication alone (Aman et al., 2009). Combining these two approaches and implementing them from early on may therefore be the best way forward to treating ASD. Early intervention, however, will only be possible once valid biomarkers have been developed, and so the search for these markers remains an important future direction.

8.5. Limitations and considerations for future research

Although the problems encountered within each study have been discussed in previous chapters, there are some limitations worthy of mentioning here. For example, we should be cautious not to over interpret findings due to the small sample size. Studies of larger sample sizes are therefore needed to replicate results, but also to enable an initial exploration of the underlying aetiological pathways leading to distinct ASD subtypes.

The lack of outcome data in some of the studies included here is yet another limitation, which restricts the interpretation of results. It was not within the scope of this thesis, for instance, to correlate the fetal, neonatal, and infant brain measures (collated as part of project 2) with later autistic and other related symptoms. However, as the infants begin to reach 36 months of age, outcome measures will soon become available. This will allow for the data to be analysed both in a categorical and dimensional manner, which will help to elucidate whether alterations in brain volume and chemistry during early prenatal and postnatal life, could be used as early predictors of risk and/or resilience for poor neurodevelopmental outcomes. It will be particularly interesting to examine whether these identified brain differences are specific to ASD, or whether they are present in individuals with associated co-morbidities, thus representing shared risk factors and elucidating on common pathways to clinically related difficulties. In addition, while the *in utero* diagnosis of ASD remains an ambitious goal that may never fully materialise, this thesis has shown that it is possible to study fetuses at risk of ASD and that this is an avenue worth pursuing. In future, once automated protocols for fetal segmentation are routinely implemented, fetal MRI may become an important research tool, which will hopefully encourage the development of early screening, and help to identify high-risk infants most in need of early intervention.

There are also specific limitations associated with studying infants at risk. Families of children with ASD may experience pressures beyond that of a typical family, which may lead to increased levels of stress and depression amongst parents (Baker et al., 2011; Ingersoll and Hambrick, 2011). Key features of stress such as social withdrawal, fatigue, and irritability may, in some cases, impact on early mother-infant interactions (Coyl et al., 2002; Murray et al., 2010). Parents of high-risk infants may also demonstrate characteristics of the BAP and thus be less sensitive to their infant's' mental state (Bolton et al., 1998; Gerdts and Bernier, 2011). Altogether, this may negatively impact upon infant brain and behavioural outcomes. Consequently, future studies of infants at risk of ASD should aim to acquire comprehensive information on parental autistic traits and mood.

Another issue not yet addressed concerns the specificity of findings. For example, although the subcortical region was enlarged by 4-6 months in high-risk infants who received a clinical diagnosis of ASD, it is not possible to be sure that these results are ASD-specific. Anatomical abnormalities of the basal ganglia (of which the subcortical region is part of) have been reported in relation to other neurodevelopmental disorders, including ADHD (Seidman et al., 2011). ADHD also shares genetic risk factors with ASD (Rommelse et al., 2010) and so, these shared factors could be what influence the (initial) abnormal development of the basal ganglia. Identifying which brain differences are related to subsequent behavioural difficulties may prove important in future, particularly when it comes to understanding the causal pathways to symptom development in a range of other related disorders. Future longitudinal research into high-risk infants would therefore benefit from the inclusion of a neurodevelopmental comparison group, to ascertain the specificity of findings. In line with this, an interesting question for future research is why – given the overlapping family histories and shared risk factors associated with a range of neurodevelopmental conditions (Consortium, 2013) – do some infants go on to be diagnosed with a disorder, whilst others born into the same family, do not? Also, what determines which infant will develop one disorder over another? And why is it that some individuals develop ASD, whilst others only show ASD-like traits, reminiscent of the BAP? Besides paving the way for more research, these questions should also prompt the search for protective, rather than just predictive, biomarkers.

Finally, although an exploratory longitudinal analysis was conducted as part of this thesis, the fact that only 8 high-risk participants were scanned at both fetal and neonatal timepoints, limited the analysis and interpretation of results. Nonetheless, preliminary findings were suggestive of a possible interaction effect between timepoint and risk group, which was in line with results from the main cross-sectional analysis. By now, many more fetuses, neonates, and infants will have been scanned as part of project 2. The majority of participants will also have imaging data at more than one timepoint. Therefore, once the infant data has been segmented and analysed, the obvious next step will be to run a thorough longitudinal analysis. This will help to determine whether the individuals that have small total and regional brain

volumes in fetal and neonatal life, are the same ones that have enlarged volumes at 4-6 months, and who then go on to develop ASD. In addition, this will allow for metabolic and volumetric trajectories to be compared between risk groups, rather than relying on comparisons of static measures alone. In a recent longitudinal study, the severity of repetitive behaviours in children with ASD was significantly correlated with an increased growth rate of the caudate, and not with caudate volume *per se* (Langen et al., 2014). As a result, it is likely that growth rates will allow for more subtle differences to be identified, and my future work with fetal, neonatal, and infant datasets will ensure that similar analyses be conducted.

8.6. Conclusion

The studies incorporated in this thesis have provided an important first step in identifying very early (fetal, neonatal, and infant) brain abnormalities that may underlie the emergence of ASD and other behavioural difficulties. Specifically, the neurodevelopmental trajectory of individuals genetically predisposed to ASD exhibits a deviation from the typical neurodevelopmental tract, evident from the fetal period onwards. This deviation occurs well before the onset of behavioural symptoms in ASD and therefore has important implications for the management of the disorder and its associated symptoms, particularly with regards to early identification and intervention.

Appendices

Appendix 1: Post-hoc power calculations

Study 2 – Chapter 4: Regional brain volumes and behavioural outcomes in infants with a familial risk of ASD

This study reported that 4-6-month-old infants at risk of ASD had significantly larger cerebellum [$F(1,44) = 6.92$, $p = 0.012$] and subcortical volumes [$F(1,44) = 4.64$, $p = 0.037$] than age-matched low-risk controls. The results of the post-hoc calculations revealed an achieved power of 0.50 and 0.46 for the cerebellum and subcortical findings, respectively. The effect size for the cerebellum finding was larger than that for the subcortical, but both were considered to be of moderate size (cerebellum: $\eta_p^2 = 0.136$; subcortical: $\eta_p^2 = 0.095$).

Study 3 – Chapter 5: Brain volumes in fetuses with and without a familial risk of ASD

In the third study of this thesis, significant group differences were identified for the cortex [$F(1,35) = 5.21$, $p = 0.029$], with high-risk fetuses having smaller cortical volumes than low-risk controls. Post-hoc power calculations revealed an achieved power of 0.46, with moderate effect size ($\eta_p^2 = 0.130$) reported for this finding.

Study 4 – Chapter 6: Brain volumes in neonates with and without a familial risk of ASD

In this experimental chapter, significant group differences were identified within the first month of postnatal life. Results revealed that high-risk neonates had a significantly smaller volume of the total brain tissue [$F(1,47) = 4.76$, $p = 0.034$] and intracranium [$F(1,47) = 5.40$, $p = 0.024$], when compared to low-risk controls. The results of the post-hoc calculations established an achieved power of a mere 0.13 and 0.11 for the total brain tissue and intracranium findings, respectively. Both these findings, however, revealed moderate effect sizes (total brain tissue: $\eta_p^2 = 0.092$; intracranium: $\eta_p^2 = 0.103$). In addition, this study identified significant differences in head-to-body proportions between groups [$F(1,48) = 14.87$, $p < 0.001$], with the high-risk group weighing considerably more than the low-risk, but having significantly smaller

intracranial volumes. The achieved power for this group difference was 0.99 and the effect size was large (η_p^2 = 0.237).

Finally, significant difference in the volume of the lentiform nucleus were also identified [F(1,46) = 4.62, *p* = 0.037], with high-risk neonates having significantly smaller volumes than low-risk controls. Post-hoc power calculations revealed an achieved power of 0.36 for this finding, with moderate effect size (η_p^2 = 0.091).

Study 5 – Chapter 7: Subcortical biochemistry from prenatal to early postnatal life, and metabolic differences in infants with and without a familial risk of ASD

The final study provided evidence that 4-6-month-old infants at risk of ASD have significantly higher levels of Glx/Cho [F(1,21) = 4.86, *p* = 0.039] and Glx/Cr [F(1,21) = 6.04, *p* = 0.023], as compared to age-matched controls. The results of the post-hoc calculations revealed an achieved power of 0.34 and 0.28 for the Glx/Cho and Glx/Cr findings, respectively. Despite this, the effect sizes were large for both findings (Glx/Cho: η_p^2 = 0.188; Glx/Cr: η_p^2 = 0.227).

References

Abrahams, B.S., and Geschwind, D.H. (2008). Advances in autism genetics: on the threshold of a new neurobiology. Nat. Rev. Drug Discov. *9*, 341–355.

Abrahams, B.S., and Geschwind, D.H. (2010). Connecting Genes to Brain in the Autism Spectrum Disorders. Arch. Neurol. *67*, 395–399.

Allen, G. (2005). The Cerebellum in Autism. Clin. Neuropsychiatry *2*, 321–337.

Allene, C., and Cossart, R. (2010). Early NMDA receptor-driven waves of activity in the developing neocortex: physiological or pathological network oscillations? J. Physiol. *588*, 83–91.

Alsdorf, R., and Wyszynski, D.F. (2005). Teratogenicity of sodium valproate. Expert Opin. Drug Saf. *4*, 345–353.

Aman, M.G., McDougle, C.J., Scahill, L., Handen, B., Arnold, L.E., Johnson, C., Stigler, K. a, Bearss, K., Butter, E., Swiezy, N.B., et al. (2009). Medication and Parent Training in Children With Pervasive Developmental Disorders and Serious Behavior Problems: Results From a Randomized Clinical Trial. J. Am. Acad. Child Adolesc. Psychiatry *48*, 1143–1154.

American Psychiatric Association (2013). DSM-V.

Anderson, S.A., Eisenstat, D.D., Shi, L., and Rubenstein, J.L. (1997). Interneuron Migration from Basal Forebrain to Neocortex: Dependence on Dlx Genes. Science (80-.). *278*, 474–476.

Anderson, S.A., Marín, O., Horn, C., Jennings, K., and Rubenstein, J.L. (2001). Distinct cortical migrations from the medial and lateral ganglionic eminences. Development *128*, 353–363.

Andre, J.B., Bresnahan, B.W., Mossa-Basha, M., Hoff, M.N., Patrick Smith, C., Anzai, Y., and Cohen, W.A. (2015). Toward quantifying the prevalence, severity, and cost associated with patient motion during clinical MR examinations. J. Am. Coll. Radiol. *12*, 689–695.

Angevine, J.B., and Sidman, R.L. (1961). Autoradiographic study of cell migration during histogenesis of cerebral cortex in the mouse. Nature *192*, 766–768.

Aoki, Y., Kasai, K., and Yamasue, H. (2012). Age-related change in brain metabolite abnormalities in autism: a meta-analysis of proton magnetic resonance spectroscopy studies. Transl. Psychiatry *2*, e69.

Arichi, T. (2012). Functional MRI of the developing neonatal brain: potential and challenges for the future. Dev. Med. Child Neurol. *54*, 676–683.

Ariyannur, P.S., Madhavarao, C.N., and Namboodiri, A.M.A. (2008). N-acetylaspartate synthesis in the brain: mitochondria vs. microsomes. Brain Res. *1227*, 34–41.

Ashburner, J., and Friston, K.J. (2005). Unified segmentation. Neuroimage *26*, 839–851.

Atkinson, L., Gonzalez, A., Kashy, D.A., Santo Basile, V., Masellis, M., Pereira, J., Chisholm, V., and Levitan, R. (2013). Maternal sensitivity and infant and mother adrenocortical function across challenges. Psychoneuroendocrinology *38*, 2943–2951.

Atladóttir, H.O., Schendel, D.E., Parner, E.T., and Henriksen, T.B. (2015). A Descriptive Study on the Neonatal Morbidity Profile of Autism Spectrum Disorders, Including a Comparison with Other Neurodevelopmental Disorders. J. Autism Dev. Disord. *45*, 2429–2442.

Atladóttir, H.Ó., Thorsen, P., Østergaard, L., Schendel, D.E., Lemcke, S., Abdallah, M., and Parner, E.T. (2010). Maternal Infection Requiring Hospitalization During Pregnancy and Autism Spectrum Disorders. J. Autism Dev. Disord. *40*, 1423–1430.

Avino, T.A., and Hutsler, J.J. (2010). Abnormal cell patterning at the cortical gray-white matter boundary in autism spectrum disorders. Brain Res. *1360*, 138–146.

Back, S. a, Luo, N.L., Borenstein, N.S., Volpe, J.J., and Kinney, H.C. (2002). Arrested oligodendrocyte lineage progression during human cerebral white matter development: dissociation between the timing of progenitor differentiation and myelinogenesis. J. Neuropathol. Exp. Neurol. *61*, 197–211.

Bailey, A., Luthert, P., Dean, A., Harding, B., Janota, I., Montgomery, M., Rutter, M., and Lantos, P. (1998). A clinicopathological study of autism. Brain *121*, 889–905.

Baird, G., Simonoff, E., Pickles, A., Chandler, S., Loucas, T., Meldrum, D., and Charman, T. (2006). Prevalence of disorders of the autism spectrum in a population cohort of children in South Thames: the Special Needs and Autism Project (SNAP). Lancet *368*, 210–215.

Bak, L.K., Schousboe, A., and Waagepetersen, H.S. (2006). The glutamate/GABA-glutamine cycle: aspects of transport, neurotransmitter homeostasis and ammonia transfer. J. Neurochem. *98*, 641–653.

Baker, J.K., Seltzer, M.M., and Greenberg, J.S. (2011). Longitudinal effects of adaptability on behavior problems and maternal depression in families of adolescents with autism. J. Fam. Psychol. *25*, 601–609.

Bale, T.L., Baram, T.Z., Brown, A.S., Goldstein, J.M., Insel, T.R., McCarthy, M.M., Nemeroff, C.B., Reyes, T.M., Simerly, R.B., Susser, E.S., et al. (2010). Early Life Programming and Neurodevelopmental Disorders. Biol. Psychiatry *68*, 314–319.

Ball, G., Counsell, S.J., Anjari, M., Merchant, N., Arichi, T., Doria, V., Rutherford, M.A., Edwards, A.D., Rueckert, D., and Boardman, J.P. (2010). An optimised tract-based spatial statistics protocol for neonates: Applications to prematurity and chronic lung disease. Neuroimage *53*, 94–102.

Ball, G., Boardman, J.P., Rueckert, D., Aljabar, P., Arichi, T., Merchant, N., Gousias, I.S., Edwards, A.D., and Counsell, S.J. (2012). The effect of preterm birth on thalamic and cortical development. Cereb. Cortex *22*, 1016–1024.

Barkovich, A.J., Baranski, K., Vigneron, D., Partridge, J.C., Hallam, D.K., Hajnal, B.L., and Ferriero, D.M. (1999). Proton MR Spectroscopy for the Evaluation of Brain Injury in Asphyxiated, Term Neonates. Am. J. Neuroradiol. *20*, 1399–1405.

Baron-Cohen, S., Scott, F.J., Allison, C., Williams, J., Bolton, P., Matthews, F.E., and Brayne, C. (2009). Prevalence of autism-spectrum conditions: UK school-based population study. Br. J. Psychiatry *194*, 500–509.

Baron-Cohen, S., Auyeung, B., Nørgaard-Pedersen, B., Hougaard, D.M., Abdallah, M.W., Melgaard, L., Cohen, A.S., Chakrabarti, B., Ruta, L., and Lombardo, M. V (2015). Elevated fetal steroidogenic activity in autism. Mol. Psychiatry *20*, 369–376.

Barr, R.F., and Hayne, H. (2003). It's Not What You Know, It's Who You Know: Older siblings facilitate imitation during infancy. Int. J. Early Years Educ. *11*, 7–21.

Bartholomeusz, H.H., Courchesne, E., and Karns, C.M. (2002). Relationship between head circumference and brain volume in healthy normal toddlers, children, and adults. Neuropediatrics *33*, 239–241.

Baruth, J.M., Wall, C.A., Patterson, M.C., and Port, J.D. (2013). Proton Magnetic Resonance Spectroscopy as a Probe into the Pathophysiology of Autism Spectrum Disorders (ASD): A Review. Autism Res. *6*, 119–133.

Bates, E., and Dick, F. (2002). Language, gesture, and the developing brain. Dev. Psychobiol. *40*, 293–310.

Batki, A., Baron-Cohen, S., Wheelwright, S., Connellan, J., and Ahluwalia, J. (2000). Is there an innate gaze module? Evidence from human neonates. Infant Behav. Dev. *23*, 223–229.

Bauman, M.L., and Kemper, T.L. (2005). Neuroanatomic observations of the brain in autism: a review and future directions. Int. J. Dev. Neurosci. *23*, 183–187.

Bavdekar, S.B. (2013). Pediatric clinical trials. Perspect. Clin. Res. *4*, 89–99.

Becker, E.B.E., and Stoodley, C.J. (2013). Autism Spectrum Disorder and the Cerebellum. In International Review of Neurobiology, pp. 1–34.

Bedford, R., Elsabbagh, M., Gliga, T., Pickles, A., Senju, A., Charman, T., and Johnson, M.H. (2012). Precursors to Social and Communication Difficulties in Infants At-Risk for Autism: Gaze Following and Attentional Engagement. J. Autism Dev. Disord. *42*, 2208–2218.

Bejjani, A., O'Neill, J., Kim, J.A., Frew, A.J., Yee, V.W., Ly, R., Kitchen, C., Salamon, N., McCracken, J.T., Toga, A.W., et al. (2012). Elevated Glutamatergic Compounds in Pregenual Anterior Cingulate in Pediatric Autism Spectrum Disorder Demonstrated by 1H MRS and 1H MRSI. PLoS One *7*, e38786.

Belmonte, M.K., Allen, G., Beckel-Mitchener, A., Boulanger, L.M., Carper, R.A., and Webb, S.J. (2004). Autism and Abnormal Development of Brain Connectivity. J. Neurosci. *24*, 9228–9231.

Belsky, J., and De Haan, M. (2011). Annual Research Review: Parenting and children's brain development: the end of the beginning. J. Child Psychol. Psychiatry *52*, 409–428.

Ben-Ari, Y. (2002). Excitatory Actions of GABA during Development: The Nature of the Nurture. Nat Rev Neurosci *3*, 728–739.

Ben-Ari, Y. (2015). Is birth a critical period in the pathogenesis of autism spectrum disorders? Nat. Rev. Neurosci. *16*, 498–505.

Bergelson, E., and Swingley, D. (2012). At 6-9 months, human infants know the meanings of many common nouns. Proc. Natl. Acad. Sci. *109*, 3253–3258.

Bernardi, S., Anagnostou, E., Shen, J., Kolevzon, A., Buxbaum, J.D., Hollander, E., Hof, P.R., and Fan, J. (2011). In vivo 1H-magnetic resonance spectroscopy study of the attentional networks in autism. Brain Res. *1380*, 198–205.

Berry-Kravis, E., Hessl, D., Coffey, S., Hervey, C., Schneider, a, Yuhas, J., Hutchison, J., Snape, M., Tranfaglia, M., Nguyen, D. V, et al. (2009). A pilot open label, single dose trial of fenobam in adults with fragile X syndrome. J. Med. Genet. *46*, 266–271.

Bertholdo, D., Watcharakorn, A., and Castillo, M. (2013). Brain Proton Magnetic Resonance Spectroscopy: Introduction and Overview. Neuroimaging Clin. N. Am. *23*, 359–380.

Bhakoo, K.K., and Pearce, D. (2000). In Vitro Expression of N-Acetyl Aspartate by Oligodendrocytes: Implications for Proton Magnetic Resonance Spectroscopy Signal In Vivo. J. Neurochem. *74*, 254–262.

Billstedt, E., Gillberg, I.C., and Gillberg, C. (2011). Aspects of quality of life in adults diagnosed with autism in childhood: a population-based study. Autism *15*, 7–20.

Black, M.M. (2008). Effects of vitamin B12 and folate deficiency on brain development in children. Food Nutr. Bull. *29*, S126–S131.

Blackmon, K., Ben-Avi, E., Wang, X., Pardoe, H.R., Di Martino, A., Halgren, E., Devinsky, O., Thesen, T., and Kuzniecky, R. (2016). Periventricular white matter abnormalities and restricted repetitive behavior in autism spectrum disorder. NeuroImage Clin. *10*, 36–45.

Blasi, A., Mercure, E., Lloyd-Fox, S., Thomson, A., Brammer, M., Sauter, D., Deeley, Q., Barker, G.J., Renvall, V., Deoni, S., et al. (2011). Early specialization for voice and emotion processing in the infant brain. Curr. Biol. *21*, 1220–1224.

Blasi, A., Lloyd-Fox, S., Sethna, V., Brammer, M.J., Mercure, E., Murray, L., Williams, S.C.R., Simmons, A., Murphy, D.G.M., and Johnson, M.H. (2015). Atypical processing of voice sounds in infants at risk for autism spectrum disorder. Cortex *71*, 122–133.

Blüml, S., Seymour, K.J., and Ross, B.D. (1999). Developmental Changes in Choline- and Ethanolamine-Containing Compounds Measured With Proton-Decoupled 31P MRS in In Vivo Human Brain. Magn. Reson. Med. *42*, 643–654.

Blüml, S., Wisnowski, J.L., Nelson, M.D., Paquette, L., Gilles, F.H., Kinney, H.C., and Panigrahy, A. (2013). Metabolic Maturation of the Human Brain From Birth Through Adolescence: Insights Fom In Vivo Magnetic Resonance Spectroscopy. Cereb. Cortex 2944–2955.

Bly, L. (1994). Motor Skills Acquisition in the First Year: An Illustrated Guide to Normal Development. (Tucson: Therapy Skill Builders).

Bolton, P.F., Murphy, M., MacDonald, H., Whitlock, B., Pickles, A., and Rutter, M. (1997). Obstetric Complications in Autism: Consequences or Causes of the Condition? J. Am. Acad. Child Adolesc. Psychiatry *36*, 272–281.

Bolton, P.F., Pickles, a, Murphy, M., and Rutter, M. (1998). Autism, affective and other psychiatric disorders: patterns of familial aggregation. Psychol. Med. *28*, 385–395.

Borrelli, E., Nestler, E.J., Allis, C.D., and Sassone-Corsi, P. (2008). Decoding the Epigenetic Language of Neuronal Plasticity. Neuron *60*, 961–974.

Boukhris, T., Sheehy, O., Mottron, L., and Bérard, A. (2015). Antidepressant Use During Pregnancy and the Risk of Autism Spectrum Disorder in Children. JAMA Pediatr. 1.

Brand, A., Richter-Landsberg, C., and Leibfritz, D. (1993). Multinuclear NMR studies on the energy metabolism of glial and neuronal cells. Dev Neurosci *15*, 289–298.

Brighina, E., Bresolin, N., Pardi, G., and Rango, M. (2009). Human Fetal Brain Chemistry as Detected by Proton Magnetic Resonance Spectroscopy. Pediatr. Neurol. *40*, 327–342.

Brito, N.H., and Noble, K.G. (2014). Socioeconomic status and structural brain development. Front. Neurosci. *8*, 1–12.

Brix, M.K., Ersland, L., Hugdahl, K., Grüner, R., Posserud, M.-B., Hammar, Å., Craven, A.R., Noeske, R., Evans, C.J., Walker, H.B., et al. (2015). "Brain MR spectroscopy in autism spectrum disorder—the GABA excitatory/inhibitory imbalance theory revisited." Front. Hum. Neurosci. *9*, 1–12.

Brody, B.A., Kinney, H.C., Kloman, A.S., and Gilles, F.H. (1987). Sequence of Central Nervous System Myelination in Human Infancy. I. An Autopsy Study of Myelination. J. Neuropathol. Exp. Neurol. *46*, 283–301.

Brown, M.S., Singel, D., Hepburn, S., and Rojas, D.C. (2013). Increased glutamate concentration in the auditory cortex of persons with autism and first-degree relatives: A 1H-MRS study. Autism Res. *6*, 1–10.

Brune, C.W., Kim, S.J., Hanna, G.L., Courchesne, E., Lord, C., Leventhal, B.L., and Cook, E.H. (2008). Family-based association testing of OCD-associated SNPs of SLC1A1 in an autism sample. Autism Res. *1*, 108–113.

Bryson, S.E., Zwaigenbaum, L., Brian, J., Roberts, W., Szatmari, P., Rombough, V., and McDermott, C. (2007). A prospective case series of high-risk infants who developed autism. J. Autism Dev. Disord. *37*, 12–24.

Bushnell, I.W.R. (2001). Mother's Face Recognition in Newborn Infants: Learning and Memory. Infant Child Dev. *10*, 67–74.

Buss, R.R., and Oppenheim, R.W. (2004). Role of programmed cell death in normal neuronal development and function. Anat. Sci. Int. *79*, 191–197.

Buwe, A., Guttenbach, M., and Schmid, M. (2005). Effect of paternal age on the frequency of cytogenetic abnormalities in human spermatozoa. Cytogenet Genome Res *111*, 213–228.

Buxhoeveden, D.P., Semendeferi, K., Buckwalter, J., Schenker, N., Switzer, R., and Courchesne, E. (2006). Reduced minicolumns in the frontal cortex of patients with autism. Neuropathol. Appl. Neurobiol. *32*, 483–491.

Bystron, I., Blakemore, C., and Rakic, P. (2008). Development of the human cerebral cortex: Boulder Committee revisited. Nat. Rev. Neurosci. *9*, 110–122.

Cabrera, N.J., Fagan, J., and Schadler, C. (2011). The influene of mother, father, and child risk on parenting and children's cognitive and social behaviors. Child Dev. *82*, 1985–2005.

Cady, E.B., Penrice, J., Amess, P.N., Lorek, A., Wylezinska, M., Aldridge, R.F., Franconi, F., Wyatt, J.S., and Reynolds, E.O. (1996). Lactate, N-acetylaspartate, Choline and Creatine

Concentrations, and Spin-Spin Relaxation in Thalamic and Occipito-Parietal Regions of Developing Human Brain. Magn. Reson. Med. *36*, 878–886.

Calderoni, S., Bellani, M., Hardan, A., Muratori, F., and Brambilla, P. (2014). Basal ganglia and restricted and repetitive behaviours in Autism Spectrum Disorders: current status and future perspectives. Epidemiol. Psychiatr. Sci. *23*, 235–238.

Cannell, J.J. (2008). Autism and vitamin D. Med. Hypotheses *70*, 750–759.

Cardoso, C., Boys, A., Parrini, E., Mignon-Ravix, C., McMahon, J.M., Khantane, S., Bertini, E., Pallesi, E., Missirian, C., Zuffardi, O., et al. (2009). Periventricular heterotopia, mental retardation, and epilepsy associated with 5q14.3-q15 deletion. Neurology *72*, 784–792.

Carpenter, M., Nagell, K., and Tomasello, M. (1998). Social cognition, joint attention, and communicative competence from 9 to 15 months of age. Monogr Soc Res Child Dev *63*, i–vi, 1-143.

Carper, R.A., and Courchesne, E. (2005). Localized Enlargement of the Frontal Cortex in Early Autism. Biol. Psychiatry *57*, 126–133.

Carper, R.A., Moses, P., Tigue, Z.D., and Courchesne, E. (2002). Cerebral Lobes in Autism: Early Hyperplasia and Abnormal Age Effects. Neuroimage *16*, 1038–1051.

Carvill, S., and Marston, G. (2002). People with intellectual disability, sensory impairments and behaviour disorder: A case series. J. Intellect. Disabil. Res. *46*, 264–272.

Casanova, E.L., and Casanova, M.F. (2014). Genetics studies indicate that neural induction and early neuronal maturation are disturbed in autism. Front. Cell. Neurosci. *8*, 1–13.

Casanova, M.F., Buxhoeveden, D.P., Switala, A.E., and Roy, E. (2002). Minicolumnar pathology in autism. Neurology *58*, 428–432.

Casanova, M.F., van Kooten, I.A.J., Switala, A.E., van Engeland, H., Heinsen, H., Steinbusch, H.W.M., Hof, P.R., Trippe, J., Stone, J., and Schmitz, C. (2006). Minicolumnar abnormalities in autism. Acta Neuropathol. *112*, 287–303.

Caviness, V.S., and Sidman, R.L. (1973). Time of origin or corresponding cell classes in the cerebral cortex of normal and reeler mutant mice: an autoradiographic analysis. J. Comp. Neurol. *148*, 141–151.

Cayre, M., Canoll, P., and Goldman, J.E. (2009). Cell migration in the normal and pathological postnatal mammalian brain. Prog. Neurobiol. *88*, 41–63.

Cellot, G., and Cherubini, E. (2014). GABAergic signaling as therapeutic target for autism spectrum disorders. Front. Pediatr. *2*, 1–11.

Cerliani, L., Mennes, M., Thomas, R.M., Di Martino, A., Thioux, M., and Keysers, C. (2015). Increased Functional Connectivity Between Subcortical and Cortical Resting-State Networks in Autism Spectrum Disorder. JAMA Psychiatry *72*, 1–11.

Chambers, C.D., Johnson, K.A., Dick, L.M., Felix, R.J., and Jones, K.L. (1998). Maternal fever and birth outcome: A prospective study. Teratology *58*, 251–257.

Chan, W.Y., Kohsaka, S., and Rezaie, P. (2007). The origin and cell lineage of microglia - New concepts. Brain Res. Rev. *53*, 344–354.

Charman, T. (2002). The prevalence of autism spectrum disorders. Recent evidence and future challenges. Eur. Child Adolesc. Psychiatry *11*, 249–256.

Charman, T. (2003). Why is joint attention a pivotal skill in autism? Philos. Trans. R. Soc. Lond. B. Biol. Sci. *358*, 315–324.

Chawarska, K., Klin, A., and Volkmar, F. (2003). Automatic attention cueing through eye movement in 2-year-old children with autism. Child Dev. *74*, 1108–1122.

Chawarska, K., Macari, S., and Shic, F. (2013). Decreased spontaneous attention to social scenes in 6-month-old infants later diagnosed with autism spectrum disorders. Biol. Psychiatry *74*, 195–203.

Cheon, K.A., Kim, Y.S., Oh, S.H., Park, S.Y., Yoon, H.W., Herrington, J., Nair, A., Koh, Y.J., Jang, D.P., Kim, Y.B., et al. (2011). Involvement of the anterior thalamic radiation in boys with high functioning autism spectrum disorders: A Diffusion Tensor Imaging study. Brain Res. *1417*, 77–86.

Chess, S. (1977). Follow-Up Report on Autism in Congenital Rubella. J. Autism Child. Schizophr. *7*, 69–81.

Chez, M.G., Burton, Q., Dowling, T., Chang, M., Khanna, P., and Kramer, C. (2007). Memantine as Adjunctive Therapy in Children Diagnosed With Autistic Spectrum Disorders: An Observation of Initial Clinical Response and Maintenance Tolerability. J. Child Neurol. *22*, 574–579.

Chi, J.G., Dooling, E.C., and Gilles, F.H. (1977). Gyral development of the human brain. Ann. Neurol. *1*, 86–93.

Chow, M.L., Pramparo, T., Winn, M.E., Barnes, C.C., Li, H.R., Weiss, L., Fan, J.B., Murray, S., April, C., Belinson, H., et al. (2012). Age-Dependent Brain Gene Expression and Copy Number Anomalies in Autism Suggest Distinct Pathological Processes at Young Versus Mature Ages. PLoS Genet. *8*.

Christensen, J., Grønborg, T.K., Sørensen, M.J., Schendel, D., Parner, E.T., Pedersen, L.H., and Vestergaard, M. (2013). Prenatal Valproate Exposure and Risk of Autism Spectrum Disorders and Childhood Autism. JAMA *309*, 1696–1703.

Christensen, L., Hutman, T., Rozga, A., Young, G.S., Ozonoff, S., Rogers, S.J., Baker, B., and Sigman, M. (2010). Play and developmental outcomes in infant siblings of children with autism. J. Autism Dev. Disord. *40*, 946–957.

Chugani, D.C., Sundram, B.S., Behen, M., Lee, M.L., and Moore, G.J. (1999). Evidence of altered energy metabolism in autistic children. Prog. Neuropsychopharmacol. Biol. Psychiatry *23*, 635–641.

Clark, J.B. (1998). N-Acetyl Aspartate: A Marker for Neuronal Loss or Mitochondrial Dysfunction. Dev. Neurosci. *20*, 271–276.

Clouchoux, C., Guizard, N., Evans, A.C., Du Plessis, A.J., and Limperopoulos, C. (2012). Normative fetal brain growth by quantitative in vivo magnetic resonance imaging. Am. J. Obstet. Gynecol. *206*, 173.e1-173.e8.

Cochran, D.M., Sikoglu, E.M., Hodge, S.M., Edden, R. a. E., Foley, A., Kennedy, D.N., Moore, C.M., and Frazier, J. a. (2015). Relationship among glutamine, γ-Aminobutyric Acid, and Social Cognition In Autism Spectrum Disorders. J. Child Adolesc. Psychopharmacol. *25*, 314–322.

Cohen, J. (1988). Statistical power analysis for the behavioral sciences. Stat. Power Anal. Behav. Sci. *2nd*, 567.

Cohn, J.F., Matias, R., Tronick, E.Z., Connell, D., and Lyons-Ruth, K. (1986). Face-to-face interactions of depressed mothers and their infants. New Dir. Child Adolesc. Dev. *1986*, 31–45.

Colvert, E., Tick, B., McEwen, F., Stewart, C., Curran, S.R., Woodhouse, E., Gillan, N., Hallett, V., Lietz, S., Garnett, T., et al. (2015). Heritability of Autism Spectrum Disorder in a UK Population-Based Twin Sample. JAMA Psychiatry *72*, 415–423.

Consortium, C.-D.G. of the P.G. (2013). Identification of risk loci with shared effects on five major psychiatric disorders: a genome-wide analysis. Lancet *381*, 1371–1379.

Constantino, J.N., and Todd, R.D. (2003). Autistic Traits in the General Population. JAMA *60*.

Constantino, J.N., Zhang, Y., Frazier, T., Abbacchi, A.M., and Law, P. (2010). Sibling recurrence and the genetic epidemiology of autism. Am. J. Psychiatry *167*, 1349–1356.

Cooper, P.J., Tomlinson, M., Swartz, L., Woolgar, M., Murray, L., and Molteno, C. (1999). Post-partum depression and the mother-infant relationship in a South African peri-urban settlement. Br. J. Psychiatry *175*, 554–558.

Copp, A.J., and Greene, N.D.E. (2013). Neural tube defects – disorders of neurulation and related embryonic processes. Wiley Interdiscip Rev Dev Biol *2*, 213–227.

Copp, A.J., Greene, N.D.E., and Murdoch, J.N. (2003). The genetic basis of mammalian neurulation. Nat. Rev. Genet. *4*, 784–793.

Corbin, J.G., Nery, S., and Fishell, G. (2001). Telencephalic cells take a tangent: non-radial migration in the mammalian forebrain. Nat. Neurosci. *4 Suppl*, 1177–1182.

Cordero-Grande, L., Hughes, E., Price, A., Hutter, J., Edwards, D.A., and Hajnal, J. V. (2016). 3D Motion Corrected SENSE Reconstruction for Multishot Multislice MRI. In Proceedings of the 24th Annual Meeting of the International Society for Magnetic Resonance in Medicine, (Singapore), p.

Corkum, V., and Moore, C. (1998). The Origins of Joint Visual Attention in Infants. Dev. Psychol. *34*, 28–38.

Corrigan, N.M., Shaw, D.W.W., Estes, A.M., Richards, T.L., Munson, J., Friedman, S.D., Dawson, G., Artru, A. a, and Dager, S.R. (2013). Atypical developmental patterns of brain chemistry in children with autism spectrum disorder. JAMA Psychiatry *70*, 964–974.

Counsell, S.J., and Rutherford, M. a (2002). Magnetic resonance imaging of the newborn brain. Curr. Paediatr. *12*, 401.

Counsell, S.J., Maalouf, E.F., Fletcher, A.M., Duggan, P., Battin, M., Lewis, H.J., Herlihy, A.H., Edwards, A.D., Bydder, G.M., and Rutherford, M.A. (2002). MR imaging assessment of myelination in the very preterm brain. Am. J. Neuroradiol. *23*, 872–881.

Courchesne, E. (1997). Brainstem, cerebellar and limbic neuroanatomical abnormalities in autism. Curr. Opin. Neurobiol. *7*, 269–278.

Courchesne, E. (2002). Abnormal early brain development in autism. Mol. Psychiatry *7*, S21–S23.

Courchesne, E., Yeung-Courchesne, R., Press, G.A., Hesselink, J.R., and Jernigan, T.L. (1988). Hypoplasia of Cerebellar Vermal Lobules VI and VII in Autism. N. Engl. J. Med. *318*, 1349–1354.

Courchesne, E., Saitoh, O., Yeung-Courchesne, R., Press, G.A., Lincoln, A.J., Haas, R.H., and Schreibman, L. (1994). Abnormality of Cerebellar Verrmian Lobules VI and VII in Patients with Infantile Autism: Identification of Hypoplastic and Hyperplastic Subgroups with MR Imaging. AJR *162*, 123–130.

Courchesne, E., Karns, C.M., Davis, H.R., Ziccardi, R., Carper, R.A., Tigue, Z.D., Chisum, H.J., Moses, P., Pierce, K., Lord, C., et al. (2001). Unusual brain growth patterns in early life in patients with autistic disorder: An MRI study. Neurology *57*, 245–254.

Courchesne, E., Carper, R., and Akshoomoff, N. (2003). Evidence of Brain Overgrowth in the First Year of Life in Autism. JAMA *290*, 337–344.

Courchesne, E., Pierce, K., Schumann, C.M., Redcay, E., Buckwalter, J.A., Kennedy, D.P., and Morgan, J. (2007). Mapping Early Brain Development in Autism. Neuron *56*, 399–413.

Courchesne, E., Campbell, K., and Solso, S. (2011). Brain growth across the life span in autism: Age-specific changes in anatomical pathology. Brain Res. *1380*, 138–145.

Coyl, D.D., Roggman, L. a., and Newland, L. a. (2002). Stress, maternal depression, and negative mother-infant interactions in relation to infant attachment. Infant Ment. Health J. *23*, 145–163.

Coyle, J.T., Leski, M.L., and Morrison, J.H. (2002). The diverse roles of L-glutamic acid in brain signal transduction. In Neuropsychopharmacology, The Fifth Generation of Progress, E. Davis KL, Charney D, Coyle JT, Nemeroff C, ed. (Philadelphia: Lippincott, Williams, and Wilkins), pp. 71–90.

Crandell, L.E., Patrick, M.P.H., and Hobson, R.P. (2003). “Still-face” interactions between mothers with borderline personality disorder and their 2-month-old infants. Br. J. Psychiatry *183*, 239–247.

Croen, L.A., Najjar, D. V., Fireman, B., and Grether, J.K. (2007). Maternal and Paternal Age and Risk of Autism Spectrum Disorders. Arch. Pediatr. Adolesc. Med. *161*, 334–340.

Croen, L. a., Grether, J.K., Yoshida, C.K., Odouli, R., and Hendrick, V. (2011). Antidepressant Use During Pregnancy and Childhood Autism Spectrum Disorders. Arch. Gen. Psychiatry *68*, 1104–1112.

Crow, J.F. (2000). The origins, patterns and implications of human spontaneous mutation. Nat. Rev. Genet. *1*, 40–47.

D'Ercole, C., Girard, N., Boubli, L., Potier, A., Chagnon, C., Raybaud, C., Blanc, B., C., D., N., G., L., B., et al. (1993). Prenatal diagnosis of fetal cerebral abnormalities by ultrasonography and magnetic resonance imaging. Eur. J. Obstet. Gynecol. Reprod. Biol. *50*, 177–184.

D'Mello, A.M., Crocetti, D., Mostofsky, S.H., and Stoodley, C.J. (2015). Cerebellar gray matter and lobular volumes correlate with core autism symptoms. NeuroImage Clin. *7*, 631–639.

Damodaram, M.S., Story, L., Eixarch, E., Patkee, P., Patel, A., Kumar, S., and Rutherford, M. (2012). Foetal volumetry using Magnetic Resonance Imaging in intrauterine growth restriction. Early Hum. Dev. *88*, S35–S40.

Davis, E.P., Buss, C., Muftuler, L.T., Head, K., Hasso, A., Wing, D.A., Hobel, C., and Sandman, C.A. (2011). Children's brain development benefits from longer gestation. Front. Psychol. *2*, 1–7.

Dawson, G., Munson, J., Webb, S.J., Nalty, T., Abbott, R., and Toth, K. (2007). Rate of Head Growth Decelerates and Symptoms Worsen in the Second Year of Life in Autism. Biol. Psychiatry *61*, 458–464.

Dawson, G., Rogers, S., Munson, J., Smith, M., Winter, J., Greenson, J., Donaldson, A., and Varley, J. (2010). Randomized, controlled trial of an intervention for toddlers with autism: the Early Start Denver Model. Pediatrics *125*, e17–e23.

Debanne, D., Daoudal, G., Sourdet, V., and Russier, M. (2003). Brain plasticity and ion channels. J Physiol Paris *97*, 403–414.

Degnan, A.J., Ceschin, R., Lee, V., Schmithorst, V.J., Bluml, S., and Panigrahy, A. (2014). Early Metabolic Development of Posteromedial Cortex and Thalamus in Humans Analyzed Via In Vivo Quantitative Magnetic Resonance Spectroscopy. J. Comp. Neurol. *522*, 3717–3732.

Delgado, J., Toro, R., Rascovsky, S., Arango, A., Angel, G.J., Calvo, V., and Delgado, J.A. (2014). Chloral hydrate in pediatric magnetic resonance imaging: evaluation of a 10-year sedation experience administered by radiologists. Pediatr. Radiol. *45*, 108–114.

Dementieva, Y.A., Vance, D.D., Donnelly, S.L., Elston, L.A., Wolpert, C.M., Ravan, S.A., Delong, G.R., Abramson, R.K., Wright, H.H., and Cuccaro, M.L. (2005). Accelerated Head Growth in Early Development of Individuals with Autism. Pediatr. Neurol. *32*, 102–108.

Demougeot, C., Garnier, P., Mossiat, C., Bertrand, N., Giroud, M., Beley, A., and Marie, C. (2001). N-Acetylaspartate, a marker of both cellular dysfunction and neuronal loss: Its relevance to studies of acute brain injury. J. Neurochem. *77*, 408–415.

Dempster, A.P., Laird, N.M., and Rubin, D.B. (1977). Maximum Likelihood from Incomplete Data via the EM Algorithm. J. R. Stat. Soc. Ser. B *39*, 1–38.

Deoni, S.C.L., Mercure, E., Blasi, A., Gasston, D., Thomson, A., Johnson, M., Williams, S.C.R., and Murphy, D.G.M. (2011). Mapping infant brain myelination with magnetic resonance imaging. J. Neurosci. *31*, 784–791.

Desai, A.R., and McConnell, S.K. (2000). Progressive restriction in fate potential by neural progenitors during cerebral cortical development. Development *127*, 2863–2872.

DeVito, T.J., Drost, D.J., Neufeld, R.W.J., Rajakumar, N., Pavlosky, W., Williamson, P., and Nicolson, R. (2007). Evidence for cortical dysfunction in autism: a proton magnetic resonance spectroscopic imaging study. Biol. Psychiatry *61*, 465–473.

Dey, S.K. (2010). How we are born. J. Clin. Invest. *120*, 952–955.

Dezortova, M., and Hajek, M. (2008). 1H MR spectroscopy in pediatrics. Eur J Radiol *67*, 240–249.

Doria, V., Beckmann, C.F., Arichi, T., Merchant, N., Groppo, M., Turkheimer, F.E., Counsell, S.J., Murgasova, M., Aljabar, P., Nunes, R.G., et al. (2010). Emergence of resting state networks in the preterm human brain. Proc. Natl. Acad. Sci. U. S. A. *107*, 20015–20020.

Doussard-Roosevelt, J.A., Joe, C.M., Bazhenova, O. V, and Porges, S.W. (2003). Mother-child interaction in autistic and nonautistic children: characteristics of maternal approach behaviors and child social responses. Dev. Psychopathol. *15*, 277–295.

Doyle-Thomas, K. a R., Card, D., Soorya, L. V., Ting Wang, a., Fan, J., and Anagnostou, E. (2014). Metabolic mapping of deep brain structures and associations with symptomatology in autism spectrum disorders. Res. Autism Spectr. Disord. *8*, 44–51.

Drenthen, G.S., Barendse, E.M., Aldenkamp, A.P., van Veenendaal, T.M., Puts, N.A.J., Edden, R.A.E., Zinger, S., Thoonen, G., Hendriks, M.P.H., Kessels, R.P.C., et al. (2016). Altered neurotransmitter metabolism in adolescents with high-functioning autism. Psychiatry Res. Neuroimaging *256*, 44–49.

Durand, C.M., Betancur, C., Boeckers, T.M., Bockmann, J., Chaste, P., Fauchereau, F., Nygren, G., Rastam, M., Gillberg, I.C., Anckarsäter, H., et al. (2007). Mutations in the gene encoding the synaptic scaffolding protein SHANK3 are associated with autism spectrum disorders. Nat. Genet. *39*, 25–27.

Ecker, C., Rocha-Rego, V., Johnston, P., Mourao-Miranda, J., Marquand, A., Daly, E.M., Brammer, M.J., Murphy, C., and Murphy, D.G. (2010). Investigating the predictive value of whole-brain structural MR scans in autism: A pattern classification approach. Neuroimage *49*, 44–56.

Ecker, C., Spooren, W., and Murphy, D. (2013a). Developing new pharmacotherapies for autism. J. Intern. Med. *274*, 308–320.

Ecker, C., Ginestet, C., Feng, Y., Johnston, P., Lombardo, M. V, Lai, M.-C., Suckling, J., Palaniyappan, L., Daly, E., Murphy, C.M., et al. (2013b). Brain Surface Anatomy in Adults With Autism The Relationship Between Surface Area, Cortical Thickness, and Autistic SymptomsBrain Surface Anatomy in Adults With Autism. JAMA Psychiatry *70*, 59–70.

Edwards, M.J., Saunders, R.D., and Shiota, K. (2003). Effects of heat on embryos and foetuses. Int. J. Hyperthermia *19*, 295–324.

Elsabbagh, M., Gliga, T., Pickles, A., Hudry, K., Charman, T., and Johnson, M.H. (2013a). The development of face orienting mechanisms in infants at-risk for autism. Behav. Brain Res. *251*, 147–154.

Elsabbagh, M., Fernandes, J., Jane Webb, S., Dawson, G., Charman, T., and Johnson, M.H. (2013b). Disengagement of visual attention in infancy is associated with emerging autism in toddlerhood. Biol. Psychiatry *74*, 189–194.

Emde, R.N., and Harmon, R.J. (1972). Endogenous and Exogenous Smiling Systems in Early Infancy. J. Am. Acad. Child Psychiatry *11*, 177–200.

Erickson, C.A., Wink, L.K., Early, M.C., Stiegelmeyer, E., Mathieu-Frasier, L., Patrick, V., and McDougle, C.J. (2014). Brief report: Pilot single-blind placebo lead-in study of acamprosate in youth with autistic disorder. J. Autism Dev. Disord. *44*, 981–987.

Eriksson, P.S., Perfilieva, E., Bjork-Eriksson, T., Alborn, A.M., Nordborg, C., Peterson, D.A., and Gage, F.H. (1998). Neurogenesis in the adult human hippocampus. Nat. Med. *4*, 1313–1317.

Esposito, G., Venuti, P., Apicella, F., and Muratori, F. (2011). Analysis of unsupported gait in toddlers with autism. Brain Dev. *33*, 367–373.

Estes, A., Shaw, D.W.W., Sparks, B.F., Friedman, S., Giedd, J.N., Dawson, G., Bryan, M., and Dager, S.R. (2011). Basal Ganglia Morphometry and Repetitive Behavior in Young Children with Autism Spectrum Disorder. Autism Res. *4*, 212–220.

Estrada, M., Varshney, A., and Ehrlich, B.E. (2006). Elevated Testosterone Induces Apoptosis in Neuronal Cells. J. Biol. Chem. *281*, 25492–25501.

Evangelou, I.E., du Plessis, A.J., Vezina, G., Noeske, R., and Limperopoulos, C. (2016). Elucidating Metabolic Maturation in the Healthy Fetal Brain Using 1H-MR Spectroscopy. Pediatrics 1–7.

Farroni, T., Csibra, G., Simion, F., and Johnson, M.H. (2002). Eye contact detection in humans from birth. Proc. Natl. Acad. Sci. U. S. A. *99*, 9602–9605.

Farroni, T., Massaccesi, S., Pividori, D., and Johnson, M.H. (2004). Gaze following in newborns. Infancy *5*, 39–60.

Fatemi, S.H. (2008). The hyperglutamatergic hypothesis of autism. Prog. Neuro-Psychopharmacology Biol. Psychiatry *32*, 911.

Fatemi, S.H., Halt, A.R., Stary, J.M., Kanodia, R., Schulz, S.C., and Realmuto, G.R. (2002). Glutamic Acid Decarboxylase 65 and 67 kDa Proteins are Reduced in Autistic Parietal and Cerebellar Cortices. Biol. Psychiatry *52*, 805–810.

Fatemi, S.H., Snow, A. V., Stary, J.M., Araghi-Niknam, M., Reutiman, T.J., Lee, S., Brooks, A.I., and Pearce, D.A. (2005). Reelin Signaling is Impaired in Autism. Biol. Psychiatry *57*, 777–787.

Fatemi, S.H., Aldinger, K. a., Ashwood, P., Bauman, M.L., Blaha, C.D., Blatt, G.J., Chauhan, A., Chauhan, V., Dager, S.R., Dickson, P.E., et al. (2012). Consensus Paper: Pathological Role of the Cerebellum in Autism. Cerebellum *11*, 777–807.

Fayed, N., and Modrego, P.J. (2005). Comparative Study of Cerebral White Matter in Autism and Attention-Deficit/Hyperactivity Disorder by Means of Magnetic Resonance Spectroscopy. Acad. Radiol. *12*, 566–569.

Fayed, N., Olmos, S., Morales, H., and Modrego, P.J. (2006). Physical Basis of Magnetic Resonance Spectroscopy and its Application to Central Nervous System Diseases. Am. J. Appl. Sci. *3*, 1836–1845.

Feinberg, J.I., Bakulski, K.M., Jaffe, A.E., Tryggvadottir, R., Brown, S.C., Goldman, L.R., Croen, L.A., Hertz-Picciotto, I., Newschaffer, C.J., Daniele Fallin, M., et al. (2015). Paternal sperm DNA methylation associated with early signs of autism risk in an autism-enriched cohort. Int. J. Epidemiol. *44*, 1199–1210.

Feldman, M.A., Ward, R.A., Savona, D., Regehr, K., Parker, K., Hudson, M., Penning, H., and Holden, J.J.A. (2012). Development and initial validation of a parent report measure of the behavioral development of infants at risk for autism spectrum disorders. J. Autism Dev. Disord. *42*, 13–22.

Fenson, L., Dale, P., Reznick, J., Thal, D., Bates, E., Hartung, J., Pethick, S., and Reilly, J. (1993). The MacArthur Communicative Development Inventories: User's guide and technical manual. Baltimore.

Fenson, L., Dale, P.S., Reznick, J.S., Bates, E., Thal, D.J., Pethick, S.J., Tomasello, M., Mervis, C.B., and Stiles, J. (1994). Variability in Early Communicative Development. Monogr. Soc. Res. Child Dev. *59*, 1–185.

Finnemore, A., Toulmin, H., Merchant, N., Arichi, T., Tusor, N., Cox, D., Ederies, A., Nongena, P., Ko, C., Dias, R., et al. (2014). Chloral hydrate sedation for magnetic resonance imaging in newborn infants. Paediatr. Anaesth. *24*, 190–195.

Fisher, S.K., Novak, J.E., and Agranoff, B.W. (2002). Inositol and higher inositol phosphates in neural tissues: Homeostasis, metabolism and functional significance. J. Neurochem. *82*, 736–754.

Flanagan, J.E., Landa, R., Bhat, A., and Bauman, M. (2012). Head lag in infants at risk for autism: A preliminary study. Am. J. Occup. Ther. *66*, 577–585.

Flanagan, J.M., Popendikyte, V., Pozdniakovaite, N., Sobolev, M., Assadzadeh, A., Schumacher, A., Zangeneh, M., Lau, L., Virtanen, C., Wang, S.-C., et al. (2006). Intra- and interindividual epigenetic variation in human germ cells. Am. J. Hum. Genet. *79*, 67.

Fleming, A.S., O'Day, D.H., and Kraemer, G.W. (1999). Neurobiology of mother-infant interactions: Experience and central nervous system plasticity across development and generations. Neurosci. Biobehav. Rev. *23*, 673–685.

Focaroli, V., Taffoni, F., Parsons, S.M., Keller, F., and Iverson, J.M. (2016). Performance of Motor Sequences in Children at Heightened vs. Low Risk for ASD: A Longitudinal Study from 18 to 36 Months of Age. Front. Psychol. *7*, 1–9.

Fombonne, E. (2005). The Changing Epidemiology of Autism. In Journal of Applied Research in Intellectual Disabilities, pp. 281–294.

Ford, T.C., and Crewther, D.P. (2016). A Comprehensive Review of the 1H-MRS Metabolite Spectrum in Autism Spectrum Disorder. Front. Mol. Neurosci. *9*, 1–14.

Franklin, T.B., and Mansuy, I.M. (2010). Epigenetic inheritance in mammals: Evidence for the impact of adverse environmental effects. Neurobiol. Dis. *39*, 61–65.

Frantz, G.D., and McConnell, S.K. (1996). Restriction of Late Cerebral Cortical Progenitors to an Upper-Layer Fate. Neuron *17*, 55–61.

Friedman, S.D., Shaw, D.W., Artru, a a, Richards, T.L., Gardner, J., Dawson, G., Posse, S.,

and Dager, S.R. (2003). Regional brain chemical alterations in young children with autism spectrum disorder. Neurology *60*, 100–107.

Friedman, S.D., Shaw, D.W.W., Artru, A.A., Dawson, G., Petropoulos, H., and Dager, S.R. (2006). Gray and White Matter Brain Chemistry in Young Children With Autism. Arch Gen Psychiatry *63*, 786–794.

Fujii, E., Mori, K., Miyazaki, M., Hashimoto, T., Harada, M., and Kagami, S. (2010). Function of the frontal lobe in autistic individuals: a proton magnetic resonance spectroscopic study. J Med Invest *57*, 35–44.

Gabis, L., Wei Huang, Azizian, A., DeVincent, C., Tudorica, A., Kesner-Baruch, Y., Roche, P., and Pomeroy, J. (2008). 1H-Magnetic Resonance Spectroscopy Markers of Cognitive and Language Ability in Clinical Subtypes of Autism Spectrum Disorders. J. Child Neurol. *23*, 766–774.

Gabriels, R.L., Cuccaro, M.L., Hill, D.E., Ivers, B.J., and Goldson, E. (2005). Repetitive behaviors in autism: Relationships with associated clinical features. Res. Dev. Disabil. *26*, 169–181.

Gaetz, W., Bloy, L., Wang, D.J., Port, R.G., Blaskey, L., Levy, S.E., and Roberts, T.P.L. (2014). GABA estimation in the Brains of Children on the Autism Spectrum: Measurement precision and regional cortical variation. Neuroimage *86*, 1–9.

Gallagher, D., Voronova, A., Zander, M.A., Cancino, G.I., Bramall, A., Krause, M.P., Abad, C., Tekin, M., Neilsen, P.M., Callen, D.F., et al. (2015). Ankrd11 is a Chromatin Regulator Involved in Autism that is Essential for Neural Development. Dev. Cell *32*, 31–42.

Gallo, V., and Ghiani, C.A. (2000). Glutamate receptors in glia: New cells, new inputs and new functions. Trends Pharmacol. Sci. *21*, 252–258.

Gamliel, M., Ebstein, R., Yirmiya, N., and Mankuta, D. (2012). Minor Fetal Sonographic Findings in Autism Spectrum Disorder. Obstet. Gynecol. Surv. *67*, 176–186.

Gardener, H., Spiegelman, D., and Buka, S.L. (2009). Prenatal risk factors for autism: comprehensive meta-analysis. Br. J. Psychiatry *195*, 7–14.

Gardener, H., Spiegelman, D., and Buka, S.L. (2011). Perinatal and Neonatal Risk Factors for Autism: A Comprehensive Meta-Analysis. Pediatrics *128*, 344–355.

Garel, C., Chantrel, E., Brisse, H., Elmaleh, M., Luton, D., Oury, J.F., Sebag, G., and Hassan, M. (2001). Fetal cerebral cortex: Normal gestational landmarks identified using prenatal MR imaging. Am. J. Neuroradiol. *22*, 184–189.

Gatto, C.L., and Broadie, K. (2010). Genetic controls balancing excitatory and inhibitory synaptogenesis in neurodevelopmental disorder models. Front. Synaptic Neurosci. *2*, 4.

Geangu, E., Benga, O., Stahl, D., and Striano, T. (2010). Contagious crying beyond the first days of life. Infant Behav. Dev. *33*, 279–288.

Georgiades, S., Szatmari, P., Zwaigenbaum, L., Bryson, S., Brian, J., Roberts, W., Smith, I., Vaillancourt, T., Roncadin, C., and Garon, N. (2013). A Prospective Study of Autistic-Like Traits in Unaffected Siblings of Probands With Autism Spectrum Disorder. JAMA Psychiatry *70*, 42–48.

Gerdts, J., and Bernier, R. (2011). The Broader Autism Phenotype and Its Implications on the Etiology and Treatment of Autism Spectrum Disorders. Autism Res. Treat. 1–19.

Geschwind, D.H., and Levitt, P. (2007). Autism spectrum disorders: developmental disconnection syndromes. Curr. Opin. Neurobiol. *17*, 103–111.

Ghaleiha, A., Asadabadi, M., Mohammadi, M.-R., Shahei, M., Tabrizi, M., Hajiaghaee, R., Hassanzadeh, E., and Akhondzadeh, S. (2013). Memantine as adjunctive treatment to risperidone in children with autistic disorder: a randomized, double-blind, placebo-controlled trial. Int. J. Neuropsychopharmacol. *16*, 783–789.

Gholipour, A., Estroff, J.A., Barnewolt, C.E., Connolly, S.A., and Warfield, S.K. (2011). Fetal brain volumetry through MRI volumetric reconstruction and segmentation. Int. J. Comput. Assist. Radiol. Surg. *6*, 329–339.

Ghosh, A., and Shatz, C.J. (1993). A role for subplate neurons in the patterning of connections from thalamus to neocortex. Development *117*, 1031–1047.

Gillberg, C., Ehlers, S., Schaumann, H., Jakobsson, G., Dahlgren, S.O., Lindblom, R., Bågenholm, a, Tjuus, T., and Blidner, E. (1990). Autism under age 3 years: a clinical study of 28 cases referred for autistic symptoms in infancy. J. Child Psychol. Psychiatry. *31*, 921–934.

Gilmore, J.H., Van Tol, J.J., Streicher, H.L., Williamson, K., Cohen, S.B., Greenwood, R.S., Charles, H.C., Kliewer, M.A., Whitt, J.K., Silva, S.G., et al. (2001). Outcome in children with fetal mild ventriculomegaly: A case series. Schizophr. Res. *48*, 219–226.

Gilmore, J.H., Lin, W., Prastawa, M.W., Looney, C.B., Vetsa, Y.S.K., Knickmeyer, R.C., Evans, D.D., Smith, J.K., Hamer, R.M., Lieberman, J.A., et al. (2007). Regional Gray Matter Growth, Sexual Dimorphism, and Cerebral Asymmetry in the Neonatal Brain. J. Neurosci. *27*, 1255–1260.

Girard, N., Gouny, S.C., Viola, A., Le Fur, Y., Viout, P., Chaumoitre, K., D'Ercole, C., Gire, C., Figarella-Branger, D., and Cozzone, P.J. (2006a). Assessment of normal fetal brain maturation in utero by proton magnetic resonance spectroscopy. Magn. Reson. Med. *56*, 768–775.

Girard, N., Fogliarini, C., Viola, A., Confort-Gouny, S., Fur, Y.L., Viout, P., Chapon, F., Levrier, O., and Cozzone, P. (2006b). MRS of normal and impaired fetal brain development. Eur. J. Radiol. *57*, 217–225.

Glasson, E.J., Bower, C., Petterson, B., de Klerk, N., Chaney, G., and Hallmayer, J.F. (2004). Perinatal Factors and the Development of Autism. A Population Study. Arch. Gen. Psychiatry *61*, 618–627.

Gleeson, J.G., and Walsh, C.A. (2000). Neuronal migration disorders: from genetic diseases to developmental mechanisms. Trends Neurosci. *23*, 352–359.

Glenn, O.A. (2006). Fetal central nervous system MR imaging. Neuroimaging Clin. N. Am. *16*, 1–17.

Goffinet, A.M. (1984). Events governing organization of postmigratory neurons: Studies on brain development in normal and reeler mice. Brain Res. Rev. *7*, 261–296.

Goldin, R.L., and Matson, J.L. (2016). Premature birth as a risk factor for autism spectrum disorder. Dev. Neurorehabil. *19*, 203–206.

Goodman, R., Ford, T., Richards, H., Gatward, R., and Meltzer, H. (2000). The Development and Well-Being Assessment: description and initial validation of an integrated assessment of child and adolescent psychopathology. J. Child Psychol. Psychiatry. *41*, 645–655.

Gotham, K., Pickles, A., and Lord, C. (2009). Standardizing ADOS Scores for a Measure of Severity in Autism Spectrum Disorders. J Autism Dev Disord *39*, 693–705.

Gould, J.B., and LeRoy, S. (1988). Socioeconomic Status and Low Birth Weight: A Racial Comparison. Pediatrics *82*, 896–904.

Gousias, I.S., Edwards, A.D., Rutherford, M.A., Counsell, S.J., Hajnal, J. V., Rueckert, D., and Hammers, A. (2012). Magnetic resonance imaging of the newborn brain: Manual segmentation of labelled atlases in term-born and preterm infants. Neuroimage *62*, 1499–1509.

Govindaraju, V., Young, K., and Maudsley, A.A. (2000). Proton NMR chemical shifts and coupling constants for brain metabolites. NMR Biomed. *13*, 129–153.

van der Graaf, M. (2010). In vivo magnetic resonance spectroscopy: basic methodology and clinical applications. Eur. Biophys. J. *39*, 527–540.

Gredebäck, G., Theuring, C., Hauf, P., and Kenward, B. (2008). The microstructure of infants' gaze as they view adult shifts in overt attention. Infancy *13*, 533–543.

Green, J., Charman, T., Pickles, A., Wan, M.W., Elsabbagh, M., Slonims, V., Taylor, C., McNally, J., Booth, R., Gliga, T., et al. (2015). Parent-mediated intervention versus no intervention for infants at high risk of autism: a parallel, single-blind, randomised trial. Lancet Psychiatry *2*, 133–140.

Greenough, W.T., Black, J.E., and Wallace, C.S. (1987). Experience and Brain Development. Child Dev. *58*, 539–559.

Grossman, R., Hoffman, C., Mardor, Y., and Biegon, A. (2006). Quantitative MRI measurements of human fetal brain development in utero. Neuroimage *33*, 463–470.

Guinchat, V., Thorsen, P., Laurent, C., Cans, C., Bodeau, N., and Cohen, D. (2012). Pre-, peri- and neonatal risk factors for autism. Acta Obstet. Gynecol. Scand. *91*, 287–300.

Gunning, M., Conroy, S., Valoriani, V., Figueiredo, B., Kammerer, M.H., Muzik, M., Glatigny-Dallay, E., and Murray, L. (2004). Measurement of mother-infant interactions and the home environment in a European setting: preliminary results from a cross-cultural study. Br. J. Psychiatry *184*, s38–s44.

Gürkan, C.K., and Hagerman, R.J. (2012). Targeted treatments in autism and fragile X syndrome. Res. Autism Spectr. Disord. *6*, 1311–1320.

Guy, A., Seaton, S.E., Boyle, E.M., Draper, E.S., Field, D.J., Manktelow, B.N., Marlow, N., Smith, L.K., and Johnson, S. (2015). Infants Born Late/ Moderately Preterm Are at Increased Risk for a Positive Autism Screen at 2 Years of Age. J. Pediatr. *166*, 269–275.e3.

Hackman, D.A., and Farah, M.J. (2009). Socioeconomic status and the developing brain. Trends Cogn. Sci. *13*, 65–73.

Hadjikhani, N., Joseph, R.M., Snyder, J., and Tager-Flusberg, H. (2006). Anatomical Differences in the Mirror Neuron System and Social Cognition Network in Autism. Cereb. Cortex *16*, 1276–1282.

Hagerman, R.J., Ono, M.Y., and Hagerman, P.J. (2005). Recent advances in fragile X: a model for autism and neurodegeneration. Curr. Opin. Psychiatry *18*, 490–496.

Halligan, S.L., Cooper, P.J., Fearon, P., Wheeler, S.L., Crosby, M., and Murray, L. (2013). The longitudinal development of emotion regulation capacities in children at risk for externalizing disorders. Dev. Psychopathol. *25*, 391–406.

Hallmayer, J., Cleveland, S., Torres, A., Phillips, J., Cohen, B., Torigoe, T., Miller, J., Fedele, A., Collins, J., Smith, K., et al. (2011). Genetic Heritability and Shared Environmental Factors Among Twin Pairs With Autism. Arch. Gen. Psychiatry *68*, 1095–1102.

Han, S., Tai, C., Westenbroek, R.E., Yu, F.H., Cheah, C.S., Potter, G.B., Rubenstein, J.L., Scheuer, T., de la Iglesia, H.O., and Catterall, W.A. (2012). Autistic behavior in Scn1a+/− mice and rescue by enhanced GABAergic transmission. Nature *489*, 385–390.

Han, S., Tai, C., Jones, C.J., Scheuer, T., and Catterall, W.A. (2014). Enhancement of Inhibitory Neurotransmission by $GABA_A$ Receptors Having α$_{2,3}$-Subunits Ameliorates Behavioral Deficits in a Mouse Model of Autism. Neuron *81*, 1282–1289.

Harada, M., Taki, M.M., Nose, A., Kubo, H., Mori, K., Nishitani, H., and Matsuda, T. (2011). Non-invasive evaluation of the GABAergic/glutamatergic system in autistic patients observed by MEGA-editing proton MR spectroscopy using a clinical 3 Tesla instrument. J. Autism Dev. Disord. *41*, 447–454.

Hardan, A.Y., Jou, R.J., Keshavan, M.S., Varma, R., and Minshew, N.J. (2004). Increased frontal cortical folding in autism: a preliminary MRI study. Psychiatry Res. Neuroimaging *131*, 263–268.

Hardan, A.Y., Girgis, R.R., Adams, J., Gilbert, A.R., Keshavan, M.S., and Minshew, N.J. (2006a). Abnormal brain size effect on the thalamus in autism. Psychiatry Res. *147*, 145–151.

Hardan, A.Y., Muddasani, S., Vemulapalli, M., Keshavan, M.S., and Minshew, N.J. (2006b). An MRI Study of Increased Cortical Thickness in Autism. Am. J. Psychiatry *163*, 1290–1292.

Hardan, A.Y., Minshew, N.J., Melhem, N.M., Srihari, S., Jo, B., Bansal, R., Keshavan, M.S., and Stanley, J.A. (2008). An MRI and proton spectroscopy study of the thalamus in children with Autism. Psychiatry Res. *163*, 97–105.

Hardan, A.Y., Libove, R.A., Keshavan, M.S., Melhem, N.M., and Minshew, N.J. (2009). A Preliminary Longitudinal MRI Study of Brain Volume and Cortical Thickness in Autism. Biol. Psychiatry *66*, 320–326.

Hashimoto, T., Tayama, M., Miyazaki, M., Yoneda, Y., Yoshimoto, T., Harada, M., Miyoshi, H., Tanouchi, M., and Kuroda, Y. (1997). Differences in Brain Metabolites Between Patients With Autism and Mental Retardation as Detected by in Vivo Localized Proton Magnetic Resonance Spectroscopy. J. Child Neurol. *12*, 91–96.

Hassan, T.H., Abdelrahman, H.M., Abdel Fattah, N.R., El-Masry, N.M., Hashim, H.M., El-Gerby, K.M., and Abdel Fattah, N.R. (2013). Blood and brain glutamate levels in children with autistic disorder. Res. Autism Spectr. Disord. *7*, 541–548.

Hayat, T.T.A., Nihat, A., Martinez-Biarge, M., McGuinness, A., Allsop, J.M., Hajnal, J. V., and Rutherford, M.A. (2011). Optimization and Initial Experience of a Multisection Balanced Steady-State Free Precession Cine Sequence for the Assessment of Fetal Behavior in Utero. Am. J. Neuroradiol. *32*, 331–338.

Hayes, A. (2012). PROCESS: A versatile computational tool for observed variable moderation, mediation, and conditional process modeling. http://is.muni.cz/el/1423/podzim2014/PSY704/ 50497615/hayes_2012_navod_process.pdf 1–39.

Hazlett, H.C., Poe, M., Gerig, G., Smith, R.G., Provenzale, J., Ross, A., Gilmore, J., and Piven, J. (2005). Magnetic Resonance Imaging and Head Circumference Study of Brain Size in Autism. Birth Through Age 2 Years. Arch. Gen. Psychiatry *62*, 1366–1376.

Hazlett, H.C., Poe, M., Gerig, G., Styner, M., Chappell, C., Smith, R.G., Vachet, C., and Piven, J. (2011). Early Brain Overgrowth in Autism Associated with an Increase in Cortical Surface Area Before Age 2 years. Arch. Gen. Psychiatry *68*, 467–476.

Hazlett, H.C., Gu, H., McKinstry, R.C., Shaw, D.W.W., Botteron, K.N., Dager, S.R., Styner, M., Vachet, C., Gerig, G., Paterson, S.J., et al. (2012). Brain Volume Findings in 6-Month-Old Infants at High Familial Risk for Autism. Am. J. Psychiatry *169*, 601–608.

Haznedar, M.M., Buchsbaum, M.S., Hazlett, E.A., LiCalzi, E.M., Cartwright, C., and Hollander, E. (2006). Volumetric Analysis and Three-Dimensional Glucose Metabolic Mapping of the Striatum and Thalamus in Patients With Autism Spectrum Disorders. Am. J. Psychiatry *163*, 1252–1263.

He, Q., Nomura, T., Xu, J., and Contractor, A. (2014). The Developmental Switch in GABA Polarity Is Delayed in Fragile X Mice. J. Neurosci. *34*, 446–450.

Heckemann, R.A., Hajnal, J. V., Aljabar, P., Rueckert, D., and Hammers, A. (2006). Automatic anatomical brain MRI segmentation combining label propagation and decision fusion. Neuroimage *33*, 115–126.

Heerschap, A., Kok, R.D., and van den Berg, P.P. (2003). Antenatal proton MR spectroscopy of the human brain in vivo. Childs Nerv. Syst. *19*, 418–421.

Henderson, C., Wijetunge, L., Kinoshita, M.N., Shumway, M., Hammond, R.S., Postma, F.R., Brynczka, C., Rush, R., Thomas, A., Paylor, R., et al. (2012). Reversal of disease-related pathologies in the fragile X mouse model by selective activation of GABAB receptors with arbaclofen. Sci. Transl. Med. *4*, 152ra128.

Herbert, M.R., Ziegler, D. a., Deutsch, C.K., O'Brien, L.M., Lange, N., Bakardjiev, a., Hodgson, J., Adrien, K.T., Steele, S., Makris, N., et al. (2003). Dissociations of cerebral cortex, subcortical and cerebral white matter volumes in autistic boys. Brain *126*, 1182–1192.

Heulens, I., D'Hulst, C., Van Dam, D., De Deyn, P.P., and Kooy, R.F. (2012). Pharmacological treatment of fragile X syndrome with GABAergic drugs in a knockout mouse model. Behav Brain Res *229*, 244–249.

Hirvikoski, T., Mittendorfer-Rutz, E., Boman, M., Larsson, H., Lichtenstein, P., and Bölte, S. (2015). Premature mortality in autism spectrum disorder. Br. J. Psychiatry *208*, 1–7.

Hobbs, K., Kennedy, A., DuBray, M., Bigler, E.D., Petersen, P.B., McMahon, W., and Lainhart, J.E. (2007). A Retrospective Fetal Ultrasound Study of Brain Size in Autism. Biol. Psychiatry *62*, 1048–1055.

Hodapp, R.M., Goldfield, E.C., and Boyatzis, C.J. (1984). The use and effectiveness of maternal scaffolding in mother-infant games. Child Dev. *55*, 772–781.

Hoekstra, R. a, Bartels, M., Verweij, C.J.H., and Boomsma, D.I. (2007). Heritability of autistic traits in the general population. Arch. Pediatr. Adolesc. Med. *161*, 372–377.

Holland, D., Chang, L., Ernst, T.M., Curran, M., Buchthal, S.D., Alicata, D., Skranes, J., Johansen, H., Hernandez, A., Yamakawa, R., et al. (2014). Structural Growth Trajectories and Rates of Change in the First 3 Months of Infant Brain Development. JAMA Neurol. *71*, 1266–1274.

Hollander, E., Anagnostou, E., Chaplin, W., Esposito, K., Haznedar, M.M., Licalzi, E., Wasserman, S., Soorya, L., and Buchsbaum, M. (2005). Striatal Volume on Magnetic Resonance Imaging and Repetitive Behaviors in Autism. Biol. Psychiatry *58*, 226–232.

Horder, J., Lavender, T., Mendez, M. a, O'Gorman, R., Daly, E., Craig, M.C., Lythgoe, D.J., Barker, G.J., and Murphy, D.G. (2013). Reduced subcortical glutamate/glutamine in adults with autism spectrum disorders: a [^{1}H]MRS study. Transl. Psychiatry *3*, e279.

Hoshino, Y., Kaneko, M., Yashima, Y., Kumashiro, H., Volkmar, F.R., and Cohen, D.J. (1987). Clinical Features of Autistic Children with Setback Course in Their Infancy. Psychiatry Clin. Neurosci. *41*, 237–245.

Howlin, P., Goode, S., Hutton, J., and Rutter, M. (2004). Adult outcome for children with autism. J. Child Psychol. Psychiatry *45*, 212–229.

Howlin, P., Savage, S., Moss, P., Tempier, A., and Rutter, M. (2014). Cognitive and language skills in adults with autism: A 40-year follow-up. J. Child Psychol. Psychiatry Allied Discip. *55*, 49–58.

Hua, X., Thompson, P., Leow, A., Madsen, S., Caplan, R., Alger, J., O'Neill, J., Joshi, K., Smalley, S., Toga, A., et al. (2013). Brain Growth Rate Abnormalities Visualized in Adolescents with Autism. Hum. Brain Mapp. *34*, 425–436.

Huang, Z. (2009). Molecular regulation of neuronal migration during neocortical development. Mol. Cell. Neurosci. *42*, 11–22.

Hughes, E., Wichmann, T., Padormo, F., Teixeira, R., Wure, J., Sharma, M., Fox, M., Hutter, J., Cordero-Grande, L., Price, A., et al. (2016). A Dedicated Neonatal Brain Imaging System. Magn. Reson. Med. 1–11.

Hultman, C., Sandin, S., Levine, S., Lichtenstein, P., and Reichenberg, A. (2011). Advancing paternal age and risk of autism: new evidence from a population-based study and a meta-analysis of epidemiological studies. Mol. Psychiatry *16*, 1203–1212.

Hultman, C.M.., Sparén, P., and Cnattingius, S. (2002). Perinatal Risk Factors for Infantile Autism. Epidemiology *13*, 417–423.

Huppi, P.S., Fusch, C., Boesch, C., Burri, R., Bossi, E., Amato, M., and Herschkowitz, N. (1995). Regional Metabolic Assessment of Human Brain During Development by Proton Magnetic-Resonance Spectroscopy In-Vivo and by High-Performance Liquid Chromatography/Gas Chromatography in Autopsy Tissue. Pediatr. Res. *37*, 145–150.

Huttenlocher, P.R. (1979). Synaptic density in human frontal cortex - Developmental changes and effects of aging. Brain Res. *163*, 195–205.

Huttenlocher, P.R., and Dabholkar, A.S. (1997). Regional Differences in Synaptogenesis in Human Cerebral Cortex. J. Comp. Neurol. *387*, 167–178.

Huttenlocher, P., de Courten, C., Garey, L., and Van der Loos, H. (1982). Synaptogenesis in human visual cortex-evidence for synapse elimination during normal development. Neurosci. Lett. *33*, 247–252.

Inder, T.E., Warfield, S.K., Wang, H., Hüppi, P.S., and Volpe, J.J. (2005). Abnormal Cerebral Structure Is Present at Term in Premature Infants. Pediatrics *115*, 286–294.

Ingersoll, B., and Hambrick, D.Z. (2011). The relationship between the broader autism phenotype, child severity, and stress and depression in parents of children with autism spectrum disorders. Res. Autism Spectr. Disord. *5*, 337–344.

Innocenti, G.M., and Price, D.J. (2005). Exuberance in the development of cortical networks. Nat. Rev. Neurosci. *6*, 955–965.

Iossifov, I., Ronemus, M., Levy, D., Wang, Z., Hakker, I., Rosenbaum, J., Yamrom, B., Lee, Y. ha, Narzisi, G., Leotta, A., et al. (2012). De Novo Gene Disruptions in Children on the Autistic Spectrum. Neuron *74*, 285–299.

Iossifov, I., O'roak, B.J., Sanders, S.J., Ronemus, M., Krumm, N., Levy, D., Stessman, H.A., Witherspoon, K., Vives, L., Patterson, K.E., et al. (2014). The contribution of de novo coding mutations to autism spectrum disorder. Nature *13*, 216–221.

Ipser, J.C., Syal, S., Bentley, J., Adnams, C.M., Steyn, B., and Stein, D.J. (2012). 1H-MRS in autism spectrum disorders: A systematic meta-analysis. Metab. Brain Dis. *27*, 275–287.

Ismail, F.Y., Fatemi, A., and Johnston, M. V. (2016). Cerebral plasticity: Windows of opportunity in the developing brain. Eur. J. Paediatr. Neurol. *21*, 23–48.

Iverson, J.M., and Wozniak, R.H. (2007). Variation in vocal-motor development in infant siblings of children with autism. J. Autism Dev. Disord. *37*, 158–170.

Jakovcevski, I., and Zecevic, N. (2005). Sequence of oligodendrocyte development in the human fetal telencephalon. Glia *49*, 480–491.

Jamain, S., Betancur, C., Quach, H., Philippe, a, Fellous, M., Giros, B., Gillberg, C., Leboyer, M., and Bourgeron, T. (2002). Linkage and association of the glutamate receptor 6 gene with autism. Mol. Psychiatry *7*, 302–310.

James, S.J., Cutler, P., Melnyk, S., Jernigan, S., Janak, L., Gaylor, D.W., and Neubrander, J.A. 1 (2004). Metabolic biomarkers of increased oxidative stress and impaired methylation capacity in children with autism. Am. J. Clin. Nutr. *80*, 1611–1617.

Jansen, J.F. a, Backes, W.H., Nicolay, K., and Kooi, M.E. (2006). 1H MR spectroscopy of the brain: absolute quantification of metabolites. Radiology *240*, 318–332.

Janson, C.G., McPhee, S.W.J., Francis, J., Shera, D., Assadi, M., Freese, A., Hurh, P., Haselgrove, J., Wang, D.J., Bilaniuk, L., et al. (2006). Natural History of Canavan Disease Revealed by Proton Magnetic Resonance Spectroscopy (1H-MRS) and Diffusion-weighted MRI. Neuropediatrics *37*, 209–221.

Jessen, K.R. (2004). Glial cells. Int. J. Biochem. Cell Biol. *36*, 1861–1867.

Jiang, S., Xue, H., Glover, A., Rutherford, M., Rueckert, D., and Hajnal, J. V. (2007). MRI of moving subjects using multislice Snapshot images with Volume Reconstruction (SVR): Application to fetal, neonatal, and adult brain studies. IEEE Trans. Med. Imaging *26*, 967–980.

Jin, Y., Wee, C.-Y., Shi, F., Thung, K.-H., Yap, P.-T., and Shen, D. (2015). Identification of Infants at Risk for Autism Using Multi-parameter Hierarchical White Matter Connectomes. Mach. Learn. Med. Imaging *9352*, 170–177.

Johnson, C.P., and Myers, S.M. (2007). Identification and evaluation of children with autism spectrum disorders. Pediatrics *120*, 1183–1215.

Johnson, M.H., Dziurawiec, S., Ellis, H., and Morton, J. (1991). Newborns' preferential tracking of face-like stimuli and its subsequent decline. Cognition *40*, 1–19.

Johnson, S., Hollis, C., Kochhar, P., Hennessy, E., Wolke, D., and Marlow, N. (2010). Autism Spectrum Disorders in Extremely Preterm Children. J. Pediatr. *156*, 525–531.e2.

Jonas, R.K., Montojo, C. a., and Bearden, C.E. (2014). The 22q11.2 deletion syndrome as a window into complex neuropsychiatric disorders over the lifespan. Biol. Psychiatry *75*, 351–360.

Jones, E.J.H., Gliga, T., Bedford, R., Charman, T., and Johnson, M.H. (2014). Developmental pathways to autism: A review of prospective studies of infants at risk. Neurosci. Biobehav. Rev. *39*, 1–33.

Joshi, G., Wozniak, J., Petty, C., Martelon, M.K., Fried, R., Bolfek, A., Kotte, A., Stevens, J., Furtak, S.L., Bourgeois, M., et al. (2013). Psychiatric comorbidity and functioning in a clinically referred population of adults with autism spectrum disorders: A comparative study. J. Autism Dev. Disord. *43*, 1314–1325.

Jou, R.J., Minshew, N.J., Keshavan, M.S., and Hardan, A.Y. (2010). Cortical Gyrification in Autistic and Asperger Disorders: A Preliminary Magnetic Resonance Imaging Study. J. Child Neurol. *25*, 1462–1467.

Kates, W.R., Burnette, C.P., Eliez, S., Strunge, L.A., Kaplan, D., Landa, R., Reiss, A.L., and Pearlson, G.D. (2004). Neuroanatomic Variation in Monozygotic Twin Pairs Discordant for the Narrow Phenotype for Autism. Am. J. Psychiatry *161*, 539–546.

Kaufmann, W.E., Cooper, K.L., Mostofsky, S.H., Capone, G.T., Kates, W.R., Newschaffer, C.J., Bukelis, I., Stump, M.H., Jann, A.E., and Lanham, D.C. (2003). Specificity of Cerebellar Vermian Abnormalities in Autism: A Quantitative Magnetic Resonance Imaging Study. J. Child Neurol. *18*, 463–470.

Kern, J.K. (2003). Purkinje cell vulnerability and autism: a possible etiological connection. Brain Dev. *25*, 377–382.

Kertes, D.A., Donzella, B., Talge, N.M., Garvin, M.C., Van Ryzin, M.J., and Gunnar, M.R. (2009). Inhibited temperament and parent emotional availability differentially predict young children's cortisol responses to novel social and nonsocial events. Dev. Psychobiol. *51*, 521–532.

Kessaris, N., Fogarty, M., Iannarelli, P., Grist, M., Wegner, M., and Richardson, W.D. (2006). Competing waves of oligodendrocytes in the forebrain and postnatal elimination of an embryonic lineage. Nat. Neurosci. *9*, 173–179.

Khazipov, R., and Luhmann, H.J. (2006). Early patterns of electrical activity in the developing cerebral cortex of humans and rodents. Trends Neurosci. *29*, 414–418.

Kimura, H., Fujii, Y., Itoh, S., Matsuda, T., Iwasaki, T., Maeda, M., Konishi, Y., and Ishii, Y. (1995). Metabolic Alterations in the Neonate and Infant Brain during Development: Evaluation with Proton MR Spectroscopy. Radiology *194*, 483–489.

Kinney, D.K., Munir, K.M., Crowley, D.J., and Miller, A.M. (2008). Prenatal stress and risk for autism. Neurosci. Biobehav. Rev. *32*, 1519–1532.

Kinney, H.C., Karthigasan, J., Borenshteyn, N.I., Flax, J.D., and Kirschner, D.A. (1994). Myelination in the developing human brain: Biochemical correlates. Neurochem. Res. *19*, 983–996.

Kinoshita, Y., Okudera, T., Tsuru, E., and Yokota, A. (2001). Volumetric Analysis of the Germinal Matrix and Lateral Ventricles Performed Using MR Images of Postmortem Fetuses. Am. J. Neuroradiol. *22*, 382–388.

Klahr, A.M., and Burt, S.A. (2014). Elucidating the etiology of individual differences in parenting: A meta-analysis of behavioral genetic research. Psychol. Bull. *140*, 544–586.

Kleinhans, N.M., Schweinsburg, B.C., Cohen, D.N., Müller, R.-A., and Courchesne, E. (2007). N-acetyl aspartate in autism spectrum disorders: Regional effects and relationship to fMRI activation. Brain Res. *1162*, 85–97.

Kleinhans, N.M., Richards, T., Weaver, K.E., Liang, O., Dawson, G., and Aylward, E. (2009). Brief Report: Biochemical Correlates of Clinical Impairment in High Functioning Autism and Asperger's Disorder. J. Autism Dev. Disord. *39*, 1079–1086.

Klin, A., Jones, W., Schultz, R., and Volkmar, F. (2003). The enactive mind, or from actions to cognition: lessons from autism. Philos. Trans. R. Soc. London. Biol. Sci. *358*, 345–360.

Kline, J., Stein, Z., Susser, M., and Warburton, D. (1985). Fever during pregnancy and spontaneous abortion. Am J Epidemiol *121*, 832–842.

van der Knaap, M.S., van der Grond, J., van Rijen, P.C., Faber, J.A., Valk, J., and Willemse, K. (1990). Age-dependent Changes in Localized Proton and Phosphorus MR Spectroscopy of the Brain. Radiology *176*, 509–515.

Knapp, M., Romeo, R., and Beecham, J. (2009). Economic cost of autism in the UK. Autism *13*, 317–336.

Knickmeyer, R.C., Gouttard, S., Kang, C., Evans, D., Wilber, K., Smith, J.K., Hamer, R.M., Lin, W., Gerig, G., and Gilmore, J.H. (2008). A Structural MRI Study of Human Brain Development from Birth to 2 Years. J. Neurosci. *28*, 12176–12182.

Kok, R., Thijssen, S., Bakermans-Kranenburg, M.J., Jaddoe, V.W.V., Verhulst, F.C., White, T., van IJzendoorn, M.H., and Tiemeier, H. (2015). Normal Variation in Early Parental Sensitivity Predicts Child Structural Brain Development. J. Am. Acad. Child Adolesc. Psychiatry *54*, 824–831.

Kok, R.D., van den Bergh, a J., Heerschap, A., Nijland, R., and van den Berg, P.P. (2001). Metabolic information from the human fetal brain obtained with proton magnetic resonance spectroscopy. Am. J. Obstet. Gynecol. *185*, 1011–1015.

Kok, R.D., van den Berg, P.P., van den Bergh, A.J., Nijland, R., and Heerschap, A. (2002). Maturation of the Human Fetal Brain as Observed by 1H MR Spectroscopy. Magn. Reson. Med. *48*, 611–616.

Kok, R.D., De Vries, M.M., Heerschap, A., and Van Den Berg, P.P. (2004). Absence of harmful effects of magnetic resonance exposure at 1.5 T in utero during the third trimester of pregnancy: A follow-up study. Magn. Reson. Imaging *22*, 851–854.

Kong, A., Frigge, M.L., Masson, G., Besenbacher, S., Sulem, P., Magnusson, G., Gudjonsson, S.A., Sigurdsson, A., Jonasdottir, A., Jonasdottir, A., et al. (2012). Rate of de novo mutations and the importance of father's age to disease risk. Nature *488*, 471–475.

Kornhuber, M.E., Kornhuber, J., Retz, W., and Riederer, P. (1993). L-Glutamate and L-aspartate concentrations in the developing and aging human putamen tissue. J. Neural Transm. *93*, 145–150.

Kostovic, I. (2002). Laminar Organization of the Human Fetal Cerebrum Revealed by Histochemical Markers and Magnetic Resonance Imaging. Cereb. Cortex *12*, 536–544.

Kostovic, I., and Rakic, P. (1990). Developmental history of the transient subplate zone in the visual and somatosensory cortex of the macaque monkey and human brain. J. Comp. Neurol. *297*, 441–470.

Kostović, I., and Jovanov-Milošević, N. (2006). The development of cerebral connections during the first 20-45 weeks' gestation. Semin. Fetal Neonatal Med. *11*, 415–422.

Kousi, E., Tsougos, I., and Eftychia, K. (2013). Proton Magnetic Resonance Spectroscopy of the Central Nervous System. Nov. Front. Adv. Neuroimaging 19–50.

Kreis, R., Ernst, T., and Ross, B.D. (1993). Development of the Human Brain: In Vivo Quantification of Metabolite and Water Content with Proton Magnetic Resonance Spectroscopy. Magn. Reson. Med. *30*, 424–437.

Kreis, R., Hofmann, L., Kuhlmann, B., Boesch, C., Bossi, E., and Hüppi, P.S. (2002). Brain Metabolite Composition During Early Human Brain Development as Measured by Quantitative In Vivo 1H Magnetic Resonance Spectroscopy. Magn. Reson. Med. *48*, 949–958.

Kubas, B., Kulak, W., Sobaniec, W., Tarasow, E., Lebkowska, U., and Walecki, J. (2012). Metabolite alterations in autistic children: a 1H MR spectroscopy study. Adv. Med. Sci. *57*, 152–156.

Kuklisova-Murgasova, M., Aljabar, P., Srinivasan, L., Counsell, S.J., Doria, V., Serag, A., Gousias, I.S., Boardman, J.P., Rutherford, M. a., Edwards, a. D., et al. (2011). A dynamic 4D probabilistic atlas of the developing brain. Neuroimage *54*, 2750–2763.

Kuklisova-Murgasova, M., Quaghebeur, G., Rutherford, M. a., Hajnal, J. V., and Schnabel, J. a. (2012). Reconstruction of fetal brain MRI with intensity matching and complete outlier removal. Med. Image Anal. *16*, 1550–1564.

Kumar, R.A., Karamohamed, S., Sudi, J., Conrad, D.F., Brune, C., Badner, J.A., Gilliam, T.C., Nowak, N.J., Cook, E.H., Dobyns, W.B., et al. (2008). Recurrent 16p11.2 microdeletions in autism. Hum. Mol. Genet. *17*, 628–638.

Kuzniewicz, M.W., Wi, S., Qian, Y., Walsh, E.M., Armstrong, M.A., and Croen, L.A. (2014). Prevalence and Neonatal Factors Associated with Autism Spectrum Disorders in Preterm Infants. J. Pediatr. *164*, 20–25.

Kyriakopoulou, V., Vatansever, D., Elkommos, S., Dawson, S., McGuinness, A., Allsop, J., Molnár, Z., Hajnal, J., and Rutherford, M. (2014). Cortical Overgrowth in Fetuses With Isolated Ventriculomegaly. Cereb. Cortex *24*, 2141–2150.

Kyriakopoulou, V., Vatansever, D., Davidson, A., Patkee, P., Elkommos, S., Chew, A., Martinez-Biarge, M., Hagberg, B., Damodaram, M., Allsop, J., et al. (2016). Normative biometry of the fetal brain using magnetic resonance imaging. Brain Struct. Funct. 1–13.

Lai, M.-C., Lombardo, M. V., Auyeung, B., Chakrabarti, B., and Baron-Cohen, S. (2015). Sex/Gender Differences and Autism: Setting the Scene for Future Research. J. Am. Acad. Child Adolesc. Psychiatry *54*, 11–24.

Lainhart, J.E., Piven, J., Wzorek, M., Landa, R., Santangelo, S.L., Coon, H., and Folstein, S.E. (1997). Macrocephaly in children and adults with autism. J. Am. Acad. Child Adolesc. Psychiatry *36*, 282–290.

Lam, K.S.L., Aman, M.G., and Arnold, L.E. (2006). Neurochemical correlates of autistic disorder: A review of the literature. Res. Dev. Disabil. *27*, 254–289.

Lam, K.S.L., Bodfish, J.W., and Piven, J. (2008). Evidence for three subtypes of repetitive behavior in autism that differ in familiality and association with other symptoms. J. Child Psychol. Psychiatry Allied Discip. *49*, 1193–1200.

Lan, L.M., Yamashita, Y., Tang, Y., Sugahara, T., Takahashi, M., Ohba, T., and Okamura, H. (2000). Normal fetal brain development: MR imaging with a half-Fourier rapid acquisition with relaxation enhancement sequence. Radiology *215*, 205–210.

Landa, R.J., Holman, K.C., and Garrett-mayer, E. (2007). Social and Communication Development in Toddlers With Early and Later Diagnosis of Autism Spectrum Disorders. Arch Gen Psychiatry *64*, 853–864.

Landrigan, P.J. (2010). What causes autism? Exploring the environmental contribution. Curr. Opin. Pediatr. *22*, 219–225.

Lange, N., Travers, B.G., Bigler, E.D., Prigge, M.B.D., Froehlich, A.L., Nielsen, J. a., Cariello, A.N., Zielinski, B. a., Anderson, J.S., Fletcher, P.T., et al. (2015). Longitudinal Volumetric Brain Changes in Autism Spectrum Disorder Ages 6-35 Years. Autism Res. *8*, 82–93.

Langen, M., Durston, S., Staal, W.G., Palmen, S.J.M.C., and van Engeland, H. (2007). Caudate Nucleus Is Enlarged in High-Functioning Medication-Naive Subjects with Autism. Biol. Psychiatry *62*, 262–266.

Langen, M., Bos, D., Noordermeer, S.D.S., Nederveen, H., Van Engeland, H., and Durston, S. (2014). Changes in the development of striatum are involved in repetitive behavior in autism. Biol. Psychiatry *76*, 405–411.

Laurence, J.A., and Fatemi, S.H. (2005). Glial fibrillary acidic protein is elevated in superior frontal, parietal and cerebellar cortices of autistic subjects. The Cerebellum *4*, 206–210.

LeBlanc, J.J., and Fagiolini, M. (2011). Autism: A "Critical Period" Disorder? Neural Plast. *2011*, 1–17.

Ledig, C., Wolz, R., Aljabar, P., Lötjönen, J., Heckemann, R. a., Hammers, A., and Rueckert, D. (2012). Multi-class brain segmentation using atlas propagation and EM-based refinement. Proc. - Int. Symp. Biomed. Imaging 896–899.

Lemonnier, E., and Ben-Ari, Y. (2010). The diuretic bumetanide decreases autistic behaviour in five infants treated during 3 months with no side effects. Acta Paediatr. Int. J. Paediatr. *99*, 1885–1888.

Lemonnier, E., Degrez, C., Phelep, M., Tyzio, R., Josse, F., Grandgeorge, M., Hadjikhani, N., and Ben-Ari, Y. (2012). A randomised controlled trial of bumetanide in the treatment of autism in children. Transl. Psychiatry *2*, e202.

Lenroot, R.K., Gogtay, N., Greenstein, D.K., Wells, E.M., Wallace, G.L., Clasen, L.S., Blumenthal, J.D., Lerch, J., Zijdenbos, A.P., Evans, A.C., et al. (2007). Sexual Dimorphism of Brain Developmental Trajectories during Childhood and Adolescence. Neuroimage *36*, 1065–1073.

Levitt, J.G., Blanton, R., Capetillo-Cunliffe, L., Guthrie, D., Toga, A., and McCracken, J.T. (1999). Cerebellar Vermis Lobules VIII-X in Autism. Prog. Neuropsychopharmacol. Biol. Psychiatry *23*, 625–633.

Levitt, J.G., Blanton, R.E., Smalley, S., Thompson, P.M., Guthrie, D., McCracken, J.T., Sadoun, T., Heinichen, L., and Toga, A.W. (2003a). Cortical Sulcal Maps in Autism. Cereb. Cortex *13*, 728–735.

Levitt, J.G., O'Neill, J., Blanton, R.E., Smalley, S., Fadale, D., McCracken, J.T., Guthrie, D., Toga, A.W., and Alger, J.R. (2003b). Proton Magnetic Resonance Spectroscopic Imaging of the Brain in Childhood Autism. Biol. Psychiatry *54*, 1355–1366.

Levy, D., Ronemus, M., Yamrom, B., Lee, Y. ha, Leotta, A., Kendall, J., Marks, S., Lakshmi, B., Pai, D., Ye, K., et al. (2011). Rare De Novo and Transmitted Copy-Number Variation in Autistic Spectrum Disorders. Neuron *70*, 886–897.

Li, X., Chauhan, A., Sheikh, A.M., Patil, S., Chauhan, V., Li, X.M., Ji, L., Brown, T., and Malik, M. (2009). Elevated immune response in the brain of autistic patients. J. Neuroimmunol. *207*, 111–116.

Lichtenstein, P., Carlström, E., Råstam, M., Gillberg, C., and Anckarsäter, H. (2010). The genetics of autism spectrum disorders and related neuropsychiatric disorders in childhood. Am. J. Psychiatry *167*, 1357–1363.

Liew, Z., Ritz, B., Virk, J., and Olsen, J. (2015). Maternal Use of Acetaminophen during Pregnancy and Risk of Autism Spectrum Disorders in Childhood: A Danish National Birth Cohort Study. Autism Res. 1–8.

Limperopoulos, C. (2009). Autism Spectrum Disorders in Survivors of Extreme Prematurity. Clin. Perinatol. *36*, 791–805.

Limperopoulos, C., Bassan, H., Gauvreau, K., Robertson, R.L., Sullivan, N.R., Benson, C.B., Avery, L., Stewart, J., Soul, J.S., Ringer, S. a, et al. (2007). Does Cerebellar Injury in Premature Infants Contribute to the High Prevalence of Long-term Cognitive, Learning, and Behavioral Disability in Survivors? Pediatrics *120*, 584–593.

Limperopoulos, C., Bassan, H., Sullivan, N.R., Soul, J.S., Robertson, R.L., Moore, M., Ringer, S.A., Volpe, J.J., and du Plessis, A.J. (2008). Positive Screening for Autism in Ex-preterm Infants: Prevalence and Risk Factors. Pediatrics *121*, 758–765.

Lin, A., Ross, B.D., Harris, K., and Wong, W. (2005). Efficacy of Proton Magnetic Resonance Spectroscopy in Neurological Diagnosis and Neurotherapeutic Decision Making. NeuroRx *2*, 197–214.

Lloyd-Fox, S., Blasi, A., Pasco, G., Gliga, T., Murphy, D., Elwell, C.E., Charman, T., Johnson, M.H., and Team, T.B. Neural signature of autism evident before six months of life. PNAS.

Lloyd-Fox, S., Blasi, A., Elwell, C.E., Charman, T., Murphy, D., and Johnson, M.H. (2013). Reduced neural sensitivity to social stimuli in infants at risk for autism. Proc. R. Soc. B Biol. Sci. *280*, 20123026–20123026.

Lockwood Estrin, G., Kyriakopoulou, V., Makropoulos, A., Ball, G., Kuhendran, L., Chew, A., Hagberg, B., Martinez-Biarge, M., Allsop, J., Fox, M., et al. (2016). Altered white matter and cortical structure in neonates with antenatally diagnosed isolated ventriculomegaly. NeuroImage Clin. *11*, 139–148.

Loftin, R.L., Odom, S.L., and Lantz, J.F. (2008). Social interaction and repetitive motor behaviors. J. Autism Dev. Disord. *38*, 1124–1135.

Lord, C., Rutter, M., and Le Couteur, A. (1994). Autism Diagnostic Interview-Revised: a revised version of a diagnostic interview for caregivers of individuals with possible pervasive developmental disorders. J. Autism Dev. Disord. *24*, 659–685.

Lord, C., Wagner, A., Rogers, S., Szatmari, P., Aman, M., Charman, T., Dawson, G., Durand, V.M., Grossman, L., Guthrie, D., et al. (2005). Challenges in evaluating psychosocial interventions for autistic spectrum disorders. J. Autism Dev. Disord. *35*, 695–708.

Lord, C., Rutter, M., Dilavore, P.C., Risi, S., Gotham, K., and Bishop, S. (2012). Autism Diagnostic Observation Schedule, Second Edition (ADOS-2) Manual (Part I): Modules 1–4 (Torrance, CA: Western Psychological Services).

Lotspeich, L.J., Kwon, H., Schumann, C.M., Fryer, S.L., Goodlin-Jones, B.L., Buonocore, M.H., Lammers, C.R., Amaral, D.G., and Reiss, A.L. (2004). Investigation of neuroanatomical differences between autism and Asperger syndrome. Arch. Gen. Psychiatry *61*, 291–298.

Luecken, L.J. (1998). Childhood attachment and loss experiences affect adult cardiovascular and cortisol function. Psychosom. Med. *60*, 765–772.

Lugo-Gil, J., and Tamis-LeMonda, C.S. (2008). Family Resources and Parenting Quality: Links to Children's Cognitive Development Across the First 3 Years. Child Dev. *79*, 1065–1085.

Luijk, M.P.C.M., Saridjan, N., Tharner, A., Van Ijzendoorn, M.H., Bakermans-Kranenburg, M.J., Jaddoe, V.W. V, Hofman, A., Verhulst, F.C., and Tiemeier, H. (2010). Attachment, depression, and cortisol: Deviant patterns in insecure-resistant and disorganized infants. Dev. Psychobiol. *52*, 441–452.

Lupien, S.J., Parent, S., Evans, A.C., Tremblay, R.E., Zelazo, P.D., Corbo, V., Pruessner, J.C., and Séguin, J.R. (2011). Larger amygdala but no change in hippocampal volume in 10-year-old children exposed to maternal depressive symptomatology since birth. PNAS *108*, 14324–14329.

Makris, N., Schlerf, J.E., Hodge, S.M., Haselgrove, C., Albaugh, M.D., Seidman, L.J., Rauch, S.L., Harris, G., Biederman, J., Caviness, V.S., et al. (2005). MRI-based surface-assisted parcellation of human cerebellar cortex: An anatomically specified method with estimate of reliability. Neuroimage *25*, 1146–1160.

Makropoulos, A., Gousias, I.S., Ledig, C., Aljabar, P., Serag, A., Hajnal, J. V., Edwards, A.D., Counsell, S.J., and Rueckert, D. (2014). Automatic whole brain MRI segmentation of the developing neonatal brain. IEEE Trans. Med. Imaging *33*, 1818–1831.

Makropoulos, A., Aljabar, P., Wright, R., Huning, B., Merchant, N., Arichi, T., Tusor, N., Hajnal, J. V., Edwards, A.D., Counsell, S.J., et al. (2015). Regional growth and atlasing of the developing human brain. Neuroimage.

Malamateniou, C., Mcguinness, A.K., Allsop, J.M., O'Regan, D.P., Rutherford, M.A., and Hajnal, J. V (2011). Snapshot Inversion Recovery: An Optimized Single-Shot T1-weighted Inversion-Recovery Sequence for Improved Fetal Brain Anatomic Delineation. Radiology *258*, 229–235.

Malamateniou, C., Malik, S.J., Counsell, S.J., Allsop, J.M., McGuinness, A.K., Hayat, T., Broadhouse, K., Nunes, R.G., Ederies, A.M., Hajnal, J. V., et al. (2013). Motion-compensation techniques in neonatal and fetal MR imaging. Am. J. Neuroradiol. *34*, 1124–1136.

Mandy, W., and Lai, M.-C. (2016). Annual Research Review: The role of the environment in the developmental psychopathology of autism spectrum condition. J. Child Psychol. Psychiatry.

Marchetto, M., Belinson, H., Tian, Y., BC, F., Fu, C., Vadodaria, K., Beltrao-Braga, P., Trujillo, C., Mendes, A., Padmanabhan, K., et al. (2016). Altered proliferation and networks in neural cells derived from idiopathic autistic individuals. Mol. Psychiatry 1–16.

Marieb, E.N., and Hoehn, K. (2007). Human Anatomy & Physiology (San Francisco, CA: Pearson Education, Inc).

Marín, O., and Rubenstein, J.L. (2001). A long, remarkable journey: tangential migration in the telencephalon. Nat. Rev. Neurosci. *2*, 780–790.

Marin-Padilla, M. (1978). Dual origin of the mammalian neocortex and evolution of the cortical plate. Anat. Embryol. (Berl). *152*, 109–126.

Marquardt, D.W. (1963). An Algorithm for Least-Squares Estimation of Nonlinear Parameters. J. Soc. Ind. Appl. Math. *11*, 431–441.

Masur, E.F. (1995). Infants' early verbal imitation and their later lexical development. Merrill. Palmer. Q. *41*, 286–306.

Masur, E.F., Eichorst, D.L., Elise Frank Masur, and Doreen L. Eichorst (2002). Infants' Spontaneous Imitation of Novel Versus Familiar Words: Relations to Observational and Maternal Report Measures of Their Lexicons. Merrill. Palmer. Q. *48*, 405–426.

Matson, J.L., and Nebel-Schwalm, M.S. (2007). Comorbid psychopathology with autism spectrum disorder in children: An overview. Res. Dev. Disabil. *28*, 341–352.

McAlonan, G.M., Daly, E., Kumari, V., Critchley, H.D., Van Amelsvoort, T., Suckling, J., Simmons, A., Sigmundsson, T., Greenwood, K., Russell, A., et al. (2002). Brain anatomy and sensorimotor gating in Asperger's syndrome. Brain *127*, 1594–1606.

McConnell, S.K., and Kaznowski, C.E. (1991). Cell Cycle Dependence of Laminar Determination in Developing Neocortex. Science (80-.). *254*, 282–285.

McKavanagh, R., Buckley, E., and Chance, S.A. (2015). Wider minicolumns in autism: A neural basis for altered processing? Brain *138*, 2034–2045.

McTigue, D.M., and Tripathi, R.B. (2008). The life, death, and replacement of oligodendrocytes in the adult CNS. J. Neurochem. *107*, 1–19.

Mevissen, M., Buntenkotter, S., and Loscher, W. (1994). Effects of Static and Time-Varying (50-Hz) Magnetic Fields on Reproduction and Fetal Development in Rats. Teratology *50*, 229–237.

Michalon, A., Bruns, A., Risterucci, C., Honer, M., Ballard, T.M., Ozmen, L., Jaeschke, G., Wettstein, J.G., Von Kienlin, M., Künnecke, B., et al. (2014). Chronic metabotropic glutamate receptor 5 inhibition corrects local alterations of brain activity and improves cognitive performance in fragile X mice. Biol. Psychiatry *75*, 189–197.

Michel, S.C. a, Rake, A., Götzmann, L., Seifert, B., Ferrazzini, M., Chaoui, R., Treiber, K., Keller, T.M., Marincek, B., and Kubik-Huch, R. a (2002). Pelvimetry and patient acceptability compared between open 0.5-T and closed 1.5-T MR systems. Eur. Radiol. *12*, 2898–2905.

Miles, J.H. (2011). Autism spectrum disorders - A genetics review. Genet. Med. *13*, 278–294.

Mitchell, S., Brian, J., Zwaigenbaum, L., Roberts, W., Szatmari, P., Smith, I., and Bryson, S. (2006). Early language and communication development of infants later diagnosed with autism spectrum disorder. J. Dev. Behav. Pediatr. *27*, S69–S78.

Moffett, J.R., and Namboodiri, A.M.A. (2006). Expression of N-acetylaspartate and N-acetylaspartylglutamate in the nervous system. Adv. Exp. Med. Biol. *576*, 7–26.

Moffett, J.R., Ross, B., Arun, P., Madhavarao, C.N., and Namboodiri, A.M.A. (2007). N-Acetylaspartate in the CNS: From Neurodiagnostics to Neurobiology. Prog. Neurobiol. *81*, 89–131.

Mooney, E.L., Gray, K.M., and Tonge, B.J. (2006). Early features of autism: Repetitive behaviours in young children. Eur. Child Adolesc. Psychiatry *15*, 12–18.

Moretti, P., and Zoghbi, H.Y. (2006). MeCP2 dysfunction in Rett syndrome and related disorders. Curr Opin Genet Dev *16*, 276–281.

Morgan, J.T., Chana, G., Pardo, C.A., Achim, C., Semendeferi, K., Buckwalter, J., Courchesne, E., and Everall, I.P. (2010). Microglial activation and increased microglial density observed in the dorsolateral prefrontal cortex in autism. Biol. Psychiatry *68*, 368–376.

Mosconi, M.W., Cody-Hazlett, H., Poe, M.D., Gerig, G., Gimpel-Smith, R., and Piven, J. (2009). Longitudinal Study of Amygdala Volume and Joint Attention in 2- to 4-Year-Old Children With Autism. Arch. Gen. Psychiatry *66*, 509–516.

Mraz, K.D., Green, J., Dumont-Mathieu, T., Makin, S., and Fein, D. (2007). Correlates of Head Circumference Growth in Infants Later Diagnosed With Autism Spectrum Disorders. J. Child Neurol. *22*, 700–713.

Mullen, E.M. (1995). Mullen Scales of Early Learning: AGS Edition. (Circle Pines, MN: American Guidance Service).

Mullins, P.G., McGonigle, D.J., O'Gorman, R.L., Puts, N.A.J.J., Vidyasagar, R., Evans, C.J., and Edden, R.A.E.E. (2014). Current practice in the use of MEGA-PRESS spectroscopy for the detection of GABA. Neuroimage *86*, 43–52.

Mundy, P., Sigman, M., Ungerer, J., and Sherman, T. (1986). Defining Defining the social deficits of autism - the contribution of nonverbal-communication measures. J. Child Psychol. Psychiatry *27*, 657–669.

Munson, J., Dawson, G., Abbott, R., Faja, S., Webb, S.J., Friedman, S.D., Shaw, D., Artru, A., and Dager, S.R. (2006). Amygdalar volume and behavioral development in autism. Arch. Gen. Psychiatry *63*, 686–693.

Murphy, D.G., Critchley, H.D., Schmitz, N., McAlonan, G., Van Amelsvoort, T., Robertson, D., Daly, E., Rowe, A., Russell, A., Simmons, A., et al. (2002). Asperger Syndrome: A Proton Magnetic Resonance Spectroscopy Study of Brain. Arch. Gen. Psychiatry *59*, 885–891.

Murray, L., Fiori-Cowley, A., Hooper, R., and Cooper, P. (1996a). The Impact of Postnatal Depression and Associated Adversity on Early Mother-Infant Interactions and Later Infant Outcome. Child Dev. *67*, 2512–2526.

Murray, L., Hipwell, A., Hooper, R., Stein, A., and Cooper, P. (1996b). The cognitive development of 5-year-old children of postnatally depressed mothers. J. Child Psychol. Psychiatry *37*, 927–935.

Murray, L., Halligan, S., and Cooper, P. (2010). Effects of postnatal depression on mother-infant interactions and child development. In Handbook of Infant Development, B.G.W. T., ed. (Wiley-Blackwell), pp. 192–220.

Myers, S.M., and Johnson, C.P. (2007). Management of children with autism spectrum disorders. Pediatrics *120*, 1162–1182.

Nadarajah, B., and Parnavelas, J.G. (2002). Modes of Neuronal Migration in the Developing Cerebral Cortex. Nat. Rev. Neurosci. *3*, 423–432.

Nadarajah, B., Brunstrom, J.E., Grutzendler, J., Wong, R.O., and Pearlman, a L. (2001). Two modes of radial migration in early development of the cerebral cortex. Nat. Neurosci. *4*, 143–150.

Nadarajah, B., Alifragis, P., Wong, R.O.L., and Parnavelas, J.G. (2003). Neuronal Migration in the Developing Cerebral Cortex: Observations Based on Real-time Imaging. Cereb. Cortex *13*, 607–611.

Nair, A., Treiber, J.M., Shukla, D.K., Shih, P., and M??ller, R.A. (2013). Impaired thalamocortical connectivity in autism spectrum disorder: A study of functional and anatomical connectivity. Brain *136*, 1942–1955.

Nair, A., Carper, R.A., Abbott, A.E., Chen, C.P., Solders, S., Nakutin, S., Datko, M.C., Fishman, I., and Müller, R.A. (2015). Regional specificity of aberrant thalamocortical connectivity in autism. Hum. Brain Mapp.

Nave, K.-A., and Werner, H.B. (2014). Myelination of the Nervous System: Mechanisms and Functions. Annu. Rev. Cell Dev. Biol. *30*, 503–533.

Nelson, S.J. (2003). Multivoxel Magnetic Resonance Spectroscopy of Brain Tumors. Mol. Cancer Ther. *2*, 497–507.

Nelson, S.B., and Valakh, V. (2015). Excitatory/Inhibitory Balance and Circuit Homeostasis in Autism Spectrum Disorders. Neuron *87*, 684–698.

Nicolson, N.A. (2004). Childhood parental loss and cortisol levels in adult men. Psychoneuroendocrinology *29*, 1012–1018.

Noble, K.G., Houston, S.M., Kan, E., and Sowell, E.R. (2012). Neural correlates of socioeconomic status in the developing human brain. Dev. Sci. *15*, 516–527.

Noble, K.G., Houston, S.M., Brito, N.H., Bartsch, H., Kan, E., Kuperman, J.M., Akshoomoff, N., Amaral, D.G., Bloss, C.S., Libiger, O., et al. (2015). Family income, parental education and brain structure in children and adolescents. Nat. Neurosci. *18*, 773–780.

Nordahl, C.W., Dierker, D., Mostafavi, I., Schumann, C.M., Rivera, S.M., Amaral, D.G., and Van Essen, D.C. (2007). Cortical Folding Abnormalities in Autism Revealed by Surface-Based Morphometry. J. Neurosci. *27*, 11725–11735.

Nordahl, C.W., Lange, N., Li, D.D., Barnett, L.A., Lee, A., Buonocore, M.H., Simon, T.J., Rogers, S., Ozonoff, S., and Amaral, D.G. (2011). Brain enlargement is associated with regression in preschool-age boys with autism spectrum disorders. PNAS *108*, 20195–20200.

Nordahl, C.W., Scholz, R., Yang, X., Buonocore, M.H., Simon, T., Rogers, S., and Amaral, D.G. (2012). Increased Rate of Amygdala Growth in Children Aged 2 to 4 Years with Autism Spectrum Disorders: A Longitudinal Study. Arch Gen Psychiatry *69*, 53–61.

Nordengen, K., Heuser, C., Rinholm, J.E. gge, Matalon, R., and Gundersen, V. (2015). Localisation of N-acetylaspartate in oligodendrocytes/myelin. Brain Struct. Funct. *220*, 899–917.

Novak, J.E., Turner, R.S., Agranoff, B.W., and Fisher, S.K. (1999). Differentiated human NT2-N neurons possess a high intracellular content of myo-inositol. J. Neurochem. *72*, 1431–1440.

O'Rahilly, R., and Müller, F. (2008). Significant features in the early prenatal development of the human brain. Ann. Anat. *190*, 105–118.

O'Roak, B.J., Vives, L., Girirajan, S., Karakoc, E., Krumm, N., Coe, B.P., Levy, R., Ko, A., Lee, C., Smith, J.D., et al. (2012). Sporadic autism exomes reveal a highly interconnected protein network of de novo mutations. Nature *485*, 246–250.

Ohta, H., Nordahl, C.W., Iosif, A.M., Lee, A., Rogers, S., and Amaral, D.G. (2016). Increased Surface Area, but not Cortical Thickness, in a Subset of Young Boys With Autism Spectrum Disorder. Autism Res. *9*, 232–248.

Okereafor, A., Allsop, J., Counsell, S.J., Fitzpatrick, J., Azzopardi, D., Rutherford, M.A., and Cowan, F.M. (2008). Patterns of Brain Injury in Neonates Exposed to Perinatal Sentinel Events. Pediatrics *121*, 906–914.

Oller, D.K. (1978). Infant vocalization and the development of speech. Allied Heal. Behav Sci. *1*, 523–549.

Olsén, P., Pääkkö, E., Vainionpää, L., Pyhtinen, J., and Järvelin, M.R. (1997). Magnetic Resonance Imaging of Periventricular Leukomalacia and its Clinical Correlation in Children. Ann. Neurol. *41*, 754–761.

Oono, I.P., Honey, E.J., and McConachie, H. (2013). Parent-mediated early intervention for young children with autism spectrum disorders (ASD). Cochrane Database Syst. Rev. *4*, 1–100.

Oppenheim, R.W. (1989). The neurotrophic theory and naturally occurring motoneuron death. Trends Neurosci. *12*, 252–255.

Ornoy, A. (2009). Valproic acid in pregnancy: How much are we endangering the embryo and fetus? Reprod. Toxicol. *28*, 1–10.

Otsuka, H., Harada, M., Mori, K., Hisaoka, S., and Nishitani, H. (1999). Brain metabolites in the hippocampus-amygdala region and cerebellum in autism: An 1H-MR spectroscopy study. Neuroradiology *41*, 517–519.

Ozonoff, S., Iosif, A.-M., Baguio, F., Cook, I.C., Hill, M.M., Hutman, T., Rogers, S.J., Rozga, A., Sangha, S., Sigman, M., et al. (2010). A Prospective Study of the Emergence of Early Behavioral Signs of Autism. J. Am. Acad. Child Adolesc. Psychiatry *49*, 256-66-2.

Ozonoff, S., Young, G.S., Carter, A., Messinger, D., Yirmiya, N., Zwaigenbaum, L., Bryson, S., Carver, L.J., Constantino, J.N., Dobkins, K., et al. (2011). Recurrence Risk for Autism Spectrum Disorders: A Baby Siblings Research Consortium Study. Pediatrics *128*, e488-95.

Padilla, N., Eklöf, E., Mårtensson, G.E., Bölte, S., Lagercrantz, H., and Ådén, U. (2015). Poor Brain Growth in Extremely Preterm Neonates Long Before the Onset of Autism Spectrum Disorder Symptoms. Cereb. Cortex 1–8.

Page, L.A., Daly, E., Schmitz, N., Simmons, A., Toal, F., Deeley, Q., Ambery, F., McAlonan, G.M., Murphy, K.C., and Murphy, D.G.M. (2006). In Vivo 1H-Magnetic Resonance Spectroscopy Study of Amygdala-Hippocampal and Parietal Regions in Autism. Am. J. Psychiatry *163*, 2189–2192.

Palmen, S.J.M.C., van Engeland, H., Hof, P.R., and Schmitz, C. (2004). Neuropathological findings in autism. Brain *127*, 2572–2583.

Palmen, S.J.M.C., Hulshoff Pol, H.E., Kemner, C., Schnack, H.G., Durston, S., Lahuis, B.E., Kahn, R.S., and Van Engeland, H. (2005). Increased gray-matter volume in medication-naive high-functioning children with autism spectrum disorder. Psychol. Med. *35*, 561–570.

Paolicelli, R.C., and Gross, C.T. (2011). Microglia in development: linking brain wiring to brain environment. Neuron Glia Biol. *7*, 77–83.

Paridaen, J.T., and Huttner, W.B. (2014). Neurogenesis during development of the vertebrate central nervous system. EMBO Rep. *15*, 351–364.

Parker, J.D., Schoendorf, K.C., and Kiely, J.L. (1994). Associations between measures of socioeconomic status and low birth weight, small for gestational age, and premature delivery in the United States. Ann. Epidemiol. *4*, 271–278.

Patel, T.B., and Clark, J.B. (1979). Synthesis of N-acetyl-L-aspartate by rat brain mitochondria and its involvement in mitochondrial/cytosolic carbon transport. Biochem. J. *184*, 539–546.

Patenaude, Y., Pugash, D., Lim, K., Morin, L., Bly, S., Butt, K., Cargill, Y., Davies, G., Denis, N., Hazlitt, G., et al. (2014). The use of magnetic resonance imaging in the obstetric patient. J. Obstet. Gynaecol. Canada *36*, 349–363.

Paul, R., Fuerst, Y., Ramsay, G., Chawarska, K., and Klin, A. (2011). Out of the mouths of babes: Vocal production in infant siblings of children with ASD. J. Child Psychol. Psychiatry Allied Discip. *52*, 588–598.

Pearlman, A.L., Faustt, P.L., Hatten, M.E., and Brunstrom, J.E. (1998). New directions for neuronal migration. Curr. Opin. Neurobiol. *8*, 45–54.

Pennock, J.M. (2002). Patient preparation, safety and hazards in imaging infants and children. In MRI of the Neonatal Brain, M.A. Rutherford, ed. (London, United Kingdom: WB Saunders), p.

Peterson, B.S., Anderson, A.W., Ehrenkranz, R., Staib, L.H., Tageldin, M., Colson, E., Gore, J.C., Duncan, C.C., Makuch, R., and Ment, L.R. (2003). Regional brain volumes and their later neurodevelopmental correlates in term and preterm infants. Pediatrics *111*, 939–948.

Pierce, K., and Courchesne, E. (2001). Evidence for a cerebellar role in reduced exploration and stereotyped behavior in autism. Biol. Psychiatry *49*, 655–664.

Pinto, D., Pagnamenta, A.T., Klei, L., Anney, R., Merico, D., Regan, R., Conroy, J., Magalhaes, T.R., Correia, C., Brett, S., et al. (2010). Functional Impact of Global Rare Copy Number Variation in Autism Spectrum Disorder. Nature *466*, 368–372.

Pisula, E., and Ziegart-Sadowska, K. (2015). Broader Autism Phenotype in Siblings of Children with ASD—A Review.

Piven, J., Berthier, M.L., Starkstein, S.E., Nehme, E., Pearlson, G., and Folstein, S. (1990). Magnetic resonance imaging evidence for a defect of cerebral cortical development in autism. Am J Psychiatry *147*, 734–739.

Piven, J., Bailey, J., Havercamp, S., Andreasen, N., and Palmer, P. (1995). An MRI study of brain size in autism. Am. J. Psychiatry *152*, 1145–1149.

Piven, J., Arndt, S., Bailey, J., and Andreasen, N. (1996). Regional brain enlargement in autism: a magnetic resonance imaging study. J. Am. Acad. Child Adolesc. Psychiatry *35*, 530–536.

Piven, J., Palmer, P., Jacobi, D., Childress, D., and Arndt, S. (1997). Broader Autism Phenotype: Evidence From a Family History Study of Multiple-Incidence Autism Families. Am. J. Psychiatry *154*, 185–190.

du Plessis, A.J., and Volpe, J.J. (2002). Perinatal brain injury in the preterm and term newborn. Curr. Opin. Neurol. *15*, 151–157.

Plomin, R., DeFries, J.C., Knopik, V.S., and Neiderhiser, J.M. (2016). Top 10 Replicated Findings From Behavioral Genetics. Perspect. Psychol. Sci. *11*, 3–23.

Polleux, F., and Lauder, J.M. (2004). Toward a Developmental Neurobiology of Autism. Ment. Retard. Dev. Disabil. Res. Rev. *10*, 303–317.

Pop, A.S., Gomez-Mancilla, B., Neri, G., Willemsen, R., and Gasparini, F. (2013). Fragile X syndrome: a preclinical review on metabotropic glutamate receptor 5 (mGluR5) antagonists and drug development. Psychopharmacology (Berl). *5*.

Port, R.G., Gaetz, W., Bloy, L., Wang, D.-J., Blaskey, L., Kuschner, E.S., Levy, S.E., Brodkin, E.S., and Roberts, T.P.L. (2016). Exploring the Relationship Between Cortical GABA Concentrations, Auditory Gamma-Band Responses and Development in ASD: Evidence for an Altered Maturational Trajectory in ASD. Autism Res. 1–15.

Portney, L.G., Watkins, M.P., and Portney G, W.P. (2009). Foundations of Clinical Research: Applications to Practice.

Poutamo, J., Partanen, K., Vanninen, R., Vainio, P., and Kirkinen, P. (1998). MRI does not change fetal cardiotocographic parameters. Prenat. Diagn. *18*, 1149–1154.

Pouwels, P.J.W., and Frahm, J. (1998). Regional Metabolite Concentrations in Human Brain as Determined by Quantitative Localized Proton MRS. Magn. Reson. Med. *39*, 53–60.

Pouwels, P.J., Brockmann, K., Kruse, B., Wilken, B., Wick, M., Hanefeld, F., and Frahm, J. (1999). Regional Age Dependence of Human Brain Metabolites from Infancy to Adulthood as Detected by Quantitative Localized Proton MRS. Pediatr. Res. *46*, 474–485.

Pritchard, M.A., de Dassel, T., Beller, E., Bogossian, F., Johnston, L., Paynter, J., Russo, S., and Scott, J. (2016). Autism in Toddlers Born Very Preterm. Pediatrics *137*, 1–8.

Pufulete, M., Al-Ghnaniem, R., Khushal, A., Appleby, P., Harris, N., Gout, S., Emery, P.W., and Sanders, T.A.B. (2005). Effect of folic acid supplementation on genomic DNA methylation in patients with colorectal adenoma. Gut *54*, 648–653.

Purcell, A.E., Jeon, O.H., Zimmerman, A.W., Blue, M.E., and Pevsner, J. (2001). Postmortem brain abnormalities of the glutamate neurotransmitter system in autism. Neurology *57*, 1618–1628.

Puts, N.A.J., Wodka, E.L., Harris, A.D., Crocetti, D., Tommerdahl, M., Mostofsky, S.H., and Edden, R.A.E. (2016). Reduced GABA and Altered Somatosensory Function in Children with Autism Spectrum Disorder. Autism Res. 1–12.

Qiu, A., Adler, M., Crocetti, D., Miller, M.I., and Mostofsky, S.H. (2010). Basal ganglia shapes predict social, communication, and motor dysfunctions in boys with autism spectrum disorder. J. Am. Acad. Child Adolesc. Psychiatry *49*, 539–551, 551-4.

Rabi, I.I., Millman, S., Kusch, P., and Zacharias, J.R. (1939). The molecular beam resonance method for measuring nuclear magnetic moments. Phys. Rev. *55*, 526–535.

Rabinowicz, T., de Courten-Myers, G.M., Petetot, J.M.-C., Xi, G., and de los Reyes, E. (1996). Human Cortex Development: Estimates of Neuronal Numbers Indicate Major Loss Late During Gestation. J. Neuropathol. Exp. Neurol. *55*, 320–328.

Rae, C.D. (2014). A Guide to the Metabolic Pathways and Function of Metabolites Observed in Human Brain 1H Magnetic Resonance Spectra. Neurochem. Res. *39*, 1–36.

Rai, D., Lee, B.K., Dalman, C., Golding, J., Lewis, G., and Magnusson, C. (2013). Parental depression, maternal antidepressant use during pregnancy, and risk of autism spectrum disorders: population based case-control study`. BMJ *346*, f2059.

Rajagopalan, V., Scott, J., Habas, P.A., Kim, K., Corbett-Detig, J., Rousseau, F., Barkovich, A.J., Glenn, O.A., and Studholme, C. (2011). Local tissue growth patterns underlying normal fetal human brain gyrification quantified in utero. J. Neurosci. *31*, 2878–2887.

Rakic, P. (1971). Neuron-glia relationship during granule cell migration in developing cerebellar cortex. A Golgi and electronmicroscopic study in Macacus Rhesus. J Comp Neurol. *141*, 283–312.

Rakic, P. (1972). Mode of Cell Migration to the Superficial Layers of Fetal Monkey Neocortex. J. Comp. Neurol. *145*, 61–83.

Rakic, P. (1995). Corticogenesis in human and nonhuman primates. In The Cognitive Neurosciences, M.S. Gazzaniga, ed. (Cambridge: The MIT Press), pp. 127–145.

Rakic, P. (2006). A century of progress in corticoneurogenesis: From silver impregnation to genetic engineering. Cereb. Cortex *16*, 3–17.

Rakic, S., and Zecevic, N. (2000). Programmed cell death in the developing human telencephalon. Eur. J. Neurosci. *12*, 2721–2734.

Ramenghi, L.A., Rutherford, M., Fumagalli, M., Bassi, L., Messner, H., Counsell, S., and Mosca, F. (2009). Neonatal neuroimaging: Going beyond the pictures. Early Hum. Dev. *85*.

Ramoz, N., Reichert, J.G., Smith, C.J., Silverman, J.M., Bespalova, I.N., Davis, K.L., and Buxbaum, J.D. (2004). Linkage and Association of the Mitochondrial Aspartate/Glutamate Carrier SLC25A12 Gene with Autism. Am. J. Psychiatry *161*, 662–669.

Ray, J.G., Vermeulen, M.J., Bharatha, A., Montanera, W.J., and Park, A.L. (2016). Association Between MRI Exposure During Pregnancy and Fetal and Childhood Outcomes. JAMA *316*, 952–961.

Raznahan, A., Wallace, G.L., Antezana, L., Greenstein, D., Lenroot, R., Thurm, A., Gozzi, M., Spence, S., Martin, A., Swedo, S.E., et al. (2013). Compared to What? Early Brain Overgrowth in Autism and the Perils of Population Norms. Biol. Psychiatry *74*, 563–575.

Redcay, E., and Courchesne, E. (2005). When Is the Brain Enlarged in Autism? A Meta-Analysis of All Brain Size Reports. Biol. Psychiatry *58*, 1–9.

Reeves, M.J., Brandreth, M., Whitby, E.H., Hart, A.R., Paley, M.N.J., Griffiths, P.D., and Stevens, J.C. (2010). Neonatal cochlear function: measurement after exposure to acoustic noise during in utero MR imaging. Radiology *257*, 802–809.

Reichenberg, A., Gross, R., Weiser, M., Bresnahan, M., Silverman, J., Harlap, S., Rabinowitz, J., Shulman, C., Malaspina, D., Lubin, G., et al. (2006). Advancing Paternal Age and Autism. Arch. Gen. Psychiatry *63*, 1026–1032.

Rice, D.S., and Curran, T. (2001). Role of the Reelin Signalling Pathway in Central Nervous System Development. Annu. Rev. Neurosci. *24*, 1005–1039.

Riordan, D., Appleby, L., and Faragher, B. (1999). Mother-infant interaction in post-partum women with schizophrenia and affective disorders. Psychol. Med. *29*, 991–995.

Ritvo, E.R., Freeman, B.J., Scheibel, A.B., Duong, T., Robinson, H., Guthrie, D., and Ritvo, A. (1986). Lower Purkinje Cell Counts in the Cerebella of Four Autistic Subjects: Initial Findings of the UCLA-NSAC Autopsy Research Report. Am. J. Psychiatry *143*, 862–866.

Robertson, N.J., and Cox, I.J. (2002). Magnetic resonance spectroscopy of the neonatal brain. In MRI of the Neonatal Brain, M.A. Rutherford, ed. (London, United Kingdom: WB Saunders), p.

Robertson, C., Hermann, K., Ratai, E.-M., and Kanwisher, N. (2015). GABA Measured in Visual Cortex using MRS Predicts Atypical Dynamics of Binocular Rivalry Associated with Autism. J. Vis. *15*, 917.

Rodriguez, M., Sabate, M., Rodriguez-Sabate, C., and Morales, I. (2013). The role of non-synaptic extracellular glutamate. Brain Res. Bull. *93*, 17–26.

Rogers, S.J., and Vismara, L.A. (2008). Evidence-Based Comprehensive Treatments for Early Autism.

Rogers, T.D., McKimm, E., Dickson, P.E., Goldowitz, D., Blaha, C.D., and Mittleman, G. (2013). Is autism a disease of the cerebellum? An integration of clinical and pre-clinical research. Front. Syst. Neurosci. *7*, 1–16.

Rojas, D.C., Peterson, E., Winterrowd, E., Reite, M.L., Rogers, S.J., and Tregellas, J.R. (2006). Regional gray matter volumetric changes in autism associated with social and repetitive behavior symptoms. BMC Psychiatry *6*, 1–13.

Rojas, D.C., Singel, D., Steinmetz, S., Hepburn, S., and Brown, M.S. (2014). Decreased left perisylvian GABA concentration in children with autism and unaffected siblings. Neuroimage *86*, 28–34.

Rojas, D.C., Becker, K.M., and Wilson, L.B. (2015). Magnetic Resonance Spectroscopy Studies of Glutamate and GABA in Autism: Implications for Excitation-Inhibition Imbalance Theory. Curr. Dev. Disord. Reports *2*, 46–57.

Rommelse, N.N.J., Franke, B., Geurts, H.M., Hartman, C. a., and Buitelaar, J.K. (2010). Shared heritability of attention-deficit/hyperactivity disorder and autism spectrum disorder. Eur. Child Adolesc. Psychiatry *19*, 281–295.

Rorke, L.B., and Spiro, A.J. (1967). Cerebral lesions in congenital rubella syndrome. J. Pediatr. *70*, 243–255.

Rosenberg, P.A., Dai, W., Gan, X.D., Ali, S., Fu, J., Back, S.A., Sanchez, R.M., Segal, M.M., Follett, P.L., Jensen, F.E., et al. (2003). Mature myelin basic protein-expressing oligodendrocytes are insensitive to kainate toxicity. J. Neurosci. Res. *71*, 237–245.

Rosenberg, R.E., Law, J.K., Yenokyan, G., McGready, J., Kaufmann, W.E., and Law, P. a (2009). Characteristics and concordance of autism spectrum disorders among 277 twin pairs. Arch. Pediatr. Adolesc. Med. *163*, 907–914.

Ross, B., and Bluml, S. (2001). Magnetic Resonance Spectroscopy of the Human Brain. Anat. Rec. *265*, 54–84.

Roth, T.L., and Sweatt, J.D. (2011). Annual research review: Epigenetic mechanisms and environmental shaping of the brain during sensitive periods of development. J. Child Psychol. Psychiatry *52*, 398–408.

Rozga, A., Hutman, T., Young, G.S., Rogers, S.J., Ozonoff, S., Dapretto, M., and Sigman, M. (2011). Behavioral profiles of affected and unaffected siblings of children with autism: Contribution of measures of mother-infant interaction and nonverbal communication. J. Autism Dev. Disord. *41*, 287–301.

Rubeis, S. De, He, X., Goldberg, A.P., Poultney, C.S., and Samocha, K. (2014). Synaptic, transcriptional, and chromatin genes disrupted in autism A. Nature *515*, 209–215.

Rubenstein, J.L.R. (2011). Annual Researc Review: Development of the cerebral cortex: Implications for neurodevelopmental disorders. J. Child Psychol. Psychiatry *52*, 339–355.

Rubenstein, J.L.R., and Merzenich, M.M. (2003). Model of autism: increased ratio of excitation/inhibition in key neural systems. Genes. Brain. Behav. *2*, 255–267.

Rutherford, M.A. (2009). Magnetic resonance imaging of the fetal brain. Curr. Opin. Obstet. Gynecol. *21*, 180–186.

Rutherford, M., Jiang, S., Allsop, J., Perkins, L., Srinivasan, L., Hayat, T., Kumar, S., and Hajnal, J. (2008). MR imaging methods for assessing fetal brain development. Dev. Neurobiol. *68*, 700–711.

Rutter, M. (2005). Aetiology of autism: findings and questions. J. Intellect. Disabil. Res. *49*, 231–238.

Rutter, M., Bailey, A., and Lord, C. (2003). Social Communication Questionnaire. Los Angeles, CA.

Rutter, M., Moffitt, T.E., and Caspi, A. (2006). Gene-environment interplay and psychopathology: Multiple varieties but real effects. J. Child Psychol. Psychiatry Allied Discip. *47*, 226–261.

Sale, A., Berardi, N., and Maffei, L. (2014). Environment and Brain Plasticity: Towards an Endogenous Pharmacotherapy. Physiol. Rev. *94*, 189–234.

Sanders, S.J., Ercan-Sencicek, A.G., Hus, V., Luo, R., Murtha, M.T., Moreno-De-Luca, D., Chu, S.H., Moreau, M.P., Gupta, A.R., Thomson, S.A., et al. (2011). Multiple Recurrent De Novo CNVs, Including Duplications of the 7q11.23 Williams Syndrome Region, Are Strongly Associated with Autism. Neuron *70*, 863–885.

Sanders, S.J., Murtha, M.T., Gupta, A.R., Murdoch, J.D., Raubeson, M.J., Willsey, A.J., Ercan-Sencicek, A.G., DiLullo, N.M., Parikshak, N.N., Stein, J.L., et al. (2012). De novo mutations revealed by whole-exome sequencing are strongly associated with autism. Nature *485*, 237–241.

Sandin, S., Lichtenstein, P., Kuja-Halkola, R., Larsson, H., Hultman, C.M., and Reichenberg, A. (2014). The Familial Risk of Autism. JAMA *311*, 1770–1777.

Sarkar, S., Craig, M.C., Dell'acqua, F., O'Connor, T.G., Catani, M., Deeley, Q., Glover, V., and Murphy, D.G.M. (2014). Prenatal stress and limbic-prefrontal white matter microstructure in children aged 6-9 years: a preliminary diffusion tensor imaging study. World J. Biol. Psychiatry *15*, 346–352.

Sato, W., Kubota, Y., Kochiyama, T., Uono, S., Yoshimura, S., Sawada, R., Sakihama, M., and Toichi, M. (2014). Increased putamen volume in adults with autism spectrum disorder. Front. Hum. Neurosci. *8*, 957.

Schendel, D.E., Overgaard, M., Christensen, J., Hjort, L., Jørgensen, M., Vestergaard, M., and Parner, E.T. (2016). Association of Psychiatric and Neurologic Comorbidity With Mortality Among Persons With Autism Spectrum Disorder in a Danish Population. JAMA Pediatr. *170*, 243–250.

Schieve, L.A., Clayton, H.B., Durkin, M.S., Wingate, M.S., and Drews-Botsch, C. (2015). Comparison of Perinatal Risk Factors Associated with Autism Spectrum Disorder (ASD), Intellectual Disability (ID), and Co-occurring ASD and ID. J. Autism Dev. Disord. *45*, 2361–2372.

Schifter, T., Hoffman, J.M., Hatten, P., Hanson, M.W., Coleman, R.E., and DeLong, G.R. (1994). Neuroimaging in infantile autism. J. Child Neurol. *9*, 155–161.

Schmahmann, J.D. (2001). The cerebrocerebellar system: anatomic substrates of the cerebellar contribution to cognition and emotion. Int. Rev. Psychiatry *13*, 247–260.

Schmahmann, J.D., and Sherman, J.C. (1998). The cerebellar cognitive affective syndrome. Brain *121*, 561–579.

Schmidt, R.J., Tancredi, D.J., Ozonoff, S., Hansen, R.L., Hartiala, J., Allayee, H., Schmidt, L.C., Tassone, F., and Hertz-Picciotto, I. (2012). Maternal periconceptional folic acid intake and risk for developmental delay and autism spectrum disorder: A case-control study. Am. J. Clin. Nutr. *96*, 80–89.

Schroder, H.J., and Power, G.G. (1997). Engine and radiator: Fetal and placental interactions for heat dissipation. Exp. Physiol. *82*, 403–414.

Schumann, C.M., Barnes, C.C., Lord, C., and Courchesne, E. (2009). Amygdala Enlargement in Toddlers with Autism Related to Severity of Social and Communication Impairments. Biol. Psychiatry *66*, 942–949.

Schumann, C.M., Bloss, C.S., Barnes, C.C., Wideman, G.M., Carper, R. a, Pierce, K., Hagler, D., Schork, N., Lord, C., Courchesne, E., et al. (2010). Longitudinal MRI Study of Cortical Development through Early Childhood in Autism. J. Neurosci. *30*, 4419–4427.

Scott, J., Underwood, J., Garvey, L.J., Mora-Peris, B., and Winston, A. (2016). A comparison of two post-processing analysis methods to quantify cerebral metabolites measured via proton magnetic resonance spectroscopy in HIV disease. Br. Inst. Radiol. *89*, 20150979.

Scott, J.A., Habas, P.A., Kim, K., Rajagopalan, V., Hamzelou, K.S., Corbett-Detig, J.M., Barkovich, A.J., Glenn, O.A., and Studholme, C. (2011). Growth trajectories of the human fetal brain tissues estimated from 3D reconstructed in utero MRI. Int. J. Dev. Neurosci. *29*, 529–536.

Scott, J.A., Hamzelou, K.S., Rajagopalan, V., Habas, P.A., Kim, K., Barkovich, A.J., Glenn, O.A., and Studholme, C. (2012). 3D Morphometric Analysis of Human Fetal Cerebellar Development. Cerebellum *11*, 761–770.

Sears, L.L., Vest, C., Mohamed, S., Bailey, J., Ranson, B.J., and Piven, J. (1999). An MRI study of the basal ganglia in autism. Prog. Neuro-Psychopharmacology Biol. Psychiatry *23*, 613–624.

Seidman, L.J., Biederman, J., Liang, L., Valera, E.M., Monuteaux, M.C., Brown, A., Kaiser, J., Spencer, T., Faraone, S. V., and Makris, N. (2011). Gray Matter Alterations in Adults with Attention-Deficit/Hyperactivity Disorder Identified by Voxel Based Morphometry. Biol. Psychiatry *69*, 857–866.

Senju, A., Csibra, G., and Johnson, M.H. (2008). Understanding the referential nature of looking: Infants' preference for object-directed gaze. Cognition *108*, 303–319.

Sepulveda, M.A., Lapez, G., Azar, M.C., and et al. (1999). Diseño de un modelo de intervencion temprana en sectores marginales. An. La Univ. Metrop. *8*, 231–248.

Serajee, F.J., Zhong, H., Nabi, R., and Huq, A.H.M.M. (2003). The metabotropic glutamate receptor 8 gene at 7q31: partial duplication and possible association with autism. J. Med. Genet. *40*, e42.

Sévely, A., and Manelfe, C. (2002). Magnetic resonance imaging of the fetal brain. In MRI of the Neonatal Brain, M.A. Rutherford, ed. (London, United Kingdom: WB Saunders), p.

Shafali, S.J. (2015). Neurodevelopmental Behavioral and Cognitive Disorders. Continuum (N. Y). *21*, 690–714.

Shalak, L., and Perlman, J.M. (2004). Hypoxic-ischemic brain injury in the term infant-current concepts. Early Hum. Dev. *80*, 125–141.

Shen, M.D., Nordahl, C.W., Young, G.S., Wootton-Gorges, S.L., Lee, A., Liston, S.E., Harrington, K.R., Ozonoff, S., and Amaral, D.G. (2013). Early brain enlargement and elevated extra-axial fluid in infants who develop autism spectrum disorder. Brain *136*, 2825–2835.

Sheridan, M. (2008). From Birth to Five Years: Children's Developmental Progress (Routledge).

Shimmura, C., Suda, S., Tsuchiya, K.J., Hashimoto, K., Ohno, K., Matsuzaki, H., Iwata, K., Matsumoto, K., Wakuda, T., Kameno, Y., et al. (2011). Alteration of plasma glutamate and glutamine levels in children with high-functioning autism. PLoS One *6*, e25340.

Shonkoff, J.P., Garner, a. S., Siegel, B.S., Dobbins, M.I., Earls, M.F., Garner, a. S., McGuinn, L., Pascoe, J., and Wood, D.L. (2012). The Lifelong Effects of Early Childhood Adversity and Toxic Stress. Pediatrics *129*, e232–e246.

Short, A.B., and Schopler, E. (1988). Factors relating to age of onset in autism. J. Autism Dev. Disord. *18*, 207–216.

Sibtain, N.A., Howe, F.A., and Saunders, D.E. (2007). The clinical value of proton magnetic resonance spectroscopy in adult brain tumours. Clin. Radiol. *62*, 109–119.

Silverman, J.L., Smith, D.L.D.L.G., Rizzo, S.J.S., Karras, M.N., Turner, S.M., Tolu, S.S., Bryce, D.K., Smith, D.L.D.L.G., Fonseca, K., Ring, R.H., et al. (2012). Negative allosteric modulation of the mGluR5 receptor reduces repetitive behaviors and rescues social deficits in mouse models of autism. Sci. Transl. Med. *4*, 131ra51.

Simmons, M.L., Frondoza, C.G., and Coyle, J.T. (1991). Immunocytochemical localization of N-acetyl-aspartate with monoclonal antibodies. Neuroscience *45*, 37–45.

Simões, R. V., Cruz-Lemini, M., Bargalló, N., Gratacós, E., and Sanz-Cortes, M. (2015). Brain metabolite differences in one-year-old infants born small at term and association with neurodevelopmental outcome. Am. J. Obstet. Gynecol. *213*, 210e.1-11.

Simonoff, E., Pickles, A., Charman, T., Chandler, S., Loucas, T., and Baird, G. (2008). Psychiatric Disorders in Children With Autism Spectrum Disorders: Prevalence, Comorbidity, and Associated Factors in a Population-Derived Sample. J. Am. Acad. Child Adolesc. Psychiatry *47*, 921–929.

Skefos, J., Cummings, C., Enzer, K., Holiday, J., Weed, K., Levy, E., Yuce, T., Kemper, T., and Bauman, M. (2014). Regional Alterations in Purkinje Cell Density in Patients with Autism. PLoS One *9*, 1–12.

Smith, S.M. (2002). Fast robust automated brain extraction. Hum. Brain Mapp. *17*, 143–155.

Smith, F.W., MacLennan, F., Abramovich, D.R., MacGilivray, I., and Hutchison, J.M.S. (1984). NMR Imaging in Human Pregnancy: A Preliminary Study. Magn. Reson. Imaging *2*, 57–64.

Smithells, R.W., Sheppard, S., Schorah, C.J., Seller, M.J., Nevin, N.C., Harris, R., Read, A.P., and Fielding, D.W. (1980). Possible prevention of neural-tube defects by periconceptional vitamin supplementation. Lancet *1*, 339–340.

Smithells, R.W., Sheppard, S., Schorah, C.J., Seller, M.J., Nevin, N.C., Harris, R., Read, A.P., and Fielding, D.W. (2011). Apparent prevention of neural tube defects by periconceptional vitamin supplementation. Int. J. Epidemiol. *40*, 1146–1154.

Soares, D.P., and Law, M. (2009). Magnetic resonance spectroscopy of the brain: review of metabolites and clinical applications. Clin. Radiol. *64*, 12–21.

Solon, O., Riddell, T.J., Quimbo, S.A., Butrick, E., Aylward, G.P., Lou Bacate, M., and Peabody, J.W. (2008). Associations between cognitive function, blood lead concentration, and nutrition among children in the central Philippines. J. Pediatr. *152*, 237–243.

Sparks, B.F., Friedman, S.D., Shaw, D.W., Aylward, E.H., Echelard, D., Artru, a a, Maravilla, K.R., Giedd, J.N., Munson, J., Dawson, G., et al. (2002). Brain structural abnormalities in young children with autism spectrum disorder. Neurology *59*, 184–192.

Stanfield, A.C., McIntosh, A.M., Spencer, M.D., Philip, R., Gaur, S., and Lawrie, S.M. (2008). Towards a neuroanatomy of autism: A systematic review and meta-analysis of structural magnetic resonance imaging studies. Eur. Psychiatry *23*, 289–299.

Stein, A., Craske, M.G., Lehtonen, A., Harvey, A., Savage-McGlynn, E., Davies, B., Goodwin, J., Murray, L., Cortina-Borja, M., and Counsell, N. (2012). Maternal Cognitions and Mother–Infant Interaction in Postnatal Depression and Generalized Anxiety Disorder. J. Abnorm. Psychol. *121*, 795–809.

Stiles, J. (2008). The fundamentals of brain development: Integrating nature and nurture (Cambridge, MA: Harvard University Press).

Stiles, J., and Jernigan, T.L. (2010). The Basics of Brain Development. Neuropsychol. Rev. *20*, 327–348.

Stoner, R., Chow, M.L., Boyle, M.P., Sunkin, S.M., Mouton, P.R., Roy, S., Wynshaw-Boris, A., Colamarino, S.A., Lein, E.S., and Courchesne, E. (2014). Patches of disorganization in the neocortex of children with autism. N. Engl. J. Med. *370*, 1209–1219.

Story, L., Damodaram, M.S., Allsop, J.M., McGuinness, A., Wylezinska, M., Kumar, S., and Rutherford, M.A. (2011). Proton magnetic resonance spectroscopy in the fetus. Eur. J. Obstet. Gynecol. Reprod. Biol. *158*, 3–8.

Story, L., Damodaram, M.S., Supramaniam, V., Allsop, J.M., McGuinness, A., Patel, A., Wylezinska, M., Kumar, S., and Rutherford, M. a. (2013). Myo-inositol metabolism in appropriately grown and growth-restricted fetuses: A proton magnetic resonance spectroscopy study. Eur. J. Obstet. Gynecol. Reprod. Biol. *170*, 77–81.

Strömland, K., Nordin, V., Miller, M., Akerström, B., and Gillberg, C. (1994). Autism in thalidomide embryopathy: a population study. Dev. Med. Child Neurol. *36*, 351–356.

Sugita, K., Ando, M., Makino, M., Takanashi, J., Fujimoto, N., and Niimi, H. (1991). Magnetic resonance imaging of the brain in congenital rubella virus and cytomegalovirus infections. Neuroradiology *33*, 239–242.

Sur, M., and Rubenstein, J.L.R. (2005). Patterning and plasticity of the cerebral cortex. Science (80-.). *310*, 805–810.

Suren, P., Bresnahan, M., Haugen, M., Hornig, M., Hirtz, D., and Smith, G.D. (2013). Association Between Maternal Use of Folic Acid Supplements and Risk of Autism Spectrum Disorders in Children. J. Am. Med. Assoc. *309*, 570–577.

Surén, P., Stoltenberg, C., Bresnahan, M., Hirtz, D., Lie, K.K., Lipkin, W.I., Magnus, P., Reichborn-Kjennerud, T., Schjølberg, S., Susser, E., et al. (2013). Early Growth Patterns in Children witth Autism. Epidemiology *24*, 660–670.

Suzuki, K., Nishimura, K., Sugihara, G., Nakamura, K., Tsuchiya, K.J., Matsumoto, K., Takebayashi, K., Isoda, H., Sakahara, H., Sugiyama, T., et al. (2010). Metabolite alterations in the hippocampus of high-functioning adult subjects with autism. Int. J. Neuropsychopharmacol. *13*, 529–534.

Sweatt, J.D. (2009). Experience-Dependent Epigenetic Modifications in the Central Nervous System. Biol. Psychiatry *65*, 191–197.

Szafranski, P., Schaaf, C.P., Person, R.E., Gibson, I.B., Xia, Z., Mahadevan, S., Wiszniewska, J., Bacino, C.A., Lalani, S., Potocki, L., et al. (2010). Structures and molecular mechanisms for common 15q13.3 microduplications involving CHRNA7: Benign or pathological? Hum. Mutat. *31*, 840–850.

Szatmari, P. (2011). Is Autism, at Least in Part, a Disorder of Fetal Programming? Arch. Gen. Psychiatry *68*, 1091–1092.

Tau, G.Z., and Peterson, B.S. (2010). Normal Development of Brain Circuits. Neuropsychopharmacology *35*, 147–168.

Tebartz Van Elst, L., Maier, S., Fangmeier, T., Endres, D., Mueller, G., Nickel, K., Ebert, D., Lange, T., Hennig, J., Biscaldi, M., et al. (2014). Disturbed cingulate glutamate metabolism in adults with high-functioning autism spectrum disorder: evidence in support of the excitatory/inhibitory imbalance hypothesis. Mol. Psychiatry *19*, 1314–1325.

Teicher, M.H., Tomoda, A., and Andersen, S.E. (2006). Neurobiological consequences of early stress and childhood maltreatment: Are results from human and animal studies comparable? In Annals of the New York Academy of Sciences, pp. 313–323.

Tomasello, M., Carpenter, M., Call, J., Behne, T., and Moll, H. (2005). Understanding and sharing intentions: the origins of cultural cognition. Behav. Brain Sci. *28*, 675–691.

Tsatsanis, K.D., Rourke, B.P., Klin, A., Volkmar, F.R., Cicchetti, D., and Schultz, R.T. (2003). Reduced Thalamic Volume in High-Functioning Individuals with Autism. Biol. Psychiatry *53*, 121–129.

Tuchman, R., Cuccaro, M., and Alessandri, M. (2010). Autism and epilepsy: Historical perspective. Brain Dev. *32*, 709–718.

Tupler, L.A., and De Bellis, M.D. (2006). Segmented hippocampal volume in children and adolescents with posttraumatic stress disorder. Biol. Psychiatry *59*, 523–529.

Turner, C.E., and Gant, N. (2014). The Biochemistry of Creatine. In Magnetic Resonance Spectroscopy, C.S. Rothmanpages, ed. (San Diego, CA: Academic Press), pp. 91–103.

Turner, A.H., Greenspan, K.S., and van Erp, T.G.M.M. (2016). Pallidum and lateral ventricle volume enlargement in autism spectrum disorder. Psychiatry Res. - Neuroimaging *252*, 40–45.

Tustison, N.J., Avants, B.B., Cook, P.A., Zheng, Y., Egan, A., Yushkevich, P.A., and Gee, J.C. (2010). N4ITK: Improved N3 bias correction. IEEE Trans. Med. Imaging *29*, 1310–1320.

Tyzio, R., Romain, N., Ferrari, D.C., Tsintsadze, T., Shahrokhi, A., Eftekhari, S., Khalilov, I., Tsintsadze, V., Brouchoud, C., Chazal, G., et al. (2014). Oxytocin-Mediated GABA Inhibition During Delivery Attenuates Autism Pathogenesis in Rodent Offspring. Science (80-.). *343*, 675–679.

Unwin, L.M., Maybery, M.T., Murphy, A., Lilje, W., Bellesini, M., Hunt, A.M., Granich, J., Jacoby, P., Dissanayake, C., Pennell, C.E., et al. (2016). A Prospective Ultrasound Study of Prenatal Growth in Infant Siblings of Children With Autism. Autism Res. *9*, 210–216.

Ure, A.M., Treyvaud, K., Thompson, D.K., Pascoe, L., Roberts, G., Lee, K.J., Seal, M.L., Northam, E., Cheong, J.L., Hunt, R.W., et al. (2015). Neonatal Brain Abnormalities Associated with Autism Spectrum Disorder in Children Born Very Preterm. Autism Res.

Urenjak, J., Williams, S.R., Gadian, D.G., and Noble, M. (1992). Specific Expression of N-Acetylaspartate in Neurons, Oligodendrocyte-Type-2 Astrocyte Progenitors, and Immature Oligodendrocytes In Vitro. J. Neurochem. *59*, 55–61.

Vadeyar, S.H., Moore, R.J., Strachan, B.K., Gowland, P.A., Shakespeare, S.A., James, D.K., Johnson, I.R., and Baker, P.N. (2000). Effect of fetal magnetic resonance imaging on fetal heart rate patterns. Am J Obs. Gynecol *182*, 666–669.

Valiente, M., and Marín, O. (2010). Neuronal migration mechanisms in development and disease. Curr Opin Neurobiol *20*, 68–78.

Varela, M., Groves, A.M., Arichi, T., and Hajnal, J. V. (2012). Mean cerebral blood flow measurements using phase contrast MRI in the first year of life. NMR Biomed. *25*, 1063–1072.

Vargas, D.L., Nascimbene, C., Krishnan, C., Zimmerman, A.W., and Pardo, C.A. (2005). Neuroglial Activation and Neuroinflammation in the Brain of Patients with Autism. Ann. Neurol. *57*, 67–81.

Vasconcelos, M., Brito, A., Domingues, R., da Cruz, L.C.H., Gasparetto, E., Werner, J., and Gonçalves, J.P.S. (2008). Proton Magnetic Resonance Spectroscopy in School-Aged Autistic Children. J. Neuroimaging *18*, 288–295.

Vatansever, D., Kyriakopoulou, V., Allsop, J.M., Fox, M., Chew, A., Hajnal, J. V, and Rutherford, M. a (2013). Multidimensional Analysis of Fetal Posterior Fossa in Health and Disease. Cerebellum *12*, 632–644.

Vigneron, D.B. (2006). Magnetic Resonance Spectroscopic Imaging of Human Brain Development. Neuroimaging Clin. N. Am. *16*, 75–85.

Voineagu, I., Wang, X., Johnston, P., Lowe, J.K., Tian, Y., Horvath, S., Mill, J., Cantor, R.M., Blencowe, B.J., and Geschwind, D.H. (2011). Transcriptomic analysis of autistic brain reveals convergent molecular pathology. Nature *474*, 380–384.

Volkmar, F.R., and Chawarska, K. (2008). Autism in infants: an update. World Psychiatry *7*, 19–21.

Volkmar, F.R., and Pauls, D. (2003). Autism. In Lancet, pp. 1133–1141.

Wallace, G.L., Dankner, N., Kenworthy, L., Giedd, J.N., and Martin, A. (2010). Age-related temporal and parietal cortical thinning in autism spectrum disorders. Brain *133*, 3745–3754.

Wallace, G.L., Robustelli, B., Dankner, N., Kenworthy, L., Giedd, J.N., and Martin, A. (2013). Increased gyrification, but comparable surface area in adolescents with autism spectrum disorders. Brain *136*, 1956–1967.

Wan, M.W., Green, J., Elsabbagh, M., Johnson, M., Charman, T., and Plummer, F. (2012). Parent-infant interaction in infant siblings at risk of autism. Res. Dev. Disabil. *33*, 924–932.

Wan, M.W., Green, J., Elsabbagh, M., Johnson, M., Charman, T., and Plummer, F. (2013). Quality of interaction between at-risk infants and caregiver at 12-15 months is associated with 3-year autism outcome. J. Child Psychol. Psychiatry Allied Discip. *54*, 763–771.

Wattjes, M.P., Harzheim, M., Lutterbey, G.G., Bogdanow, M., Schild, H.H., and Träber, F. (2008). High field MR imaging and 1H-MR spectroscopy in clinically isolated syndromes suggestive of multiple sclerosis: correlation between metabolic alterations and diagnostic MR imaging criteria. J. Neurol. *255*, 56–63.

Wegiel, J., Kuchna, I., Nowicki, K., Imaki, H., Wegiel, J., Marchi, E., Ma, S.Y., Chauhan, A., Chauhan, V., Bobrowicz, T.W., et al. (2010). The neuropathology of autism: defects of neurogenesis and neuronal migration, and dysplastic changes. Acta Neuropathol. *119*, 755–770.

Weiss, L. a, Shen, Y., Korn, J.M., Arking, D.E., Miller, D.T., Fossdal, R., Saemundsen, E., Stefansson, H., Ferreira, M. a R., Green, T., et al. (2008). Association between microdeletion and microduplication at 16p11.2 and autism. N. Engl. J. Med. *358*, 667–675.

Whitehouse, A.J.O., Hickey, M., Stanley, F.J., Newnham, J.P., and Pennell, C.E. (2011). Brief Report: A Preliminary Study of Fetal Head Circumference Growth in Autism Spectrum Disorder. J. Autism Dev. Disord. *41*, 122–129.

Wijlaars, L.P.M.M., Johnson, L., van Jaarsveld, C.H.M., and Wardle, J. (2011). Socioeconomic status and weight gain in early infancy. Int. J. Obes. *35*, 963–970.

Willemsen, M.H., Fernandez, B. a, Bacino, C. a, Gerkes, E., de Brouwer, A.P.M., Pfundt, R., Sikkema-Raddatz, B., Scherer, S.W., Marshall, C.R., Potocki, L., et al. (2010). Identification of ANKRD11 and ZNF778 as candidate genes for autism and variable cognitive impairment in the novel 16q24.3 microdeletion syndrome. Eur. J. Hum. Genet. *18*, 429–435.

Williams, G., King, J., Cunningham, M., Stephan, M., Kerr, B., and Hersh, J.H. (2001). Fetal valproate syndrome and autism: additional evidence of an association. Dev. Med. Child Neurol. *43*, 202–206.

Wilson, M., Reynolds, G., Kauppinen, R.A., Arvanitis, T.N., and Peet, A.C. (2011). A Constrained Least-Squares Approach to the Automated Quantitation of In Vivo (1)H Magnetic Resonance Spectroscopy Data. Magn. Reson. Med. *65*, 1–12.

Wing, L., and Potter, D. (2002). The Epidemiology of Autistic Spectrum Disorders: Is the Prevalence Rising? Ment. Retard. Dev. Disabil. Res. Rev. *8*, 151–161.

Wodarz, A., and Huttner, W.B. (2003). Asymmetric cell division during neurogenesis in Drosophila and vertebrates. Mech. Dev. *120*, 1297–1309.

Wolff, J.J., Gu, H., Gerig, G., Elison, J.T., Styner, M., Gouttard, S., Botteron, K.N., Dager, S.R., Dawson, G., Estes, A.M., et al. (2012). Differences in White Matter Fiber Tract Development Present From 6 to 24 Months in Infants with Autism. Am. J. Psychiatry *169*, 589–600.

Wolff, J.J., Gerig, G., Lewis, J.D., Soda, T., Styner, M. a., Vachet, C., Botteron, K.N., Elison, J.T., Dager, S.R., Estes, A.M., et al. (2015). Altered corpus callosum morphology associated with autism over the first 2 years of life. Brain *138*, 1–13.

Woo, C.C., Donnelly, J.H., Steinberg-Epstein, R., and Leon, M. (2015). Environmental Enrichment as a Therapy for Autism: A Clinical Trial Replication and Extension. Behav. Neurosci. *129*, 412–422.

Woolfenden, S., Sarkozy, V., Ridley, G., Coory, M., and Williams, K. (2012). A systematic review of two outcomes in autism spectrum disorder - epilepsy and mortality. Dev. Med. Child Neurol.

Wright, R., Vatansever, D., Kyriakopoulou, V., Ledig, C., Wolz, R., Serag, A., Rueckert, D., Rutherford, M.A., Hajnal, J.V., and Aljabar, P. (2012). Age dependent fetal MR segmentation using manual and automated approaches. In Workshop on Perinatal and Paediatric Imaging: PaPI, Medical Image Computing and Computer-Assisted Intervention: MICCAI., pp. 97–104.

Wright, R., Kyriakopoulou, V., Ledig, C., Rutherford, M.A., Hajnal, J. V., Rueckert, D., and Aljabar, P. (2014). Automatic quantification of normal cortical folding patterns from fetal brain MRI. Neuroimage *91*, 21–32.

Wright, R., Makropoulos, A., Kyriakopoulou, V., Patkee, P.A., Koch, L.M., Rutherford, M.A., Hajnal, J. V., Rueckert, D., and Aljabar, P. (2015). Construction of a fetal spatio-temporal cortical surface atlas from in utero MRI: Application of spectral surface matching. Neuroimage *120*, 467–480.

Xu, G., Broadbelt, K.G., Haynes, R.L., Rebecca, D., Volpe, J.J., and Kinney, H.C. (2011). Late Development of the GABAergic system in the Human Cerebral Cortex and White Matter. J. Neuropathol. Exp. Neurol. *70*, 841–858.

Xue, H., Srinivasan, L., Jiang, S., Rutherford, M., Edwards, A.D., Rueckert, D., and Hajnal, J. V. (2007). Automatic segmentation and reconstruction of the cortex from neonatal MRI. Neuroimage *38*, 461–477.

Yang, S., Perez, E., Cutright, J., Liu, R.A.N., He, Z., Day, A.L., Simpkins, J.W., Perez, E., Cutright, J., He, Z., et al. (2002). Testosterone increases neurotoxicity of glutamate in vitro and ischemia-reperfusion injury in an animal model. J. Appl. Physiol. *92*, 195–201.

Yip, Y., Capriotti, C., Talagala, S., and Yip, J. (1994). Effects of MR exposure at 1.5 T on early embryonic development of the chick. J. Magn. Reson. Imaging *4*, 742–748.

Yoshioka, A., Bacskai, B., and Pleasure, D. (1996). Pathophysiology of oligodendroglial excitotoxicity. J. Neurosci. Res. *46*, 427–437.

Yuan, X., Eisen, A.M., McBain, C.J., and Gallo, V. (1998). A role for glutamate and its receptors in the regulation of oligodendrocyte development in cerebellar tissue slices. Development *125*, 2901–2914.

Yushkevich, P.A., Piven, J., Hazlett, H.C., Smith, R.G., Ho, S., Gee, J.C., and Gerig, G. (2006). User-guided 3D active contour segmentation of anatomical structures: Significantly improved efficiency and reliability. Neuroimage *31*, 1116–1128.

Zhang, Y., Hodgson, N.W., Trivedi, M.S., Abdolmaleky, H.M., Fournier, M., Cuenod, M., Do, K.Q., and Deth, R.C. (2016). Decreased Brain Levels of Vitamin B12 in Aging, Autism and Schizophrenia. PLoS One *11*, e0146797.

Zheng, Z., Zhu, T., Qu, Y., and Mu, D. (2016). Blood Glutamate Levels in Autism Spectrum Disorder: A Systematic Review and Meta-Analysis. PLoS One *11*, e0158688.

Zhu, J.-K. (2009). Active DNA demethylation mediated by DNA glycosylases. Annu. Rev. Genet. *43*, 143–166.

Zoghbi, H.Y., and Bear, M.F. (2012). Synaptic Dysfunction in Neurodevelopmental Disorders Associated with Autism and Intellectual Disabilities. Cold Spring Harb. Perspect. Biol. *4*, 1–22.

Zwaigenbaum, L., Bryson, S., Rogers, T., Roberts, W., Brian, J., and Szatmari, P. (2005). Behavioral manifestations of autism in the first year of life. Int. J. Dev. Neurosci. *23*, 143–152.

Zwaigenbaum, L., Thurm, A., Stone, W., Baranek, G., Bryson, S., Iverson, J., Kau, A., Klin, A., Lord, C., Landa, R., et al. (2007). Studying the Emergence of Autism Spectrum Disorders in High-Risk Infants: Methodological and Practical Issues. J. Autism Dev. Disord. *37*, 466–480.

Zwaigenbaum, L., Bryson, S., and Garon, N. (2013). Early identification of autism spectrum disorders. Behav. Brain Res. *251*, 133–146.

Zwaigenbaum, L., Young, G.S., Stone, W.L., Dobkins, K., Ozonoff, S., Brian, J., Bryson, S.E., Carver, L.J., Hutman, T., Iverson, J.M., et al. (2014). Early Head Growth in Infants at Risk of Autism: A Baby Siblings Research Consortium Study. J. Am. Acad. Child Adolesc. Psychiatry *53*, 1053–1062.

Zwaigenbaum, L., Bauman, M.L., Choueiri, R., Fein, D., Kasari, C., Pierce, K., Stone, W.L., Yirmiya, N., Estes, A., Hansen, R.L., et al. (2015). Early Identification and Interventions for Autism Spectrum Disorder: Executive Summary. Pediatrics *136*, S1–S9.